Supplementary Materials for

Photobiocatalytic benzylic C–H acylation enabled by the synergy of a thiamine-dependent enzyme, an organophotocatalyst and hydrogen-atom-transfer

Xichao Peng[#], Jianqiang Feng[#], Fulu Liu[#], Wenzheng Xie[#], Hailong Sun, Yuanyuan Xu, Yang Ming, Zhongqiu Xing, Yu Zheng, Binju Wang*, Yi-Tao Long*, Xiaoqiang Huang*

[*]Corresponding author. Email: huangx513@nju.edu.cn;
yitaolong@nju.edu.cn;
wangbinju2018@xmu.edu.cn

This PDF file includes:

Supplementary Figs. 1-11

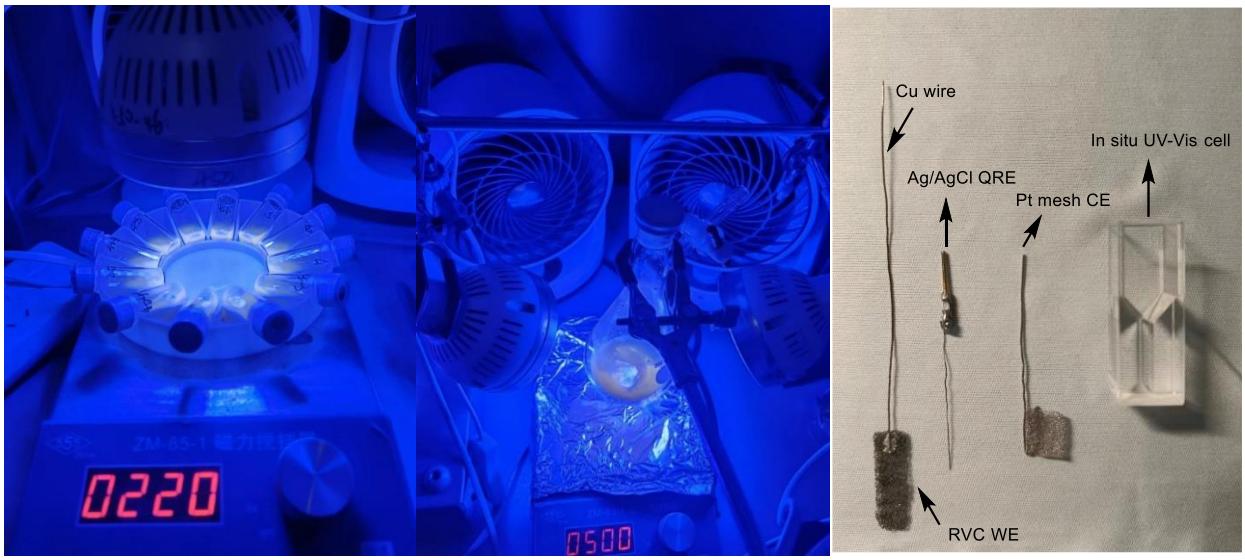

a **b** **c**

Supplementary Fig. 1 | Photobiocatalytic reaction set-up. a, Set-up for 0.004 mmol scale reactions, reaction vials were placed on the stir-plate, at a distance of ~ 10 cm from a 450-460 nm LEDs lamp, with a cooling fan. **b**, Set-up for 0.1 mmol scale reactions, the reaction was carried out in a 200 mL Schlenk flask with two 450-460 nm LEDs lamps and two cooling fans; LED lamps were purchased from the Chinese Taobao branded as "JiaDeng". Unless otherwise noted, the wavelength of the LEDs used is 450-460 nm. **c**, Devices for the spectroelectrochemical studies.

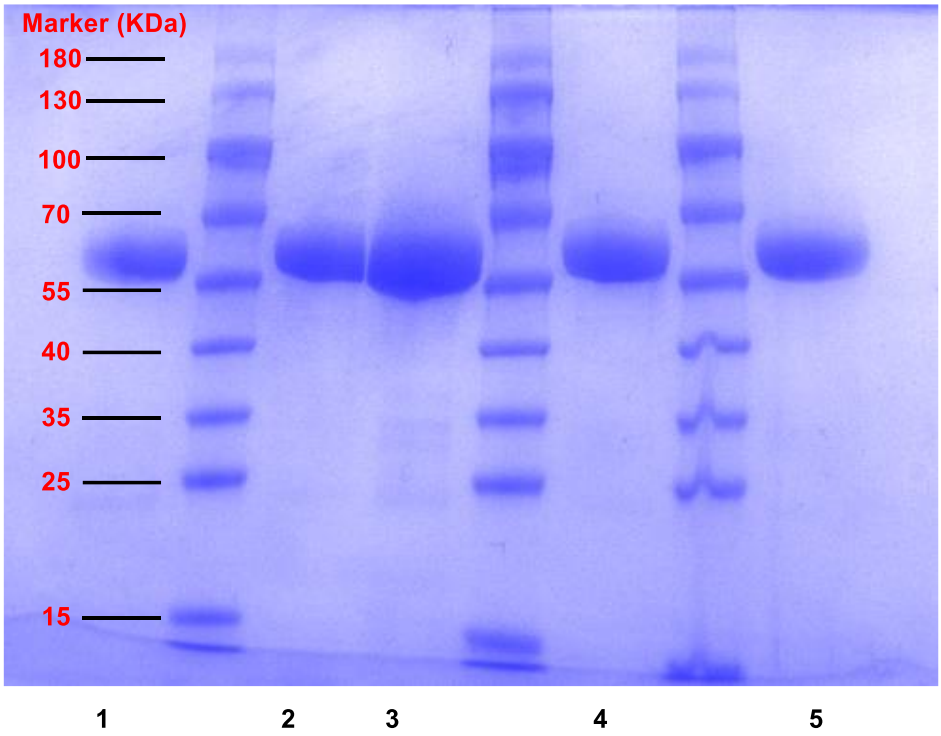

Supplementary Fig. 2 | SDS-PAGE analysis showing the purity of the enzymes. 1, *Pf*BAL; 2, *Pf*BAL_T481L; 3, *Pf*BAL_T481L-A480G; 4, *Pf*BAL_T481L-A480G-Y397A; 5, *Pf*BAL_T481L-A480G-Y397A-W163C. Other lines are makers.

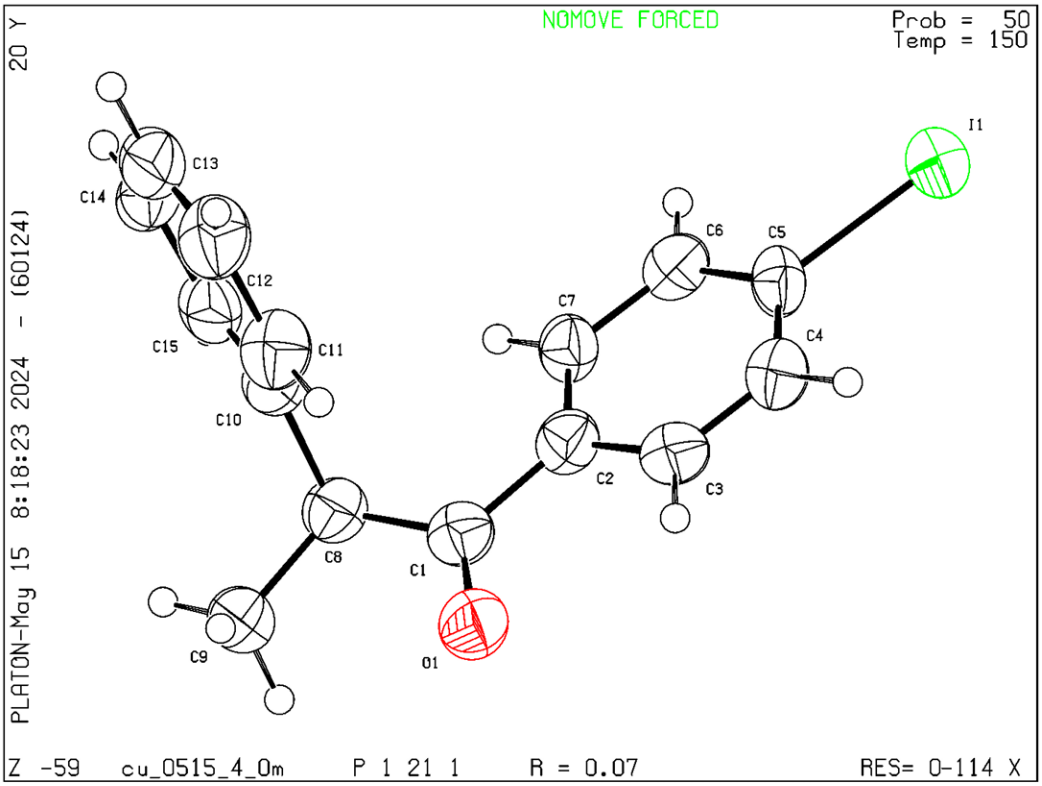

Supplementary Fig. 3 | **X-Ray diffraction data.** X-Ray diffraction data of (*S*)-**3g** (CCDC 2355842) obtained from the reactions catalysed by *Pf*BAL_T481L-A480G-Y397A-W163C. See the Supplementary Table 21 for detailed discussion.

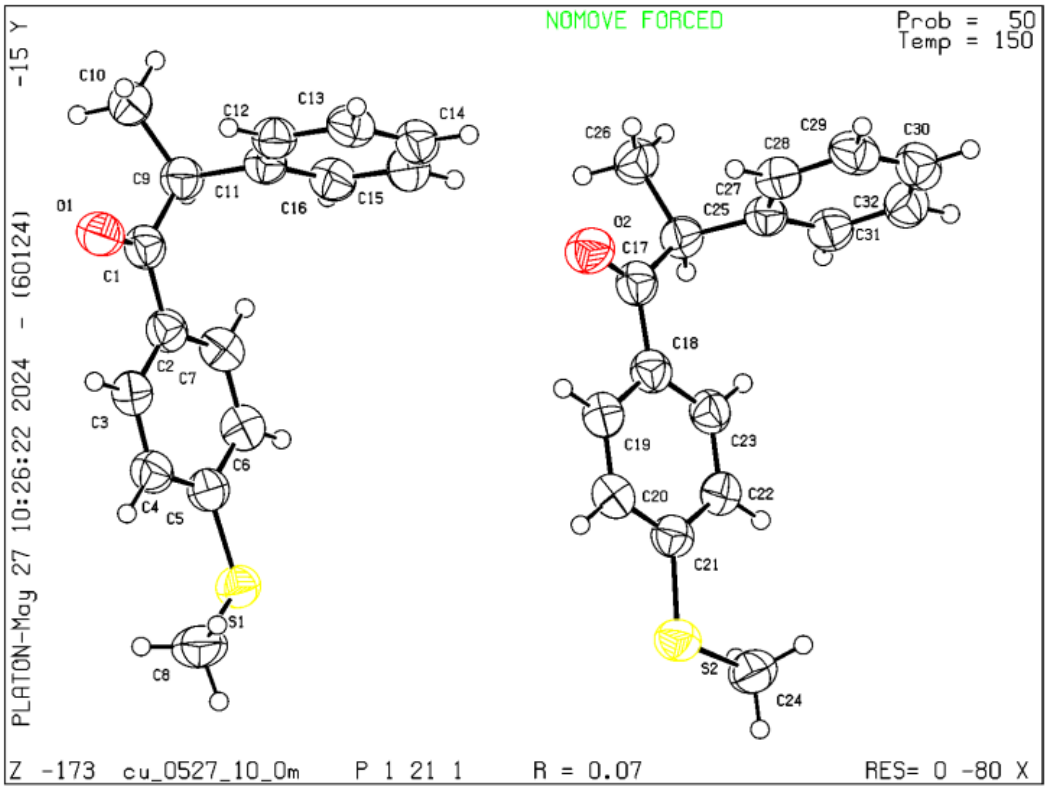

Supplementary Fig. 4 | X-Ray diffraction data. X-Ray diffraction data of (*S*)-**3k** (CCDC 2358465) obtained from the reactions catalysed by *Pf*BAL_T481L-A480G-Y397A-W163C. See the Supplementary Table 22 for detailed discussion.

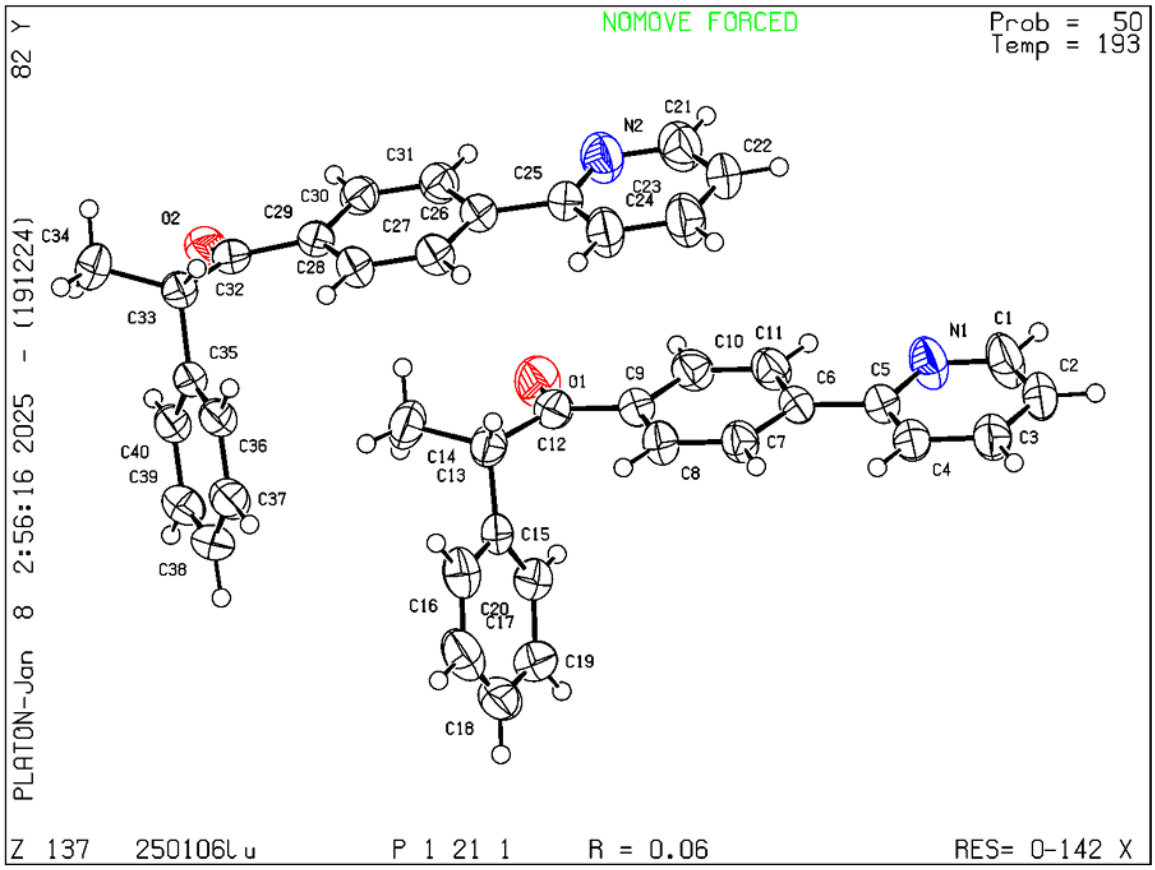

Supplementary Fig. 5 | **X-Ray diffraction data.** X-Ray diffraction data of (*S*)-**3q** (CCDC 2416063) obtained from the reactions catalysed by *Pf*BAL_T481L-A480G-Y397A-W163C. See the Supplementary Table 23 for detailed discussion.

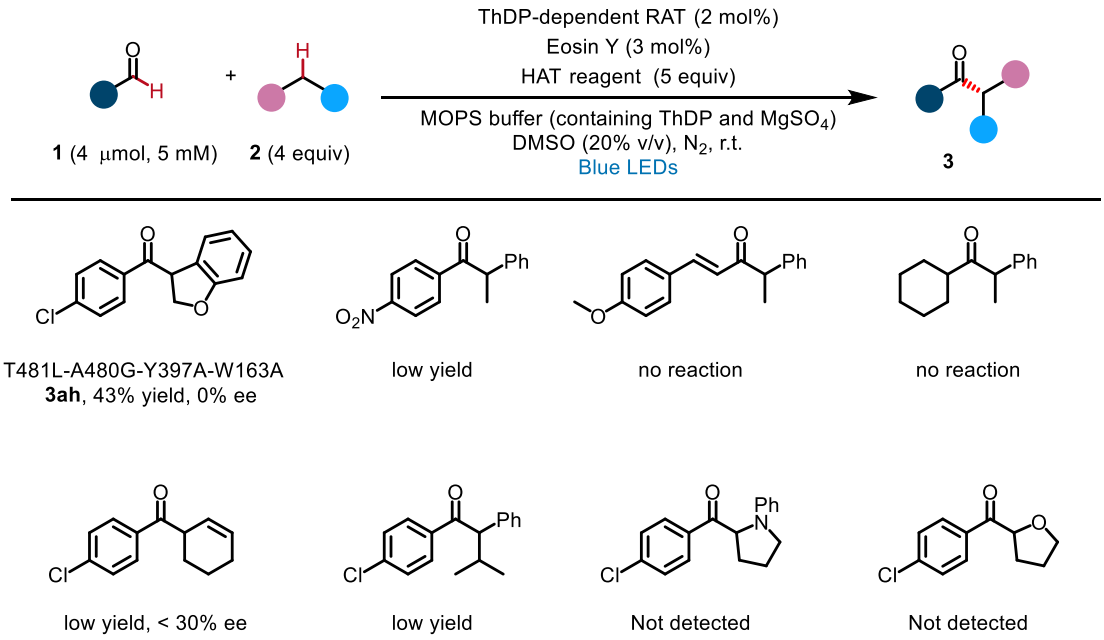

Supplementary Fig. 6 | Unsuccessful examples. Conditions: **1** (0.004 mmol), **2** (0.016 mmol), HAT reagent 2 (0.020 mmol), *Pf*BAL_T481L*;* *Pf*BAL_T481L-A480G or *Pf*BAL_T481L-A480G-Y397A-W163C (2 mol%) as biocatalysts, Eosin Y (3 mol%), 20 v/v % DMSO in 100 mM MOPS buffer (pH 8.0, containing 2.5 mM $MgSO_4$ and 0.15 mM ThDP) were stirred for 14 h at room temperature under N_2 atmosphere with the irradiation of 450-460 nm LEDs; total volume of the reaction is 0.8 mL. The reactions were detected by GC-MS.

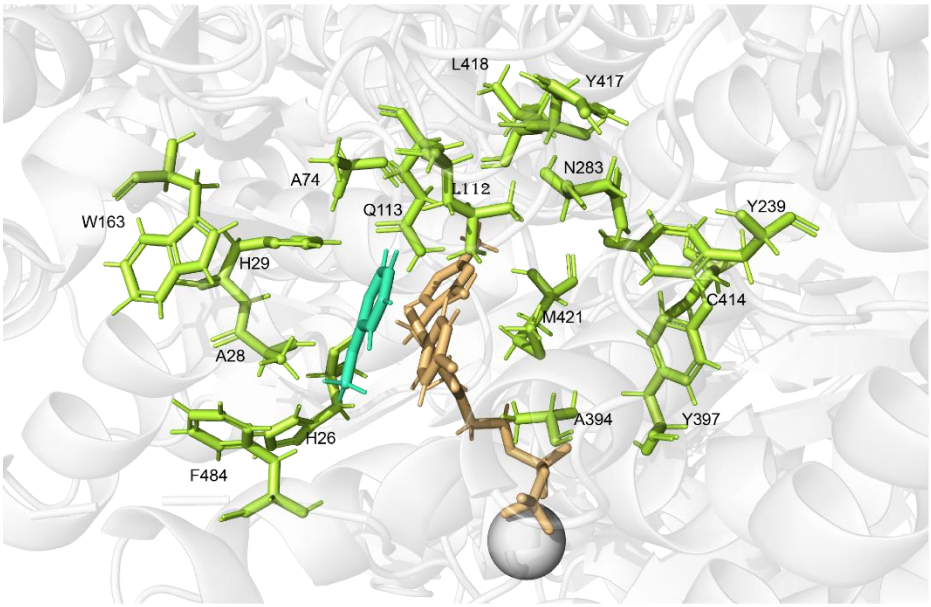

Supplementary Fig. 7 | Sites selected for evolution. Based on a MD-simulated benzylic radical within the active site of *Pf*BAL_T481L-A480G in the form of ThDP-**1a**-derived ketyl radical, sixteen residues were selected within 5 Å radius of the simulated benzylic radical intermediate.

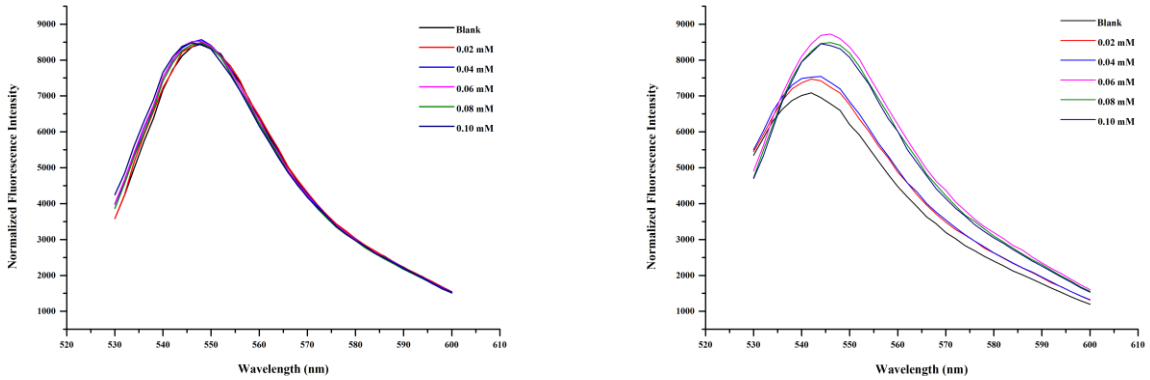

Supplementary Fig. 8 | Stern-Volmer luminescence quenching studies with different quenchers. **a**, HAT reagent 2 was used as the quencher. **b**, the mixture of **RAT$_{CH}$** and **1a** was used as the quencher. See the Method section, 6.5 Stern-Volmer Luminescence Quenching Studies, for detailed discussions.

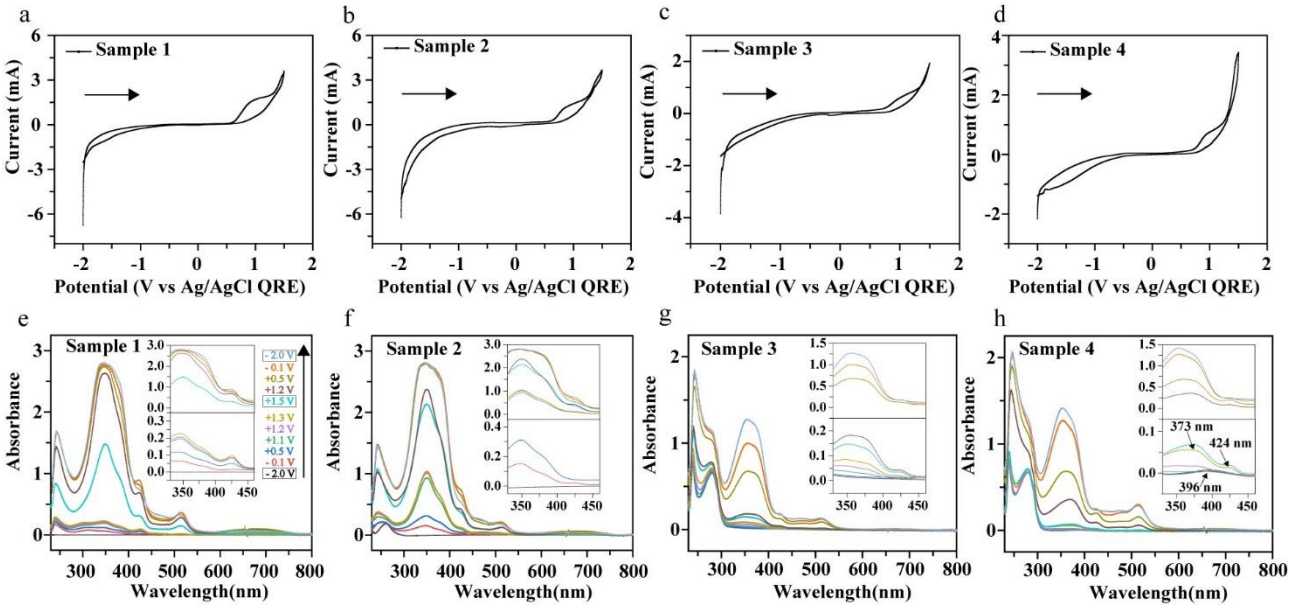

Supplementary Fig. 9 | Cyclic voltammograms of **a**, Sample 1: MOPS buffer (100 mM, pH 8.0, containing 2.5 mM $MgSO_4$ and 0.15 mM ThDP); **b**, Sample 2: MOPS buffer (100 mM, pH 8.0, containing 2.5 mM $MgSO_4$ and 0.15 mM ThDP) + 0.1 mM **1a**; **c**, Sample 3: MOPS buffer (100 mM, pH 8.0, containing 2.5 mM $MgSO_4$ and 0.15 mM ThDP) + 0.1 mM **RAT$_{CH}$**; **d**, Sample 4: MOPS buffer (100 mM, pH 8.0, containing 2.5 mM $MgSO_4$ and 0.15 mM ThDP) + 0.1 mM **1a** + 0.1 mM **RAT$_{CH}$**. Each solution was with a total volume of 0.75 mL with 20 v/v % DMSO. UV-Visible spectra of **e**, Sample 1; **f**, Sample 2; **g**, Sample 3 and **h**, Sample 4 at various potentials during CV testing. In the insets the spectra correspond to the range of 400 nm to 450 nm.

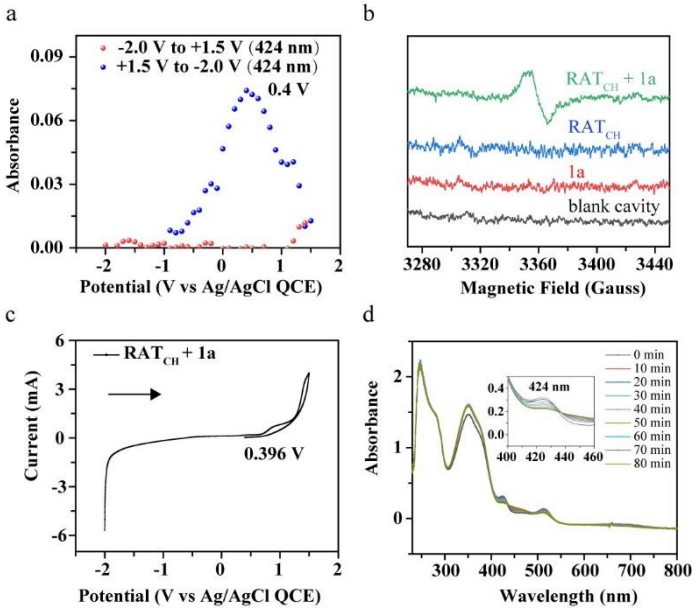

Supplementary Fig. 10 | a, In-situ UV-Vis spectroelectrochemical testing shows the variation of the UV-Vis characteristic absorption peak of Sample 4 at 424 nm with changes in potential. **b**, Low-temperature electron paramagnetic resonance (EPR) experiments. EPR experimental conditions: microwave frequency, 9.44 GHz; microwave power, 20 mW; modulation amplitude, 1.0 G; temperature, 100 K. **c**, The CV test for Sample 4 was conducted with the voltage applied until + 0.396 V was reached. **d**, After ceasing voltage application at + 0.396 V, Sample 4 exhibited radical decay. In the insets the spectra correspond to the range of 400 nm to 450 nm.

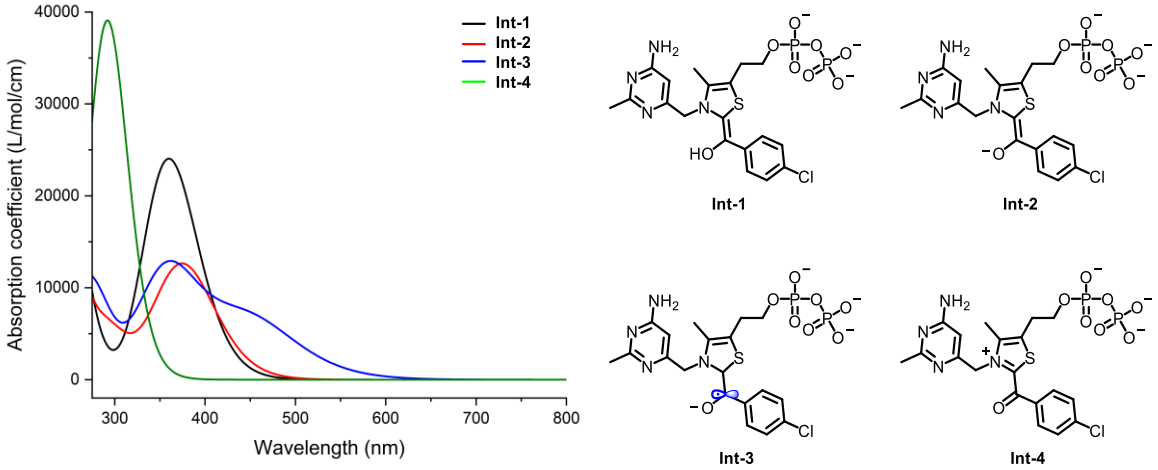

Supplementary Fig. 11 | Calculated UV-vis absorption spectra of the key intermediates. See the Method section, 7.4 Spectral Calculations for Computational Studies.

Supplementary Tables 1-25

Supplementary Table 1 | ThDP-dependent enzymes screened for enantioselective C(sp^3)–H bond radical acylation reaction. Conditions: 4-chlorobenzaldehyde **1a** (0.004 mmol), ethylbenzene **2a** (0.016 mmol), HAT reagent 1 (0.020 mmol), biocatalysts (2 mol%), Eosin Y (3 mol%), 20 v/v % DMSO in 50 mM MOPS buffer (pH 7.5, containing 2.5 mM $MgSO_4$ and 0.15 mM ThDP) were stirred for 14 h at room temperature under N_2 atmosphere with the irradiation of 530-540 nm LEDs; total volume of the reaction is 0.8 mL. The yield was determined by GC. Enantiomeric excess was determined by HPLC analysis on a chiral stationary phase. n.d. = not determined. [a]Given in numbers are NCBI accession numbers. n.a. = not applicable.

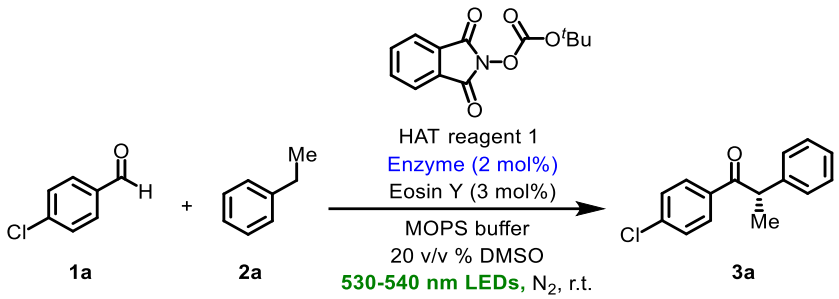

biocatalyst	accession number[a]	PDB code	yield (%)	ee (%)
*Pf*BAL	3D7K_A	3D7K	1.1	n.d.
*Pp*BFD	WP_016501746.1	1MCZ	0.6	n.d.
*Ec*MenD	WP_001295284.1	5EJ8	0	n.d.
*Ec*TK	1QGD_A	1QGD	0	n.d.
*Pa*BAL	WP_135246357.1	n.a.	0.6	n.d.
CDH	WP_169259343.1	2PGO	0	n.d.
*Ll*KdcA	QII57472.1	2VBG	0.4	n.d.
*Pf*BAL_T481L	n.a.	n.a.	2.2	n.d.
***Pf*BAL_T481L-A480G**	n.a.	n.a.	**2.5**	n.d.

Supplementary Table 2 | HAT reagents screened for enantioselective C(sp^3)–H bond radical acylation reaction. Conditions: 4-chlorobenzaldehyde **1a** (0.004 mmol), ethylbenzene **2a** (0.016 mmol), HAT reagent (0.020 mmol), *Pf*BAL_T481L-A480G (2 mol%), Eosin Y (3 mol%), 20 v/v % DMSO in 50 mM MOPS buffer (pH 7.5, containing 2.5 mM $MgSO_4$ and 0.15 mM ThDP) were stirred for 14 h at room temperature under N_2 atmosphere with the irradiation of 530-540 nm LEDs; total volume of the reaction is 0.8 mL. The yield was determined by GC. Enantiomeric excess was determined by HPLC analysis on a chiral stationary phase. n.d. = not determined.

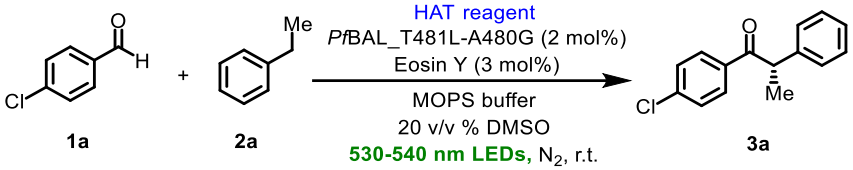

biocatalyst	yield (%)	ee (%)
HAT reagent 1	2.5	n.d.
HAT reagent 2	**24**	**92**
HAT reagent 3	15	90
HAT reagent 4	0	n.d.
HAT reagent 5	4	n.d.

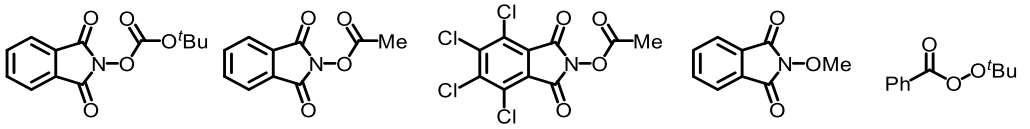

Supplementary Table 3 | Photocatalysts screened for enantioselective C(sp^3)–H bond radical acylation reaction. Conditions: 4-chlorobenzaldehyde **1a** (0.004 mmol), ethylbenzene **2a** (0.016 mmol), HAT reagent 2 (0.020 mmol), *Pf*BAL_T481L-A480G (2 mol%), Photocatalysts (X mol%), 20 v/v % DMSO in 50 mM MOPS buffer (pH 7.5, containing 2.5 mM $MgSO_4$ and 0.15 mM ThDP) were stirred for 14 h at room temperature under N_2 atmosphere with the irradiation of LEDs (PC 1, 530-540 nm or 450-460 nm; PC 2, PC 5, PC 6, 450-460 nm; PC 3, PC 4, 420-430 nm); total volume of the reaction is 0.8 mL. The yield was determined by GC. Enantiomeric excess was determined by HPLC analysis on a chiral stationary phase. n.d. = not determined.

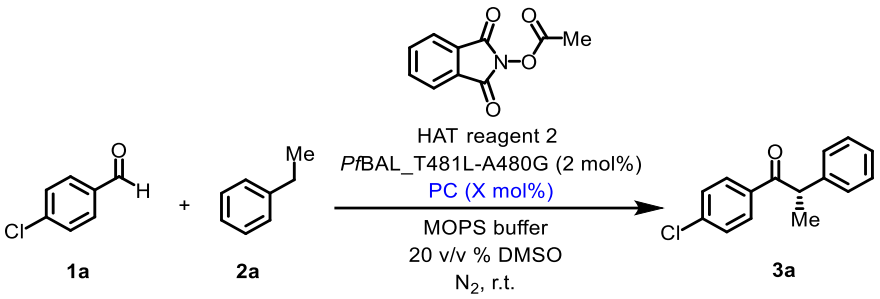

photocatalysts	LEDs wavelength	yield (%)	ee (%)
PC 1 (3 mol%)	530-540 nm	24	92
PC 1 (3 mol%)	**450-460 nm**	**26**	**92**
PC 2 (1 mol%)	450-460 nm	11	88
PC 3 (1 mol%)	420-430 nm	7	91
PC 4 (1 mol%)	420-430 nm	10	87
PC 5 (3 mol%)	450-460 nm	16	90
PC 6 (3 mol%)	450-460 nm	1	n.d.

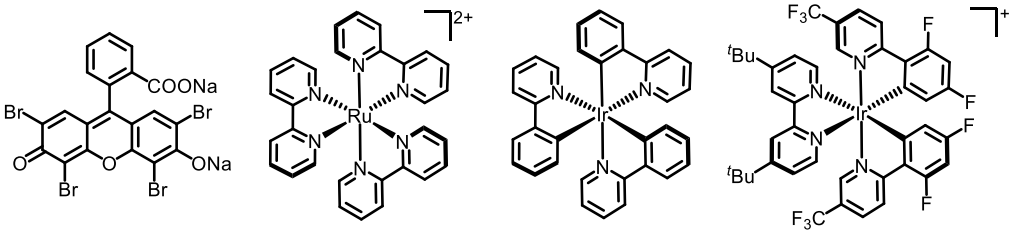

Eosin Y
PC 1

$[Ru(bpy)_3]Cl_2$
PC 2

$Ir(bpy)_3$
PC 3

$Ir[dF(CF_3)ppy]_2(dtbbpy)PF_6$
PC 4

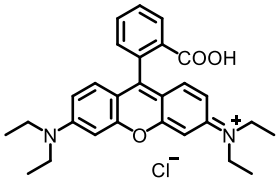

Rhodamine B
PC 5

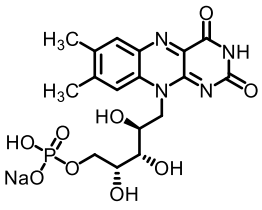

FMN-Na
PC 6

Supplementary Table 4 | The results of glycine scanning. Conditions: 4-chlorobenzaldehyde **1a** (0.004 mmol), ethylbenzene **2a** (0.016 mmol), HAT reagent 2 (0.020 mmol), mutants (2 mol%), Eosin Y (3 mol%), 20 v/v % DMSO in 50 mM MOPS buffer (pH 7.5, containing 2.5 mM $MgSO_4$ and 0.15 mM ThDP) were stirred for 14 h at room temperature under N_2 atmosphere with the irradiation of 450-460 nm LEDs; total volume of the reaction is 0.8 mL. The yield was determined by GC. Enantiomeric excess was determined by HPLC analysis on a chiral stationary phase. n.d. = not determined.

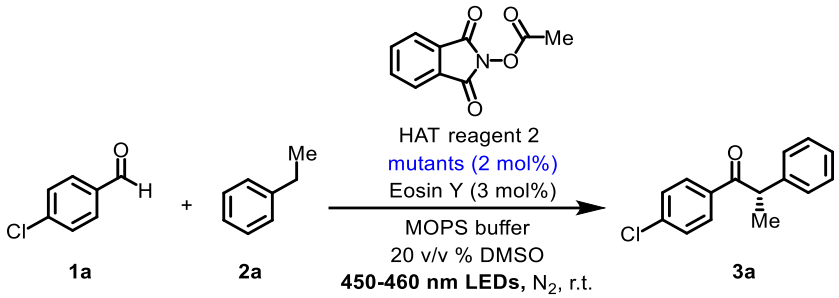

mutants	yield (%)	ee (%)
*Pf*BAL_T481L-A480G-H26G	2	n.d.
*Pf*BAL_T481L-A480G-A28G	6	71
*Pf*BAL_T481L-A480G-H29G	1	n.d.
*Pf*BAL_T481L-A480G-A74G	3	n.d.
*Pf*BAL_T481L-A480G-L112G	6	75
*Pf*BAL_T481L-A480G-Q113G	4	n.d.
*Pf*BAL_T481L-A480G-W163G	10	90
*Pf*BAL_T481L-A480G-Y239G	27	88
*Pf*BAL_T481L-A480G-N283G	17	89
*Pf*BAL_T481L-A480G-A394G	5	n.d.
*Pf*BAL_T481L-A480G-Y397G	36	89
*Pf*BAL_T481L-A480G-C414G	18	88
*Pf*BAL_T481L-A480G-Y417G	2	n.d.
*Pf*BAL_T481L-A480G-L418G	1	n.d.
*Pf*BAL_T481L-A480G-M421G	1	n.d.
*Pf*BAL_T481L-A480G-F484G	0	n.d.

Supplementary Table 5 | Saturation mutagenesis on site 397. Conditions: 4-chlorobenzaldehyde **1a** (0.004 mmol), ethylbenzene **2a** (0.016 mmol), HAT reagent 2 (0.020 mmol), mutants (2 mol%), Eosin Y (3 mol%), 20 v/v % DMSO in 50 mM MOPS buffer (pH 7.5, containing 2.5 mM $MgSO_4$ and 0.15 mM ThDP) were stirred for 14 h at room temperature under N_2 atmosphere with the irradiation of 450-460 nm LEDs; total volume of the reaction is 0.8 mL. The yield was determined by GC. Enantiomeric excess was determined by HPLC analysis on a chiral stationary phase.

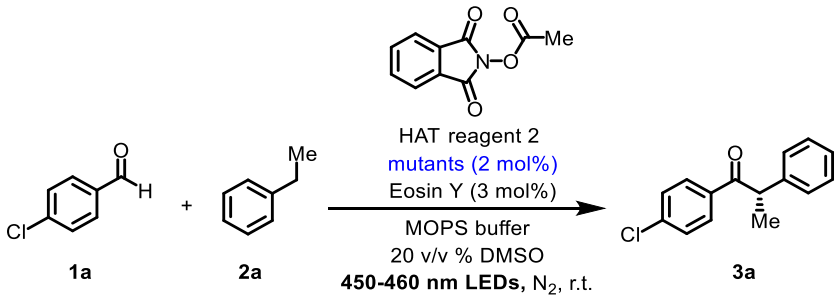

mutants	yield (%)	ee (%)
*Pf*BAL_T481L-A480G-Y397G	36	89
***Pf*BAL_T481L-A480G-Y397A**	**40**	**93**
*Pf*BAL_T481L-A480G-Y397V	23	90
*Pf*BAL_T481L-A480G-Y397I	25	87
*Pf*BAL_T481L-A480G-Y397T	21	88
*Pf*BAL_T481L-A480G-Y397L	22	89
*Pf*BAL_T481L-A480G-Y397P	28	89
*Pf*BAL_T481L-A480G-Y397K	27	86
*Pf*BAL_T481L-A480G-Y397F	32	86
*Pf*BAL_T481L-A480G-Y397W	30	91
*Pf*BAL_T481L-A480G-Y397D	18	88
*Pf*BAL_T481L-A480G-Y397N	18	89
*Pf*BAL_T481L-A480G-Y397R	30	81
*Pf*BAL_T481L-A480G-Y397E	25	94
*Pf*BAL_T481L-A480G-Y397Q	17	92
*Pf*BAL_T481L-A480G-Y397H	24	91
*Pf*BAL_T481L-A480G-Y397M	24	89

Supplementary Table 6 | Saturation mutagenesis on site 163. Conditions: 4-chlorobenzaldehyde **1a** (0.004 mmol), ethylbenzene **2a** (0.016 mmol), HAT reagent 2 (0.020 mmol), mutants (2 mol%), Eosin Y (3 mol%), 20 v/v % DMSO in 50 mM MOPS buffer (pH 7.5, containing 2.5 mM $MgSO_4$ and 0.15 mM ThDP) were stirred for 14 h at room temperature under N_2 atmosphere with the irradiation of 450-460 nm LEDs; total volume of the reaction is 0.8 mL. The yield was determined by GC. Enantiomeric excess was determined by HPLC analysis on a chiral stationary phase. n.d. = not determined.

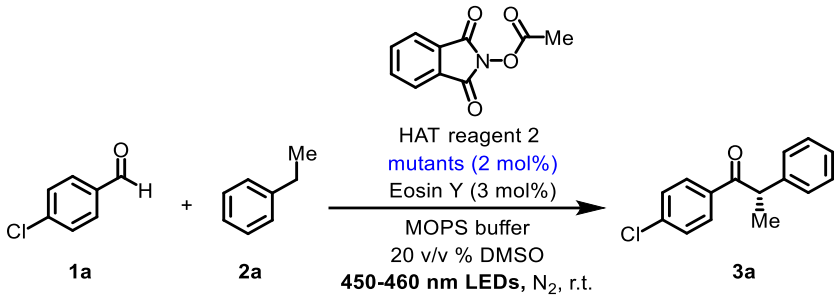

mutants	yield (%)	ee (%)
*Pf*BAL_T481L-A480G-W163S	24	91
*Pf*BAL_T481L-A480G-W163M	22	89
*Pf*BAL_T481L-A480G-W163E	28	92
*Pf*BAL_T481L-A480G-W163T	21	89
*Pf*BAL_T481L-A480G-W163C	34	90
*Pf*BAL_T481L-A480G-W163Q	23	91
*Pf*BAL_T481L-A480G-W163P	17	87
*Pf*BAL_T481L-A480G-W163D	2	n.d.
*Pf*BAL_T481L-A480G-W163K	23	90
*Pf*BAL_T481L-A480G-W163N	23	92
*Pf*BAL_T481L-A480G-W163A	41	90
*Pf*BAL_T481L-A480G-W163L	32	84
*Pf*BAL_T481L-A480G-W163V	39	92
*Pf*BAL_T481L-A480G-W163F	21	93
*Pf*BAL_T481L-A480G-W163Y	23	90
*Pf*BAL_T481L-A480G-W163H	19	89

Supplementary Table 7 | Mutagenesis on site 283. Conditions: 4-chlorobenzaldehyde **1a** (0.004 mmol), ethylbenzene **2a** (0.016 mmol), HAT reagent 2 (0.020 mmol), mutants (2 mol%), Eosin Y (3 mol%), 20 v/v % DMSO in 50 mM MOPS buffer (pH 7.5, containing 2.5 mM $MgSO_4$ and 0.15 mM ThDP) were stirred for 14 h at room temperature under N_2 atmosphere with the irradiation of 450-460 nm LEDs; total volume of the reaction is 0.8 mL. The yield was determined by GC. Enantiomeric excess was determined by HPLC analysis on a chiral stationary phase. n.d. = not determined.

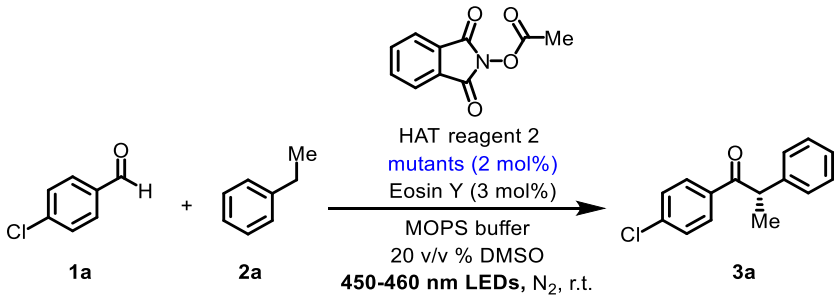

mutants	yield (%)	ee (%)
*Pf*BAL_T481L-A480G-N283V	8	n.d.
*Pf*BAL_T481L-A480G-N283G	17	89
*Pf*BAL_T481L-A480G-N283I	6	n.d.
*Pf*BAL_T481L-A480G-N283L	12	86
*Pf*BAL_T481L-A480G-N283W	26	86
*Pf*BAL_T481L-A480G-N283M	23	91
*Pf*BAL_T481L-A480G-N283D	17	85
*Pf*BAL_T481L-A480G-N283E	23	89
*Pf*BAL_T481L-A480G-N283Q	17	89
*Pf*BAL_T481L-A480G-N283H	16	84
*Pf*BAL_T481L-A480G-N283C	22	88
*Pf*BAL_T481L-A480G-N283T	20	88

Supplementary Table 8 | Site-specific mutagenesis on sites 113/239/26/414. Conditions: 4-chlorobenzaldehyde **1a** (0.004 mmol), ethylbenzene **2a** (0.016 mmol), HAT reagent 2 (0.020 mmol), mutants (2 mol%), Eosin Y (3 mol%), 20 v/v % DMSO in 50 mM MOPS buffer (pH 7.5, containing 2.5 mM $MgSO_4$ and 0.15 mM ThDP) were stirred for 14 h at room temperature under N_2 atmosphere with the irradiation of 450-460 nm LEDs; total volume of the reaction is 0.8 mL. The yield was determined by GC. Enantiomeric excess was determined by HPLC analysis on a chiral stationary phase. n.d. = not determined.

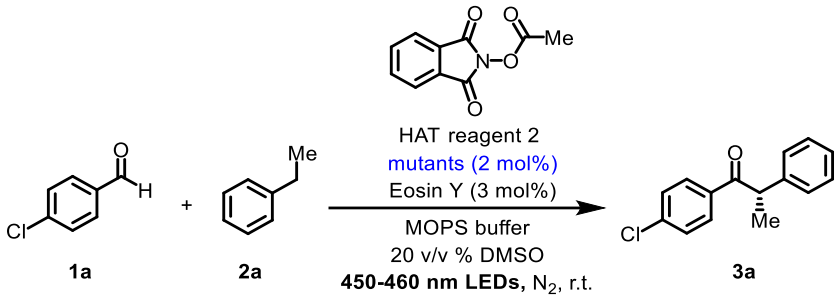

mutants	yield (%)	ee (%)
*Pf*BAL_T481L-A480G-Q113I	0	n.d.
*Pf*BAL_T481L-A480G-Q113A	0	n.d.
*Pf*BAL_T481L-A480G-Q113V	0	n.d.
*Pf*BAL_T481L-A480G-Q113L	9	77
*Pf*BAL_T481L-A480G-Y239L	7	80
*Pf*BAL_T481L-A480G-Y239T	31	83
*Pf*BAL_T481L-A480G-Y239C	16	79
*Pf*BAL_T481L-A480G-Y239F	29	92
*Pf*BAL_T481L-A480G-Y239V	17	88
*Pf*BAL_T481L-A480G-H26A	30	93
*Pf*BAL_T481L-A480G-H26L	25	92
*Pf*BAL_T481L-A480G-H26F	18	87
*Pf*BAL_T481L-A480G-H26Q	36	94
*Pf*BAL_T481L-A480G-C414A	18	89
*Pf*BAL_T481L-A480G-C414L	4	n.d.
*Pf*BAL_T481L-A480G-C414F	0	n.d.
*Pf*BAL_T481L-A480G-C414I	0	n.d.

Supplementary Table 9 | Saturation mutagenesis on site 26 using *Pf*BAL_T481L-A480G-Y397A as the parent. Conditions: 4-chlorobenzaldehyde **1a** (0.004 mmol), ethylbenzene **2a** (0.016 mmol), HAT reagent 2 (0.020 mmol), mutants (2 mol%), Eosin Y (3 mol%), 20 v/v % DMSO in 50 mM MOPS buffer (pH 7.5, containing 2.5 mM $MgSO_4$ and 0.15 mM ThDP) were stirred for 14 h at room temperature under N_2 atmosphere with the irradiation of 450-460 nm LEDs; total volume of the reaction is 0.8 mL. The yield was determined by GC. Enantiomeric excess was determined by HPLC analysis on a chiral stationary phase. n.d. = not determined.

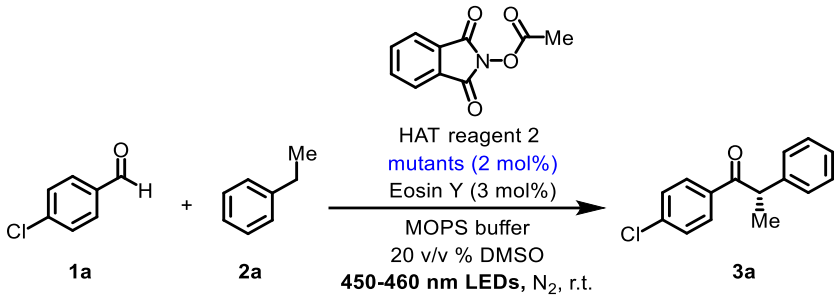

mutants	yield (%)	ee (%)
*Pf*BAL_T481L-A480G-Y397A-H26T	24	91
*Pf*BAL_T481L-A480G-Y397A-H26E	26	95
*Pf*BAL_T481L-A480G-Y397A-H26R	10	95
*Pf*BAL_T481L-A480G-Y397A-H26N	4	n.d.
*Pf*BAL_T481L-A480G-Y397A-H26L	22	95
*Pf*BAL_T481L-A480G-Y397A-H26A	15	95
*Pf*BAL_T481L-A480G-Y397A-H26Q	33	68
*Pf*BAL_T481L-A480G-Y397A-H26F	11	92
*Pf*BAL_T481L-A480G-Y397A-H26I	17	92
*Pf*BAL_T481L-A480G-Y397A-H26S	23	95
*Pf*BAL_T481L-A480G-Y397A-H26K	5	n.d.
*Pf*BAL_T481L-A480G-Y397A-H26M	2	n.d.
*Pf*BAL_T481L-A480G-Y397A-H26P	9	91
*Pf*BAL_T481L-A480G-Y397A-H26D	2	n.d.
*Pf*BAL_T481L-A480G-Y397A-H26G	5	n.d.
*Pf*BAL_T481L-A480G-Y397A-H26W	2	n.d.
*Pf*BAL_T481L-A480G-Y397A-H26C	15	93
*Pf*BAL_T481L-A480G-Y397A-H26V	13	94

Supplementary Table 10 | Saturation mutagenesis on site 163 using *Pf*BAL_T481L-A480G-Y397G as the parent. Conditions: 4-chlorobenzaldehyde **1a** (0.004 mmol), ethylbenzene **2a** (0.016 mmol), HAT reagent 2 (0.020 mmol), mutants (2 mol%), Eosin Y (3 mol%), 20 v/v % DMSO in 50 mM MOPS buffer (pH 7.5, containing 2.5 mM $MgSO_4$ and 0.15 mM ThDP) were stirred for 14 h at room temperature under N_2 atmosphere with the irradiation of 450-460 nm LEDs; total volume of the reaction is 0.8 mL. The yield was determined by GC. Enantiomeric excess was determined by HPLC analysis on a chiral stationary phase. n.d. = not determined.

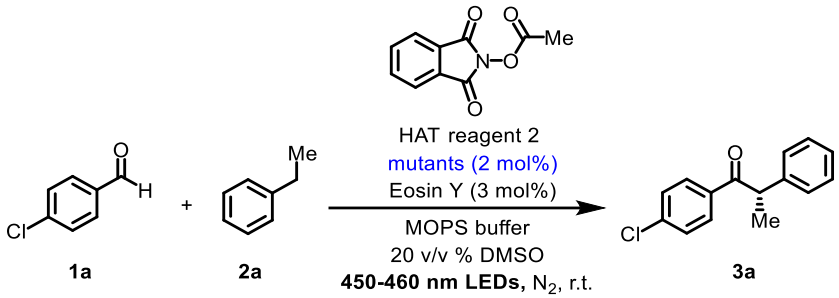

mutants	yield (%)	ee (%)
*Pf*BAL_T481L-A480G-Y397G-W163K	43	91
*Pf*BAL_T481L-A480G-Y397G-W163A	44	91
*Pf*BAL_T481L-A480G-Y397G-W163V	41	93
*Pf*BAL_T481L-A480G-Y397G-W163F	41	93
*Pf*BAL_T481L-A480G- Y397G-W163D	2	n.d.
*Pf*BAL_T481L-A480G-Y397G-W163N	27	90
*Pf*BAL_T481L-A480G-Y397G-W163H	30	91
*Pf*BAL_T481L-A480G-Y397G-W163S	29	87
*Pf*BAL_T481L-A480G-Y397G-W163P	5	n.d.
*Pf*BAL_T481L-A480G-Y397G-W163I	32	91
*Pf*BAL_T481L-A480G-Y397G-W163M	27	86
*Pf*BAL_T481L-A480G-Y397G-W163C	27	86
*Pf*BAL_T481L-A480G-Y397G-W163L	21	91
*Pf*BAL_T481L-A480G-Y397G-W163Y	26	86
*Pf*BAL_T481L-A480G- Y397G-W163G	25	89
*Pf*BAL_T481L-A480G- Y397G-W163T	28	88
*Pf*BAL_T481L-A480G- Y397G-W163Q	24	88

Supplementary Table 11 | Saturation mutagenesis on site 163 using *Pf*BAL_T481L-A480G-Y397A as the parent. Conditions: 4-chlorobenzaldehyde **1a** (0.004 mmol), ethylbenzene **2a** (0.016 mmol), HAT reagent 2 (0.020 mmol), mutants (2 mol%), Eosin Y (3 mol%), 20 v/v % DMSO in 50 mM MOPS buffer (pH 7.5, containing 2.5 mM $MgSO_4$ and 0.15 mM ThDP) were stirred for 14 h at room temperature under N_2 atmosphere with the irradiation of 450-460 nm LEDs; total volume of the reaction is 0.8 mL. The yield was determined by GC. Enantiomeric excess was determined by HPLC analysis on a chiral stationary phase.

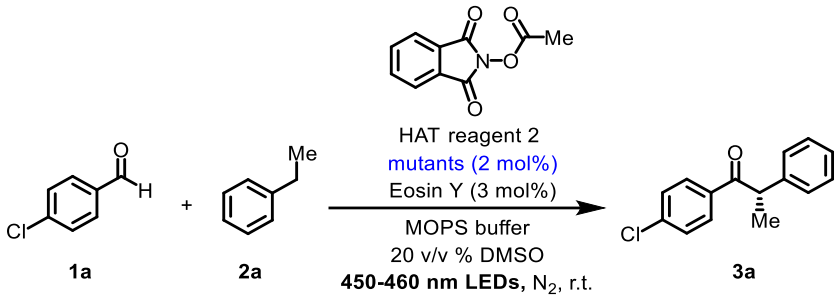

mutants	yield (%)	ee (%)
*Pf*BAL_T481L-A480G-Y397A-W163K	46	94
*Pf*BAL_T481L-A480G-Y397A-W163M	36	94
*Pf*BAL_T481L-A480G-Y397A-W163E	30	93
*Pf*BAL_T481L-A480G-Y397A-W163R	36	92
*Pf*BAL_T481L-A480G-Y397A-W163N	32	94
*Pf*BAL_T481L-A480G-Y397A-W163Q	37	93
*Pf*BAL_T481L-A480G-Y397A-W163P	21	90
*Pf*BAL_T481L-A480G-Y397A-W163F	38	94
*Pf*BAL_T481L-A480G-Y397A-W163L	40	95
*Pf*BAL_T481L-A480G-Y397A-W163G	36	93
*Pf*BAL_T481L-A480G-Y397A-W163S	36	94
*Pf*BAL_T481L-A480G-Y397A-W163I	35	93
*Pf*BAL_T481L-A480G-Y397A-W163H	34	93
***Pf*BAL_T481L-A480G-Y397A-W163C**	**52**	**94**
*Pf*BAL_T481L-A480G-Y397A-W163A	34	93
*Pf*BAL_T481L-A480G-Y397A-W163V	44	95

Supplementary Table 12 | Optimization of the ratio of co-solvent DMSO. Conditions: 4-chlorobenzaldehyde **1a** (0.004 mmol), ethylbenzene **2a** (0.016 mmol), HAT reagent 2 (0.020 mmol), *Pf*BAL_T481L-A480G-Y397A-W163C (2 mol%), Eosin Y (3 mol%), X v/v % DMSO in 50 mM MOPS buffer (pH 7.5, containing 2.5 mM $MgSO_4$ and 0.15 mM ThDP) were stirred for 14 h at room temperature under N_2 atmosphere with the irradiation of 450-460 nm LEDs; total volume of the reaction is 0.8 mL. The yield was determined by GC.

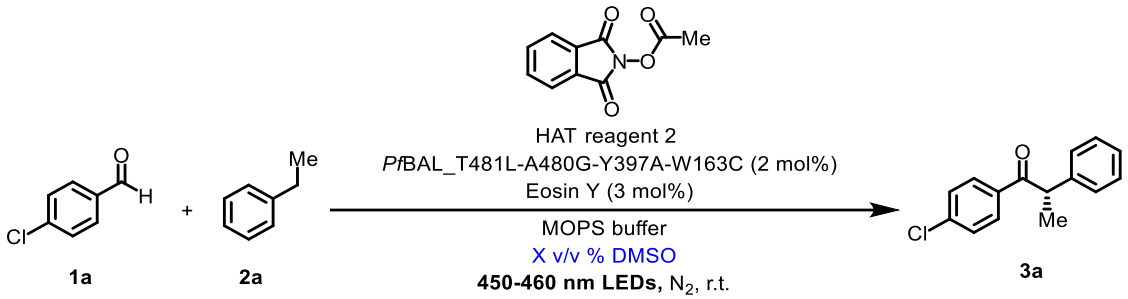

DMSO (X v/v %)	yield (%)
10	42
15	50
20	**52**
25	50
30	46

Supplementary Table 13 | Optimization of MOPS concentration. Conditions: 4-chlorobenzaldehyde **1a** (0.004 mmol), ethylbenzene **2a** (0.016 mmol), HAT reagent 2 (0.020 mmol), *Pf*BAL_T481L-A480G-Y397A-W163C (2 mol%), Eosin Y (3 mol%), 20 v/v % DMSO in MOPS buffer (pH 7.5, containing 2.5 mM $MgSO_4$ and 0.15 mM ThDP) were stirred for 14 h at room temperature under N_2 atmosphere with the irradiation of 450-460 nm LEDs; total volume of the reaction is 0.8 mL. The yield was determined by GC.

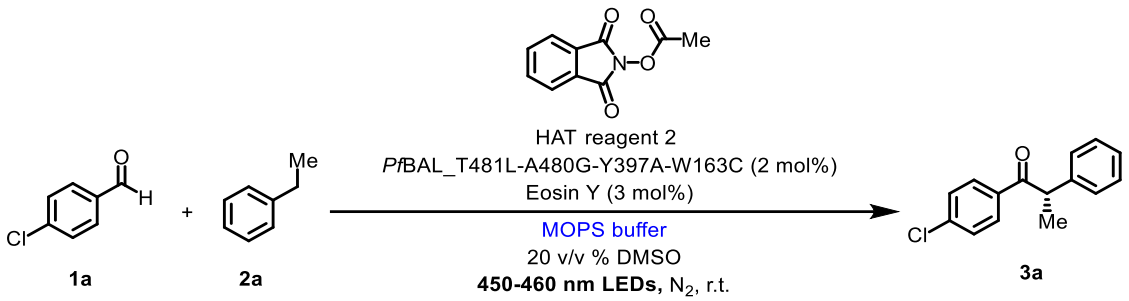

MOPS (mM)	yield (%)
25	46
50	52
75	53
100	**56**
125	54
150	43

Supplementary Table 14 | Optimization of the amount of ThDP. Conditions: 4-chlorobenzaldehyde **1a** (0.004 mmol), ethylbenzene **2a** (0.016 mmol), HAT reagent 2 (0.020 mmol), *Pf*BAL_T481L-A480G-Y397A-W163C (2 mol%), Eosin Y (3 mol%), 20 v/v % DMSO in 100 mM MOPS buffer (pH 7.5, containing 2.5 mM $MgSO_4$ and X mM ThDP) were stirred for 14 h at room temperature under N_2 atmosphere with the irradiation of 450-460 nm LEDs; total volume of the reaction is 0.8 mL. The yield was determined by GC.

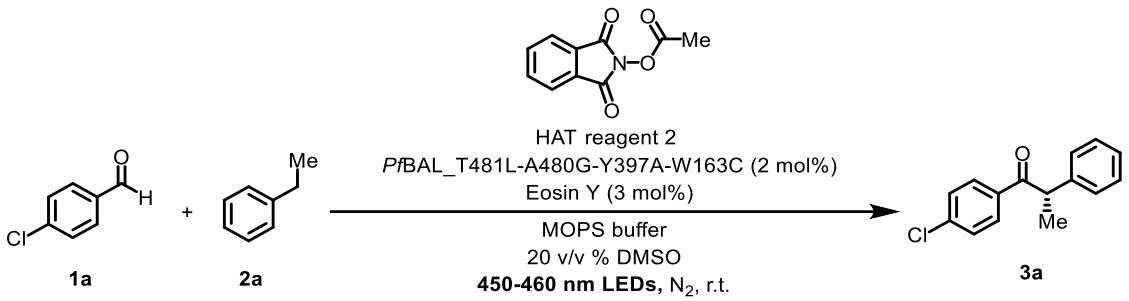

ThDP (mM)	yield (%)
0.125	49
0.15	**56**
0.175	57
0.20	50

Supplementary Table 15 | Optimization of the reaction volume. Conditions: 4-chlorobenzaldehyde **1a** (0.004 mmol), ethylbenzene **2a** (0.016 mmol), HAT reagent 2 (0.020 mmol), *Pf*BAL_T481L-A480G-Y397A-W163C (2 mol%), Eosin Y (3 mol%), 20 v/v % DMSO in 100 mM MOPS buffer (pH 7.5, containing 2.5 mM $MgSO_4$ and 0.15 mM ThDP) were stirred for 14 h at room temperature under N_2 atmosphere with the irradiation of 450-460 nm LEDs; total volume of the reaction is X µL. The yield was determined by GC.

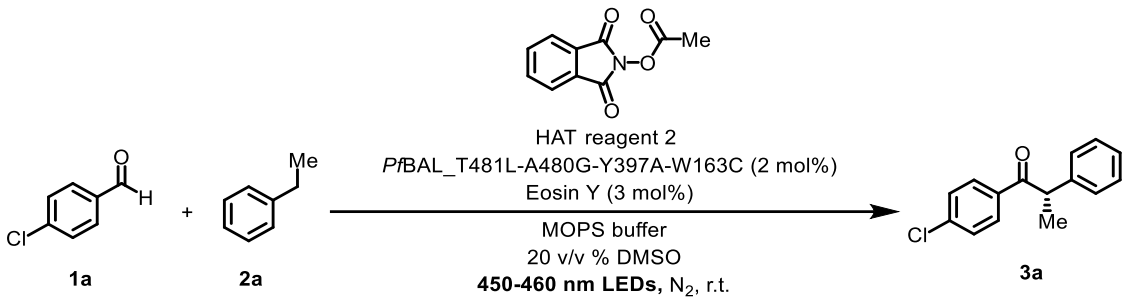

volume (µL)	yield (%)
600	27
800	**56**
1000	50
1500	37
2000	24

Supplementary Table 16 | Optimization of the pH. Conditions: 4-chlorobenzaldehyde **1a** (0.004 mmol), ethylbenzene **2a** (0.016 mmol), HAT reagent 2 (0.020 mmol), *Pf*BAL_T481L-A480G-Y397A-W163C (2 mol%), Eosin Y (3 mol%), 20 v/v % DMSO in 100 mM MOPS buffer (containing 2.5 mM $MgSO_4$ and 0.15 mM ThDP) were stirred for 14 h at room temperature under N_2 atmosphere with the irradiation of 450-460 nm LEDs; total volume of the reaction is 0.8 mL. The yield was determined by GC.

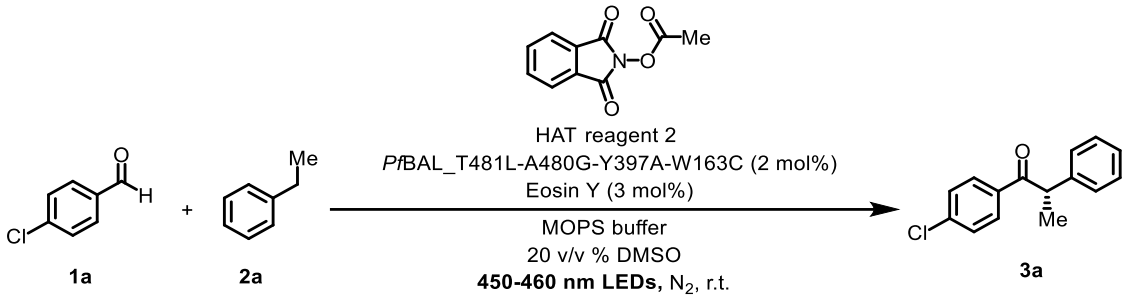

pH	yield (%)
6.5	48
7.25	56
7.5	56
7.75	60
8.0	**61**
8.25	29
8.5	24

Supplementary Table 17 | Optimization of the equiv of HAT reagent 2. Conditions: 4-chlorobenzaldehyde **1a** (0.004 mmol), ethylbenzene **2a** (0.016 mmol), HAT reagent 2 (X equiv), *Pf*BAL_T481L-A480G-Y397A-W163C (2 mol%), Eosin Y (3 mol%), 20 v/v % DMSO in 100 mM MOPS buffer (containing 2.5 mM $MgSO_4$ and 0.15 mM ThDP) were stirred for 14 h at room temperature under N_2 atmosphere with the irradiation of 450-460 nm LEDs; total volume of the reaction is 0.8 mL. The yield was determined by GC.

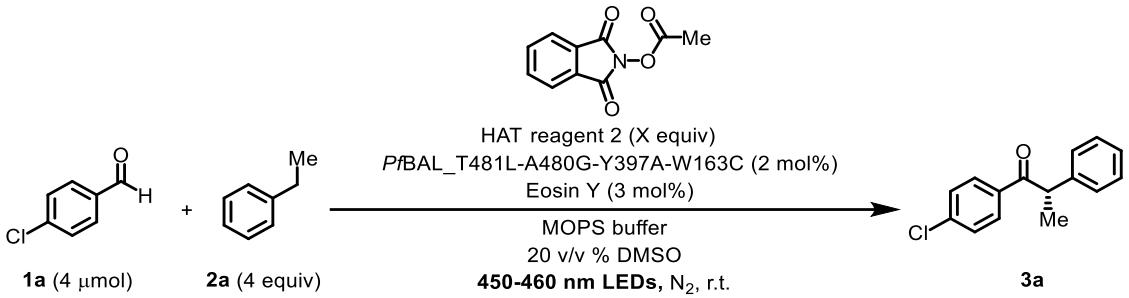

HAT reagent 2 (equiv)	yield (%)
1.0	18
2.0	41
3.0	53
4.0	55
5.0	**61**

Supplementary Table 18 | Optimization of the equiv of ethylbenzene. Conditions: 4-chlorobenzaldehyde **1a** (0.004 mmol), ethylbenzene **2a** (X equiv), HAT reagent 2 (0.020 mmol), *Pf*BAL_T481L-A480G-Y397A-W163C (2 mol%), Eosin Y (3 mol%), 20 v/v % DMSO in 100 mM MOPS buffer (containing 2.5 mM $MgSO_4$ and 0.15 mM ThDP) were stirred for 14 h at room temperature under N_2 atmosphere with the irradiation of 450-460 nm LEDs; total volume of the reaction is 0.8 mL. The yield was determined by GC.

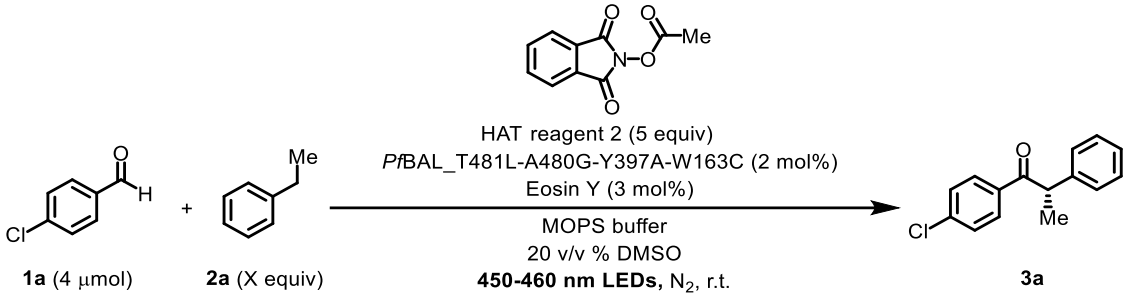

2a (equiv)	yield (%)
1.0	10
2.0	45
3.0	52
4.0	**61**
5.0	53

Supplementary Table 19 | The control experiments. Standard conditions: 4-chlorobenzaldehyde **1a** (0.004 mmol), ethylbenzene **2a** (0.016 mmol), HAT reagent 2 (0.020 mmol), *Pf*BAL_T481L-A480G-Y397A-W163C (2 mol%), Eosin Y (3 mol%), 20 v/v % DMSO in 100 mM MOPS buffer (pH 8.0, containing 2.5 mM $MgSO_4$ and 0.15 mM ThDP) were stirred for 14 h at room temperature under N_2 atmosphere with the irradiation of 450-460 nm LEDs; total volume of the reaction is 0.8 mL. The yield was determined by GC. n.a. = not applicable; n.d. = not determined.

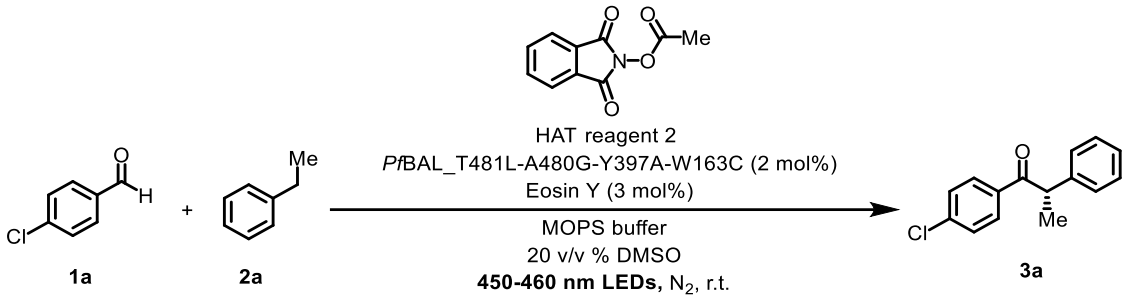

control experiment	yield (%)	ee (%)
Standard	61	94
No light	0	n.a.
No Eosin Y	0	n.a.
No HAT reagent	0	n.a.
Under air	9	n.d.
No ThDP	0	n.a.
No *Pf*BAL_T481L-A480G-Y397A-W163C	0	n.a.

Supplementary Table 20 | Mass balance of the model reaction. Standard conditions: 4-chlorobenzaldehyde **1a** (0.004 mmol), ethylbenzene **2a** (0.016 mmol), HAT reagent 2 (0.020 mmol), *Pf*BAL_T481L-A480G-Y397A-W163C (2 mol%), Eosin Y (3 mol%), 20 v/v % DMSO in 100 mM MOPS buffer (pH 8.0, containing 2.5 mM $MgSO_4$ and 0.15 mM ThDP) were stirred for 14 h at room temperature under N_2 atmosphere with the irradiation of 450-460 nm LEDs; total volume of the reaction is 0.8 mL. The yield was determined by LC and referred to **1a**.

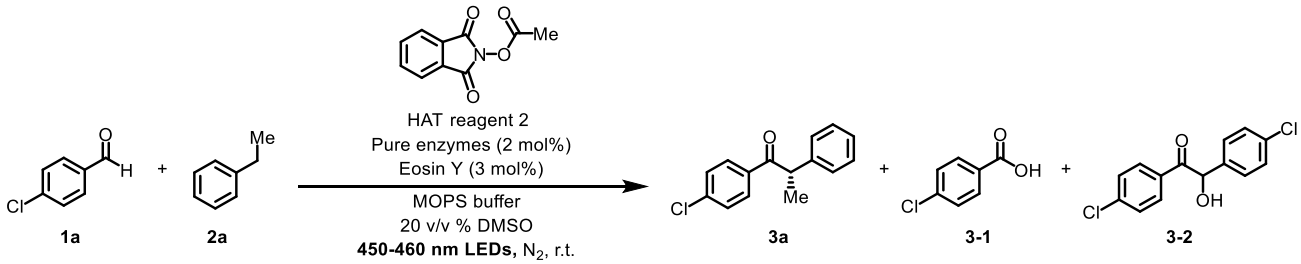

Enzyme (2 mol%)	**1a (%) remained**	**yield of 3a (%) ee in parenthesis**	**yield of 3-1 (%)**	**yield of 3-2 (%)**
*Pf*BAL	11	13 (19% ee)	21	51
*Pf*BAL_T481L	5	28 (78% ee)	34	7
*Pf*BAL_T481L-A480G	9	19 (92% ee)	26	30
*Pf*BAL_T481L-A480G-Y397A	3	40 (93% ee)	32	11
*Pf*BAL_T481L-A480G-Y397A-W163C	3	63 (61% GC yield, 94% ee)	27	5

LC calibration curve for **1a** is displayed below.

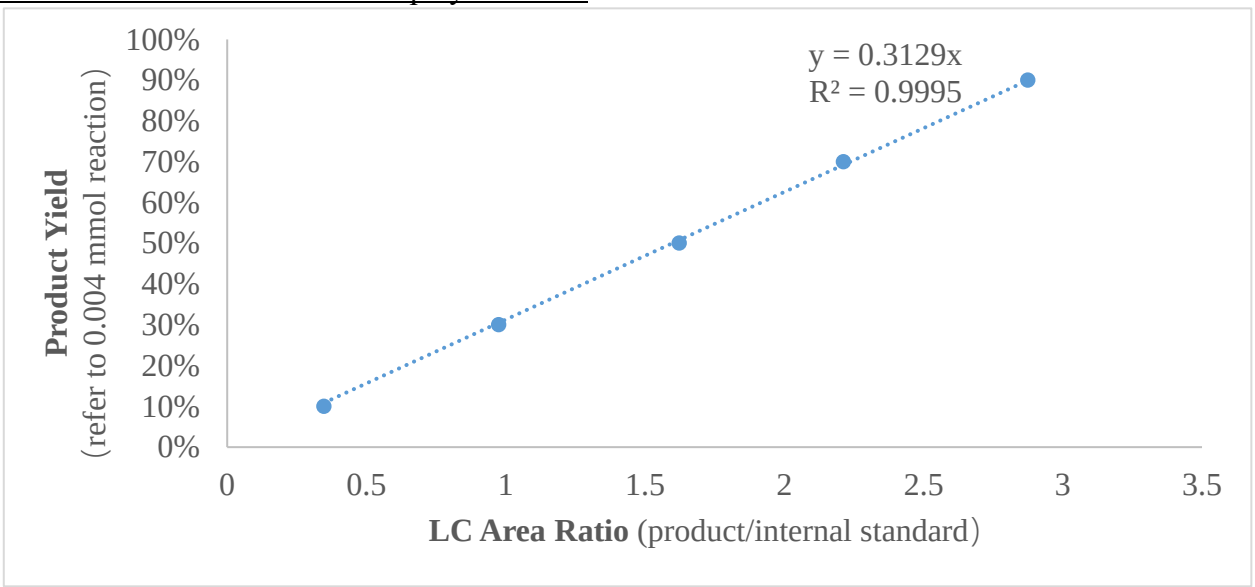

LC calibration curve for **3a** is displayed below.

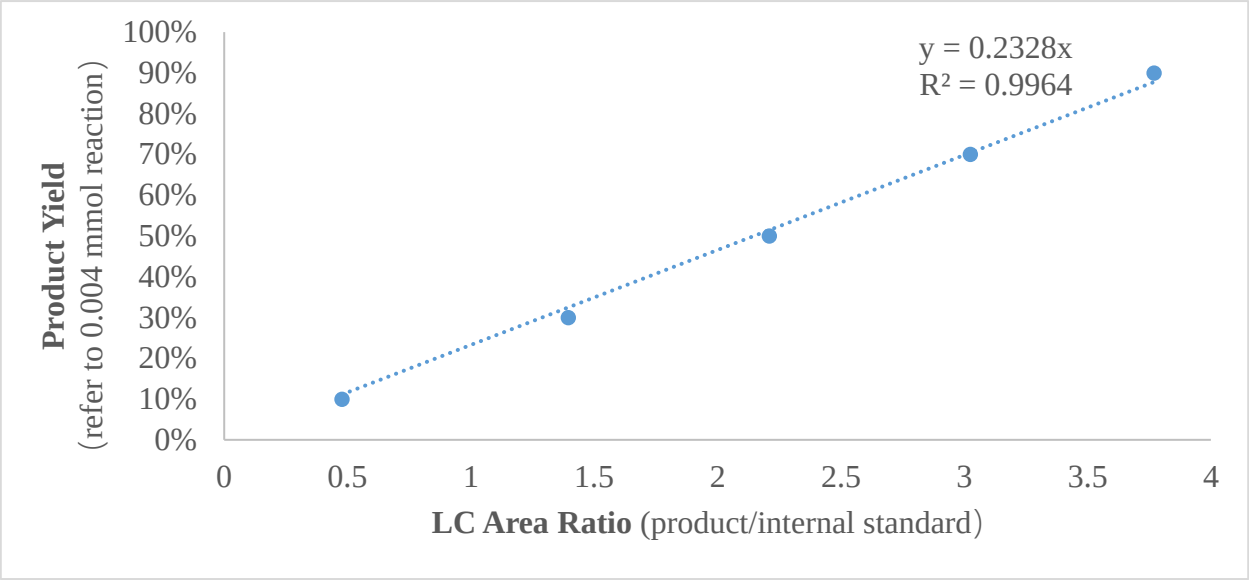

LC calibration curve for **3-1** is displayed below.

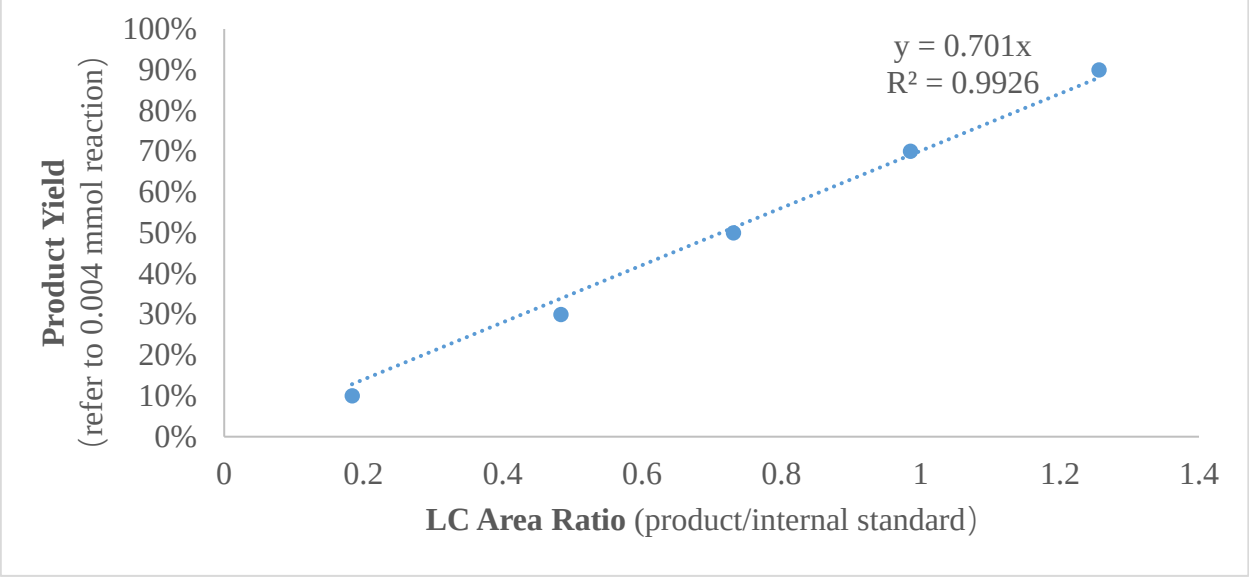

LC calibration curve for **3-2** is displayed below.

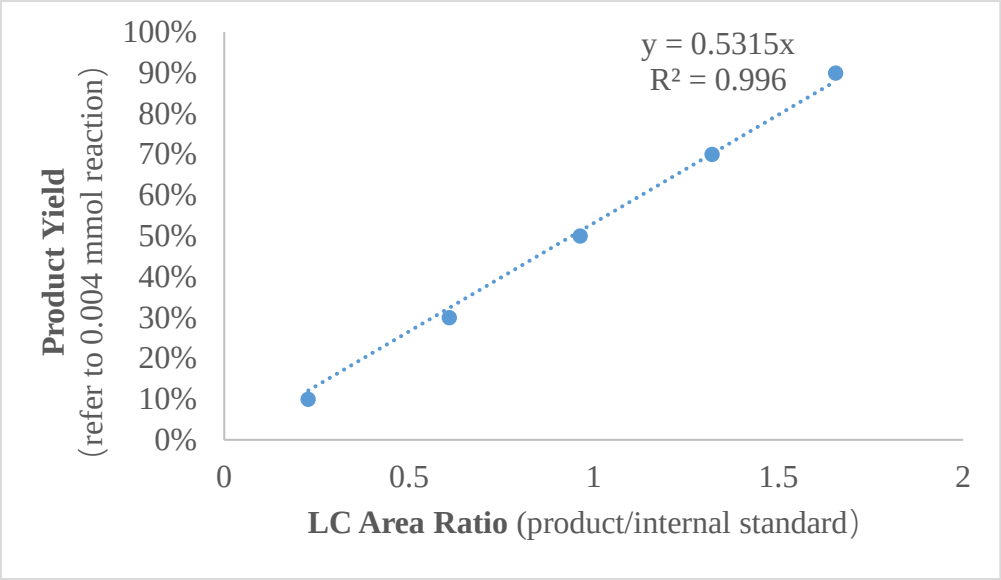

Supplementary Table 21 | Crystal data and structure refinement for (*S*)-3g.

Identification code	**3g** (CCDC: 2355842)
Empirical formula	$C_{15}H_{13}IO$
Formula weight	336.1725
Temperature	150.00 K
Wavelength	1.54178 Å
Crystal system	monoclinic
Space group	$P2_1$
Unit cell dimensions	a=6.8885 (2) Å a = 90° b=10.6012 (4) Å b = 92.109° (2) c=9.2373 (3) Å g = 90°
Volume	674.11 (4) $Å^3$
Z	2
Density (calculated)	1.656 mg/m^3
Absorption coefficient	18.505 mm^{-1}
F(000)	329.2
Crystal size	0.06×0.04×0.02 mm^3
Theta range for data collection	9.58 to 133.14°
Index ranges	$-6 \le h \le 8$, $-13 \le k \le 13$, $-11 \le l \le 11$
Reflections collected	4629
Independent reflections	2162 [R_{int} = 0.0432, R_{sigma} = 0.0775]
Completeness to theta = 133.1 °	99.1 %
Max. and min. transmission	0.0853 and 0.0061
Data/restraints/parameters	2162/1/155
Goodness-of-fit on F^2	0.955
Final R indices [I>2σ(I)]	R1 = 0.0653, wR2 = 0.1401
R indices (all data)	R1 = 0.0657, wR2 = 0.1408
Flack parameters	0.106 (12)
Largest diff. peak and hole	2.25/-0.88 e.$Å^{-3}$

Supplementary Table 22 | Crystal data and structure refinement for (*S*)-3k.

Identification code	**3k** (CCDC: 2358465)
Empirical formula	$C_{16}H_{16}OS$
Formula weight	256.363
Temperature	150.00 K
Wavelength	1.54178 Å
Crystal system	monoclinic
Space group	$P2_1$
Unit cell dimensions	a=16.0453 (4) Å a = 90° b=5.5611 (1) Å b = 114.662° (1) c=16.4961 (3) Å g = 90°
Volume	1337.68 (5) $Å^3$
Z	4
Density (calculated)	1.273 mg/m^3
Absorption coefficient	2.011 mm^{-1}
F(000)	546.8
Crystal size	0.3×0.2×0.1 mm^3
Theta range for data collection	5.9 to 149.4°
Index ranges	$-20 \leq h \leq 18$, $-6 \leq k \leq 6$, $-20 \leq l \leq 20$
Reflections collected	11980
Independent reflections	5125 [R_{int} = 0.0313, R_{sigma} = 0.0444]
Completeness to theta = 135.4 °	99.8 %
Max. and min. transmission	0.0872 and 0.0106
Data/restraints/parameters	5125/1/329
Goodness-of-fit on F^2	1.116
Final R indices [I>2σ(I)]	R1 = 0.0653, wR2 = 0.1474
R indices (all data)	R1 = 0.0667, wR2 = 0.1490
Flack parameters	0.045 (12)
Largest diff. peak and hole	0.51/-0.20 e.$Å^{-3}$

Supplementary Table 23 | Crystal data and structure refinement for (*S*)-3q.

Identification code	**3q** (CCDC: 2416063)
Empirical formula	$C_{20}H_{17}NO$
Formula weight	287.362
Temperature	193 K
Wavelength	1.54178 Å
Crystal system	monoclinic
Space group	$P2_1$
Unit cell dimensions	a=5.6914 (2) Å a = 90° b=15.3437 (1) Å b = 98.867° (2) c=17.7428 (5) Å g = 90°
Volume	1530.91 (9) $Å^3$
Z	4
Density (calculated)	1.247 mg/m^3
Absorption coefficient	0.597 mm^{-1}
F(000)	608.0
Crystal size	0.13×0.12×0.1 mm^3
Theta range for data collection	5.04° to 136.916°
Index ranges	$-6 \le h \le 6$, $-18 \le k \le 17$, $-21 \le l \le 21$
Reflections collected	22456
Independent reflections	5531 [R_{int} = 0.0719, R_{sigma} = 0.0556]
Completeness to theta = 135.4 °	100 %
Max. and min. transmission	0.753 and 0.678
Data/restraints/parameters	5531/1/400
Goodness-of-fit on F^2	1.037
Final R indices [I>2σ(I)]	R1 = 0.0555, wR2 = 0.1344
R indices (all data)	R1 = 0.0831, wR2 = 0.1622
Flack parameters	-0.2 (2)
Largest diff. peak and hole	0.33/-3.4 e.$Å^{-3}$

Supplementary Table 24 | List of primers used in the study.

Sequence of primers using for Glycine Scan (Based on pET28a-T481L_A480G)	
H26G_F	TGTTCGGCCTG**GGC**GGTGCGCATAT
A28G_F	GCCTGCACGGT**GGT**CATATTGATACC
H29G_F	TGCACGGTGCG**GGT**ATTGATACCATCT
silent primer_R (H29, A28, H29)	ATCTGGACGCGCGCCGTGC
A74G_F	TGGCGCTGGTGACG**GGT**GGCGGCGGTT
silent primer_R (A74)	AAAACCGGCACGCCGGTAG
L112G_F	AAACCAACACC**GGT**CAGGCGGGCATT
Q113_F	ACCAACACCTTA**GGT**GCGGGCATTGA
silent primer_R (L112, Q113)	TCAGCACCAGATCCGGGGCGG
W163_F	TCATCAGGATGTC**GCC**CGGCAGATCC
silent primer_R (W163)	TGGCAATGATCACCGGTGGT
Y239G_F	AGACAGACCTTC**GCC**GTCCGCGAAAA
silent primer_R (Y239)	GTTTTACCAACGCGGTGA
N283G_F	ACCGTGACCGGT**GCC**CAGGCCGAAA
silent primer_R (N283)	TGCGATGGCGGCGCCTAT
A394G_F	AGGTAGGTCAG**ACC**ACCATCCGCCA
Y397G_F	AGACAGCCACAG**GCC**GGTCAGAGCAC
silent primer_R (A394, Y397)	CGTGCCGGTTTTCGCGGA
C414G_F	CAGGTAGCCGTG**GCC**CAGGAAGCCACC
Y417G_F	TGCTGCCCAG**ACC**GCCGTGGCAC
L418G_F	CCATGCTGCC**ACC**GTAGCCGTGG
M421G_F	AAACCAACGCC**ACC**GCTGCCCAGG
silent primer_R (C414, Y417, L418, M421)	CGGTCTGGTTCAGAACCTGTAC
F484G_F	CCAGCTGCTG**ACC**GTGCAGCAGA
silent primer_R (F484)	GATGTTGGCGGCACCATCGAA

Sequence of primers using for W163, N283, Y397, H26, Q113, Y239 and C414 mutagenesis (Based on pET28a-T481L-A480G)	
N283_ATG_F	GTTTCGGCCTG**ATG**ACCGGTCACGGT
N283_NDT_F	GTTTCGGCCTG**NDT**ACCGGTCACGGT
N283_TGG_F	GTTTCGGCCTG**TGG**ACCGGTCACGGT
N283_VMA_F	GTTTCGGCCTG**VMA**ACCGGTCACGGT
silent primer_R (N283)	GTAACGAGGATGGTACGACGG
W163_ATG_F	TGGATCTGCCG**ATG**GACATCCTGATG
W163_NDT_F	TGGATCTGCCG**NDT**GACATCCTGATG
W163_VMA_F	TGGATCTGCCG**VMA**GACATCCTGATG
silent primer_R (W163)	ATGGTGCCGCCAACATCC
Y397_ATG_F	TGCTCTGACC**ATG**CTGTGGCTGTCTG
Y397_NDT_F	TGCTCTGACC**NDT**CTGTGGCTGTCTG
Y397_TGG_F	TGCTCTGACC**TGG**CTGTGGCTGTCTG
Y397_VMA_F	TGCTCTGACC**VMA**CTGTGGCTGTCTG
silent primer_R (Y397)	CCATACCGATCAGGATCAG
C414A_F	AGGTAGCCGTG**TGC**CAGGAAGCCAC
C414F_F	AGGTAGCCGTG**GAA**CAGGAAGCCAC
C414I_F	AGGTAGCCGTG**GAT**CAGGAAGCCAC
C414L_F	AGGTAGCCGTG**CAG**CAGGAAGCCAC
C414V_F	AGGTAGCCGTG**AAC**CAGGAAGCCAC
silent primer_R (C414)	ATGCGTGGCGGTCTGGTTC
H26A_F	TGTTCGGCCTG**GCA**GGTGCGCATATTG
H26F_F	TGTTCGGCCTG**TTC**GGTGCGCATATTG
H26I_F	TGTTCGGCCTG**ATC**GGTGCGCATATTG
H26L_F	TGTTCGGCCTG**CTG**GGTGCGCATATTG
H26V_F	TGTTCGGCCTG**GTT**GGTGCGCATATTG
silent primer_R (H26)	ACGCGCGCCGTGCGCAG
Q113A_F	ACCAACACCTTA**GCA**GCGGGCATTGATC

Q113F_F	ACCAACACCTTA**TTC**GCGGGCATTGATC
Q113I_F	ACCAACACCTTA**ATC**GCGGGCATTGATC
Q113L_F	ACCAACACCTTA**CTG**GCGGGCATTGATC
Q113V_F	ACCAACACCTTA**GTT**GCGGGCATTGATC
silent primer_R (Q113)	AGCATCAGCACCAGATCCG
Y239A_F	TTTTCGCGGAC**GCA**GAAGGTCTGTC
Y239F_F	TTTTCGCGGAC**TTC**GAAGGTCTGTC
Y239I_F	TTTTCGCGGAC**ATC**GAAGGTCTGTC
Y239L_F	TTTTCGCGGAC**CTG**GAAGGTCTGTC
Y239V_F	TTTTCGCGGAC**GTT**GAAGGTCTGTC
silent primer_R (Y239)	TCAGACAGCCACAGGTAGG
Sequence of primers using for W163 and H26 mutagenesis (Based on pET28a-T481L_A480G_Y397A/G)	
H26_ATG_F	ATATGCGCACC**CAT**CAGGCCGAAC
H26_NDT_F	ATATGCGCACC**AHN**CAGGCCGAAC
H26_TGG_F	ATATGCGCACC**CCA**CAGGCCGAAC
H26_VMA_F	ATATGCGCACC**TKB**CAGGCCGAAC
H26A_F	ATATGCGCACC**CGC**CAGGCCGAAC
H26E_F	ATATGCGCACC**TTC**CAGGCCGAAC
H26R_F	ATATGCGCACC**GCG**CAGGCCGAAC
H26T_F	ATATGCGCACC**GGT**CAGGCCGAAC
H26Y_F	ATATGCGCACC**GTA**CAGGCCGAAC
silent primer_R (H26)	attcgatggtgtccggga
W163_ATG_F	TGGATCTGCCG**ATG**GACATCCTGATG
W163_NDT_F	TGGATCTGCCG**NDT**GACATCCTGATG
W163_VMA_F	TGGATCTGCCG**VMA**GACATCCTGATG
W163N_F	GATCTGCCG**AAC**GACATCCTGA
W163P_F	GATCTGCCG**CCG**GACATCCTGA
W163Q_F	GATCTGCCG**CAG**GACATCCTGA

W163S_F	GATCTGCCG**TCC**GACATCCTGA
silent primer_R (W163)	GATGGTGCCGCCAACATC

Supplementary Table 25 | Molecular dynamics trajectory clustering analysis. Cluster: indicates the identifier of each cluster. Frames: represents the number of frames assigned to each cluster. Frac: shows the fraction of total frames that belong to each cluster. AvgDist: the average distance between frames and the centroid of the cluster. Stdev: the standard deviation of the distances between frames and the cluster centroid. Centroid: the position of the cluster centroid, representing the average state of all frames in the cluster. AvgCDist: the average distance between the centroid of the current cluster and the centroids of all other clusters.

Cluster	Frames	Frac	AvgDist	Stdev	Centroid	AvgCDist
0	2280	0.456	1.862	0.203	4033	1.359
1	1380	0.276	1.837	0.191	2197	1.183
2	1340	0.268	1.949	0.249	672	1.246

Supplementary Methods

1. General Information

0.004 mmol (or 0.1 mmol) catalytic reactions were performed in a 4 mL clear glass vial (or a 200 mL Schlenk flask) with a magnetic stirring, illuminated with one (or two) 450-460 nm LEDs, stirred for 14 h with one (or two) cooling fan (Supplementary Fig. 1).

Unless otherwise noted, reagents were purchased from commercial suppliers, such as Energey Chemical and Aladdin, and used without further purification. Flash column chromatography was performed with ultrapure silica gel SiliaFlash® P60 (irregularly shaped, 200-300 mesh). ^{1}H NMR, and proton decoupled ^{13}C NMR spectra were recorded on a BRUKER AVANCE III 400 MHz NMR spectrometer at ambient temperature. NMR standards were used as follows: ^{1}H NMR spectroscopy: δ = 0.00 ppm (tetramethylsilane, TMS), ^{13}C NMR spectroscopy: δ = 77.0 ppm ($CDCl_3$). ^{1}H NMR coupling constants were reported in Hz, and multiplicity was indicated as follows: s (singlet); d (doublet); t (triplet); q (quartet); m (multiplet); dd (doublet of doublets); td (triplet of doublets). High-resolution mass spectra (HRMS) were conducted at Thermo Fisher Micromass instrument with an electrospray ionization time-of-flight (ESI-TOF) detector. The GC-MS system is consisted of an Agilent 8860 (Agilent Inc, Palo Alto, CA, USA) gas chromatograph (unless noted DB-5MS UI column was used, length 30 m, inner diameter 0.25 mm, film thickness 0.25 μm) and an Agilent 5977B mass selective detector (positive electron impact mode, EI). An Agilent 8860 gas chromatograph (HP-5 column, length 30 m, inner diameter 0.32 mm, film thickness 0.25 μm) with a FID detector was used for yield determination. Enantiomeric purities of the enzymatic products were determined with a 25 cm Daicel Chiralpak AS-H column, a 25 cm Daicel Chiralpak AD-3 column, a 25 cm Daicel Chiralcel OJ-H column or a 25 cm Daicel Chiralcel OJ-3 column on an Agilent 1290 Infinity II system using *n*-hexane/isopropanol as the mobile phase.

E. coli DH5α cells, and *E. coli* BL21 (DE3) strains were purchased from GenScript Biotech Co., Ltd (Nanjing, China). Restriction enzymes were purchased from Beyotime Biotech. (Shanghai, China). Kanamycin, isopropyl-*β*-D-thiogalactoside (IPTG), tryptone and yeast extract were obtained from Sangon Biotech Co., Ltd (Shanghai, China).

All genes were synthesized by Sangon Biotech Co., Ltd (Shanghai, China). *Pp*BFD, *Pf*BAL, CDH, *Ec*MenD, *Ec*TK, *Ll*KdcA and *Pa*BAL were cloned into pET28a (+) vector with the *Nco*I and *Xho*I restriction sites and C-terminal 6xHis tag.

2. Expression, Purification, and Concentration Determination of Enzymes

For the expression of *Pf*BAL, an *E. coli* BL21 (DE3) single colony harbouring pET28a-*Pf*BAL was inoculated in 6 mL LB medium containing 50 μg/mL kanamycin and grown at 37 ºC, 250 rpm, for 12-14 h. The overnight culture was transferred into 600 mL TB medium containing 50 μg/mL kanamycin, which was then grown at 37 ºC until OD_{600} = 0.6-0.8. Isopropyl-*β*-D-thiogalactoside (IPTG) was added into the culture to a final concentration of 0.5 mM. The cells were induced at 25 ºC for 16 h, then harvested by centrifugation (8000 rpm, 4 ºC, 15 min) and the supernatant was removed and resuspended in binding buffer (50 mM Tris-HCl, 300 mM NaCl, pH 7.5) at 2.5 mL per gram wet cells. Subsequently, the cells were sonicated for 40 min (10 sec on, 10 sec off) and centrifuged (12000 rpm, 1 h, 4 ºC). Purification of the soluble his6-tagged fusion protein from supernatant was performed by using HisTrap column fitted to an ÄKTAxpress FPLC system (GE Health Life Sciences, Pittsburgh, PA). The fractions containing target proteins were collected and buffer exchanged with Kpi buffer (50 mM, pH 7.5) with an Amicon Ultra concentration tube with 50 kDa cut-off. After that, the proteins were stored in 10 v/v % glycerol as 100 μL aliquots at −80 ºC. The concentration of enzymes was determined by the absorption at 280 nm.

The DNA sequence of wild-type ***Pf*BAL**

ATGGCAATGATCACCGGTGGTGAACTGGTTGTTCGTACCCTGATCAAAGCTGGTGTTGA
ACACCTGTTCGGCCTGCACGGTGCGCATATTGATACCATCTTCCAGGCGTGCCTGGATCA
CGATGTGCCGATCATCGATACTCGCCATGAAGCTGCGGCGGGCCACGCGGCTGAAGGTT
ACGCTCGTGCGGGTGCTAAACTGGGTGTGGCGCTGGTGACGGCGGGCGGCGGTTTTAC
CAACGCGGTGACCCCGATCGCGAACGCGTGGCTGGATCGTACCCCGGTTCTGTTCCTGA
CCGGTAGCGGTGCCCTGCGCGATGATGAAACCAACACCTTACAGGCGGGCATTGATCAG
GTTGCGATGGCGGCGCCTATTACTAAATGGGCGCACCGCGTGATGGCTACCGAACACAT
CCCGCGTCTGGTGATGCAGGCGATCCGCGCAGCTCTGAGCGCGCCGCGCGGCCCGGTTC
TGCTGGATCTGCCGTGGGACATCCTGATGAACCAGATCGATGAAGATTCCGTGATCATTC
CAGATCTGGTTCTGTCTGCGCACGGCGCGCGTCCAGATCCGGCGGACCTGGATCAGGCG
CTGGCTCTGCTGCGCAAAGCGGAACGCCCGGTTATCGTGCTGGGTTCTGAAGCGTCCCG
TACCGCCCGTAAAACCGCGCTGTCCGCGTTCGTGGCGGCTACCGGCGTGCCGGTTTTCG
CGGACTACGAAGGTCTGTCTATGCTGAGCGGCCTGCCGGATGCAATGCGTGGCGGTCTG
GTTCAGAACCTGTACAGCTTCGCTAAAGCAGACGCCGCCCCGGATCTGGTGCTGATGCT
GGGCGCACGTTTCGGCCTGAACACCGGTCACGGTTCCGGCCAGCTGATCCCGCACTCTG
CGCAGGTGATCCAGGTTGATCCGGACGCATGTGAACTGGGCCGCTTACAGGGCATCGCT
CTGGGCATCGTGGCGGATGTTGGCGGCACCATCGAAGCACTGGCTCAGGCAACCGCTC
AGGATGCGGCGTGGCCGGATCGTGGCGATTGGTGCGCGAAAGTGACCGATCTGGCCCA
GGAACGCTACGCGTCGATCGCGGCTAAAAGCAGCTCCGAACACGCGCTGCACCCGTTC
CACGCAAGCCAGGTTATTGCAAAACACGTTGATGCTGGTGTTACCGTGGTGGCGGATGG
TGCTCTGACCTACCTGTGGCTGTCTGAAGTGATGAGCCGTGTTAAACCGGGTGGCTTCC
TGTGCCACGGCTACCTGGGCAGCATGGGCGTTGGTTTTGGCACCGCCCTGGGCGCGCAG
GTTGCAGACCTGGAAGCTGGCCGTCGTACCATCCTCGTTACCGGCGACGGCTCCGTTGG
CTACAGCATCGGCGAATTTGACACCCTGGTGCGTAAACAGCTGCCGCTGATCGTTATCAT
CATGAACAACCAGAGCTGGGGTGCGACCCTGCACTTCCAGCAGCTGGCGGTTGGTCCG
AACCGCGTGACCGGCACCCGTCTGGAAAACGGCTCTTACCACGGCGTGGCGGCGGCGT
TCGGTGCTGATGGTTACCACGTGGATAGCGTTGAATCCTTCTCTGCGGCGCTGGCTCAGG
CTCTGGCACACAACCGTCCGGCTTGCATCAACGTTGCGGTTGCGCTGGACCCGATCCCG
CCGGAAGAACTGATCCTGATCGGTATGGACCCGTTCGCGctcgagcaccaccaccaccaccactga

The protein sequence of wild-type ***Pf*BAL**

MAMITGGELVVRTLIKAGVEHLFGLHGAHIDTIFQACLDHDVPIIDTRHEAAAGHAAEGYA
RAGAKLGVALVTAGGGFTNAVTPIANAWLDRTPVLFLTGSGALRDDETNTLQAGIDQVAM
AAPITKWAHRVMATEHIPRLVMQAIRAALSAPRGPVLLDLPWDILMNQIDEDSVIIPDLVLS
AHGARPDPADLDQALALLRKAERPVIVLGSEASRTARKTALSAFVAATGVPVFADYEGLSM
LSGLPDAMRGGLVQNLYSFAKADAAPDLVLMLGARFGLNTGHGSGQLIPHSAQVIQVDPD
ACELGRLQGIALGIVADVGGTIEALAQATAQDAAWPDRGDWCAKVTDLAQERYASIAAKS
SSEHALHPFHASQVIAKHVDAGVTVVADGALTYLWLSEVMSRVKPGGFLCHGYLGSMGV
GFGTALGAQVADLEAGRRTILVTGDGSVGYSIGEFDTLVRKQLPLIVIIMNNQSWGATLHFQ
QLAVGPNRVTGTRLENGSYHGVAAAFGADGYHVDSVESFSAALAQALAHNRPACINVAVA
LDPIPPEELILIGMDPFALEHHHHHH

The DNA sequence of ***Pf*BAL_T481L**

ATGGCAATGATCACCGGTGGTGAACTGGTTGTTCGTACCCTGATCAAAGCTGGTGTTGA

ACACCTGTTCGGCCTGCACGGTGCGCATATTGATACCATCTTCCAGGCGTGCCTGGATCA
CGATGTGCCGATCATCGATACTCGCCATGAAGCTGCGGCGGGCCACGCGGCTGAAGGTT
ACGCTCGTGCGGGTGCTAAACTGGGTGTGGCGCTGGTGACGGCGGGCGGCGGTTTTAC
CAACGCGGTGACCCCGATCGCGAACGCGTGGCTGGATCGTACCCCGGTTCTGTTCCTGA
CCGGTAGCGGTGCCCTGCGCGATGATGAAACCAACACCTTACAGGCGGGCATTGATCAG
GTTGCGATGGCGGCGCCTATTACTAAATGGGCGCACCGCGTGATGGCTACCGAACACAT
CCCGCGTCTGGTGATGCAGGCGATCCGCGCAGCTCTGAGCGCGCCGCGCGGCCCGGTTC
TGCTGGATCTGCCGTGGGACATCCTGATGAACCAGATCGATGAAGATTCCGTGATCATTC
CAGATCTGGTTCTGTCTGCGCACGGCGCGCGTCCAGATCCGGCGGACCTGGATCAGGCG
CTGGCTCTGCTGCGCAAAGCGGAACGCCCGGTTATCGTGCTGGGTTCTGAAGCGTCCCG
TACCGCCCGTAAAACCGCGCTGTCCGCGTTCGTGGCGGCTACCGGCGTGCCGGTTTTCG
CGGACTACGAAGGTCTGTCTATGCTGAGCGGCCTGCCGGATGCAATGCGTGGCGGTCTG
GTTCAGAACCTGTACAGCTTCGCTAAAGCAGACGCCGCCCCGGATCTGGTGCTGATGCT
GGGCGCACGTTTCGGCCTGAACACCGGTCACGGTTCCGGCCAGCTGATCCCGCACTCTG
CGCAGGTGATCCAGGTTGATCCGGACGCATGTGAACTGGGCCGCTTACAGGGCATCGCT
CTGGGCATCGTGGCGGATGTTGGCGGCACCATCGAAGCACTGGCTCAGGCAACCGCTC
AGGATGCGGCGTGGCCGGATCGTGGCGATTGGTGCGCGAAAGTGACCGATCTGGCCCA
GGAACGCTACGCGTCGATCGCGGCTAAAAGCAGCTCCGAACACGCGCTGCACCCGTTC
CACGCAAGCCAGGTTATTGCAAAACACGTTGATGCTGGTGTTACCGTGGTGGCGGATGG
TGCTCTGACCTACCTGTGGCTGTCTGAAGTGATGAGCCGTGTTAAACCGGGTGGCTTCC
TGTGCCACGGCTACCTGGGCAGCATGGGCGTTGGTTTTGGCACCGCCCTGGGCGCGCAG
GTTGCAGACCTGGAAGCTGGCCGTCGTACCATCCTCGTTACCGGCGACGGCTCCGTTGG
CTACAGCATCGGCGAATTTGACACCCTGGTGCGTAAACAGCTGCCGCTGATCGTTATCAT
CATGAACAACCAGAGCTGGGGTGCG**CTG**CTGCACTTCCAGCAGCTGGCGGTTGGTCCG
AACCGCGTGACCGGCACCCGTCTGGAAAACGGCTCTTACCACGGCGTGGCGGCGGCGT
TCGGTGCTGATGGTTACCACGTGGATAGCGTTGAATCCTTCTCTGCGGCGCTGGCTCAGG
CTCTGGCACACAACCGTCCGGCTTGCATCAACGTTGCGGTTGCGCTGGACCCGATCCCG
CCGGAAGAACTGATCCTGATCGGTATGGACCCGTTCGCGctcgagcaccaccaccaccactga

The protein sequence of ***Pf*BAL_T481L**

MAMITGGELVVRTLIKAGVEHLFGLHGAHIDTIFQACLDHDVPIIDTRHEAAAGHAAEGYA
RAGAKLGVALVTAGGGFTNAVTPIANAWLDRTPVLFLTGSGALRDDETNTLQAGIDQVAM
AAPITKWAHRVMATEHIPRLVMQAIRAALSAPRGPVLLDLPWDILMNQIDEDSVIIPDLVLS
AHGARPDPADLDQALALLRKAERPVIVLGSEASRTARKTALSAFVAATGVPVFADYEGLSM
LSGLPDAMRGGLVQNLYSFAKADAAPDLVLMLGARFGLNTGHGSGQLIPHSAQVIQVDPD
ACELGRLQGIALGIVADVGGTIEALAQATAQDAAWPDRGDWCAKVTDLAQERYASIAAKS
SSEHALHPFHASQVIAKHVDAGVTVVADGALTYLWLSEVMSRVKPGGFLCHGYLGSMGV
GFGTALGAQVADLEAGRRTILVTGDGSVGYSIGEFDTLVRKQLPLIVIIMNNQSWGA**L**LHFQ
QLAVGPNRVTGTRLENGSYHGVAAAFGADGYHVDSVESFSAALAQALAHNRPACINVAVA
LDPIPPEELILIGMDPFALEHHHHHH

The DNA sequence of ***Pf*BAL_T481L-A480G**

ATGGCAATGATCACCGGTGGTGAACTGGTTGTTCGTACCCTGATCAAAGCTGGTGTTGA
ACACCTGTTCGGCCTGCACGGTGCGCATATTGATACCATCTTCCAGGCGTGCCTGGATCA
CGATGTGCCGATCATCGATACTCGCCATGAAGCTGCGGCGGGCCACGCGGCTGAAGGTT

ACGCTCGTGCGGGTGCTAAACTGGGTGTGGCGCTGGTGACGGCGGGCGGCGGTTTTAC
CAACGCGGTGACCCCGATCGCGAACGCGTGGCTGGATCGTACCCCGGTTCTGTTCCTGA
CCGGTAGCGGTGCCCTGCGCGATGATGAAACCAACACCTTACAGGCGGGCATTGATCAG
GTTGCGATGGCGGCGCCTATTACTAAATGGGCGCACCGCGTGATGGCTACCGAACACAT
CCCGCGTCTGGTGATGCAGGCGATCCGCGCAGCTCTGAGCGCGCCGCGCGGCCCGGTTC
TGCTGGATCTGCCGTGGGACATCCTGATGAACCAGATCGATGAAGATTCCGTGATCATTC
CAGATCTGGTTCTGTCTGCGCACGGCGCGCGTCCAGATCCGGCGGACCTGGATCAGGCG
CTGGCTCTGCTGCGCAAAGCGGAACGCCCGGTTATCGTGCTGGGTTCTGAAGCGTCCCG
TACCGCCCGTAAAACCGCGCTGTCCGCGTTCGTGGCGGCTACCGGCGTGCCGGTTTTCG
CGGACTACGAAGGTCTGTCTATGCTGAGCGGCCTGCCGGATGCAATGCGTGGCGGTCTG
GTTCAGAACCTGTACAGCTTCGCTAAAGCAGACGCCGCCCCGGATCTGGTGCTGATGCT
GGGCGCACGTTTCGGCCTGAACACCGGTCACGGTTCCGGCCAGCTGATCCCGCACTCTG
CGCAGGTGATCCAGGTTGATCCGGACGCATGTGAACTGGGCCGCTTACAGGGCATCGCT
CTGGGCATCGTGGCGGATGTTGGCGGCACCATCGAAGCACTGGCTCAGGCAACCGCTC
AGGATGCGGCGTGGCCGGATCGTGGCGATTGGTGCGCGAAAGTGACCGATCTGGCCCA
GGAACGCTACGCGTCGATCGCGGCTAAAAGCAGCTCCGAACACGCGCTGCACCCGTTC
CACGCAAGCCAGGTTATTGCAAAACACGTTGATGCTGGTGTTACCGTGGTGGCGGATGG
TGCTCTGACCTACCTGTGGCTGTCTGAAGTGATGAGCCGTGTTAAACCGGGTGGCTTCC
TGTGCCACGGCTACCTGGGCAGCATGGGCGTTGGTTTTGGCACCGCCCTGGGCGCGCAG
GTTGCAGACCTGGAAGCTGGCCGTCGTACCATCCTCGTTACCGGCGACGGCTCCGTTGG
CTACAGCATCGGCGAATTTGACACCCTGGTGCGTAAACAGCTGCCGCTGATCGTTATCAT
CATGAACAACCAGAGCTGGGGT**GGTCTG**CTGCACTTCCAGCAGCTGGCGGTTGGTCCG
AACCGCGTGACCGGCACCCGTCTGGAAAACGGCTCTTACCACGGCGTGGCGGCGGCGT
TCGGTGCTGATGGTTACCACGTGGATAGCGTTGAATCCTTCTCTGCGGCGCTGGCTCAGG
CTCTGGCACACAACCGTCCGGCTTGCATCAACGTTGCGGTTGCGCTGGACCCGATCCCG
CCGGAAGAACTGATCCTGATCGGTATGGACCCGTTCGCGctcgagcaccaccaccaccaccactga

The protein sequence of ***Pf*BAL_T481L-A480G**

MAMITGGELVVRTLIKAGVEHLFGLHGAHIDTIFQACLDHDVPIIDTRHEAAAGHAAEGYA
RAGAKLGVALVTAGGGFTNAVTPIANAWLDRTPVLFLTGSGALRDDETNTLQAGIDQVAM
AAPITKWAHRVMATEHIPRLVMQAIRAALSAPRGPVLLDLPWDILMNQIDEDSVIIPDLVLS
AHGARPDPADLDQALALLRKAERPVIVLGSEASRTARKTALSAFVAATGVPVFADYEGLSM
LSGLPDAMRGGLVQNLYSFAKADAAPDLVLMLGARFGLNTGHGSGQLIPHSAQVIQVDPD
ACELGRLQGIALGIVADVGGTIEALAQATAQDAAWPDRGDWCAKVTDLAQERYASIAAKS
SSEHALHPFHASQVIAKHVDAGVTVVADGALTYLWLSEVMSRVKPGGFLCHGYLGSMGV
GFGTALGAQVADLEAGRRTILVTGDGSVGYSIGEFDTLVRKQLPLIVIIMNNQSWG**GL**LHFQ
QLAVGPNRVTGTRLENGSYHGVAAAFGADGYHVDSVESFSAALAQALAHNRPACINVAVA
LDPIPPEELILIGMDPFALEHHHHHH

The DNA sequence of ***Pf*BAL_T481L-A480G-Y397A**

ATGGCAATGATCACCGGTGGTGAACTGGTTGTTCGTACCCTGATCAAAGCTGGTGTTGA
ACACCTGTTCGGCCTGCACGGTGCGCATATTGATACCATCTTCCAGGCGTGCCTGGATCA
CGATGTGCCGATCATCGATACTCGCCATGAAGCTGCGGCGGGCCACGCGGCTGAAGGTT
ACGCTCGTGCGGGTGCTAAACTGGGTGTGGCGCTGGTGACGGCGGGCGGCGGTTTTAC
CAACGCGGTGACCCCGATCGCGAACGCGTGGCTGGATCGTACCCCGGTTCTGTTCCTGA

CCGGTAGCGGTGCCCTGCGCGATGATGAAACCAACACCTTACAGGCGGGCATTGATCAG
GTTGCGATGGCGGCGCCTATTACTAAATGGGCGCACCGCGTGATGGCTACCGAACACAT
CCCGCGTCTGGTGATGCAGGCGATCCGCGCAGCTCTGAGCGCGCCGCGCGGCCCGGTTC
TGCTGGATCTGCCGTGGGACATCCTGATGAACCAGATCGATGAAGATTCCGTGATCATTC
CAGATCTGGTTCTGTCTGCGCACGGCGCGCGTCCAGATCCGGCGGACCTGGATCAGGCG
CTGGCTCTGCTGCGCAAAGCGGAACGCCCGGTTATCGTGCTGGGTTCTGAAGCGTCCCG
TACCGCCCGTAAAACCGCGCTGTCCGCGTTCGTGGCGGCTACCGGCGTGCCGGTTTTCG
CGGACTACGAAGGTCTGTCTATGCTGAGCGGCCTGCCGGATGCAATGCGTGGCGGTCTG
GTTCAGAACCTGTACAGCTTCGCTAAAGCAGACGCCGCCCCGGATCTGGTGCTGATGCT
GGGCGCACGTTTCGGCCTGAACACCGGTCACGGTTCCGGCCAGCTGATCCCGCACTCTG
CGCAGGTGATCCAGGTTGATCCGGACGCATGTGAACTGGGCCGCTTACAGGGCATCGCT
CTGGGCATCGTGGCGGATGTTGGCGGCACCATCGAAGCACTGGCTCAGGCAACCGCTC
AGGATGCGGCGTGGCCGGATCGTGGCGATTGGTGCGCGAAAGTGACCGATCTGGCCCA
GGAACGCTACGCGTCGATCGCGGCTAAAAGCAGCTCCGAACACGCGCTGCACCCGTTC
CACGCAAGCCAGGTTATTGCAAAACACGTTGATGCTGGTGTTACCGTGGTGGCGGATGG
TGCTCTGACC**GCA**CTGTGGCTGTCTGAAGTGATGAGCCGTGTTAAACCGGGTGGCTTCC
TGTGCCACGGCTACCTGGGCAGCATGGGCGTTGGTTTTGGCACCGCCCTGGGCGCGCAG
GTTGCAGACCTGGAAGCTGGCCGTCGTACCATCCTCGTTACCGGCGACGGCTCCGTTGG
CTACAGCATCGGCGAATTTGACACCCTGGTGCGTAAACAGCTGCCGCTGATCGTTATCAT
CATGAACAACCAGAGCTGGGGT**GGTCTG**CTGCACTTCCAGCAGCTGGCGGTTGGTCCG
AACCGCGTGACCGGCACCCGTCTGGAAAACGGCTCTTACCACGGCGTGGCGGCGGCGT
TCGGTGCTGATGGTTACCACGTGGATAGCGTTGAATCCTTCTCTGCGGCGCTGGCTCAGG
CTCTGGCACACAACCGTCCGGCTTGCATCAACGTTGCGGTTGCGCTGGACCCGATCCCG
CCGGAAGAACTGATCCTGATCGGTATGGACCCGTTCGCGctcgagcaccaccaccaccaccactga

The protein sequence of ***Pf*BAL_T481L-A480G-Y397A**

MAMITGGELVVRTLIKAGVEHLFGLHGAHIDTIFQACLDHDVPIIDTRHEAAAGHAAEGYA
RAGAKLGVALVTAGGGFTNAVTPIANAWLDRTPVLFLTGSGALRDDETNTLQAGIDQVAM
AAPITKWAHRVMATEHIPRLVMQAIRAALSAPRGPVLLDLPWDILMNQIDEDSVIIPDLVLS
AHGARPDPADLDQALALLRKAERPVIVLGSEASRTARKTALSAFVAATGVPVFADYEGLSM
LSGLPDAMRGGLVQNLYSFAKADAAPDLVLMLGARFGLNTGHGSGQLIPHSAQVIQVDPD
ACELGRLQGIALGIVADVGGTIEALAQATAQDAAWPDRGDWCAKVTDLAQERYASIAAKS
SSEHALHPFHASQVIAKHVDAGVTVVADGALT**A**LWLSEVMSRVKPGGFLCHGYLGSMGV
GFGTALGAQVADLEAGRRTILVTGDGSVGYSIGEFDTLVRKQLPLIVIIMNNQSWG**GL**LHFQ
QLAVGPNRVTGTRLENGSYHGVAAAFGADGYHVDSVESFSAALAQALAHNRPACINVAVA
LDPIPPEELILIGMDPFALEHHHHHH

The DNA sequence of ***Pf*BAL_T481L-A480G-Y397A-W163C**

ATGGCAATGATCACCGGTGGTGAACTGGTTGTTCGTACCCTGATCAAAGCTGGTGTTGA
ACACCTGTTCGGCCTGCACGGTGCGCATATTGATACCATCTTCCAGGCGTGCCTGGATCA
CGATGTGCCGATCATCGATACTCGCCATGAAGCTGCGGCGGGCCACGCGGCTGAAGGTT
ACGCTCGTGCGGGTGCTAAACTGGGTGTGGCGCTGGTGACGGCGGGCGGCGGTTTTAC
CAACGCGGTGACCCCGATCGCGAACGCGTGGCTGGATCGTACCCCGGTTCTGTTCCTGA
CCGGTAGCGGTGCCCTGCGCGATGATGAAACCAACACCTTACAGGCGGGCATTGATCAG
GTTGCGATGGCGGCGCCTATTACTAAATGGGCGCACCGCGTGATGGCTACCGAACACAT

CCCGCGTCTGGTGATGCAGGCGATCCGCGCAGCTCTGAGCGCGCCGCGCGGCCCGGTTC
TGCTGGATCTGCCG**TGC**GACATCCTGATGAACCAGATCGATGAAGATTCCGTGATCATTC
CAGATCTGGTTCTGTCTGCGCACGGCGCGCGTCCAGATCCGGCGGACCTGGATCAGGCG
CTGGCTCTGCTGCGCAAAGCGGAACGCCCGGTTATCGTGCTGGGTTCTGAAGCGTCCCG
TACCGCCCGTAAAACCGCGCTGTCCGCGTTCGTGGCGGCTACCGGCGTGCCGGTTTTCG
CGGACTACGAAGGTCTGTCTATGCTGAGCGGCCTGCCGGATGCAATGCGTGGCGGTCTG
GTTCAGAACCTGTACAGCTTCGCTAAAGCAGACGCCGCCCCGGATCTGGTGCTGATGCT
GGGCGCACGTTTCGGCCTGAACACCGGTCACGGTTCCGGCCAGCTGATCCCGCACTCTG
CGCAGGTGATCCAGGTTGATCCGGACGCATGTGAACTGGGCCGCTTACAGGGCATCGCT
CTGGGCATCGTGGCGGATGTTGGCGGCACCATCGAAGCACTGGCTCAGGCAACCGCTC
AGGATGCGGCGTGGCCGGATCGTGGCGATTGGTGCGCGAAAGTGACCGATCTGGCCCA
GGAACGCTACGCGTCGATCGCGGCTAAAAGCAGCTCCGAACACGCGCTGCACCCGTTC
CACGCAAGCCAGGTTATTGCAAAACACGTTGATGCTGGTGTTACCGTGGTGGCGGATGG
TGCTCTGACC**GCA**CTGTGGCTGTCTGAAGTGATGAGCCGTGTTAAACCGGGTGGCTTCC
TGTGCCACGGCTACCTGGGCAGCATGGGCGTTGGTTTTGGCACCGCCCTGGGCGCGCAG
GTTGCAGACCTGGAAGCTGGCCGTCGTACCATCCTCGTTACCGGCGACGGCTCCGTTGG
CTACAGCATCGGCGAATTTGACACCCTGGTGCGTAAACAGCTGCCGCTGATCGTTATCAT
CATGAACAACCAGAGCTGGGGT**GGTCTG**CTGCACTGGCAGCAGCTGGCGGTTGGTCCG
AACCGCGTGACCGGCACCCGTCTGGAAAACGGCTCTTACCACGGCGTGGCGGCGGCGT
TCGGTGCTGATGGTTACCACGTGGATAGCGTTGAATCCTTCTCTGCGGCGCTGGCTCAGG
CTCTGGCACACAACCGTCCGGCTTGCATCAACGTTGCGGTTGCGCTGGACCCGATCCCG
CCGGAAGAACTGATCCTGATCGGTATGGACCCGTTCGCGctcgagcaccaccaccaccaccactga

<u>The protein sequence of ***Pf*BAL_T481L-A480G-Y397A-W163C**</u>
MAMITGGELVVRTLIKAGVEHLFGLHGAHIDTIFQACLDHDVPIIDTRHEAAAGHAAEGYA
RAGAKLGVALVTAGGGFTNAVTPIANAWLDRTPVLFLTGSGALRDDETNTLQAGIDQVAM
AAPITKWAHRVMATEHIPRLVMQAIRAALSAPRGPVLLDLP**C**DILMNQIDEDSVIIPDLVLSA
HGARPDPADLDQALALLRKAERPVIVLGSEASRTARKTALSAFVAATGVPVFADYEGLSML
SGLPDAMRGGLVQNLYSFAKADAAPDLVLMLGARFGLNTGHGSGQLIPHSAQVIQVDPDA
CELGRLQGIALGIVADVGGTIEALAQATAQDAAWPDRGDWCAKVTDLAQERYASIAAKSSS
EHALHPFHASQVIAKHVDAGVTVVADGALT**A**LWLSEVMSRVKPGGFLCHGYLGSMGVGF
GTALGAQVADLEAGRRTILVTGDGSVGYSIGEFDTLVRKQLPLIVIIMNNQSWG**GL**LHWQQ
LAVGPNRVTGTRLENGSYHGVAAAFGADGYHVDSVESFSAALAQALAHNRPACINVAVAL
DPIPPEELILIGMDPFALEHHHHHH

3. Directed Evolution

3.1 Materials and General Methods for Directed Evolution

Molecular biology reagents and chemicals were purchased from Vazyme Biotech Co., Ltd, Beyotime Biotech, Inc., if not specifically noted. Primers were ordered from Beijing Tsingke Biotech Co., Ltd. and listed in Supplementary Table 24.

3.2 The Evolution Trajectory

The variants library based on wild-type *Pf*BAL built by our prior work[1] was screened for enantioselective C(sp^3)–H bond radical acylation reaction at first, and variants *Pf*BAL_T481L, *Pf*BAL_T481L-A480G were identified to be the best catalyst (Supplementary Table 1). Then, the crystal structure of *Pf*BAL_T481L-A480G was simulated by Molecular Dynamics Simulation (MD) and used as the acceptor, Breslow intermediate radical cation formed by ThDP and **1a** complex and the benzylic radical was used as the ligand for docking. Accordingly, sixteen amino acid residues within 5 Å of the ketyl radical were selected for glycine scanning (Supplementary Fig. 7). According to the results of glycine scanning (Supplementary Table 4), seven amino acid residues were selected for further mutagenesis. Four residues (H26, Q113, Y239, C414) were substituted with amino acids of different sizes: alanine (A), leucine (L), phenylalanine (F), Isoleucine (I), Valine (V); the other three residues (W163, N283, Y397) were performed by site-saturation mutagenesis using the "Tang and 22c-trick" method[2]. According to the protocol, four primers containing codons NDT, VMA, ATG and TGG, respectively, (NDT encodes I, N, S, G, D, V, R, H, L, F, Y, and C, VMA encodes E, A, Q, P, K, and L, ATG encodes M, and TGG encodes W, thereby including all 20 natural amino acids) were used for a given site of mutagenesis. These four primers were mixed in a ratio of 12:6:1:1. Analysis of the results of the reactions (Supplementary Tables 4-8), *Pf*BAL_T481L-A480G-Y397A (41% yield, 93% ee) and *Pf*BAL_T481L-A480G-Y397G (43% yield, 89% ee) were identified to be the best catalysts, and some mutagenesis of 26 and 163 sites were also proved to have improvement on yield and enantioselectivity. Then we conducted iterative site-saturation mutagenesis at positions H26, and W163 using *Pf*BAL_T481L-A480G-Y397G/A as template, respectively. Finally, analysis of the reaction outcomes of the variants (Supplementary Tables 9-11), mutant **RAT$_{CH}$** (*Pf*BAL_T481L-A480G-Y397A-W163C) was identified as the best catalyst for the model reaction.

3.3 Mutant Creation

The primers were designed by using a two-step PCR method in which one primer containing mutagenic sites and one silent primer were used to generate a short DNA fragment, which was recovered and then employed as a megaprimer to amplify the whole plasmid[3]. The PCR product of the second step was digested by *Dpn*I restriction enzyme, and 5 μL of the resulting mixture was transformed into chemically-competent *E. coli* BL21 (DE3) cells. The single colonies from the transformation plates were picked and cultured overnight at 37 ºC with kanamycin (50 μg/mL). Then the overnight cultures were pelleted and mini-prepped by Sangon Plasmid Miniprep Kit and further sequenced to confirm the mutations (Supplementary Table 24).

4. Typical Procedure for Photobiocatalytic Reactions

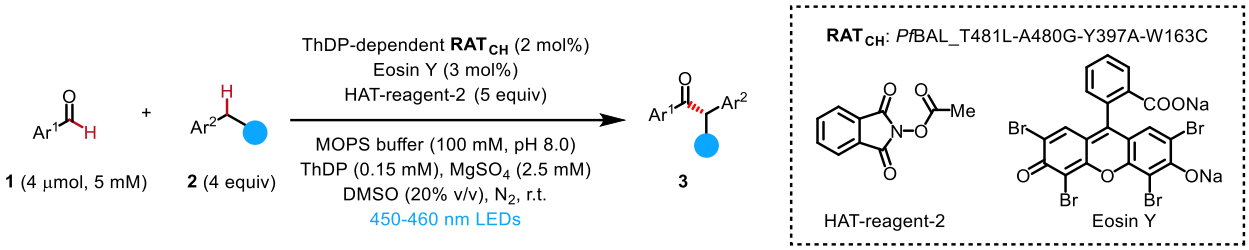

All enzymatic reactions were assembled in a Vigor glove box with an O_2 concentration below 3 ppm. Taking **1a** + **2a** → **3a** as an example, in the glove box, to a 4 mL vial containing a magnetic stir bar, solutions of *Pf*BAL_T481L-A480G-Y397A-W163C (**RAT$_{CH}$**), 4-chlorobenzaldehyde **1a** (40 μL of a 100 mM DMSO stock, 0.004 mmol), ethylbenzene **2a** (40 μL of a 400 mM DMSO stock, 0.016 mmol), HAT reagent 2 (80 μL of a 250 mM DMSO stock, 0.020 mmol) and Eosin Y (20 μL of a 6 mM stock in MOPS buffer, 3 mol%) were added to ~ 620 μL of MOPS buffer (100 mM, containing 2.5 mM $MgSO_4$, 0.15 mM ThDP, pH 8.0). The total volume of the reaction mixture was 0.8 mL and the final concentration for DMSO was 20 v/v %. The vial was sealed with a screw cap and then sealed tightly with a sealing film, removed from the glove box, illuminated with 450-460 nm LEDs, and stirred for 14 h at room temperature with a cooling fan.

For reaction work-up, ethyl acetate (1.0 mL) and 20.0 μL of an internal standard stock (2 v/v % of *n*-dodecane in ethyl acetate) were added and mixed thoroughly. The organic phase was separated and then analysed by GC, GC-MS and chiral HPLC. The product formation was confirmed by comparing MS spectra and the retention times in GC and HPLC with the racemic standards. GC yields were determined relative to the *n*-dodecane according to calibration curves. Enantioselectivity was determined by chiral HPLC. LC yields were determined using a ZORBAX SB-C18 column (2.1 x 50 mm, 1.8 μm) against an internal standard 1-benzyl-4-chlorobenzene at 210 nm.

All the 0.004 mmol reactions were repeated at least twice independently using different batches of the enzyme. Selected examples were reproduced by another person from the same group. GC yields were typically within 10% error among each run. Ee values were typically within 3% error among each run.

Substrates (**3g**, **3k**, **3q** and **3af**) were selected to be performed on a 0.1-mmol scale. Accordingly, 200 mL Schlenk flask was used. After irradiation for 14 h, the mixture was transferred into 50 mL centrifuge tubes and centrifuged at 6000 rpm for 15 min, the supernatant was extracted with ethyl acetate five times, and the precipitate was washed with ethyl acetate five times. Then, the combined organic phase was concentrated and purified by flash chromatography on silica gel (petroleum ether/ethyl acetate = 100:1) to afford isolated yield.

Unless otherwise noted, *Conditions C* were applied: aldehyde **1** (0.004 mmol), ethylbenzene **2** (0.016 mmol), HAT reagent 2 (0.020 mmol), **RAT$_{CH}$** (2 mol%), Eosin Y (3 mol%), 20 v/v % DMSO in 100 mM MOPS buffer (pH 8.0, containing 2.5 mM $MgSO_4$ and 0.15 mM ThDP) were stirred for 14 h at room temperature under N_2 atmosphere with the irradiation of 450-460 nm LEDs; total volume of the reaction is 0.8 mL; the yield was determined by GC and based on **1**; enantiomeric excess (ee) was determined by HPLC analysis on a chiral stationary phase.

5. Preparation of Racemic References

Method A:

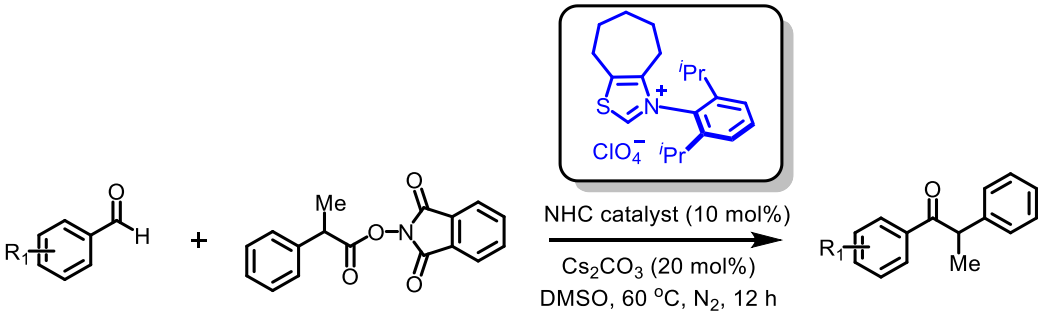

Arylaldehyde (1 mmol), *N*-(acyloxy)phthalimide (2 mmol), NHC catalyst (10 mol%) and Cs_2CO_3 (20 mol%) were added to a dry Schlenk tube equipped with a stirring bar. The mixture was evacuated and backfilled with N_2 for three times. Then, anhydrous DMSO (4 mL) was added by syringe under N_2 atmosphere. The reaction mixture was stirred at 60 °C for 12 h. The reaction was quenched by adding 10 mL water and extracted with ethyl acetate for three times. The organic layers were combined and dried with anhydrous Na_2SO_4. After concentration under reduced pressure, the crude residue was purified by flash chromatography on silica gel (petroleum ether/ethyl acetate = 100:1 to 20:1) to afford the racemic references. **Method A** was used for synthesizing racemic references **3q** and **3r**.

Method B:

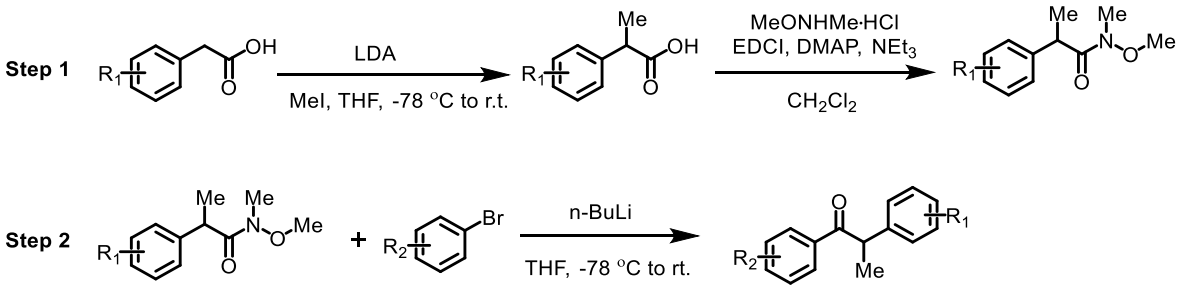

Step 1: To a solution of LDA (6 mmol, 2 eq) in anhydrous THF (15 mL) was added phenylacetic acid (3 mmol, 1 eq, in 5 mL THF) at – 78 °C. The mixture was stirred at – 78 °C for 1 h. Iodomethane (4.5 mmol, 1.5 eq) was added in one portion and then the mixture was allowed to warm to room temperature and stirred overnight. The reaction mixture was acidified with HCl (1.0 N), and extracted with ethyl acetate three times. The organic layers were combined and dried over anhydrous Na_2SO_4, then concentrated under reduced pressure. The crude product was used directly for the next step without further purification. The crude mixture of the 2-phenylpropionic acid (1.0 eq), *N*, *O*-dimethylhydroxylamine hydrochloride (1.3 eq) and DMAP (10 mol%) were added into a flask with CH_2Cl_2 (0.2 M) at 0 °C, NEt_3 (1.33 eq) and EDCI (1.3 eq) were added successively. The reaction mixture was stirred at 0 °C for 1 h, then allowed to warm to room temperature and stirred overnight. The organic layer was washed with 1.0 N HCl (3×10 mL), aqueous saturated $NaHCO_3$ (3×10 mL),

and brine (20 mL). The combined organic layers were dried over anhydrous Na_2SO_4, and concentrated under reduced pressure. The crude mixture was purified by flash chromatography on silica gel (petroleum ether/ethyl acetate = 30:1 to 10:1) to give the pure Weinreb amide.

Step 2: The aryl bromide (1.5 eq) was dissolved in THF, ^{n}BuLi (1.5 eq) was added dropwise at -78 ºC under a N_2 atmosphere. The reaction was stirred at -78 ºC for 1 h. The corresponding Weinreb amide (1.0 eq in THF) was added dropwise to the flask. The reaction was allowed to warm to room temperature and stirred overnight. The reaction was quenched with a saturated aqueous NH_4Cl solution at room temperature and extracted with ethyl acetate. After drying with anhydrous Na_2SO_4, filtration and concentration under reduced pressure, the crude residue was purified by flash chromatography on silica gel (petroleum ether/ethyl acetate = 100:1 to 5:1) to afford the racemic references. **Method B** was used for synthesizing the rest of the racemic references.

6. Mechanistic Studies

6.1 TEMPO Trapping Experiment

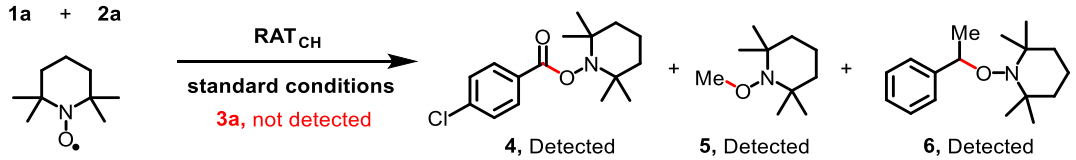

To probe the radical intermediate in our enantioselective C(sp^3)–H bond radical acylation reaction, a TEMPO trapping experiment was designed and performed. Radical trapping reagent TEMPO (5.0 eq) was added to the model reaction under *Conditions C* by using **RAT$_{CH}$** as a catalyst. The reaction mixture was analysed by GC and HRMS. We found that the formation of product **3a** was completely inhibited and products **4**, **5** and **6** were detected by HRMS which indicated the formation of the ketyl radical (**Int. C** in Fig. 2a), methyl radical (**Int. D** in Fig. 2a) and benzyl radical (**Int. E** in Fig. 2a).

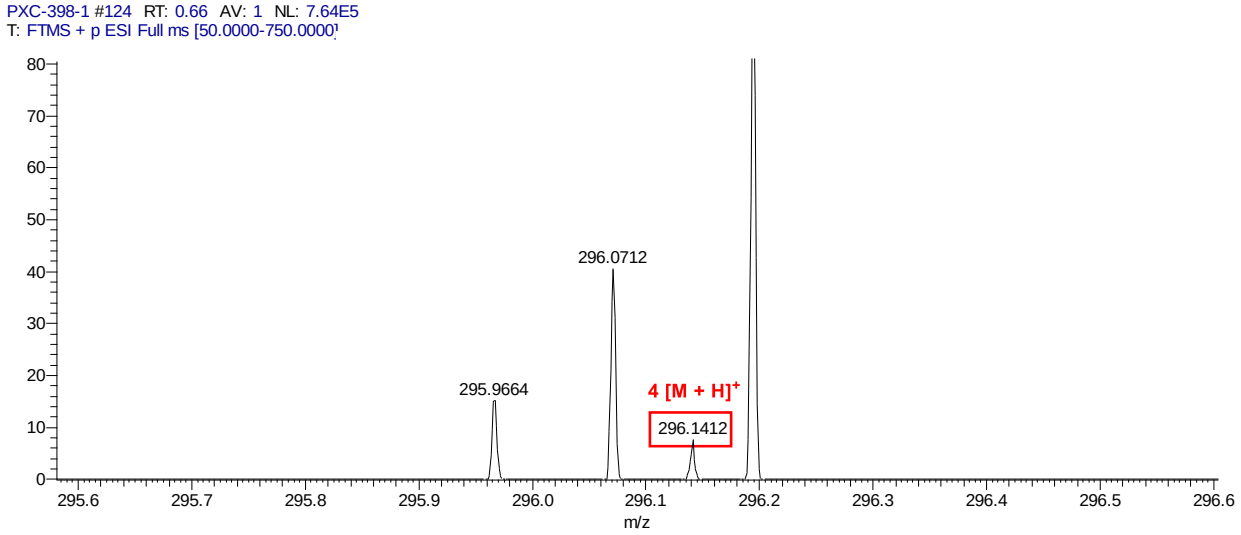

PXC-398-1 #346 RT: 1.86 AV: 1 NL: 5.16E6
T: FTMS + p ESI Full ms [50.0000-750.0000]

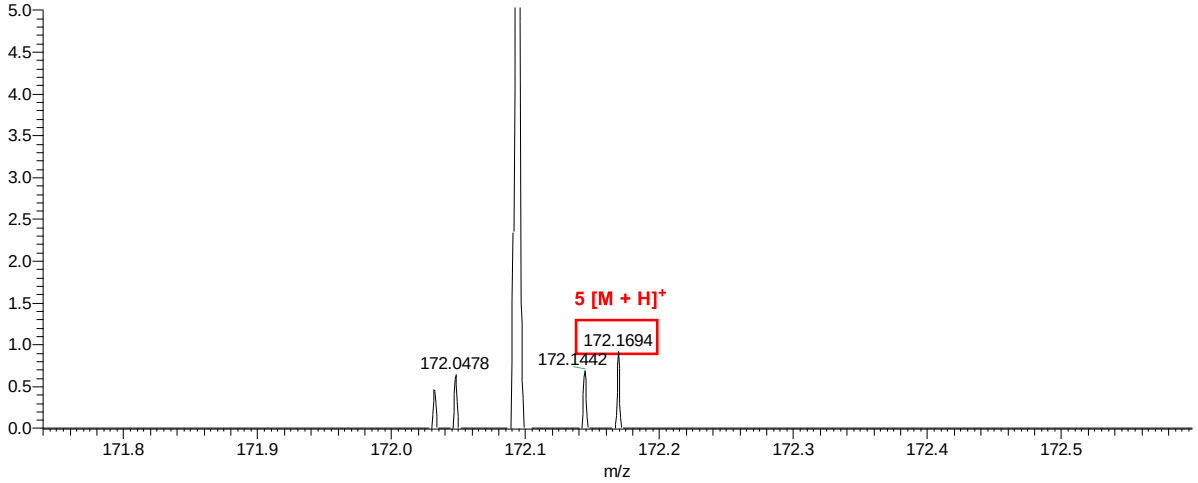

PXC-398-1 #76 RT: 0.40 AV: 1 NL: 4.31E5
T: FTMS + p ESI Full ms [50.0000-750.0000]

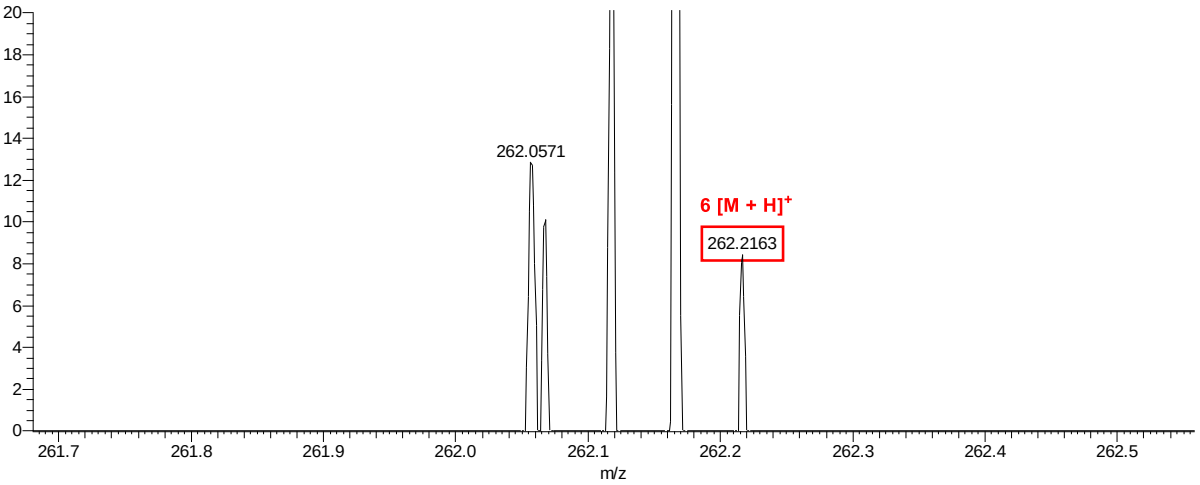

6.2 Ethene-1,1-diyldibenzene Trapping Experiment

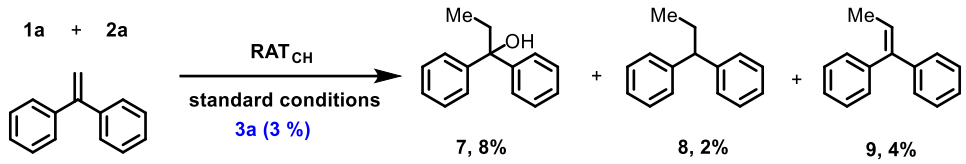

To probe the methyl radical intermediate in our enantioselective C(sp^3)–H bond radical acylation reaction, an ethene-1,1-diyldibenzene trapping experiment was designed and performed. Radical trapping reagent ethene-1,1-diyldibenzene (5.0 eq) was added to the model reaction under the standard conditions by using **RAT$_{CH}$** as a catalyst. The reaction result was analysed by GC, which showed that product **3a** formed in 3% yield. According to the comparisons with standard references, formations of **7, 8** and **9** were confirmed. Based on the GC calibration curves, the yields referring to ethene-1,1-diyldibenzene are 8%, 2%, 4%, respectively, for compounds **7-9**. These results indicated the formation of methyl radical intermediate.

GC calibration curve for **7** is displayed below.

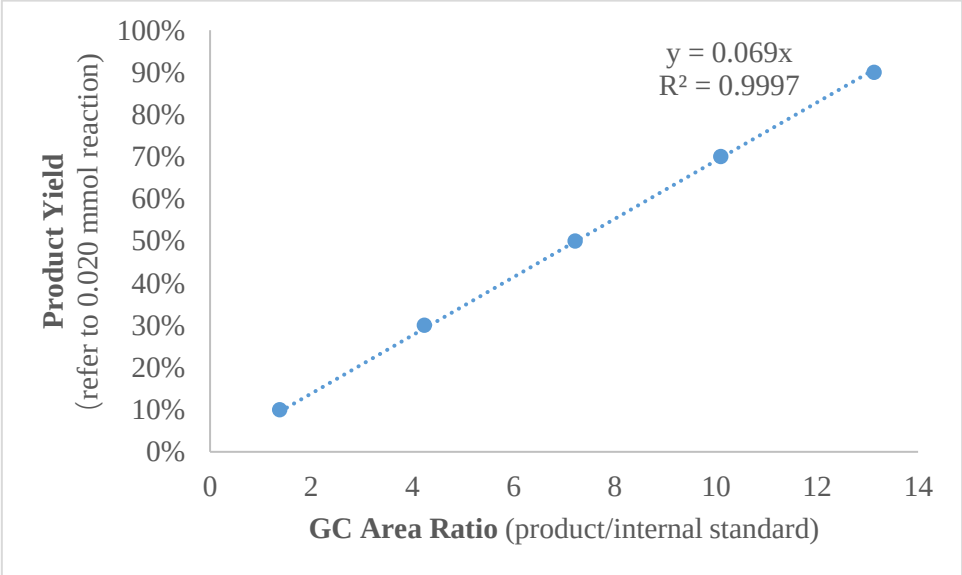

1,1-Diphenylpropan-1-ol (7)

7 is a white solid (144 mg, 68% yield) and the NMR spectra of **7** match the one previously reported in the literature[4].

^{1}H NMR (400 MHz, CDCl$_3$) δ 7.44-7.37 (m, 4H), 7.35-7.26 (m, 4H), 7.25-7.17 (m, 2H), 2.32 (q, J = 7.3 Hz, 2H), 2.06 (s, 1H), 0.88 (t, J = 7.3 Hz, 3H).

^{13}C NMR (100 MHz, CDCl$_3$) δ 146.9, 128.1, 126.7, 126.1, 78.4, 34.4, 8.1.

HRMS (ESI, m/z) calcd. for $C_{15}H_{17}O$ $[M+H-H_2O]^+$ 195.1168, found: 195.1168.

GC calibration curve for **8** is displayed below.

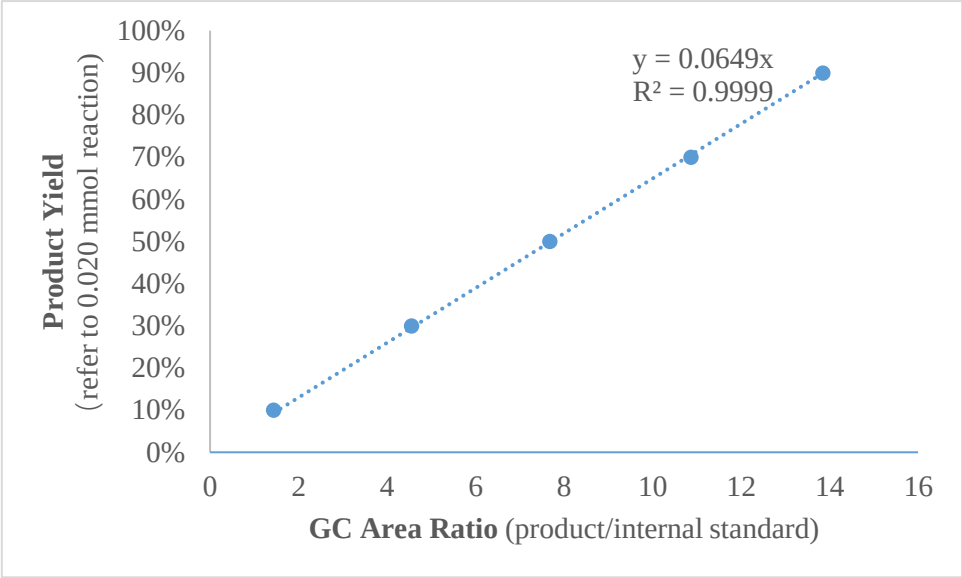

Propane-1,1-diyldibenzene (8)

8 is a colorless liquid (178 mg, 91% yield) and the NMR spectra of **8** match the one previously reported in the literature[5].

^{1}H NMR (400 MHz, $CDCl_3$) δ 7.31-7.20 (m, 8H), 7.21-7.12 (m, 2H), 3.79 (t, J = 7.8 Hz, 1H), 2.07 (p, J = 7.4 Hz, 3H), 0.90 (t, J = 7.3 Hz, 3H).

^{13}C NMR (100 MHz, $CDCl_3$) δ 145.1, 128.3, 127.9, 126.0, 53.2, 28.6, 12.8.

MS (EI, *m/z*) calcd. for $C_{15}H_{16}$ $[M]^+$ 196.1, found: 196.1.

GC calibration curve for **9** is displayed below.

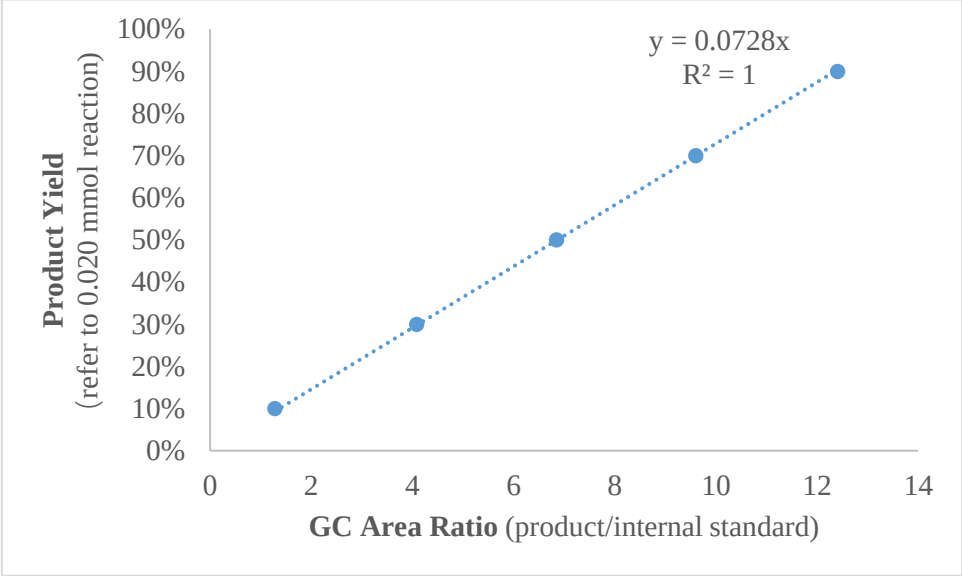

Prop-1-ene-1,1-diyldibenzene (9)

9 is a colorless liquid (413 mg, 85% yield) and the NMR spectra of **9** match the one previously reported in the literature[6].

^{1}H NMR (400 MHz, $CDCl_3$) δ 7.40-7.32 (m, 2H), 7.33-7.26 (m, 1H), 7.29-7.15 (m, 7H), 6.17 (q, J = 7.0 Hz, 1H), 1.75 (d, J = 7.0 Hz, 3H).
^{13}C NMR (100 MHz, $CDCl_3$) δ 142.9, 142.4, 140.0, 130.0, 128.1, 128.0, 127.2, 126.8, 126.7, 124.1, 15.7.
MS (EI, *m/z*) calcd. for $C_{15}H_{14}$ $[M]^+$ 194.1, found: 194.1.

6.3 BHT Trapping Experiment

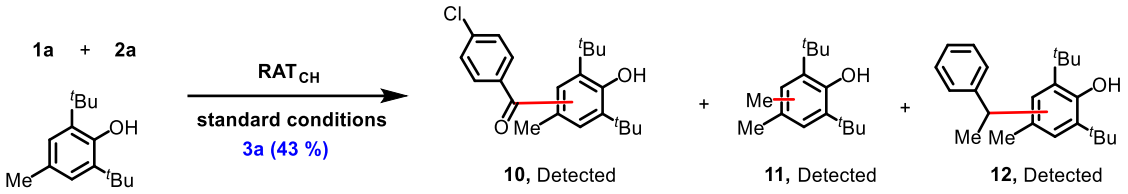

To probe the radical intermediate in our enantioselective C(sp^3)–H bond radical acylation reaction, a BHT (butylated hydroxytoluene) trapping experiment was designed and performed. Radical trapping reagent BHT (5.0 eq) was added to the model reaction under *Conditions C* by using **RAT$_{CH}$** as a catalyst. The reaction result was analysed by GC, HRMS. We found that product **3a** formed in 43% yield. Products **10**, **11** and **12** were detected by HRMS which indicated the formation of the ketyl radical (**Int. C** in Fig. 2a), methyl radical (**Int. D** in Fig. 2a) and benzyl radical (**Int. E** in Fig. 2a).

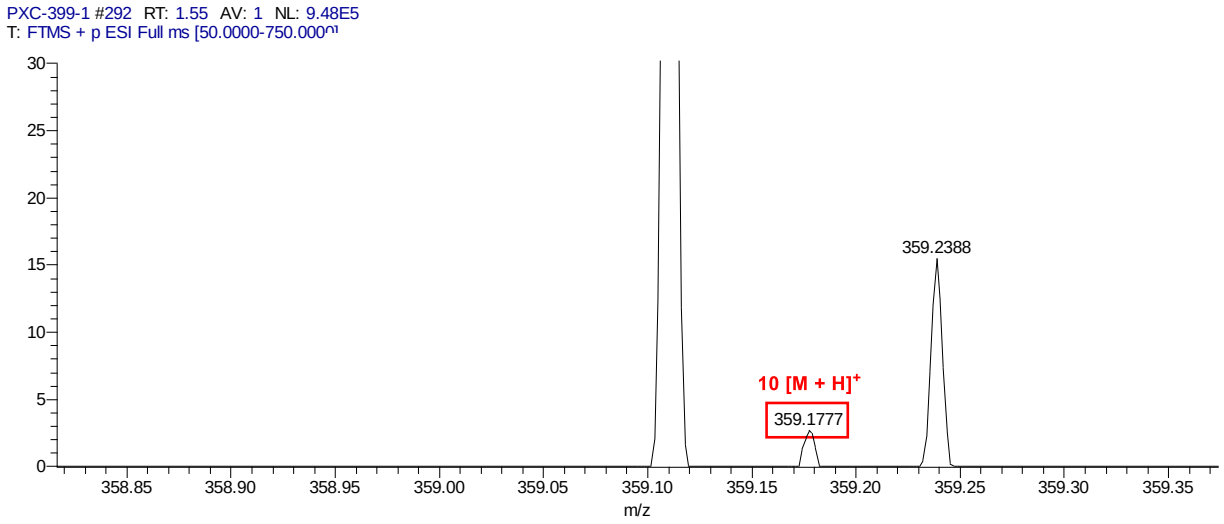

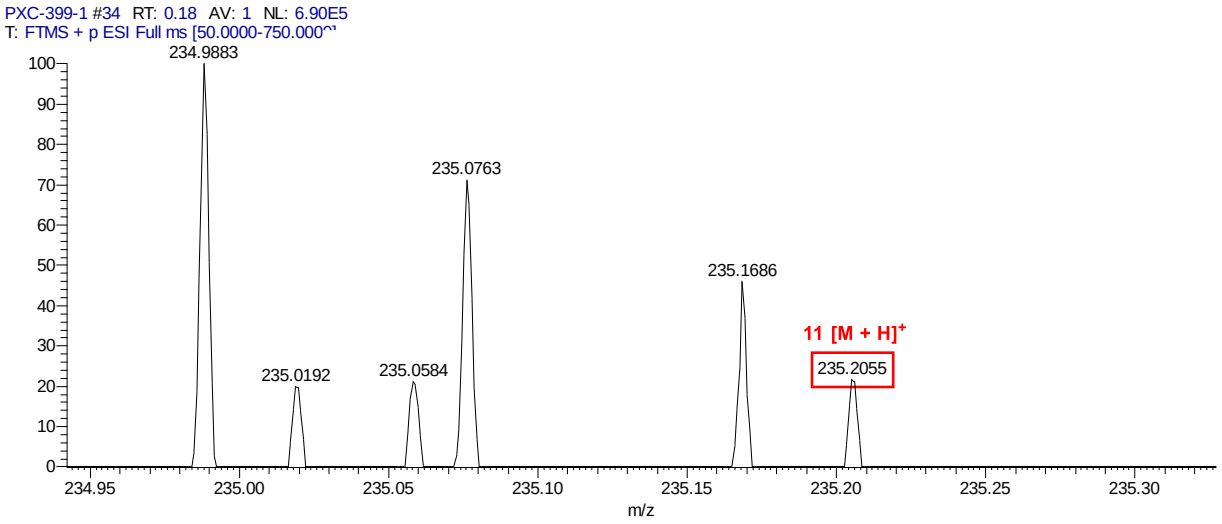
PXC-399-1 #34 RT: 0.18 AV: 1 NL: 6.90E5
T: FTMS + p ESI Full ms [50.0000-750.000^']
234.9883
235.0763
235.1686
235.0192
235.0584
11 [M + H]+
235.2055
m/z

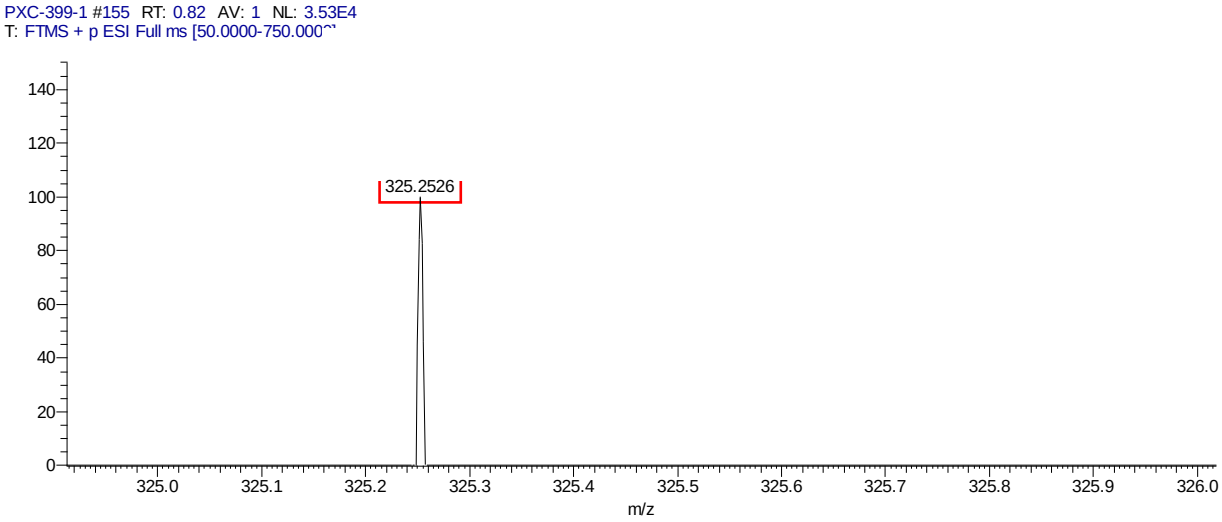
PXC-399-1 #155 RT: 0.82 AV: 1 NL: 3.53E4
T: FTMS + p ESI Full ms [50.0000-750.000^']
325.2526
m/z

6.4 Kinetic Isotope Effect Experiments

4-(Propan-2-yl-2-d)-1,1'-biphenyl (**2l-*d*$_2$**) was prepared as a white solid (164 mg, 89%) following previously reported procedure[7]. Almost 100% deuteration ratio was achieved according to the ^{1}H NMR spectrum.

^{1}H NMR (400 MHz, CDCl$_3$) δ 7.61-7.55 (m, 2H), 7.55-7.49 (m, 2H), 7.46-7.38 (m, 2H), 7.36-7.24 (m, 3H), 1.26 (s, 3H).

^{13}C NMR (100 MHz, CDCl$_3$) δ 143.3, 141.2, 138.6, 128.7, 128.3, 127.1, 127.0, 126.9, 27.8 (t, J = 19.6 Hz), 15.4.

MS (EI, *m/z*) calcd. for $C_{14}H_{12}D_2$ $[M]^+$ 184.1, found: 184.2.

Parallel reactions:

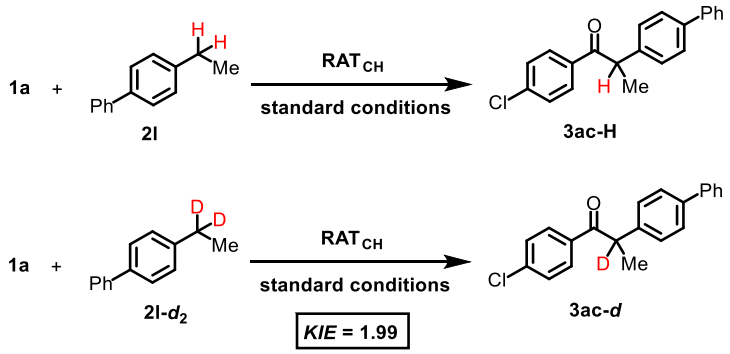

Five vials in parallel, were added 4-chlorobenzaldehyde 1a (0.004 mmol), 4-ethyl-1,1'-biphenyl (0.016 mmol), HAT reagent 2 (0.020 mmol), RAT$_{CH}$ (2 mol%), Eosin Y (3 mol%), 20 v/v % DMSO in 100 mM MOPS buffer (pH 8.0, containing 2.5 mM $MgSO_4$ and 0.15 mM ThDP); total volume of the reaction mixture was 0.8 mL each. The vials were stirred for 10 min, 20 min, 30 min, 40 min, 50 min, respectively, at room temperature under N_2 atmosphere with the irradiation of 450-460 nm LEDs. Then the mixtures were analysed by GC for the determination of yields at different time. These results were repeated twice, to get average yields for yield-time curves.

Following the same steps but using 4-(propan-2-yl-2-*d*)-1,1'-biphenyl instead, an initial rate for deuterated substrate was therefore determined.

Time (min)	**3ac-H** (GC yield) (average of duplicate runs)	**3ac-*d*** (GC yield) (average of duplicate runs)
10	6.42	3.11
20	10.64	6.39
30	16.44	8.65
40	20.27	9.23
50	22.65	11.54

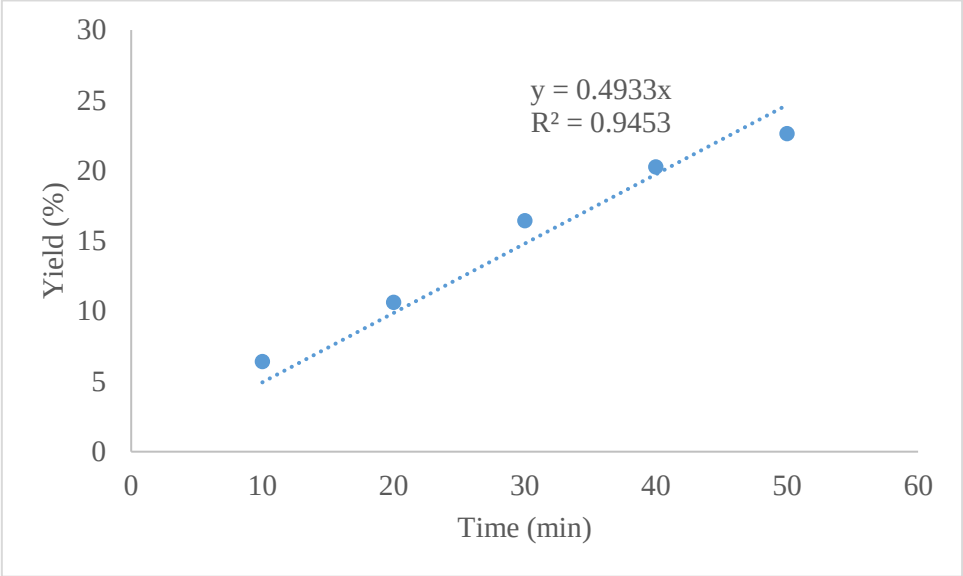

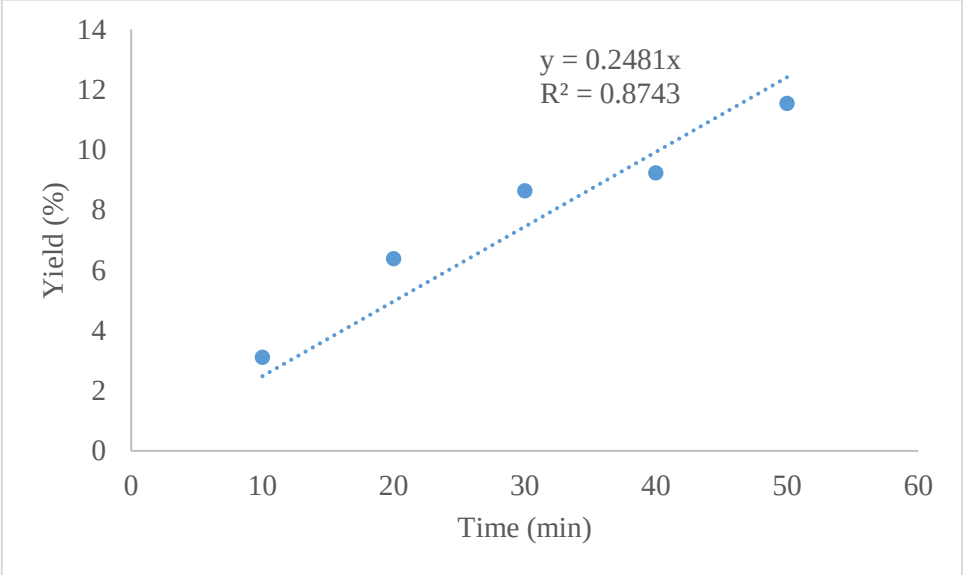

GC calibration curve for **3ac** is displayed below.

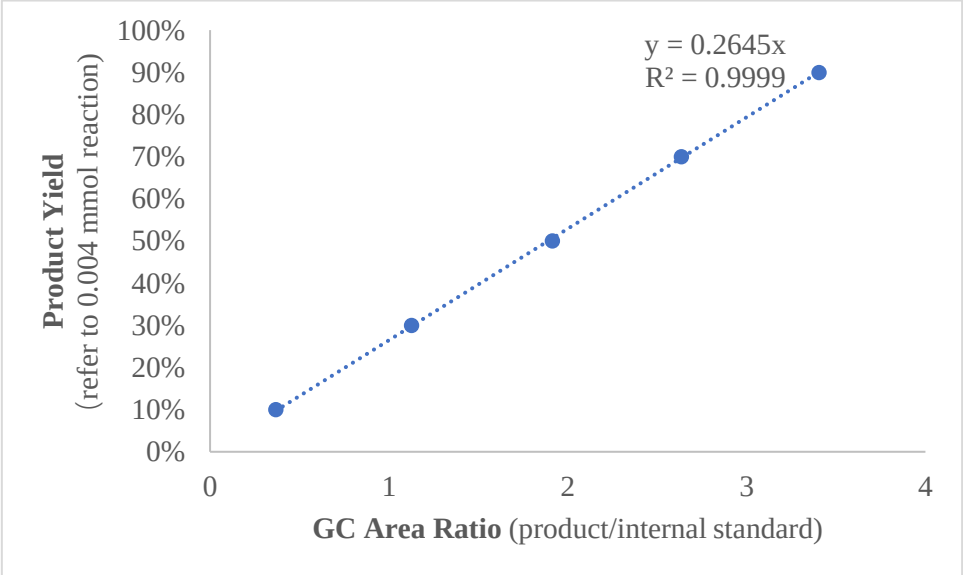

Competition reactions:

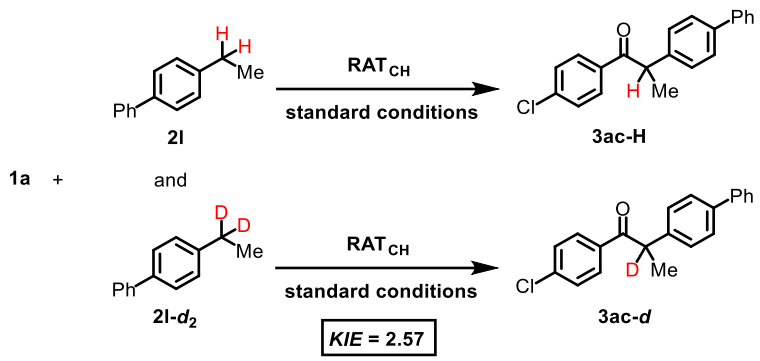

Ratio of the Product

Run	Total GC yield	Ratio of **3ac-H**, **3ac-*d*** in ^{1}H NMR	k_H/k_d
1	14.59 %	0.72 : 0.28	2.57
2	15.78 %	0.72 : 0.28	2.57

Conditions: 4-chlorobenzaldehyde **1a** (0.004 mmol), 4-ethyl-1,1'-biphenyl (0.008 mmol) and 4-(propan-2-yl-2-*d*)-1,1'-biphenyl (0.008 mmol), HAT reagent 2 (0.020 mmol), **RAT$_{CH}$** (2 mol%), Eosin Y (3 mol%), 20 v/v % DMSO in 100 mM MOPS buffer (pH 8.0, containing 2.5 mM $MgSO_4$ and 0.15 mM ThDP) were stirred for **3 h** at room temperature under N_2 atmosphere with the irradiation of 450-460 nm LEDs; total volume of the reaction is 0.8 mL. Running six reactions in parallel. After 3 h, two for GC yield determination, while the rest of reactions mixture was combined and then extracted by ethyl acetate and purified by TLC. The resultant pure **3ac** was subjected to ^{1}H NMR. The KIE ratio was therefore determined by quantitative ^{1}H NMR spectroscopy.
First run: KIE = 2.57; second run: KIE = 2.57; average: KIE = 2.57.

Note: we have not considered the pH effect of deuterium on the KIE. In our reaction scheme, the hydrogen atom transfer (HAT) pathway, occurring between the methyl radical and ethylbenzene, is responsible for the C-H/D cleavage. Thus, the pH effect of deuterium is expected to play minor roles in this radical pathway.

^{1}H NMR (400 MHz, $CDCl_3$) spectra of pure **3ac** for the two runs were showed as follows:

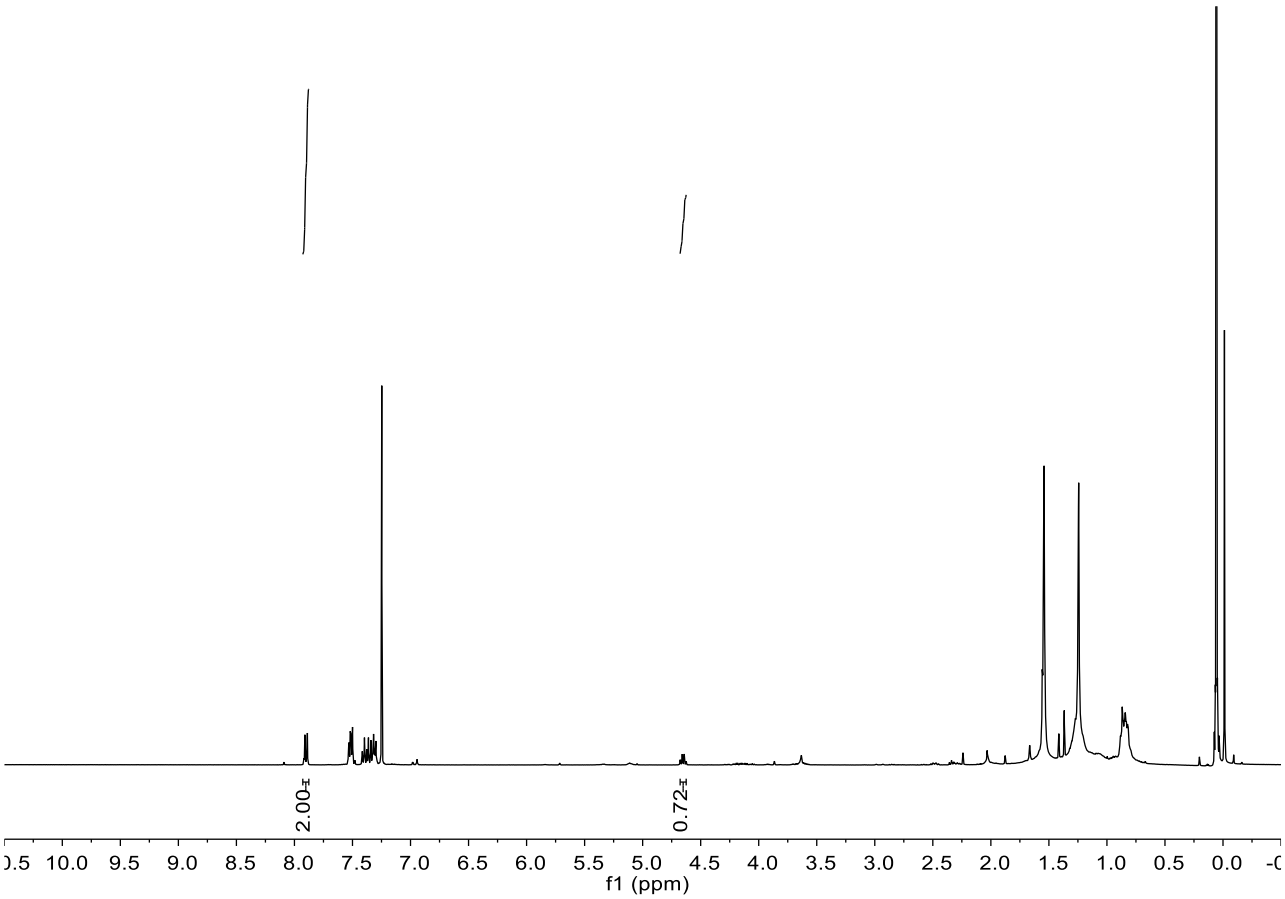
2.00
0.72
10.0 9.5 9.0 8.5 8.0 7.5 7.0 6.5 6.0 5.5 5.0 4.5 4.0 3.5 3.0 2.5 2.0 1.5 1.0 0.5 0.0
f1 (ppm)

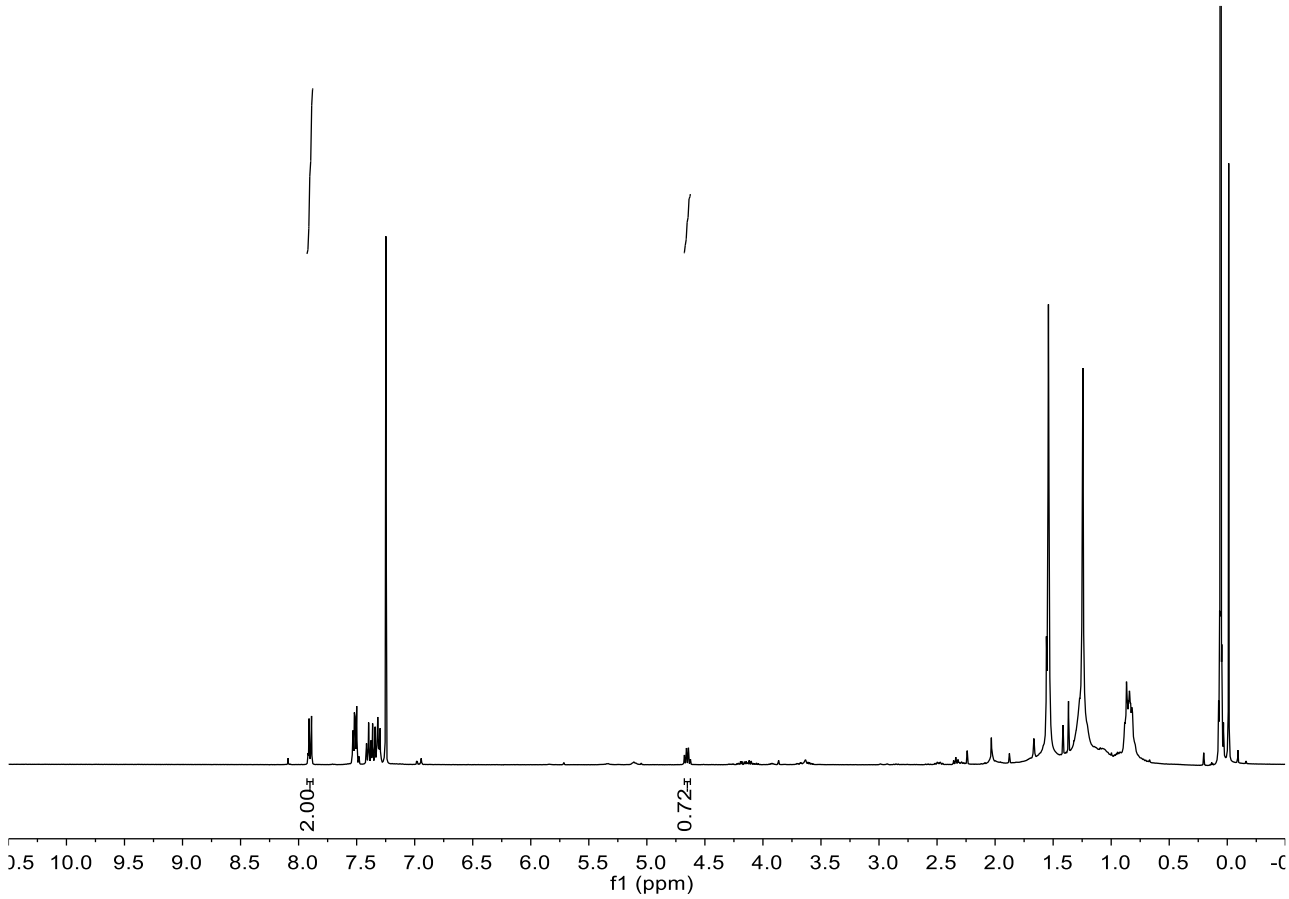
2.00
0.72
10.0 9.5 9.0 8.5 8.0 7.5 7.0 6.5 6.0 5.5 5.0 4.5 4.0 3.5 3.0 2.5 2.0 1.5 1.0 0.5 0.0
f1 (ppm)

6.5 Stern-Volmer Luminescence Quenching Studies

To identify the key species that interacts with the excited Eosin Y, Stern-Volmer luminescence quenching experiments were designed and conducted.

Emission intensities were recorded on a MolecularDevice SpectraMax M3 reader. Samples for the quenching experiments were prepared in a 4 mL screw-top quartz cuvette under a N_2 atmosphere. Solutions of different quenchers in degassed DMSO were prepared. Conditions: different amounts (0.02 mM, 0.04 mM, 0.06 mM, 0.08 mM, 0.10 mM) of quencher solution were added to a solution of the photocatalyst Eosin Y (0.02 mM) in MOPS buffer (100 mM, pH 8.0, containing 2.5 mM $MgSO_4$ and 0.15 mM ThDP). Each solution was with a total volume of 2 mL with 20 v/v % DMSO. Excitation of the sample was irradiated at 455 nm and emission was measured at 548 nm. As shown in Supplementary Fig. 8a, excited Eosin Y couldn't be quenched by HAT reagent 2. On the other hand, the quenching of the excited Eosin Y by the mixture of **RAT$_{CH}$** and **1a** were recorded although not that efficient (Supplementary Fig. 8b).

These results exclude an oxidative quenching pathway that excited Eosin Y was single electron oxidized by HAT reagent 2.

6.6 Discussion on the Organophotoredox Catalysis

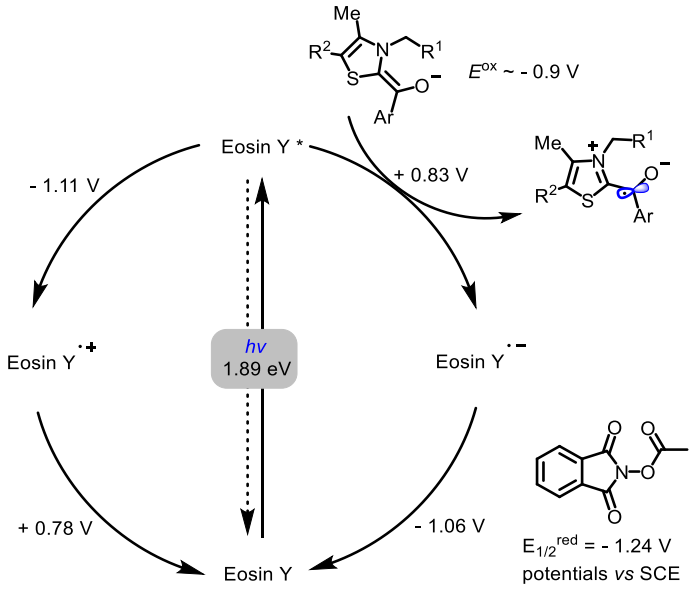

According to the literature, the oxidative potential of Breslow intermediate derivative (**Int. B** derivative) is around − 0.9 V vs SCE[8] which is easily single electron oxidized by Eosin Y* ($E_{1/2}$ (Eosin Y* / Eosin $Y^{\bullet-}$) = + 0.83 V vs SCE)[9]. Additionally, our spectroelectrochemical studies indicated the enzymatic Breslow intermediate is prone to oxidation (Supplementary Fig. 10). The reduction potential of HAT reagent 2 is around − 1.24 V vs SCE[10] and it may be reduced by Eosin $Y^{\bullet-}$ ($E_{1/2}$ (Eosin $Y^{\bullet-}$ / Eosin Y) = − 1.06 V). These means the proposed reductive quenching photoredox cycle is possible.

In the alternative oxidative quenching photoredox cycle, HAT reagent 2 was single electron reduced by ($E_{1/2}$ (Eosin Y* / Eosin $Y^{\bullet+}$) = − 1.11 V vs SCE) and then Breslow intermediate derivative (**Int. B**) was single electron oxidized by Eosin $Y^{\bullet+}$ ($E_{1/2}$ (Eosin $Y^{\bullet+}$ / Eosin Y) = + 0.78 V). This pathway was excluded by Stern-Volmer luminescence quenching studies between Eosin Y* and HAT reagent 2.

Breslow intermediate derivatives were considered as strong reductive species (Supplementary method section 6.7). But direct single electron transfer between HAT reagent 2 and Breslow intermediate **Int. B** was excluded by the control experiment in which no product was formed without Eosin Y (Supplementary Table 19).

The analysis of redox potentials suggests a reductive quenching pathway of the organophotoredox catalysis.

6.7 UV-Visible Spectroelectrochemical Studies

To investigate the transformation of the enzymatic Breslow intermediate formation between **1a** and **RAT$_{CH}$** in the MOPS buffer, in situ UV-visible spectroelectrochemical techniques was employed. Supplementary Fig. 9a-9d shows the cyclic voltammograms of the four samples, the compositions of which are MOPS buffer only, MOPS buffer + **1a**, MOPS buffer + **RAT$_{CH}$**, and MOPS buffer + **1a** + **RAT$_{CH}$**, respectively, for the samples 1, 2, 3, 4.

The experiment employed a three-electrode system comprising a reticulated vitreous carbon (RVC) working electrode, a platinum mesh counter electrode, and an Ag/AgCl quasi-reference electrode (QRE) (Supplementary Fig. 1c). The scan potential ranged from − 2.0 V → + 1.5 V → − 2.0 V, with a minimum scan rate of 1 mV/s due to the use of a thin-layer electrochemical cell. In the optical transparent thin-layer electrochemical cell (with a path length of 0.2 mm), using sample 1 as the background, UV-Vis spectra during the electrochemical reaction process were recorded for the four samples (Supplementary Fig. 9e-9h). As shown in Supplementary Fig. 9h, prior to applying the potential, sample 4 exhibited characteristic absorption peaks of protein at 280 nm. As the potential was gradually decreased from + 1.5 V to − 2.0 V, a new broad absorption band at 424 nm first appeared and then disappeared in the sample 4, as depicted in the magnified view of Supplementary Fig. 9h. This band may be characteristic of the enzymatic Breslow-int.-derived ketyl radical (**Int. C**) as no comparable changes were observed in the control.

Careful analysis of the characteristic absorption peak at 424 nm for sample 4 (Supplementary Fig. 10), we can see: (1) During the potential ramp from − 2.0 V to + 1.5 V, no significant sign observed. At + 1.5 V, the corresponding enzyme/ThDP-**1a** complex is supposed to be the Breslow-int.-derived cation intermediate, which according to literature[11] and calculated UV-vis absorption spectra (Supplementary Fig. 11), exhibits no visible light abortion band. (2) During the potential ramp from + 1.5 V to − 2.0 V, the absorption band at 424 nm was observed at + 1.2 V, suggesting the SET reduction of the Breslow-int.-derived cation intermediate to the ketyl radical. At + 0.4 V, the absorption band at 424 nm reached its maximum, indicating peak generation of the ketyl radical. Under negative potential − 2.0 V (ranging from + 1.5 V to − 2.0 V), the reverse electrochemical conditions likely resulted in reduction the ketyl radical back to the initial Breslow-int. intermediate (**Int. B**), leading to the disappearance of the absorption peak at 424 nm. Again, the visible-light absorption spectrum of the Breslow int. aligns to the literature report[11] and the calculated UV-Vis absorption spectra.

To further probe the ketyl radical intermediates at ~ + 0.4 V, samples-2, 3, 4 were taken during CV scanning at a reverse potential of − 0.1 V (ranging from + 1.5 V to − 2.0 V), followed by characterization using EPR (Supplementary Fig. 10b). A characteristic EPR signal was detected for Sample 4 (at − 0.1 V). Based on our previous report[1], this signal could be assigned to be the indicator of the enzymatic Breslow-int.-derived ketyl radical (**Int. C**). Furthermore, time-dependent decay process of the UV-vis characteristic absorption peak at 424 nm after the cessation of applying a potential of + 0.396 V was depicted in Supplementary Fig. 10c-d. After 80 minutes, the intensity of the absorption peak gradually decreases until it nearly disappears, which is consistent with the quenching process of a radical intermediate.

6.8 Michaelis Menten Kinetics Measurement

Steady-state kinetic studies were carried out using purified enzyme *Pf*BAL and **RAT$_{CH}$**, respectively, with the concentration of 4-chlorobenzaldehyde **1a** ranging from 0.5 mM to 30 mM. To determine the initial reaction rates, we measured the amount of **3a** formed at different time points: 10 min, 15 min, 20 min, 25 min, and 30 min for the *Pf*BAL-catalysed reactions, and 2 min, 4 min, 6 min, 8 min, and 10 min for the **RAT$_{CH}$**-catalysed reactions. Then, the initial rates were calculated based on the **3a**-concentration-time curves. Rates were repeated twice. Michaelis Menten curves were thereby obtained based on kinetic studies.

Experimental procedure: Stock solutions of **1a** in DMSO with varying concentrations were prepared by serial dilution (1200 mM, 800 mM, 600 mM, 400 mM, 320 mM, 240 mM, 160 mM, 80 mM, 40 mM and 20 mM; this corresponded to a final concentration of 30 mM, 20 mM, 15 mM, 10 mM, 8 mM, 6 mM, 4 mM, 2 mM, 1 mM and 0.5 mM, respectively, when 20 µL of the stock solution was used for each reaction). The initial rate measurements using *Pf*BAL or **RAT$_{CH}$** (0.05 mM) were performed in ~ 620 µL MOPS buffer (100 mM, 2.5 mM $MgSO_4$, 0.15 mM ThDP, pH 8.0) and 20 µL Eosin Y (150 µM final concentration), 140 µL DMSO containing ethylbenzene **2a** (300 mM final concentration) and HAT reagent 2 (400 mM final concentration); substrate **1a** (20 µL, 0.5 mM to 20 mM final concentration) in a 4 mL clear glass vial containing a stir bar, illuminated with a 450-460 nm LEDs. Accordingly, after illumination with stirring, ethyl acetate (1.0 mL) and 20.0 µL of an internal standard stock (2 v/v % of *n*-dodecane in ethyl acetate) were added to the reaction mixture and mixed thoroughly. The organic phase was separated and then analysed by GC to determine the amount of **3a** formed.

Initial rates under different concentrations of **1a** catalysed by *Pf*BAL:

1a (mM)	**First test: v_1** (mM/s)	**Second test: v_2** (mM/s)
0.5	0.000012221	0.0000048671
1	0.000011275	0.0000094348
2	0.000012638	0.000015099
4	0.000030771	0.000029311
6	0.000033136	0.000029404
8	0.000044347	0.000038148
10	0.000048971	0.000048494
15	0.000047546	0.000058118
20	0.000050455	0.000048137
30	0.000061991	0.00005983

Michaelis Menten curves for *Pf*BAL:

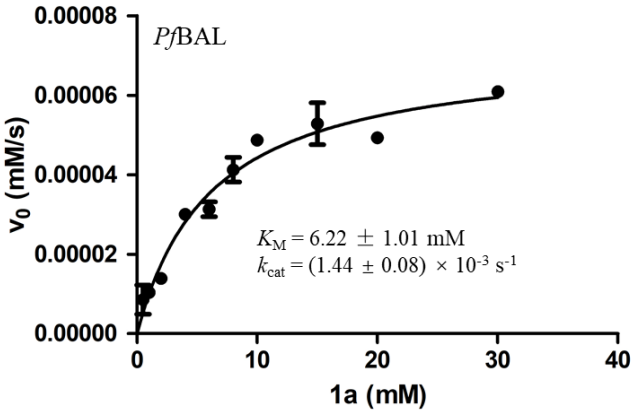

Initial rates under different concentrations of **1a** catalysed by **RAT$_{CH}$**:

1a (mM)	**First test: v_1** (mM/s)	**Second test: v_2** (mM/s)
0.5	0.000033236	0.000050165
1	0.00012037	0.00019191
2	0.00029106	0.0002392
4	0.00048471	0.00058282
6	0.00060597	0.00064264
8	0.00082953	0.00077988
10	0.00085366	0.00089468
15	0.00098636	0.00092937
20	0.00096786	0.0011296
30	0.0011138	0.0011399

Michaelis Menten curves for **RAT$_{CH}$**:

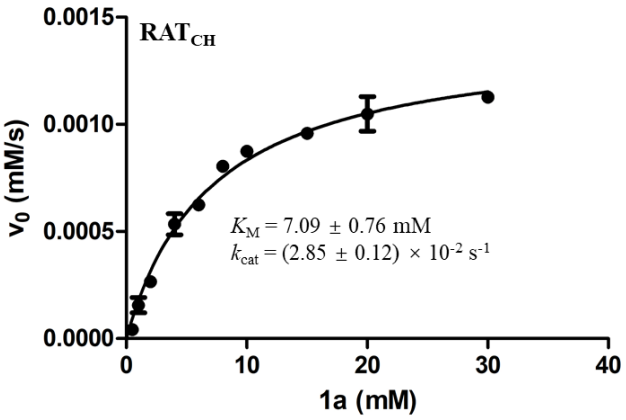

7. Computational Studies

7.1 System Setup and Molecular Dynamics (MD) Simulations

The structures of mutants (W163C/Y397A/A480G/T481L) were built based on SWISS-MODEL[12] homology modelling, the template was their wild-type structure (PDB code: 3D7K). **2a** radical (**Int. E**) was docked using AutoDock Vina[13]. It is worth noting that when **Int. E** was docked into the vacated position, two different binding modes were obtained (H-forward & H-backward, see Fig. 4f). We assigned the protonation status of titratable residues (His, Glu, Asp) based on the pKa values from the PROPKA software[14] in combination with a careful visual inspection of local hydrogen-bonded networks. His21, His29, His40, His49, His113, His130, His137, His185, His294, His318, His371, His374, and His280 were protonated at the ε position, His55, His286 and His 483 were protonated at the δ position, while all the Glu and Asp residues were deprotonated. The Amber ff14SB[15] force field was employed for the protein residues, while the general AMBER GAFF[16] was used for substrates. The partial atomic charges of substrates were obtained from the RESP[17] at the B3LYP/6-31G(d) level of theory. Sodium ions were added to the protein surface to neutralize the total charge of the systems. Finally, the resulting system was solvated in a rectangular box of TIP3P waters extending up to a minimum distance of 16 Å from the protein surface. After proper setup, the whole system was fully minimized using combined steepest descent and conjugate gradient method. Then, the system was gently annealed from 0 to 300 K under NVT ensemble for 50 ps with a weak restraint of 25 kcal/mol/Å on protein. To achieve a uniform density after heating dynamics, 1 ns of density equilibration was performed under the NPT ensemble at the target temperature of 300 K and target pressure of 1.0 atm. Afterward, further equilibrated the system for 4 ns under the NPT ensemble to get the well-settled pressure and temperature. Finally, a 200 ns productive MD simulation was performed under the NPT ensemble. During all MD simulations, the covalent bonds containing hydrogen were constrained using SHAKE[18] and an integration step of 2 fs was used. All MD simulations were performed with GPU version of Amber 20[19] package.

7.2 QM/MM Calculations for Enzymatic Reactions

All QM/MM[20] calculations were performed using ChemShell[21] combining Turbomole[22] for the QM region and DL_POLY[23] for the MM region. The electronic embedding scheme was used to account for the polarizing effect of the enzyme environment on the QM region. Hydrogen link atoms with the charge-shift model were applied to treat the QM/MM boundary. For radical cross-coupling reactions, the QM region consists of the Int. C and Int. E complex (Fig. 4f). During QM/MM geometry optimizations, the QM region was studied with the B3LYP density functional with two levels of theory. For geometry optimization, the double-ζ basis set def2-SVP, collectively labeled as B1, was used. The energies were further corrected with the larger basis set def2-TZVP for all atoms, labeled as B2. Dispersion corrections computed with Grimme's D3 method were included in all QM calculations.

7.3 QM Calculations for Radical Generation

All DFT calculations were performed with the Gaussian 16, Revision A.03 software[24]. All geometry optimizations are conducted in conjunction with the SMD[25] continuum solvation model at the B3LYP-D3/def2-SVP level of theory. The energies were further refined with the larger basis set def2-TZVP for all atoms. The solvent of chlorobenzene ($\varepsilon = 5.6$) was used to simulate the protein environment effects. Harmonic frequency calculations were performed at the same level of theory as the optimizations to estimate the Gibbs free energies corrections.

7.4 Spectral Calculations

The possible key intermediates (see Supplementary Fig. 11) were first optimized at wB97XD/6-31+G(d) level. Then, the single-point TDDFT calculations at wB97XD/6-31+G(d) levels were performed to compute the UV-Vis spectrum. All TDDFT calculations were performed with Gaussian 16, Revision A.03.

Note: Based on our mechanistic studies, it is suggested that the photoinduced generation of the prochiral radical (**Int. E**) occurs outside the active site, with minimal influence from the protein environment. Therefore, we simplified the computational model by using a QM model for the calculations related to the formation of **Int. E** (Fig. 4c and 4f). Regarding the radical cross-coupling step (**Int. E** + **Int. C** → **Int. F**), this must occur within the active site. Consequently, we used a QM/MM model for the calculations associated with this step.

Additionally, we used the B3LYP-D3/def2-SVP level to optimize the structure of key species (such as, Fig. 4f & h) in the ground state. For the excited-state properties calculations, we have applied the wB97XD/6-31+G(d) level to calculate the key excited-state species (see, Fig 4c & Supplementary Fig. 11). The function of wB97XD has been demonstrated to be practical for studying the excited properties according to extensive work from our group and other groups[26,27].

8. Experimental and Characterization Data of Racemic Products

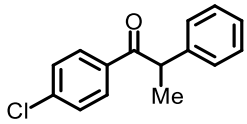

1-(4-Chlorophenyl)-2-phenylpropan-1-one (3a)

By using the typical procedure described in Section 4, the reaction of 4-chlorobenzaldehyde **1a** (0.004 mmol) and ethylbenzene **2a** (0.016 mmol) catalysed by **RAT$_{CH}$** (2 mol%) afforded **3a** in 61% **GC yield** (average of duplicate runs), with a 94% ee.

GC calibration curve for **3a** is displayed below.

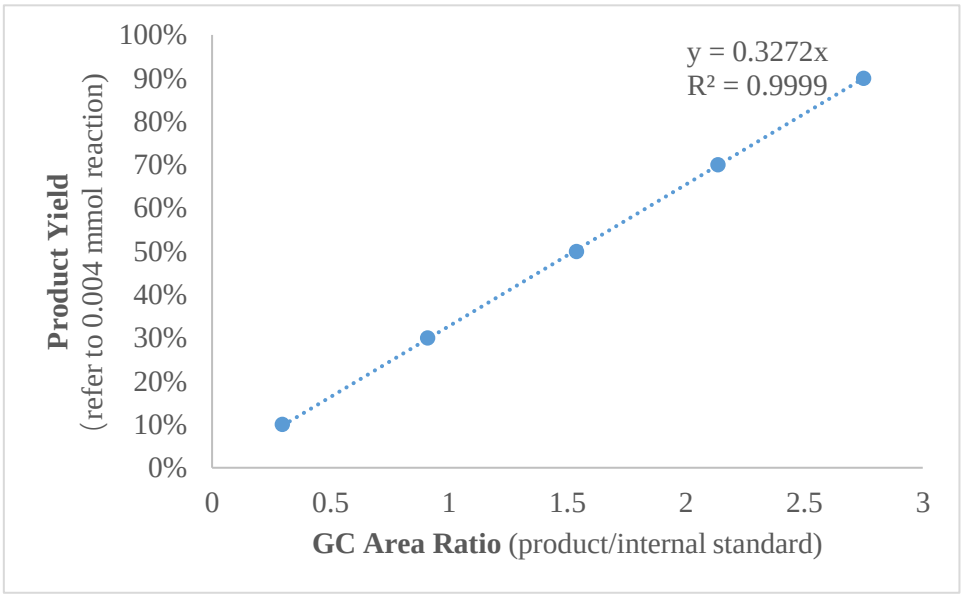

Enantiomeric excess was established by HPLC analysis using a Chiralpak AS-H column (HPLC: AS-H, 254 nm, *n*-hexane/isopropanol = 95:5, flow rate 0.5 mL/min, 30 °C, t_r (major) = 9.27 min, t_r (minor) = 10.23 min).

HPLC trace of *rac*-**3a**:

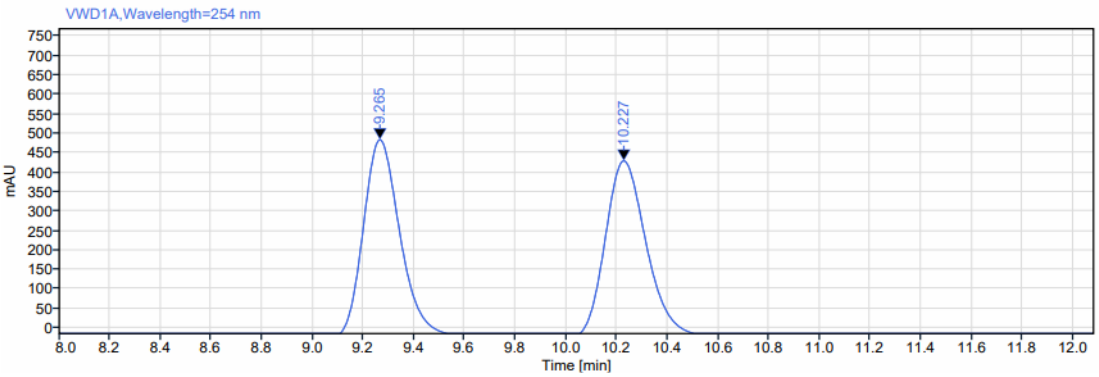

Signal: VWD1A,Wavelength=254 nm

RT [min]	Type	Area	Height	Area%
9.265	BB	5268.10	512.00	49.99
10.227	BB	5270.10	457.42	50.01
	Sum	10538.19		

HPLC trace of enantioenriched-**3a** obtained in a 0.004 mmol reaction:

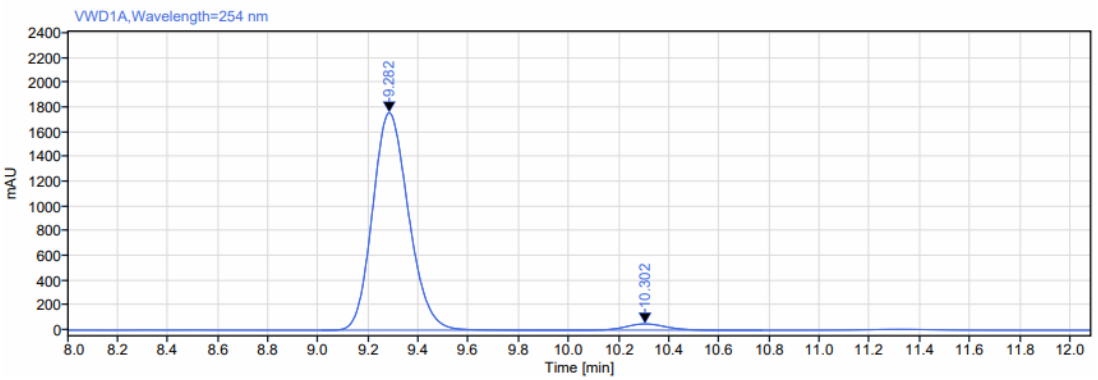

Signal: VWD1A,Wavelength=254 nm

RT [min]	Type	Area	Height	Area%
9.282	BB	17545.98	1758.64	96.86
10.302	BB	568.61	50.77	3.14
	Sum	18114.59		

Rac-**3a** is a colorless oil (1.22 g, 84%). The NMR spectra of *rac*-**3a** match the one previously reported[28].

^{1}H NMR (400 MHz, $CDCl_3$) δ 7.91-7.83 (m, 2H), 7.37-7.30 (m, 2H), 7.31-7.16 (m, 5H), 4.61 (q, J = 6.8 Hz, 1H), 1.52 (d, J = 6.8 Hz, 3H).

^{13}C NMR (100 MHz, $CDCl_3$) δ 199.0, 141.2, 139.1, 134.7, 130.2, 129.1, 128.8, 127.7, 127.0, 48.1, 19.4.

MS (EI, *m/z*) calcd. for $C_{15}H_{13}ClO$ $[M]^+$ 244.1, found: 244.0.

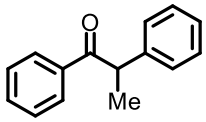

1,2-Diphenylpropan-1-one (3b)

By using the typical procedure described in Section 4, the reaction of benzaldehyde **1b** (0.004 mmol) and ethylbenzene **2a** (0.016 mmol) catalysed by **RAT$_{CH}$** (2 mol%) afforded **3b** in 59% **GC yield** (average of duplicate runs), with a 88% ee.

GC calibration curve for **3b** is displayed below.

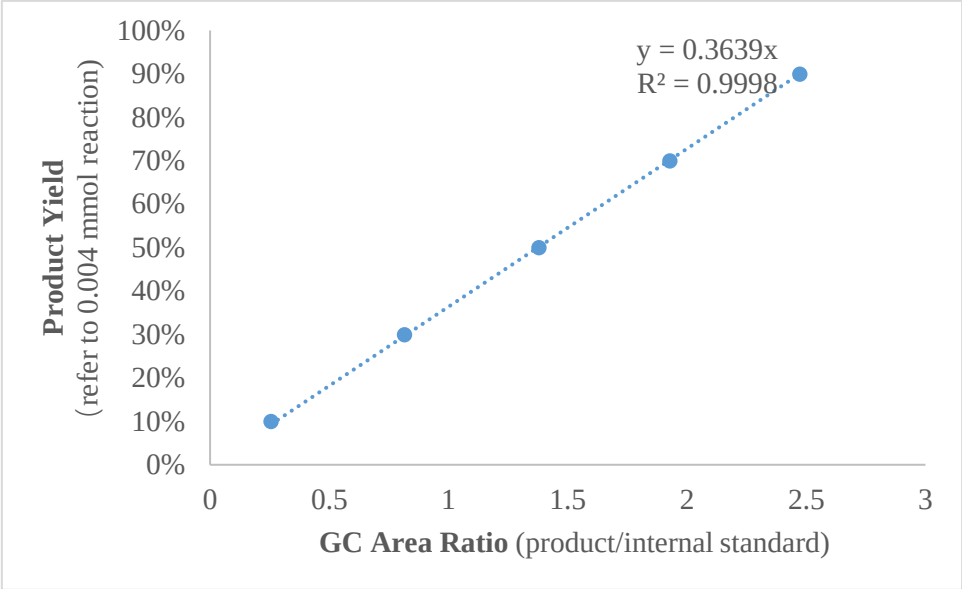

Enantiomeric excess was established by HPLC analysis using a Chiralpak AS-H column (HPLC: AS-H, 254 nm, *n*-hexane/isopropanol = 95:5, flow rate 0.5 mL/min, 30 °C, t_r (major) = 9.07 min, t_r (minor) = 9.77 min).

HPLC trace of *rac*-**3b**:

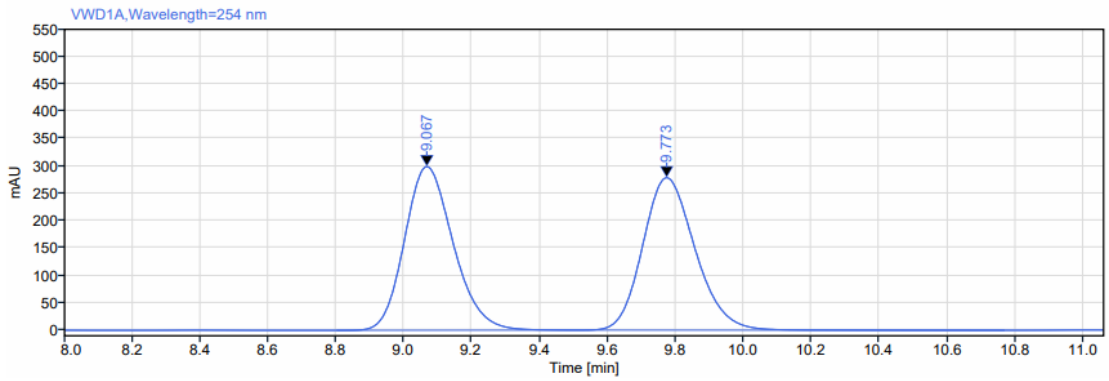

Signal: VWD1A,Wavelength=254 nm

RT [min]	Type	Area	Height	Area%
9.067	BB	2976.54	299.11	49.94
9.773	BB	2983.20	278.59	50.06
	Sum	5959.74		

HPLC trace of enantioenriched-**3b** obtained in a 0.004 mmol reaction:

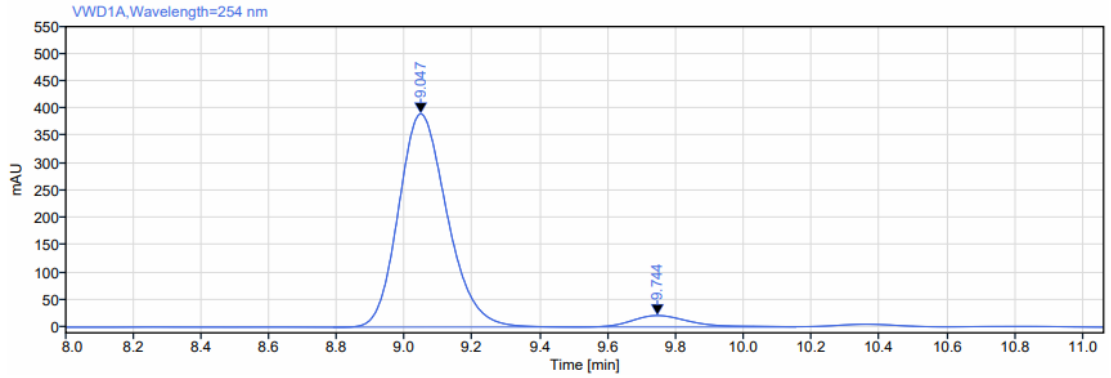

Signal: VWD1A,Wavelength=254 nm

RT [min]	Type	Area	Height	Area%
9.047	BB	3878.69	389.94	93.92
9.744	BV	251.19	20.96	6.08
	Sum	4129.87		

Rac-**3b** is a colorless oil (862 mg, 82%). The NMR spectra of *rac*-**3b** match the one previously reported[29].

^{1}H NMR (400 MHz, $CDCl_3$) δ 7.98-7.93 (m, 2H), 7.51-7.42 (m, 1H), 7.41-7.33 (m, 2H), 7.31-7.26 (m, 4H), 7.24-7.15 (m, 1H), 4.67 (q, J = 6.8 Hz, 1H), 1.53 (d, J = 6.8 Hz, 3H).

^{13}C NMR (100 MHz, $CDCl_3$) δ 200.3, 141.4, 136.5, 132.7, 128.9, 128.7, 128.4, 127.7, 126.9, 47.9, 19.5.

MS (EI, *m/z*) calcd. for $C_{15}H_{14}O$ $[M]^+$ 210.1, found: 210.1.

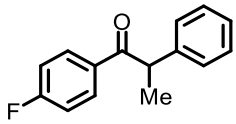

1-(4-Fluorophenyl)-2-phenylpropan-1-one (3c)

By using the typical procedure described in Section 4, the reaction of 4-fluorobenzaldehyde **1c** (0.004 mmol) and ethylbenzene **2a** (0.016 mmol) catalysed by **RAT$_{CH}$** (2 mol%) afforded **3c** in 66% **GC yield** (average of duplicate runs), with a 94% ee.

GC calibration curve for **3c** is displayed below.

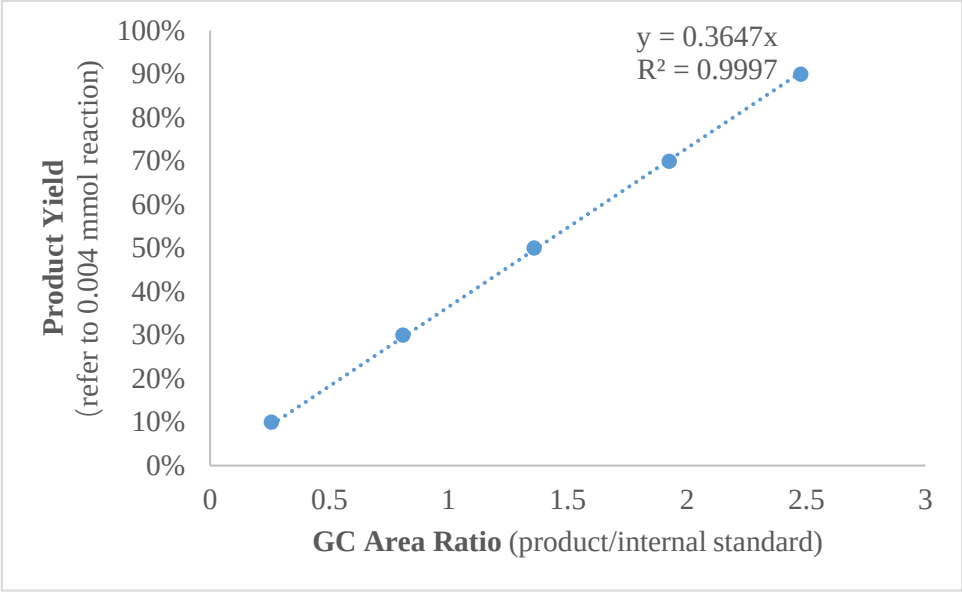

Enantiomeric excess was established by HPLC analysis using a Chiralpak AS-H column (HPLC: AS-H, 254 nm, *n*-hexane/isopropanol = 95:5, flow rate 0.5 mL/min, 30 °C, t_r (major) = 9.21 min, t_r (minor) = 10.21 min).

HPLC trace of *rac*-**3c**:

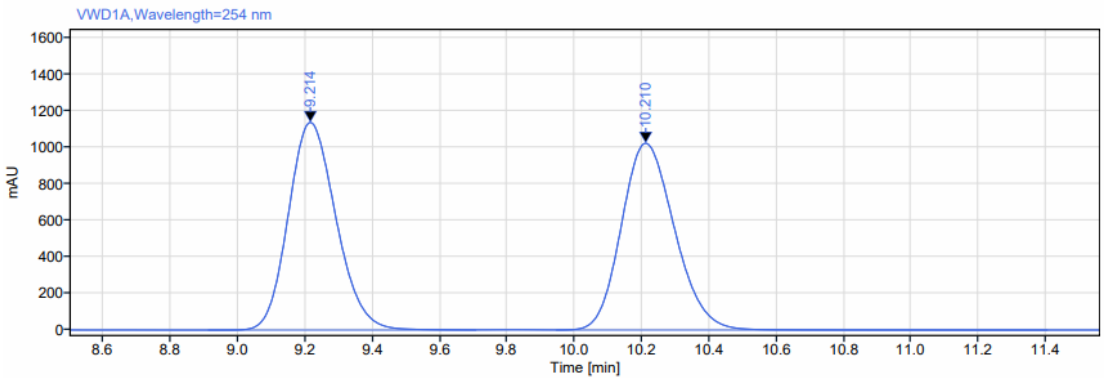

Signal: VWD1A,Wavelength=254 nm

RT [min]	Type	Area	Height	Area%
9.214	BV	11221.34	1139.83	49.89
10.210	VB	11272.59	1025.48	50.11
	Sum	22493.92		

HPLC trace of enantioenriched-**3c** obtained in a 0.004 mmol reaction:

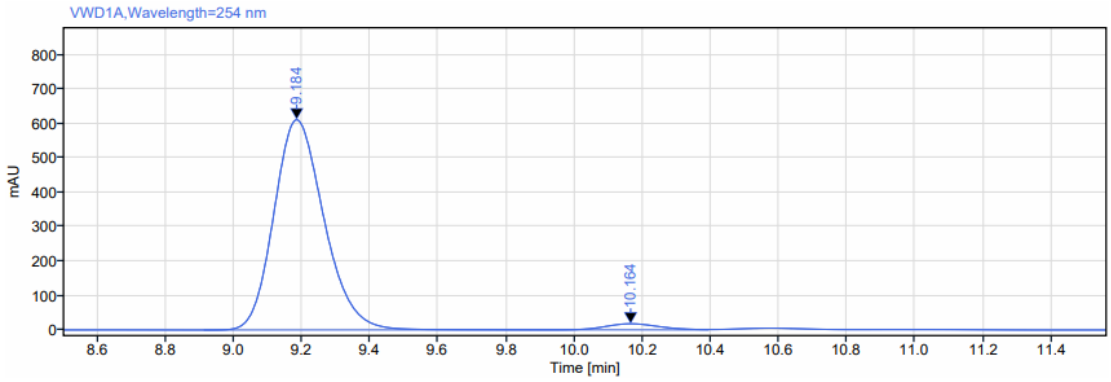

Signal: VWD1A,Wavelength=254 nm

RT [min]	Type	Area	Height	Area%
9.184	BB	6255.98	611.98	96.98
10.164	BV	194.56	17.81	3.02
	Sum	6450.54		

Rac-**3c** is a colorless oil (256 mg, 78%). The NMR spectra of *rac*-**3c** match the one previously reported[28].

^{1}H NMR (400 MHz, $CDCl_3$) δ 8.01-7.92 (m, 2H), 7.33-7.22 (m, 4H), 7.24-7.16 (m, 1H), 7.08-6.98 (m, 2H), 4.62 (q, J = 6.8 Hz, 1H), 1.52 (d, J = 6.8 Hz, 3H).

^{13}C NMR (100 MHz, $CDCl_3$) δ 198.6, 165.4 (d, J = 252.8 Hz), 141.3, 132.8, 131.4 (d, J = 9.4 Hz), 129.0, 127.6, 127.0, 115.5 (d, J = 21.7 Hz), 48.0, 19.5.

MS (EI, *m/z*) calcd. for $C_{15}H_{13}FO$ $[M]^+$ 228.1, found: 228.1.

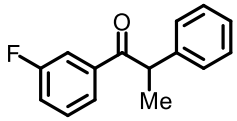

1-(3-Fluorophenyl)-2-phenylpropan-1-one (3d)

By using the typical procedure described in Section 4, the reaction of 3-fluorobenzaldehyde **1d** (0.004 mmol) and ethylbenzene **2a** (0.016 mmol) catalysed by **RAT$_{CH}$** (2 mol%) afforded **3d** in 51% **GC yield** (average of duplicate runs), with a 87% ee.

GC calibration curve for **3d** is displayed below.

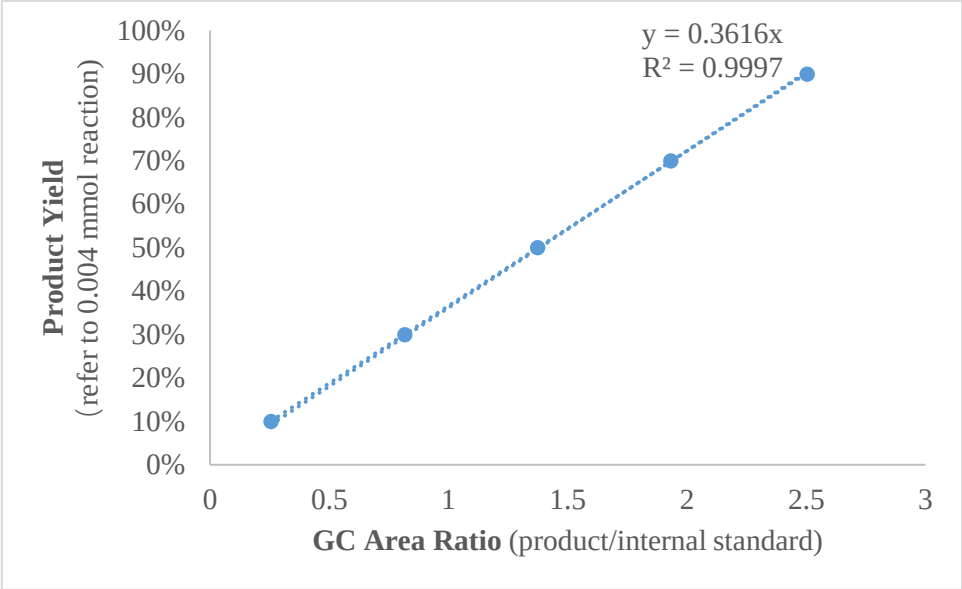

Enantiomeric excess was established by HPLC analysis using a Chiralpak AS-H column (HPLC: AS-H, 254 nm, *n*-hexane/isopropanol = 95:5, flow rate 0.5 mL/min, 30 °C, t_r (major) = 8.58 min, t_r (minor) = 9.13 min).

HPLC trace of *rac*-**3d**:

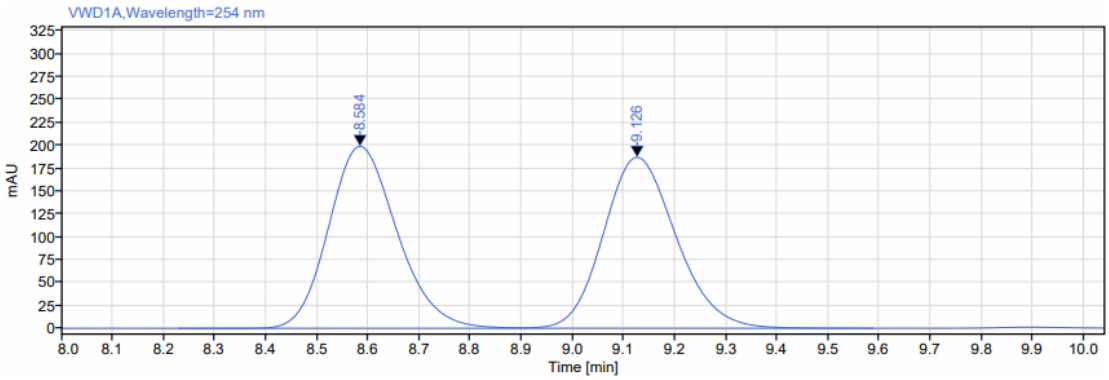

Signal: VWD1A,Wavelength=254 nm

RT [min]	Type	Area	Height	Area%
8.584	BV	1859.35	199.10	50.08
9.126	VB	1853.56	187.06	49.92
	Sum	3712.91		

HPLC trace of enantioenriched-**3d** obtained in a 0.004 mmol reaction:

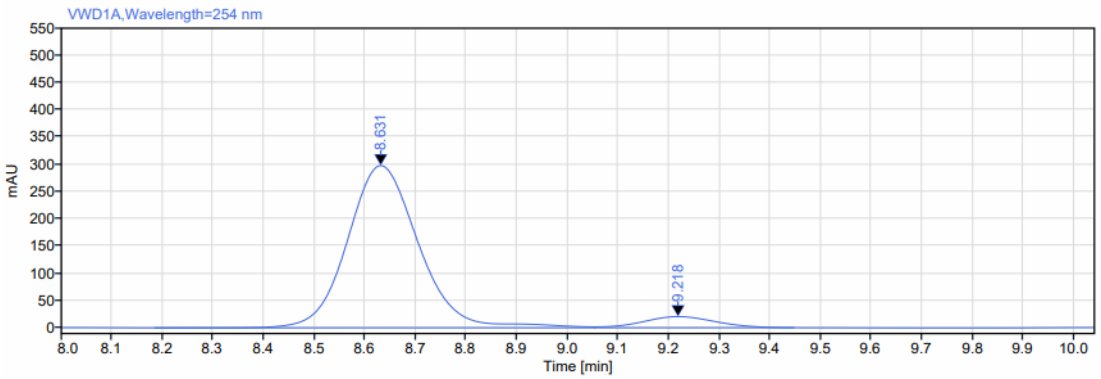

Signal: VWD1A,Wavelength=254 nm

RT [min]	Type	Area	Height	Area%
8.631	BM m	2904.05	297.56	93.49
9.218	MM m	202.10	20.42	6.51
	Sum	3106.15		

Rac-**3d** is a colorless oil (104 mg, 85%). The NMR spectra of *rac*-**3d** match the one previously reported[30].

^{1}H NMR (400 MHz, $CDCl_3$) δ 7.74-7.68 (m, 1H), 7.66-7.58 (m, 1H), 7.37 -7.23 (m, 5H), 7.24-7.16 (m, 1H), 7.19-7.10 (m, 1H), 4.61 (q, J = 6.8 Hz, 1H), 1.53 (d, J = 6.8 Hz, 3H).

^{13}C NMR (100 MHz, $CDCl_3$) δ 198.9 (d, J = 2.2 Hz), 162.7 (d, J = 246.3 Hz), 141.0, 138.6 (d, J = 6.1 Hz), 130.0 (d, J = 7.6 Hz), 129.1, 127.7, 127.0, 124.4 (d, J = 3 Hz), 119.7 (d, J = 21.2 Hz), 115.4 (d, J = 22.2 Hz), 48.2, 19.4.

MS (EI, *m/z*) calcd. for $C_{15}H_{13}FO$ $[M]^+$ 228.1, found: 228.1.

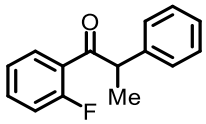

1-(2-Fluorophenyl)-2-phenylpropan-1-one (3e)

By using the typical procedure described in Section 4, the reaction of 2-fluorobenzaldehyde **1e** (0.004 mmol) and ethylbenzene **2a** (0.016 mmol) catalysed by **RAT$_{CH}$** (2 mol%) afforded **3e** in 38% **GC yield** (average of duplicate runs), with a 70% ee.

GC calibration curve for **3e** is displayed below.

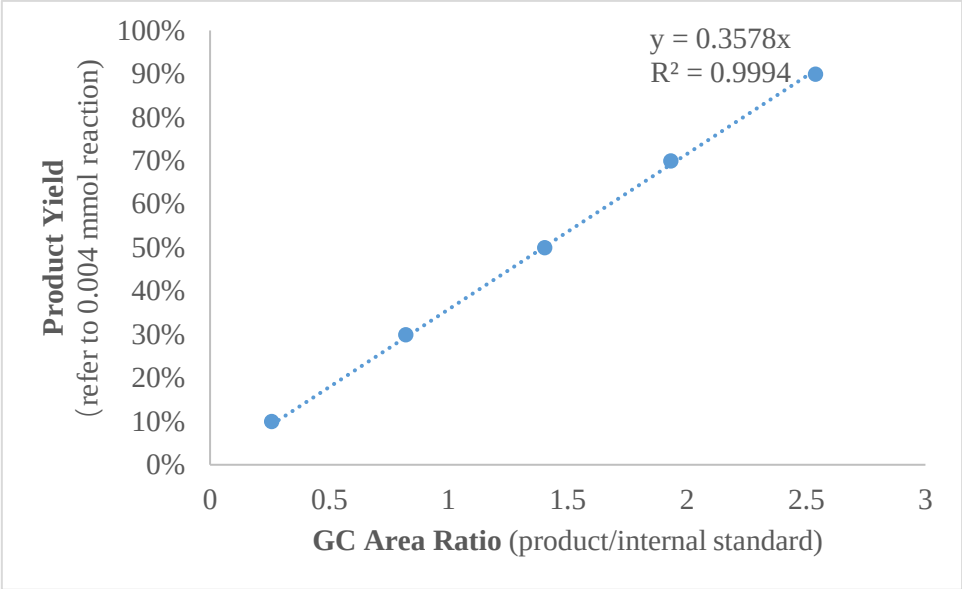

Enantiomeric excess was established by HPLC analysis using a Chiralpak AS-H column (HPLC: AS-H, 254 nm, *n*-hexane/isopropanol = 95:5, flow rate 0.5 mL/min, 30 °C, t_r (major) = 8.83 min, t_r (minor) = 9.26 min).

HPLC trace of *rac*-**3e**:

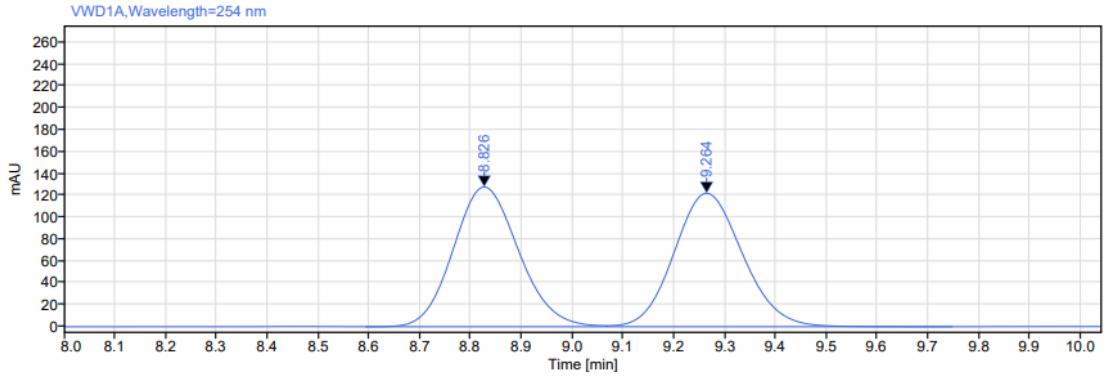

Signal: VWD1A,Wavelength=254 nm

RT [min]	Type	Area	Height	Area%
8.826	VV	1144.18	127.83	49.93
9.264	VB	1147.52	122.11	50.07
	Sum	2291.71		

HPLC trace of enantioenriched-**3e** obtained in a 0.004 mmol reaction:

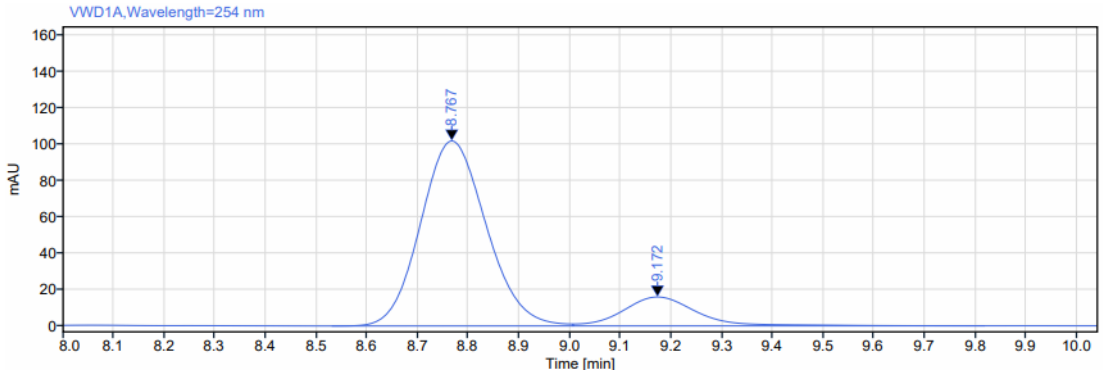

Signal: VWD1A,Wavelength=254 nm

RT [min]	Type	Area	Height	Area%
8.767	BV	917.70	101.96	85.05
9.172	VB	161.33	15.96	14.95
	Sum	1079.03		

Rac-**3e** is a colorless oil (123 mg, 65%). The NMR spectra of *rac*-**3e** match the one previously reported[31].

^{1}H NMR (400 MHz, $CDCl_3$) δ 7.71 (td, J = 7.6, 1.9 Hz, 1H), 7.45-7.35 (m, 1H), 7.29 -7.22 (m, 4H), 7.22-7.14 (m, 1H), 7.17-7.09 (m, 1H), 7.07-6.97 (m, 1H), 4.60 (q, J = 6.9 Hz, 1H), 1.53 (d, J = 6.9 Hz, 3H).

^{13}C NMR (100 MHz, $CDCl_3$) δ 199.7 (d, J = 4.3 Hz), 160.9 (d, J = 252.0 Hz), 140.5, 134.0 (d, J = 9.0 Hz), 131.0 (d, J = 2.8 Hz), 128.7, 128.1, 126.9, 126.1 (d, J = 13.2 Hz), 124.4 (d, J = 3.3 Hz), 116.5 (d, J = 23.8 Hz), 51.9 (d, J = 6.3 Hz), 18.9.

MS (EI, *m/z*) calcd. for $C_{15}H_{13}FO$ $[M]^+$ 228.1, found: 228.1.

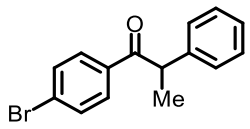

1-(4-Bromophenyl)-2-phenylpropan-1-one (3f)

By using the typical procedure described in Section 4, the reaction of 4-bromobenzaldehyde **1f** (0.004 mmol) and ethylbenzene **2a** (0.016 mmol) catalysed by **RAT$_{CH}$** (2 mol%) afforded **3f** in 59% **GC yield** (average of duplicate runs), with a 94% ee.

GC calibration curve for **3f** is displayed below.

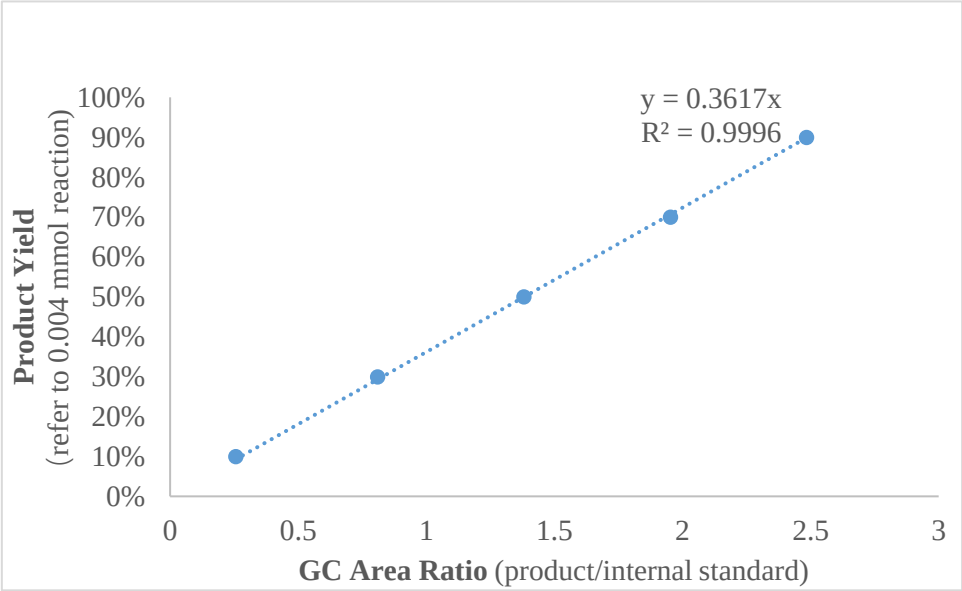

Enantiomeric excess was established by HPLC analysis using a Chiralpak AS-H column (HPLC: AS-H, 254 nm, *n*-hexane/isopropanol = 95:5, flow rate 0.5 mL/min, 30 °C, t_r (major) = 9.88 min, t_r (minor) = 10.88 min).

HPLC trace of *rac*-**3f**:

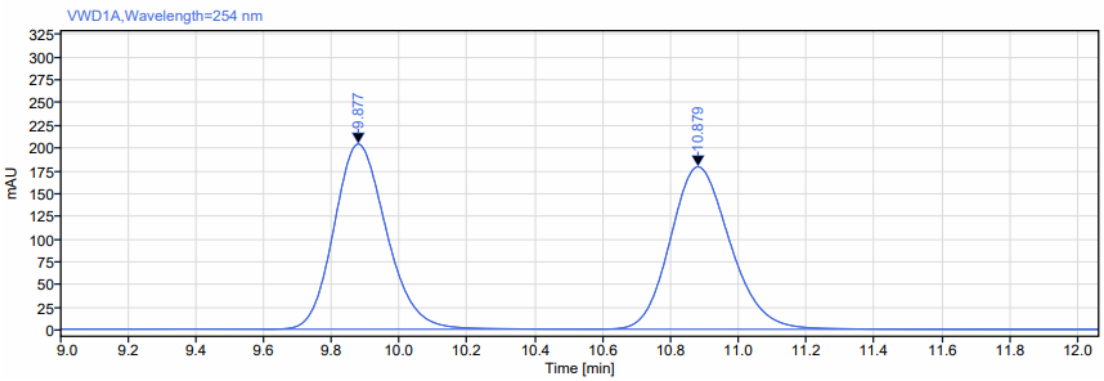

Signal: VWD1A,Wavelength=254 nm

RT [min]	Type	Area	Height	Area%
9.877	BB	2185.86	203.53	49.99
10.879	BB	2186.41	178.51	50.01
	Sum	4372.27		

HPLC trace of enantioenriched-**3f** obtained in a 0.004 mmol reaction:

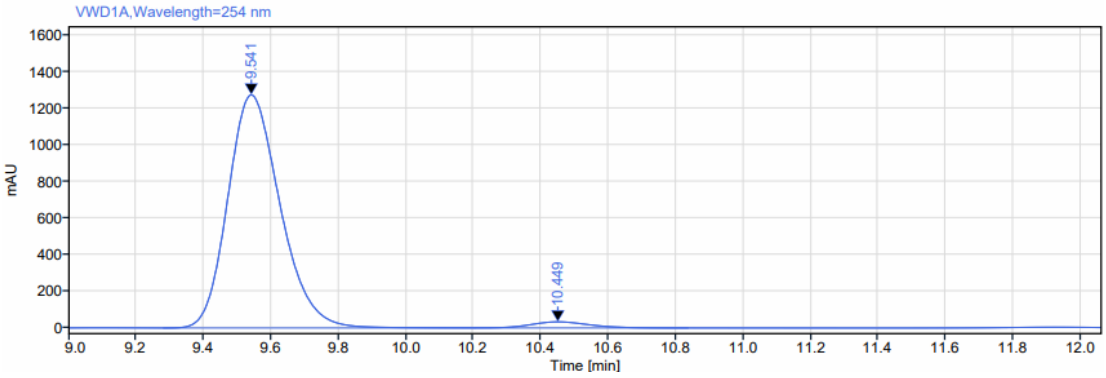

Signal: VWD1A,Wavelength=254 nm

RT [min]	Type	Area	Height	Area%
9.541	BM m	13761.25	1276.49	97.13
10.449	MM m	406.21	33.55	2.87
	Sum	14167.46		

Rac-**3f** is a colorless oil (1.11 g, 77%). The NMR spectra of *rac*-**3f** match the one previously reported[32].
^{1}H NMR (400 MHz, $CDCl_3$) δ 7.83-7.75 (m, 2H), 7.53-7.46 (m, 2H), 7.33-7.16 (m, 5H), 4.60 (q, J = 6.8 Hz, 1H), 1.52 (d, J = 7.2 Hz, 3H).
^{13}C NMR (100 MHz, $CDCl_3$) δ 199.2, 141.1, 135.1, 131.8, 130.3, 129.1, 127.9, 127.6, 127.0, 48.1, 19.4.
MS (EI, *m/z*) calcd. for $C_{15}H_{13}BrO$ $[M]^+$ 288.0, found: 288.0.

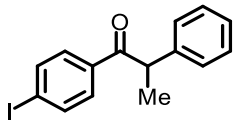

1-(4-Iodophenyl)-2-phenylpropan-1-one (3g)
By using the typical procedure described in Section 4, the reaction of 4-iodobenzaldehyde **1g** (0.004 mmol) and ethylbenzene **2a** (0.016 mmol) catalysed by **RAT$_{CH}$** (2 mol%) afforded **3g** in 54% **GC yield** (average of duplicate runs), with a 94% ee.

GC calibration curve for **3g** is displayed below.

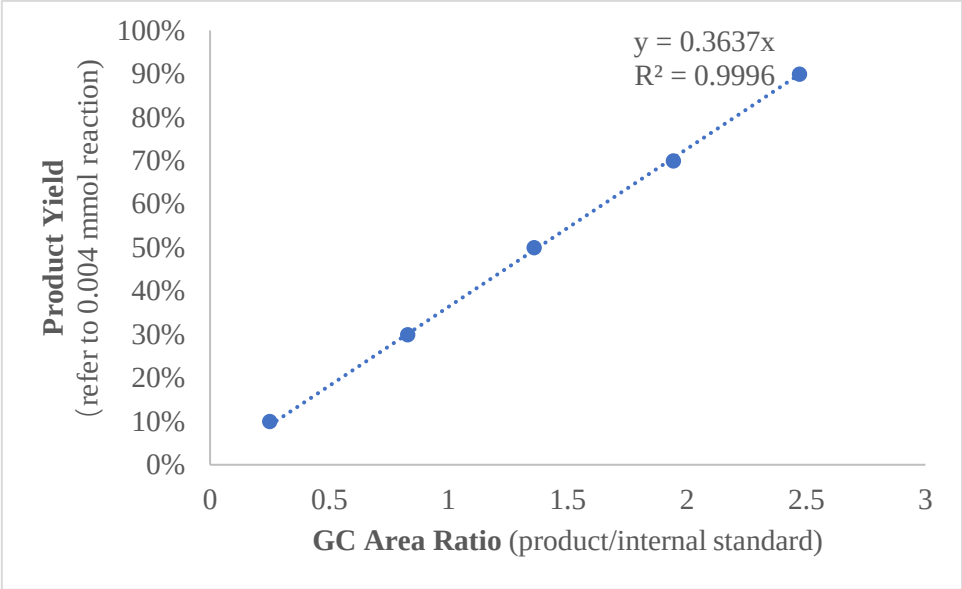

Enantiomeric excess was established by HPLC analysis using a Chiralpak AS-H column (HPLC: AS-H, 254 nm, *n*-hexane/isopropanol = 95:5, flow rate 0.5 mL/min, 30 °C, t_r (major) = 10.29 min, t_r (minor) = 11.07 min).

HPLC trace of *rac*-**3g**:

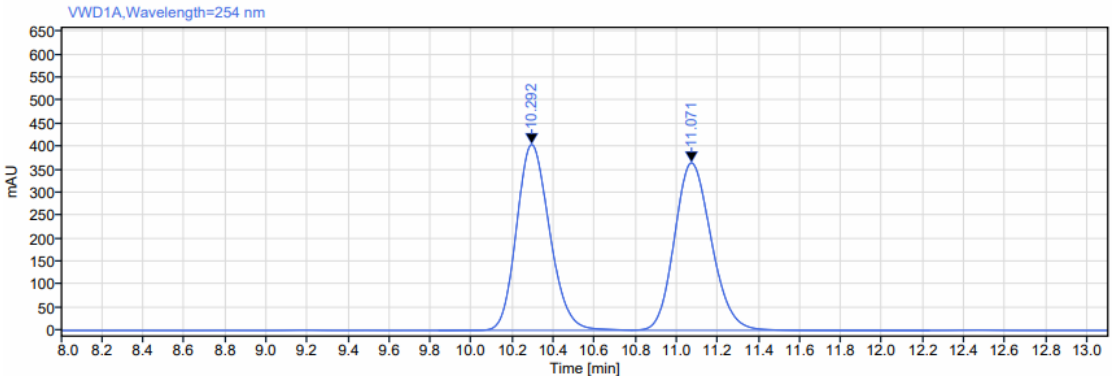

Signal: VWD1A,Wavelength=254 nm

RT [min]	Type	Area	Height	Area%
10.292	BV	4544.01	404.60	49.89
11.071	VB	4564.59	364.79	50.11
	Sum	9108.61		

HPLC trace of enantioenriched-**3g** obtained in a 0.004 mmol reaction:

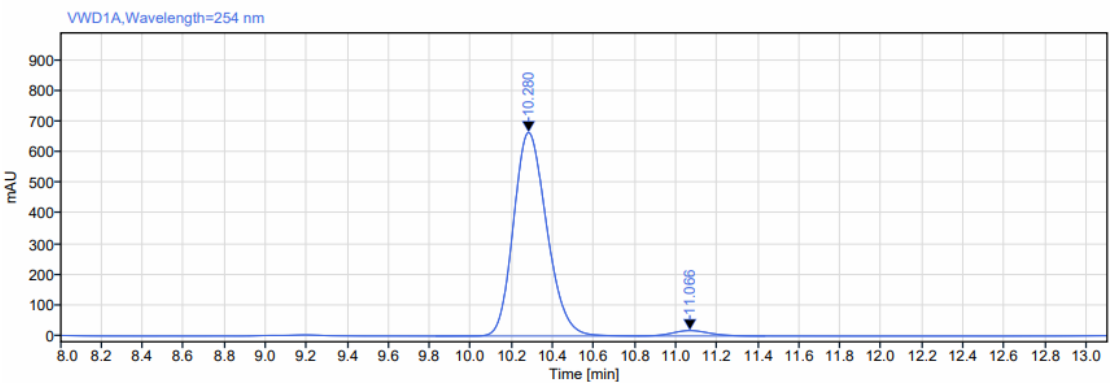

Signal: VWD1A,Wavelength=254 nm

RT [min]	Type	Area	Height	Area%
10.280	BM m	7486.52	664.11	97.06
11.066	MM m	227.08	17.84	2.94
	Sum	7713.60		

The reaction was scaled up to 0.1 mmol, which afforded 16.1 mg **3g**, corresponding to a 48% isolated yield with a 93% ee.

^{1}H NMR (400 MHz, $CDCl_3$) of enantioenriched-**3g** obtained in a 0.1 mmol reaction:

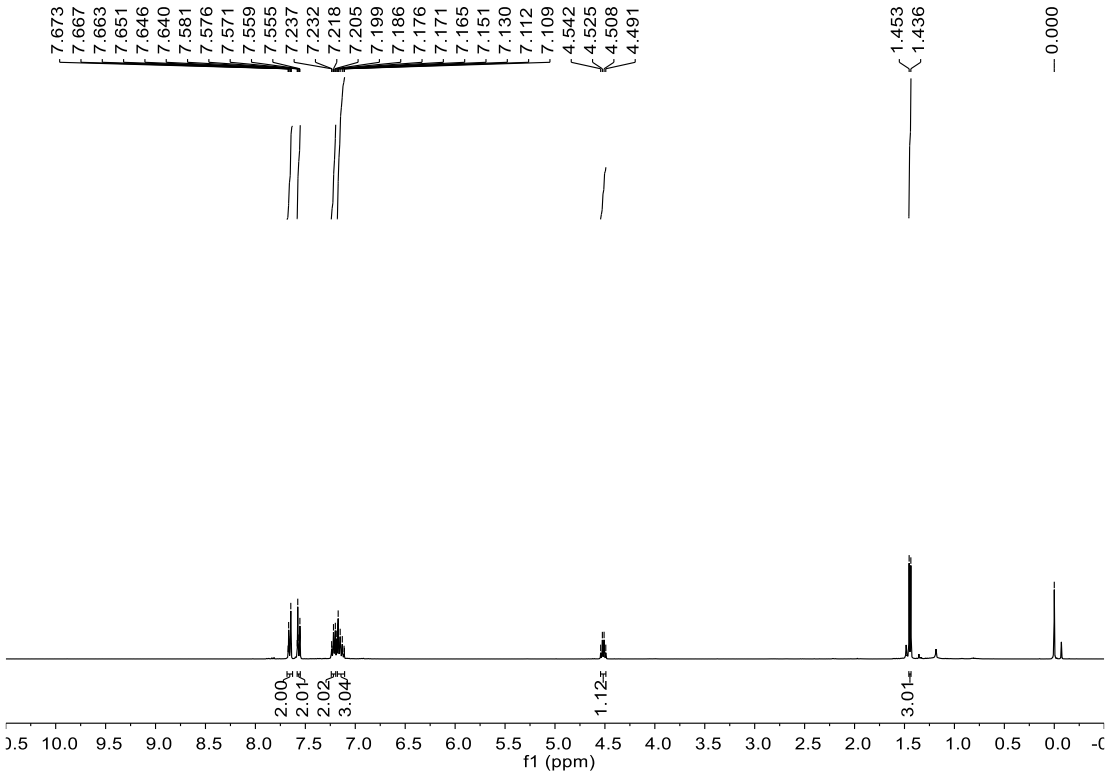

Enantiomeric excess was established by HPLC analysis using a Chiralpak AS-H column (HPLC: AS-H, 254 nm, *n*-hexane/isopropanol = 95:5, flow rate 0.5 mL/min, 30 °C, t_r (major) = 10.07 min, t_r (minor) = 10.72 min).

HPLC trace of *rac*-**3g**:

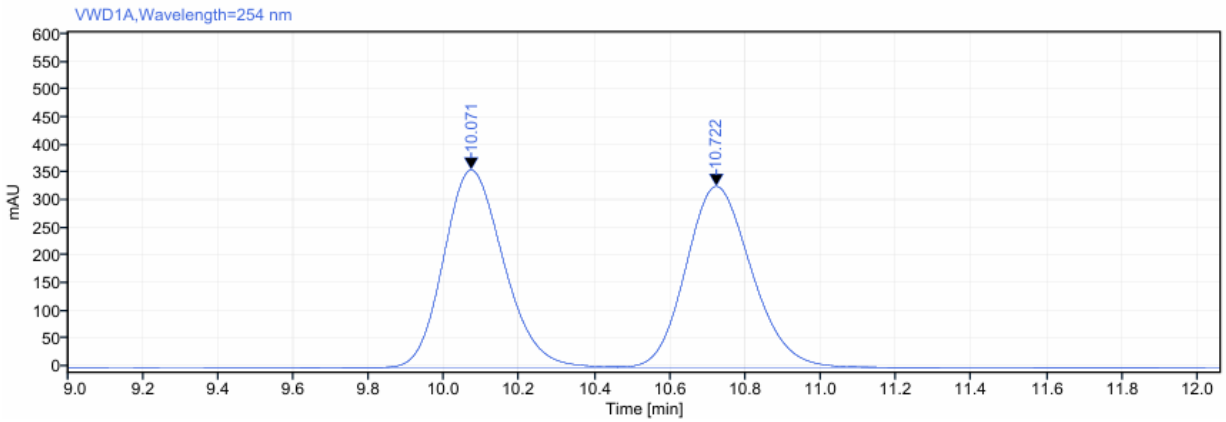

Signal: VWD1A,Wavelength=254 nm

RT [min]	Type	Area	Height	Area%
10.071	BV	3974.13	357.66	49.90
10.722	VB	3989.41	327.92	50.10
	Sum	7963.54		

HPLC trace of **3g** obtained in a 0.1 mmol reaction:

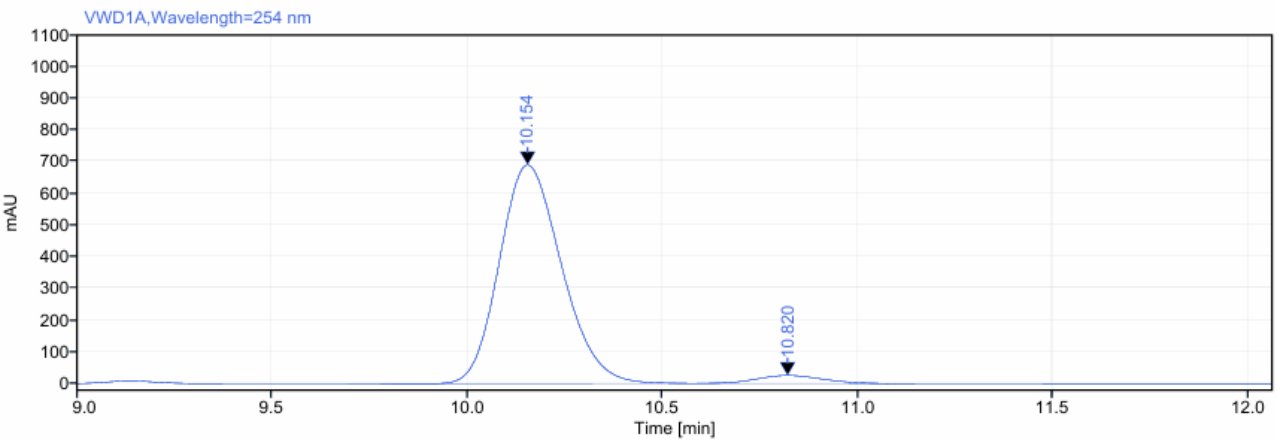

Signal: VWD1A,Wavelength=254 nm

RT [min]	Type	Area	Height	Area%
10.154	BM m	7631.10	689.80	96.35
10.820	MM m	289.41	25.09	3.65
	Sum	7920.51		

Rac-**3g** is a white solid (424 mg, 84%). The NMR spectra of *rac*-**3g** match the one previously reported[1].

^{1}H NMR (400 MHz, $CDCl_3$) δ 7.76-7.69 (m, 2H), 7.67-7.60 (m, 2H), 7.33-7.25 (m, 2H), 7.25-7.16 (m, 3H), 4.59 (q, J = 6.8 Hz, 1H), 1.51 (d, J = 6.8 Hz, 3H).

^{13}C NMR (100 MHz, $CDCl_3$) δ 199.5, 141.1, 137.8, 135.7, 130.2, 129.1, 127.6, 127.0, 100.7, 48.0, 19.4.

MS (EI, *m/z*) calcd. for $C_{15}H_{13}IO$ $[M]^+$ 336.0, found: 336.0.

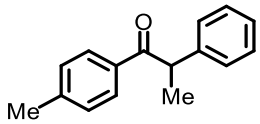

2-Phenyl-1-(*p*-tolyl)propan-1-one (3h)

By using the typical procedure described in Section 4, the reaction of 4-methylbenzaldehyde **1h** (0.004 mmol) and ethylbenzene **2a** (0.016 mmol) catalysed by **RAT$_{CH}$** (2 mol%) afforded **3h** in 48% **GC yield** (average of duplicate runs), with a 95% ee.

GC calibration curve for **3h** is displayed below.

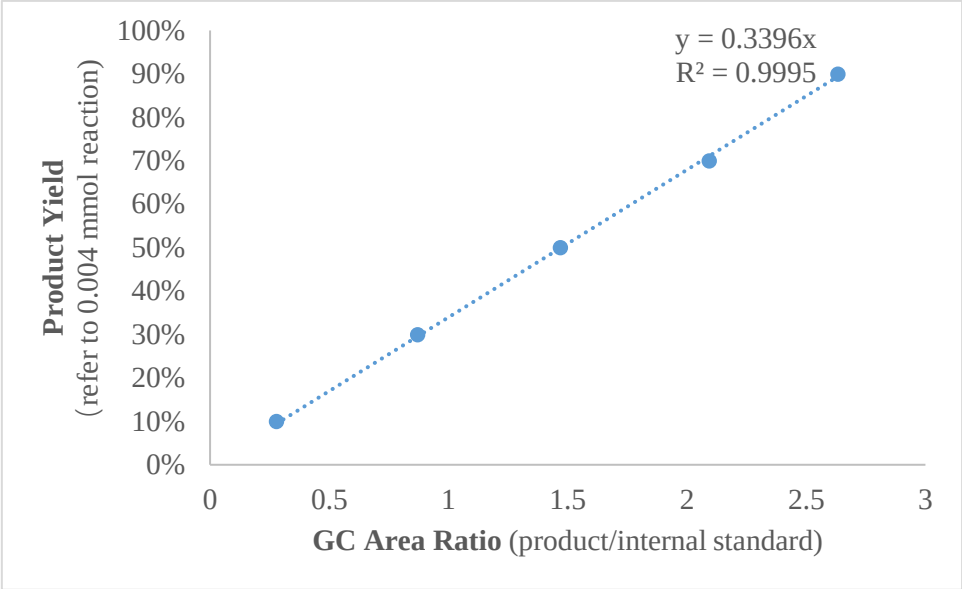

Enantiomeric excess was established by HPLC analysis using a Chiralpak AS-H column (HPLC: AS-H, 254 nm, *n*-hexane/isopropanol = 95:5, flow rate 0.5 mL/min, 30 °C, t_r (major) = 9.28 min, t_r (minor) = 10.44 min).

HPLC trace of *rac*-**3h**:

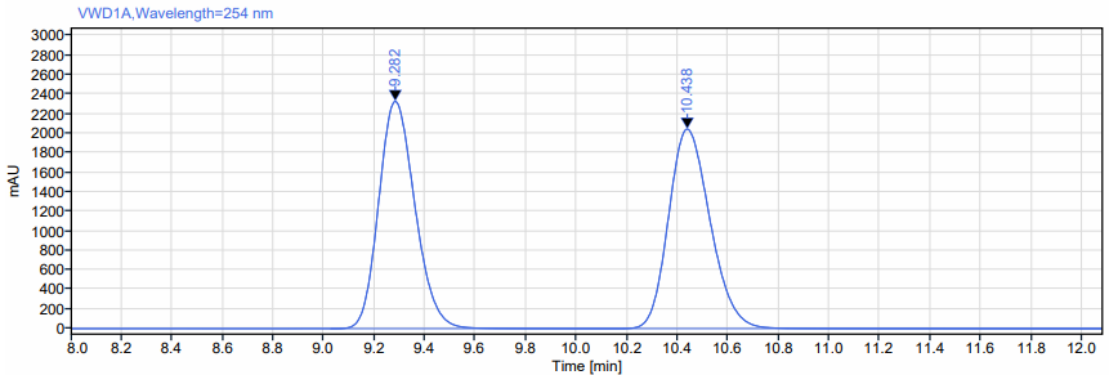

Signal: VWD1A,Wavelength=254 nm

RT [min]	Type	Area	Height	Area%
9.282	VB	23262.79	2329.87	49.88
10.438	BB	23371.18	2044.62	50.12
	Sum	46633.97		

HPLC trace of enantioenriched-**3h** obtained in a 0.004 mmol reaction:

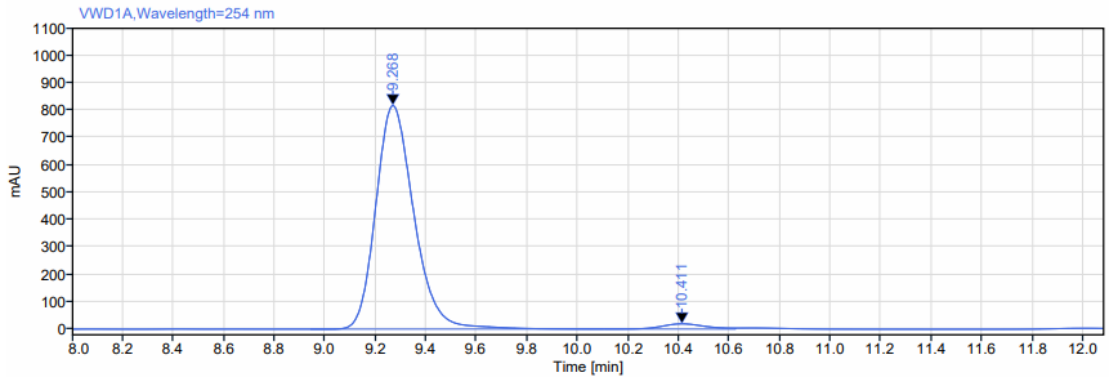

Signal: VWD1A,Wavelength=254 nm

RT [min]	Type	Area	Height	Area%
9.268	BB	8569.41	817.16	97.40
10.411	BV	228.82	19.11	2.60
	Sum	8798.23		

Rac-**3h** is a colorless oil (195 mg, 87%). The NMR spectra of *rac*-**3h** match the one previously reported[28].

^{1}H NMR (400 MHz, $CDCl_3$) δ 7.88-7.82 (m, 2H), 7.30-7.24 (m, 4H), 7.21-7.12 (m, 3H), 4.66 (q, J = 6.8 Hz, 1H), 2.32 (s, 3H), 1.52 (d, J = 6.8 Hz, 3H).

^{13}C NMR (100 MHz, $CDCl_3$) δ 199.9, 143.5, 141.7, 133.9, 129.1, 128.9, 128.8, 127.7, 126.7, 47.7, 21.5, 19.4.

MS (EI, *m/z)* calcd. for $C_{16}H_{16}O$ $[M]^+$ 224.1, found: 224.1.

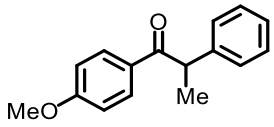

1-(4-Methoxyphenyl)-2-phenylpropan-1-one (3i)

By using the typical procedure described in Section 4, the reaction of 4-methoxybenzaldehyde **1i** (0.004 mmol) and ethylbenzene **2a** (0.016 mmol) catalysed by **RAT$_{CH}$** (2 mol%) afforded **3i** in 40% **GC yield** (average of duplicate runs), with a 96% ee.

GC calibration curve for **3i** is displayed below.

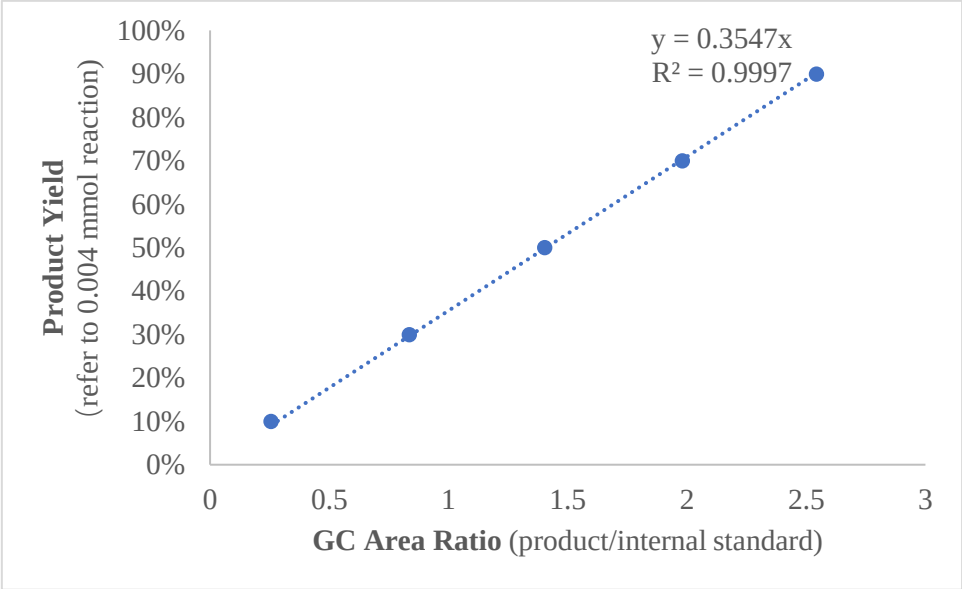

Enantiomeric excess was established by HPLC analysis using a Chiralpak AS-H column (HPLC: AS-H, 254 nm, *n*-hexane/isopropanol = 95:5, flow rate 0.5 mL/min, 30 °C, t_r (major) = 14.99 min, t_r (minor) = 16.61 min).

HPLC trace of *rac*-**3i**:

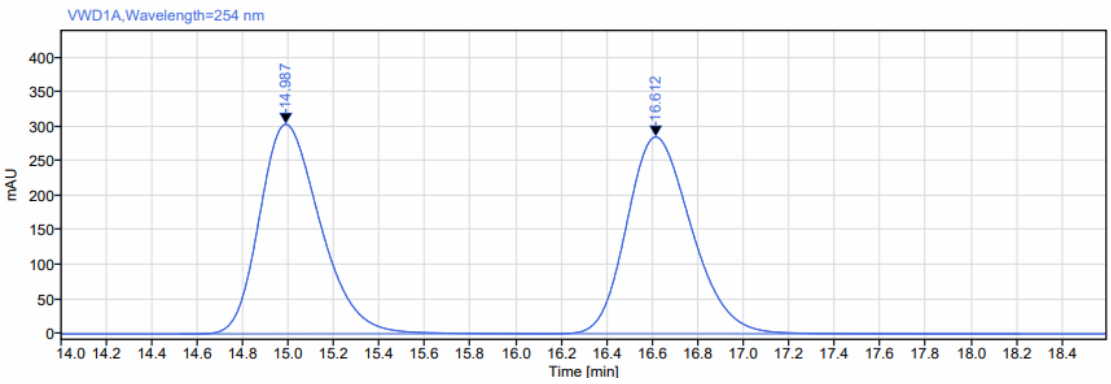

Signal: VWD1A,Wavelength=254 nm

RT [min]	Type	Area	Height	Area%
14.987	BB	5630.71	303.99	49.95
16.612	BB	5641.00	285.44	50.05
	Sum	11271.71		

HPLC trace of enantioenriched-**3i** obtained in a 0.004 mmol reaction:

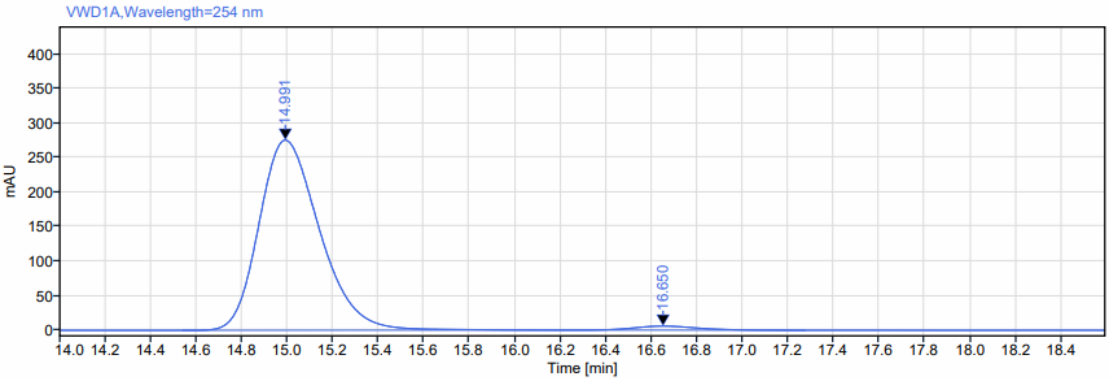

Signal: VWD1A,Wavelength=254 nm

RT [min]	Type	Area	Height	Area%
14.991	BB	5098.44	275.79	97.80
16.650	BB	114.87	5.89	2.20
	Sum	5213.31		

Rac-**3i** is a colorless oil (178 mg, 78%). The NMR spectra of *rac*-**3i** match the one previously reported[28].

^{1}H NMR (400 MHz, $CDCl_3$) δ 7.98-7.90 (m, 2H), 7.31-7.25 (m, 4H), 7.23-7.14 (m, 1H), 6.89-6.81 (m, 2H), 4.64 (q, J = 6.9 Hz, 1H), 3.80 (s, 3H), 1.51 (d, J = 6.8 Hz, 3H).

^{13}C NMR (100 MHz, $CDCl_3$) δ 198.8, 163.2, 141.9, 131.0, 129.4, 128.9, 127.7, 126.7, 113.6, 55.4, 47.5, 19.5.

MS (EI, *m/z*) calcd. for $C_{16}H_{16}O_2$ $[M]^+$ 240.1, found: 240.1.

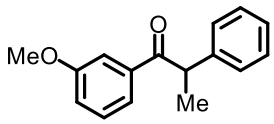

1-(3-Methoxyphenyl)-2-phenylpropan-1-one (3j)

By using the typical procedure described in Section 4, the reaction of 3-methoxybenzaldehyde **1j** (0.004 mmol) and ethylbenzene **2a** (0.016 mmol) catalysed by **RAT$_{CH}$** (2 mol%) afforded **3j** in 51%

GC yield (average of duplicate runs), with a 78% ee.

GC calibration curve for **3j** is displayed below.

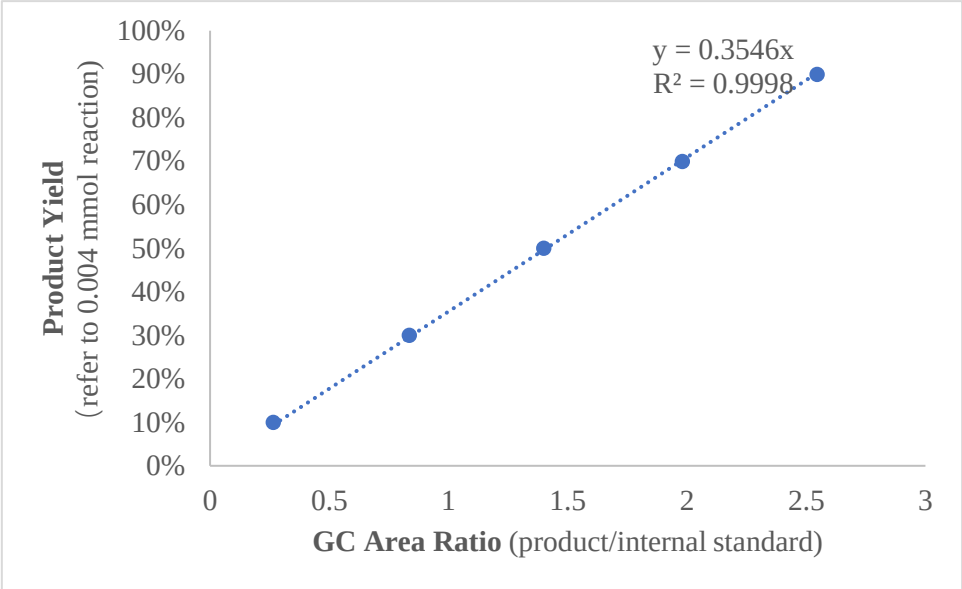

Enantiomeric excess was established by HPLC analysis using a Chiralpak AS-H column (HPLC: AS-H, 254 nm, *n*-hexane/isopropanol = 95:5, flow rate 0.5 mL/min, 30 °C, t_r (major) = 10.75 min, t_r (minor) = 12.93 min).

HPLC trace of *rac*-**3j**:

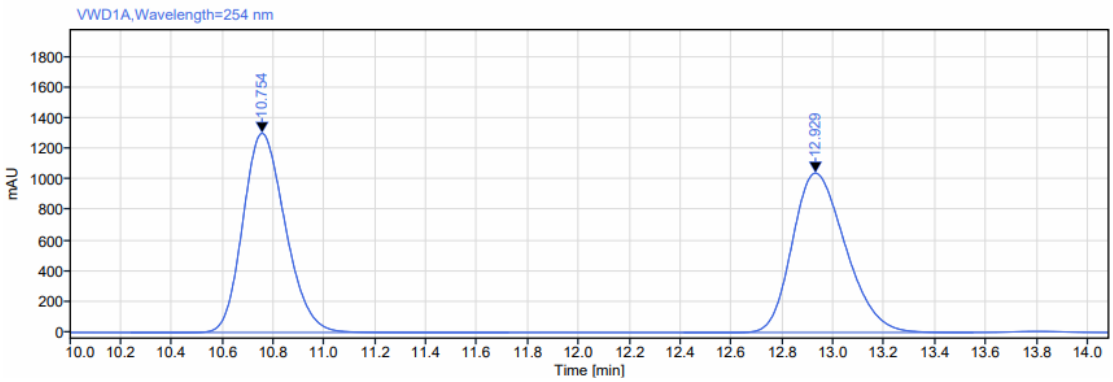

Signal: VWD1A,Wavelength=254 nm

RT [min]	Type	Area	Height	Area%
10.754	BB	15070.98	1302.36	49.89
12.929	BV	15140.30	1042.15	50.11
	Sum	30211.28		

HPLC trace of enantioenriched-**3j** obtained in a 0.004 mmol reaction:

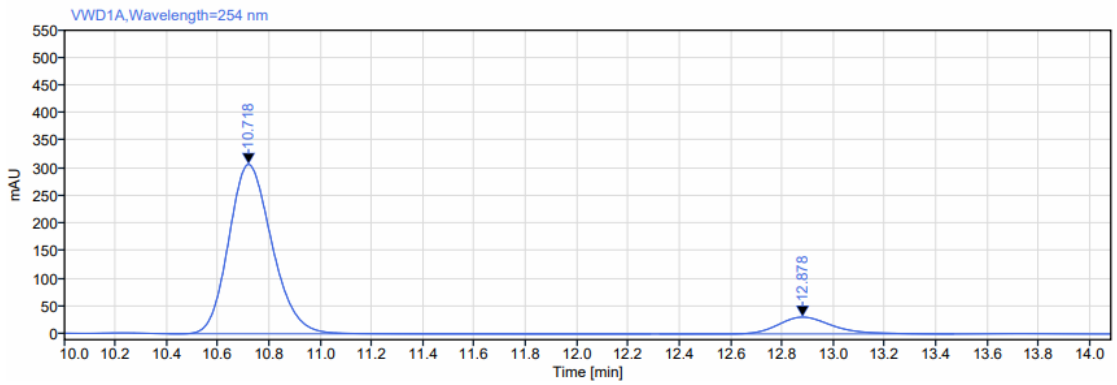

Signal: VWD1A,Wavelength=254 nm

RT [min]	Type	Area	Height	Area%
10.718	MB m	3593.27	306.63	88.91
12.878	BB	448.19	30.49	11.09
	Sum	4041.47		

Rac-**3j** is a colorless oil (164 mg, 68%). The NMR spectra of *rac*-**3j** match the one previously reported[33].

^{1}H NMR (400 MHz, $CDCl_3$) δ 7.56-7.49 (m, 1H), 7.51-7.45 (m , 1H), 7.31 -7.24 (m, 5H), 7.23-7.15 (m, 1H), 7.04-6.97 (m, 1H), 4.66 (q, J = 6.8 Hz, 1H), 3.78 (s, 3H), 1.53 (d, J = 6.9 Hz, 3H).

^{13}C NMR (100 MHz, $CDCl_3$) δ 200.1, 159.7, 141.5, 137.8, 129.4, 128.9, 127.7, 126.9, 121.3, 119.2, 113.1, 55.3, 48.0, 19.5.

MS (EI, *m/z*) calcd. for $C_{16}H_{16}O_2$ $[M]^+$ 240.1, found: 240.1.

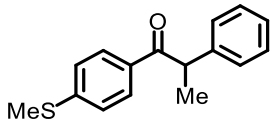

1-(4-(Methylthio)phenyl)-2-phenylpropan-1-one (3k)

By using the typical procedure described in Section 4, the reaction of 4-(methylthio)benzaldehyde **1k** (0.004 mmol) and ethylbenzene **2a** (0.016 mmol) catalysed by **RAT$_{CH}$** (2 mol%) afforded **3k** in 47% **GC yield** (average of duplicate runs), with a 97% ee.

GC calibration curve for **3k** is displayed below.

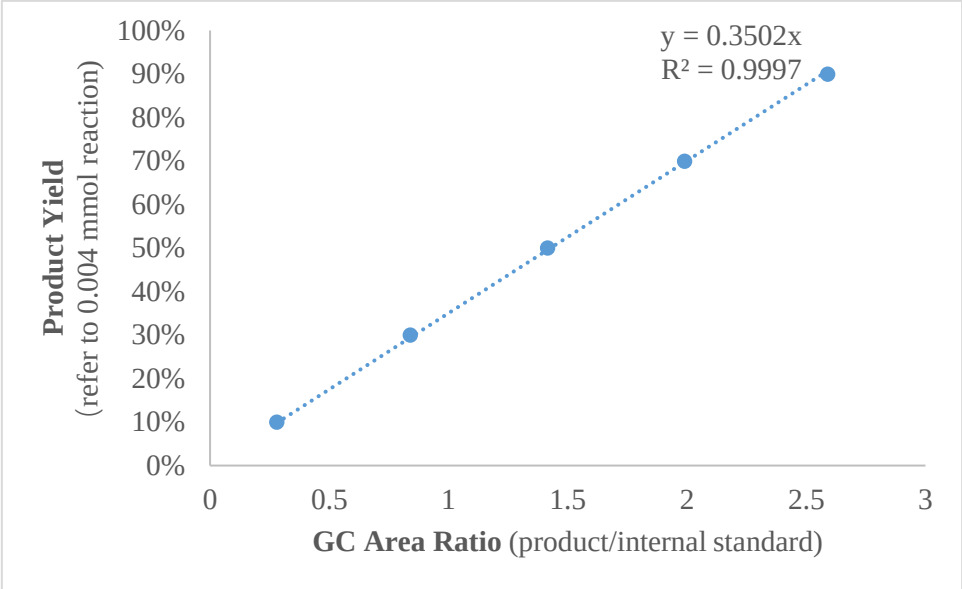

Enantiomeric excess was established by HPLC analysis using a Chiralpak AS-H column (HPLC: AS-H, 254 nm, *n*-hexane/isopropanol = 95:5, flow rate 0.5 mL/min, 30 °C, t_r (major) = 15.25 min, t_r (minor) = 16.18 min).

HPLC trace of *rac*-**3k**:

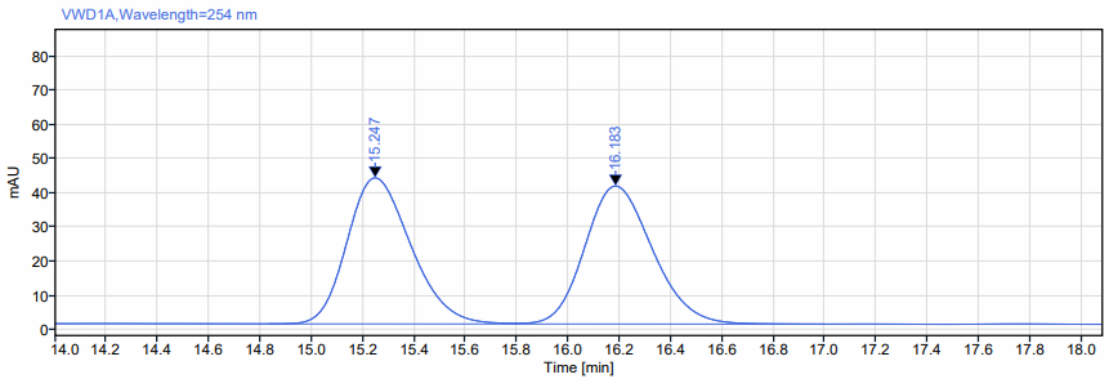

Signal: VWD1A,Wavelength=254 nm

RT [min]	Type	Area	Height	Area%
15.247	BV	739.16	42.75	49.93
16.183	VB	741.11	40.39	50.07
	Sum	1480.27		

HPLC trace of enantioenriched-**3k** obtained in a 0.004 mmol reaction:

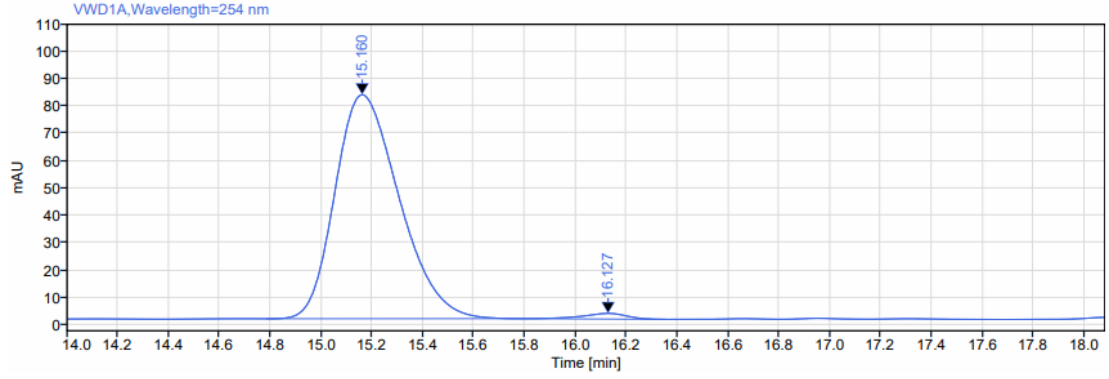

Signal: VWD1A,Wavelength=254 nm

RT [min]	Type	Area	Height	Area%
15.160	BB	1435.26	81.84	98.31
16.127	BB	24.75	2.07	1.69
	Sum	1460.01		

The reaction was scaled up to 0.1 mmol, which afforded 11.0 mg **3k**, corresponding to a 43% isolated yield with a 94% ee.

^{1}H NMR (400 MHz, $CDCl_3$) of enantioenriched-**3k** obtained in a 0.1 mmol reaction:

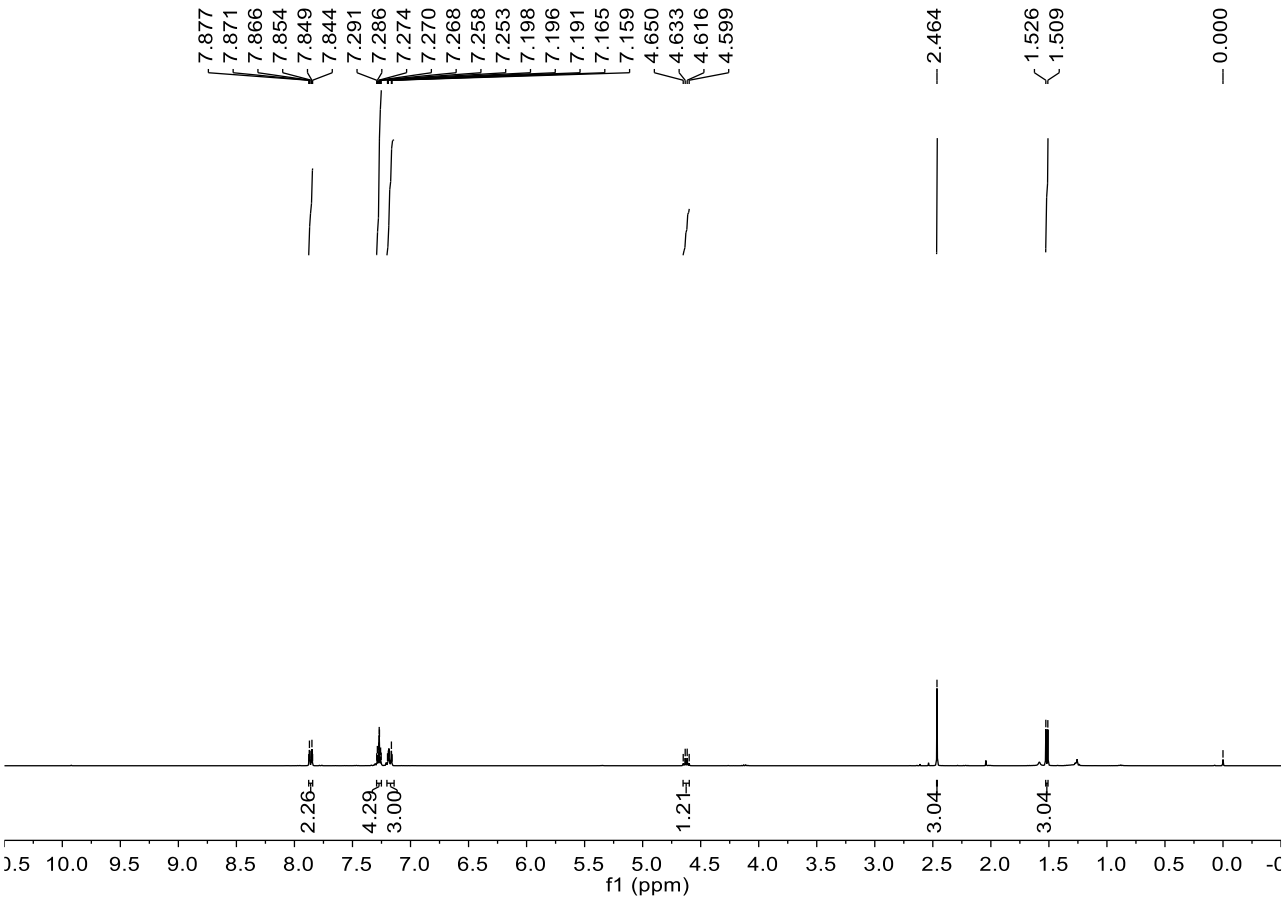

Enantiomeric excess was established by HPLC analysis using a Chiralpak AS-H column (HPLC: AS-H, 254 nm, *n*-hexane/isopropanol = 95:5, flow rate 0.5 mL/min, 30 °C, t_r (major) = 14.93 min, t_r (minor) = 15.76 min).

HPLC trace of *rac*-**3k**:

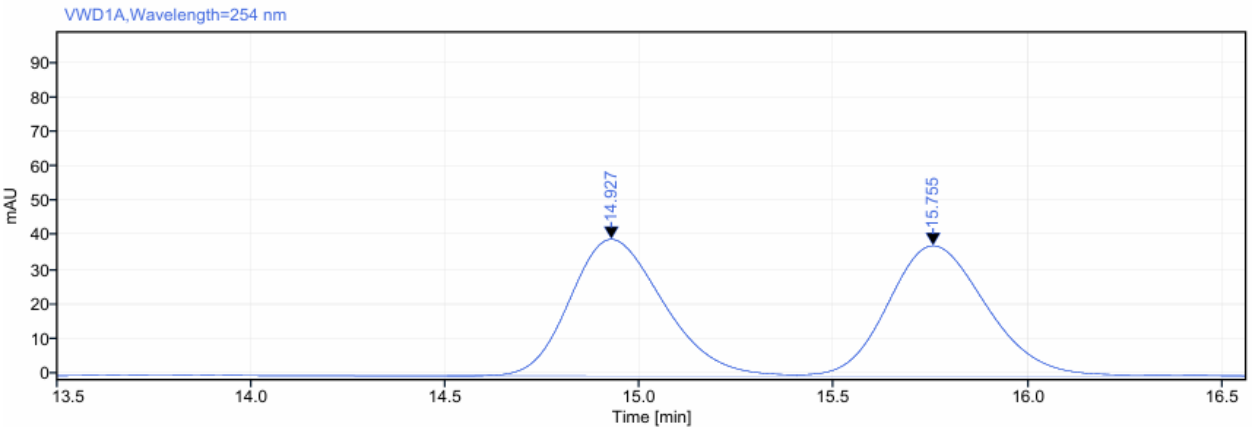

Signal:	VWD1A,Wavelength=254 nm			
RT [min]	Type	Area	Height	Area%
14.927	BV	662.01	39.59	49.77
15.755	VB	668.07	37.76	50.23
	Sum	1330.08		

HPLC trace of **3k** obtained in a 0.1 mmol reaction:

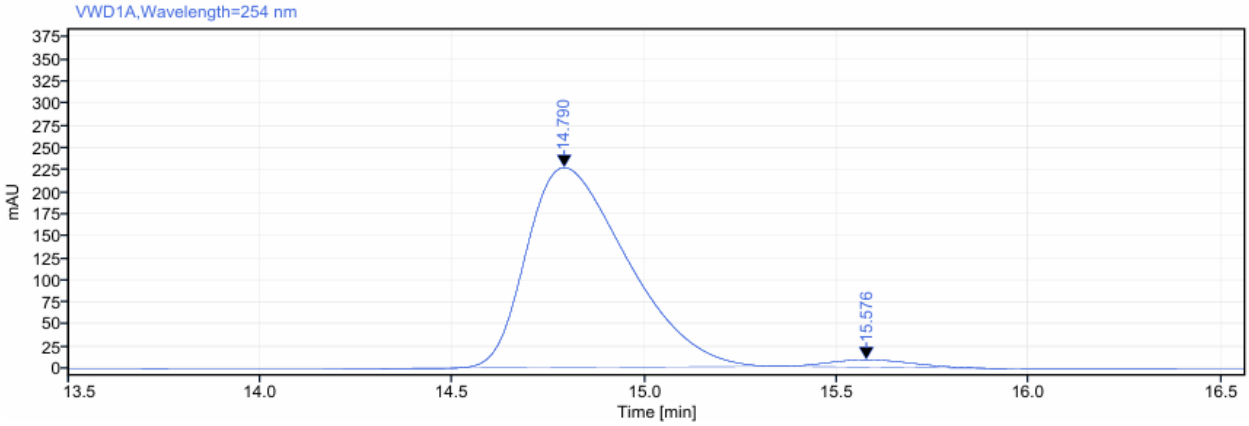

Signal:	VWD1A,Wavelength=254 nm			
RT [min]	Type	Area	Height	Area%
14.790	BM m	4104.22	226.42	97.03
15.576	MM m	125.52	8.29	2.97
	Sum	4229.73		

Rac-**3k** is a white solid (101 mg, 66%). The NMR spectra of *rac*-**3k** match the one previously reported[34].

^{1}H NMR (400 MHz, $CDCl_3$) δ 7.90-7.82 (m, 2H), 7.32-7.23 (m, 4H), 7.23-7.14 (m, 3H), 4.62 (q, J = 6.8 Hz, 1H), 2.46 (s, 3H), 1.52 (d, J = 6.8 Hz, 3H).

^{13}C NMR (100 MHz, $CDCl_3$) δ 199.2, 145.5, 141.6, 132.7, 129.2, 129.0, 127.7, 126.8, 124.9, 47.7, 19.5, 14.7.

MS (EI, *m/z*) calcd. for $C_{16}H_{16}OS$ $[M]^+$ 256.1, found: 256.1.

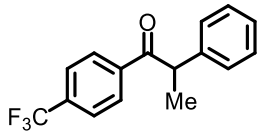

2-Phenyl-1-(4-(trifluoromethyl)phenyl)propan-1-one (3l)

By using the typical procedure described in Section 4, the reaction of 4-

(trifluoromethyl)benzaldehyde **1l** (0.004 mmol) and ethylbenzene **2a** (0.016 mmol) catalysed by **RAT$_{CH}$** (2 mol%) afforded **3l** in 47% **GC yield** (average of duplicate runs), with a 83% ee.

GC calibration curve for **3l** is displayed below.

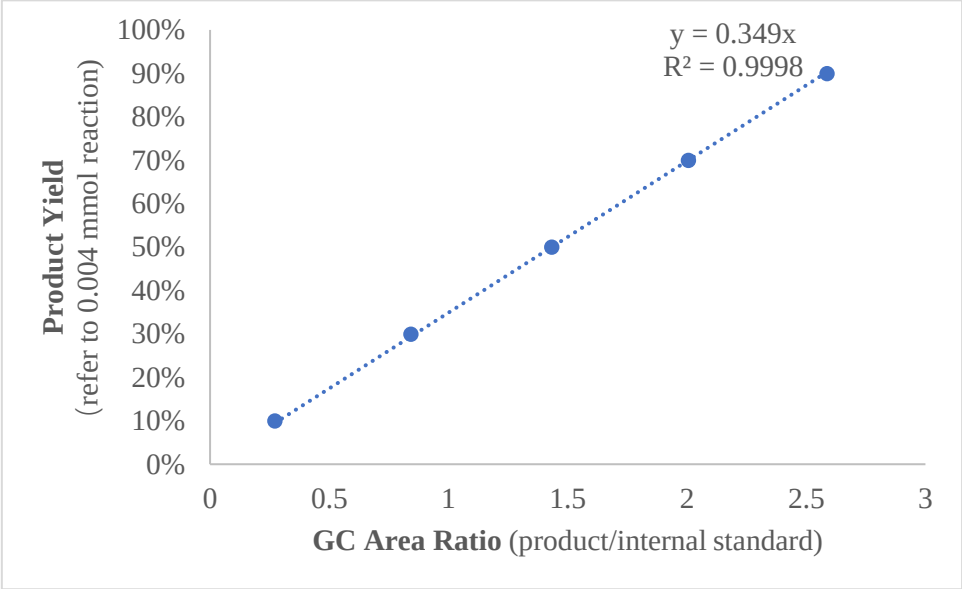

Enantiomeric excess was established by HPLC analysis using a Chiralpak AS-H column (HPLC: AS-H, 254 nm, *n*-hexane/isopropanol = 95:5, flow rate 0.5 mL/min, 30 °C, t_r (major) = 7.78 min, t_r (minor) = 8.27 min).

HPLC trace of *rac*-**3l**:

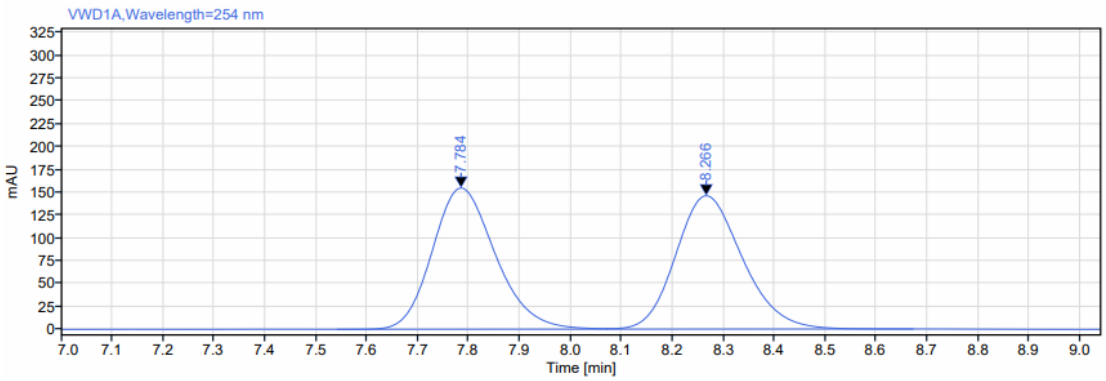

Signal: VWD1A,Wavelength=254 nm

RT [min]	Type	Area	Height	Area%
7.784	BM m	1336.45	154.88	50.05
8.266	MM m	1333.57	146.27	49.95
	Sum	2670.02		

HPLC trace of enantioenriched-**3l** obtained in a 0.004 mmol reaction:

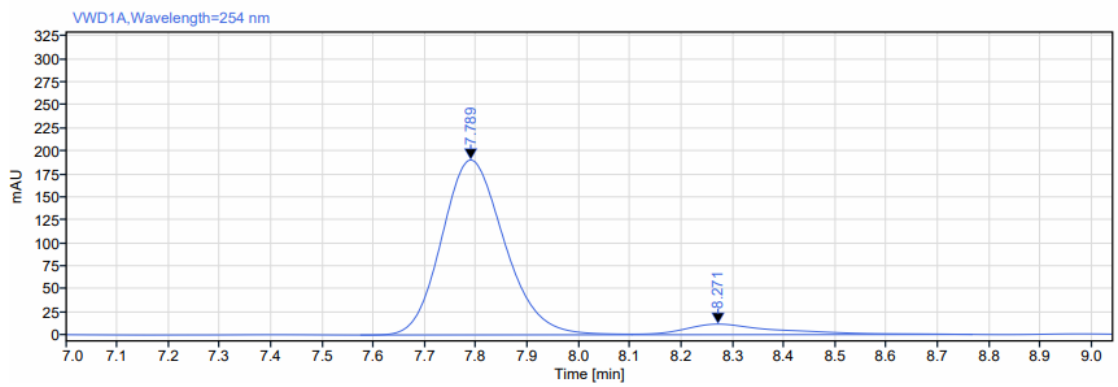

Signal: VWD1A,Wavelength=254 nm

RT [min]	Type	Area	Height	Area%
7.789	BM m	1619.09	190.37	91.69
8.271	MM m	146.81	11.50	8.31
	Sum	1765.90		

Rac-**3l** is a colorless oil (248 mg, 81%). The NMR spectra of *rac*-**3l** match the one previously reported[35].

^{1}H NMR (400 MHz, $CDCl_3$) δ 8.02 (d, J = 8.1 Hz, 2H), 7.62 (d, J = 8.2 Hz, 2H), 7.34-7.17 (m, 5H), 4.65 (q, J = 6.8 Hz, 1H), 1.55 (d, J = 6.8 Hz, 3H).

^{13}C NMR (100 MHz, $CDCl_3$) δ 199.2, 140.8, 139.2, 134.0 (q, J = 32.4 Hz), 129.2, 129.0, 127.7, 127.2, 125.5 (q, J = 3.7 Hz), 123.5 (q, J = 270.9 Hz), 48.5, 19.3.

MS (EI, *m/z*) calcd. for $C_{16}H_{13}F_3O$ $[M]^+$ 278.1, found: 278.1.

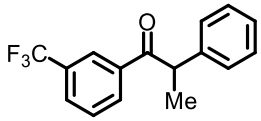

2-Phenyl-1-(3-(trifluoromethyl)phenyl)propan-1-one (3m)

By using the typical procedure described in Section 4, the reaction of 3-(trifluoromethyl)benzaldehyde **1m** (0.004 mmol) and ethylbenzene **2a** (0.016 mmol) catalysed by **RAT$_{CH}$** (2 mol%) afforded **3m** in 65% **GC yield** (average of duplicate runs), with a 71% ee.

GC calibration curve for **3m** is displayed below.

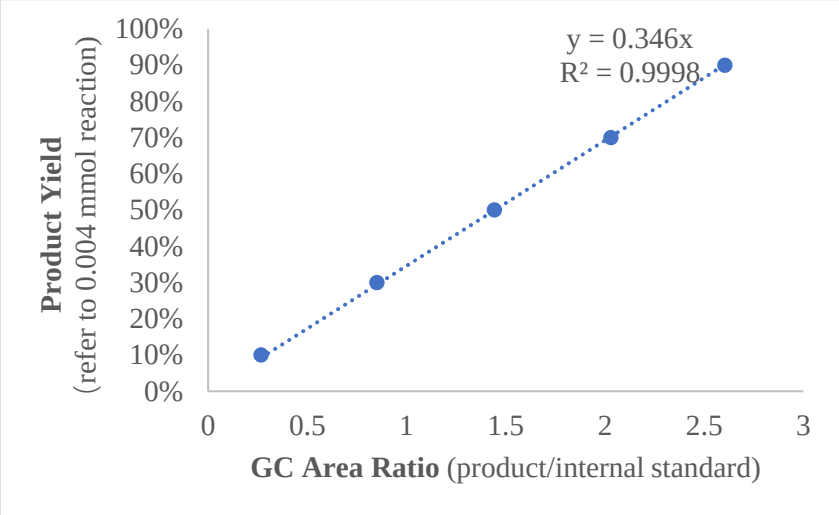

Enantiomeric excess was established by HPLC analysis using a Chiralpak AS-H column (HPLC: AS-H, 254 nm, *n*-hexane/isopropanol = 95:5, flow rate 0.5 mL/min, 30 °C, t_r (major) = 7. 69 min, t_r (minor) = 8.19 min).

HPLC trace of *rac*-**3m**:

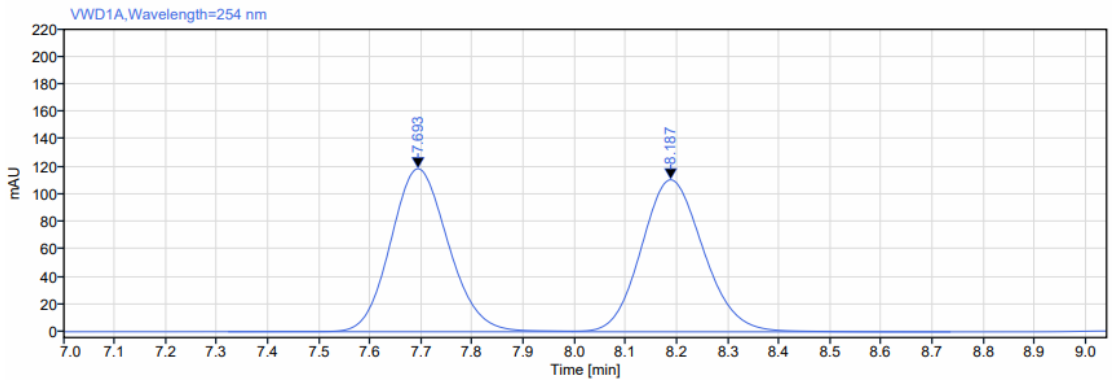

Signal: VWD1A,Wavelength=254 nm

RT [min]	Type	Area	Height	Area%
7.693	BV	932.29	118.52	49.97
8.187	VB	933.51	110.51	50.03
	Sum	1865.80		

HPLC trace of enantioenriched-**3m** obtained in a 0.004 mmol reaction:

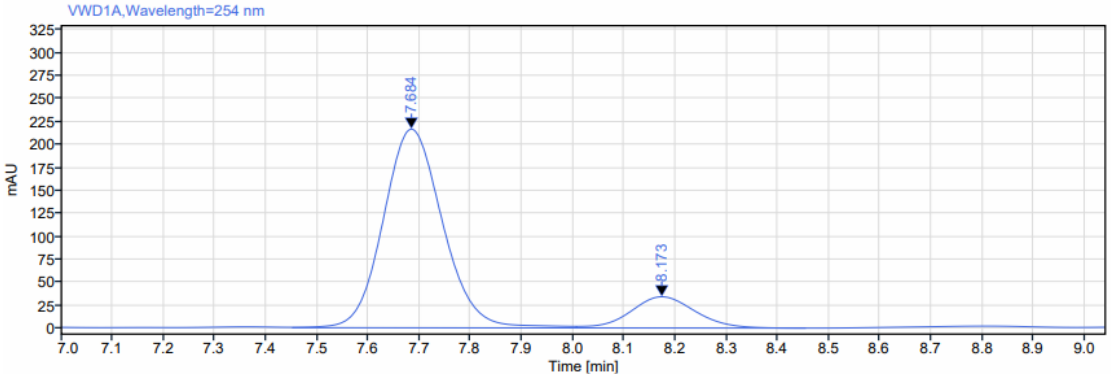

Signal: VWD1A,Wavelength=254 nm

RT [min]	Type	Area	Height	Area%
7.684	VV	1744.50	216.47	85.45
8.173	VB	297.06	34.05	14.55
	Sum	2041.56		

Rac-**3m** is a colorless oil (170 mg, 61%). The NMR spectra of *rac*-**3m** match the one previously reported[36].

^{1}H NMR (400 MHz, $CDCl_3$) δ 8.22 (s, 1H), 8.09 (d, J = 7.9 Hz, 1H), 7.70 (d, J = 7.8 Hz, 1H), 7.49 (t, J = 7.8 Hz, 1H), 7.34-7.23 (m, 4H), 7.25-7.16 (m, 1H), 4.66 (q, J = 6.8 Hz, 1H), 1.55 (d, J = 6.8 Hz, 3H).

^{13}C NMR (100 MHz, $CDCl_3$) δ 198.8, 140.7, 136.9, 131.9 (q, J = 0.6 Hz), 131.1 (q, J = 32.5 Hz), 129.2, 129.11 (q, J = 3.7 Hz), 129.09, 127.7, 127.2, 125.6 (q, J = 3.9 Hz), 123.6 (q, J = 270.8 Hz), 48.3, 19.3.

MS (EI, *m/z*) calcd. for $C_{16}H_{13}F_3O$ $[M]^+$ 278.1, found: 278.1.

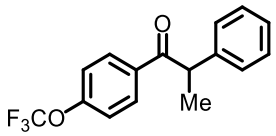

2-Phenyl-1-(4-(trifluoromethoxy)phenyl)propan-1-one (3n)

By using the typical procedure described in Section 4, the reaction of 4-(trifluoromethoxy)benzaldehyde **1n** (0.004 mmol) and ethylbenzene **2a** (0.016 mmol) catalysed by **RAT$_{CH}$** (2 mol%) afforded **3n** in 48% **GC yield** (average of duplicate runs), with a 90% ee.

GC calibration curve for **3n** is displayed below.

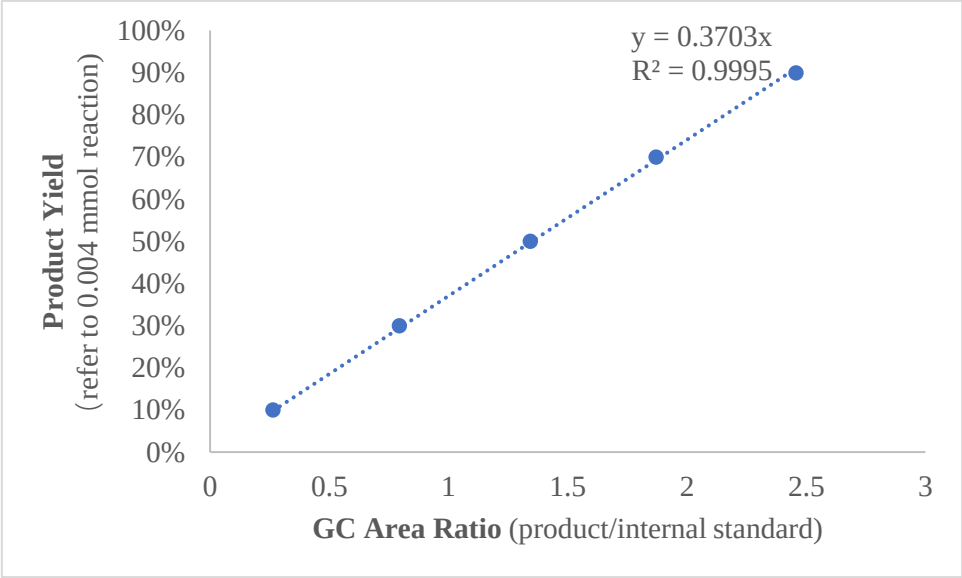

Enantiomeric excess was established by HPLC analysis using a Chiralpak AS-H column (HPLC: AS-H, 254 nm, *n*-hexane/isopropanol = 95:5, flow rate 0.5 mL/min, 30 °C, t_r (major) = 7.38 min, t_r (minor) = 7.70 min).

HPLC trace of *rac*-**3n**:

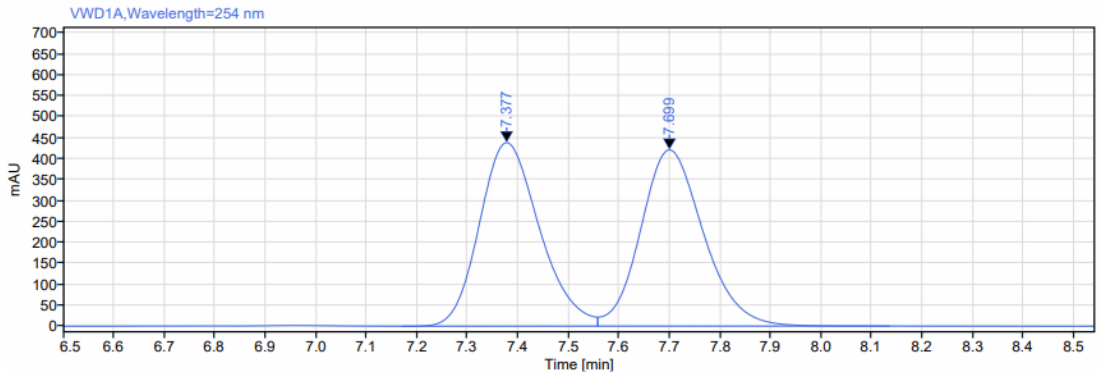

Signal: VWD1A,Wavelength=254 nm

RT [min]	Type	Area	Height	Area%
7.377	BM m	3629.28	439.21	49.91
7.699	MM m	3642.76	421.89	50.09
	Sum	7272.05		

HPLC trace of enantioenriched-**3n** obtained in a 0.004 mmol reaction:

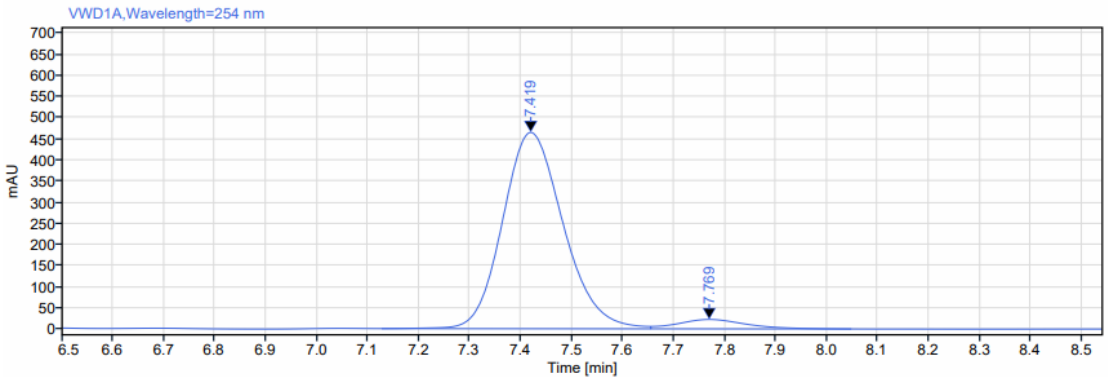

Signal: VWD1A,Wavelength=254 nm

RT [min]	Type	Area	Height	Area%
7.419	BM m	3847.42	465.29	94.90
7.769	MM m	206.84	22.32	5.10
	Sum	4054.25		

Rac-**3n** is a colorless oil (217 mg, 86%). The NMR spectra of *rac*-**3n** match the one previously reported[1].

^{1}H NMR (400 MHz, $CDCl_3$) δ 8.03-7.95 (m, 2H), 7.34-7.23 (m, 4H), 7.25-7.16 (m, 3H), 4.62 (q, J = 6.8 Hz, 1H), 1.53 (d, J = 6.8 Hz, 3H).

^{13}C NMR (100 MHz, $CDCl_3$) δ 198.6, 152.3, 141.1, 134.6, 130.8, 129.1, 127.7, 127.1, 120.19, 120.22 (q, J = 257.2 Hz), 48.2, 19.4.

MS (EI, *m/z*) calcd. for $C_{16}H_{13}F_3O_2$ $[M]^+$ 294.1, found: 294.1.

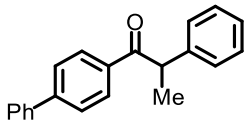

1-([1,1'-Biphenyl]-4-yl)-2-phenylpropan-1-one (3o)

By using the typical procedure described in Section 4, the reaction of [1,1'-biphenyl]-4-carbaldehyde **1o** (0.004 mmol) and ethylbenzene **2a** (0.016 mmol) catalysed by **RAT$_{CH}$** (2 mol%) afforded **3o** in 38% **GC yield** (average of duplicate runs), with a 97% ee.

GC calibration curve for **3o** is displayed below.

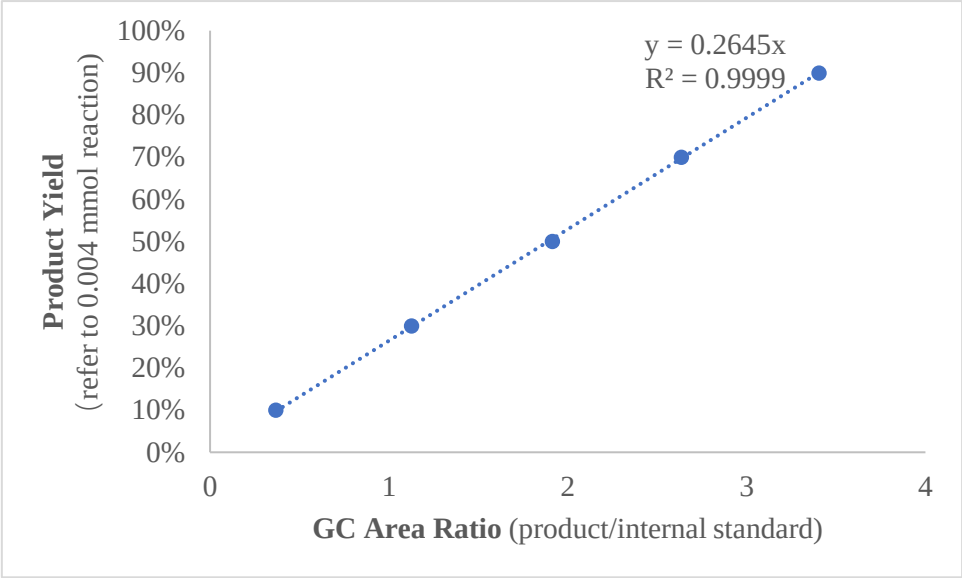

Enantiomeric excess was established by HPLC analysis using a Chiralpak AS-H column (HPLC: AS-H, 254 nm, *n*-hexane/isopropanol = 95:5, flow rate 0.5 mL/min, 30 °C, t_r (major) = 24.34 min, t_r (minor) = 22.13 min).

HPLC trace of *rac*-**3o**:

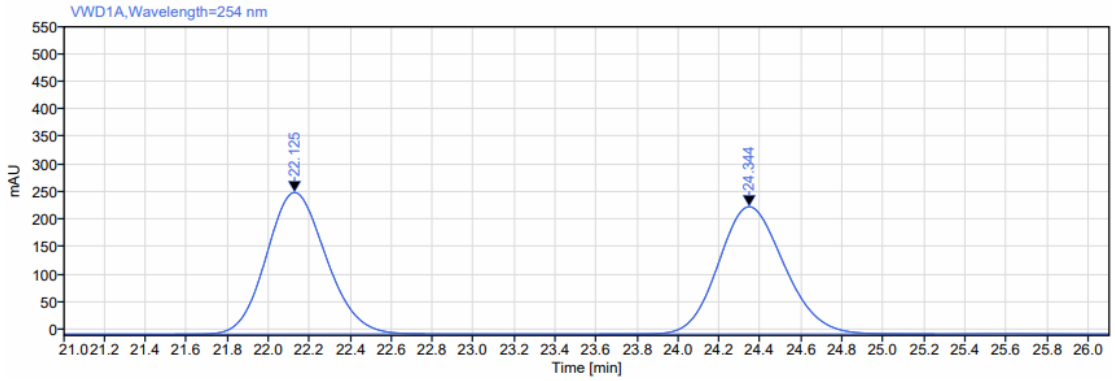

Signal: VWD1A,Wavelength=254 nm

RT [min]	Type	Area	Height	Area%
22.125	BM m	5188.25	256.74	50.20
24.344	BB	5146.18	230.89	49.80
	Sum	10334.43		

HPLC trace of enantioenriched-**3o** obtained in a 0.004 mmol reaction:

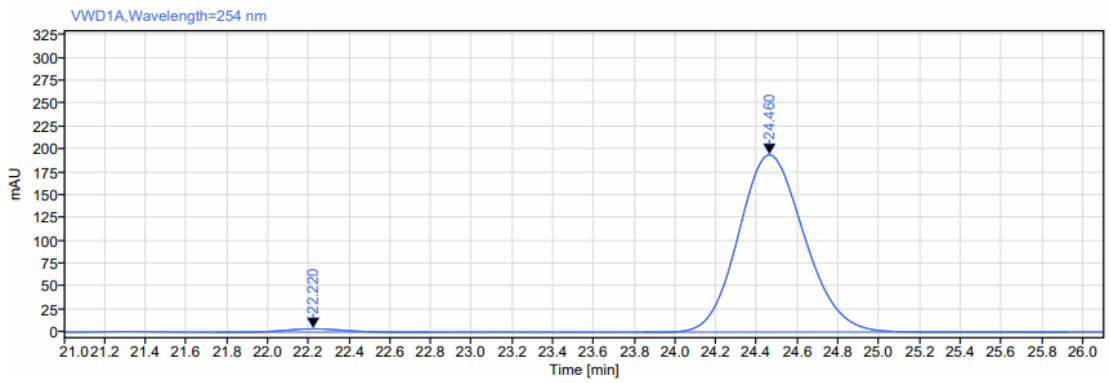

Signal: VWD1A,Wavelength=254 nm

RT [min]	Type	Area	Height	Area%
22.220	BB	74.45	3.69	1.68
24.460	BB	4354.86	194.16	98.32
	Sum	4429.31		

Rac-**3o** is a white solid (316 mg, 84%). The NMR spectra of *rac*-**3o** match the one previously reported[29].

^{1}H NMR (400 MHz, $CDCl_3$) δ 8.05-7.99 (m, 2H), 7.63-7.54 (m, 4H), 7.48-7.40 (m, 2H), 7.41-7.32 (m, 1H), 7.35-7.26 (m, 4H), 7.26-7.17 (m, 1H), 4.71 (q, J = 6.8 Hz, 1H), 1.55 (d, J = 6.9 Hz, 3H).

^{13}C NMR (100 MHz, $CDCl_3$) δ 199.8, 145.4, 141.5, 139.8, 135.1, 129.4, 129.0, 128.9, 128.1, 127.8, 127.2, 127.1, 126.9, 47.9, 19.5.

MS (EI, *m/z*) calcd. for $C_{21}H_{18}O$ $[M]^+$ 286.1, found: 286.1.

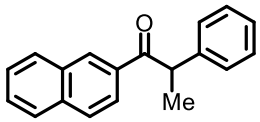

1-(Naphthalen-2-yl)-2-phenylpropan-1-one (3p)

By using the typical procedure described in Section 4, the reaction of 2-naphthaldehyde **1p** (0.004 mmol) and ethylbenzene **2a** (0.016 mmol) catalysed by **RAT$_{CH}$** (2 mol%) afforded **3p** in 30% **GC yield** (average of duplicate runs), with a 85% ee.

GC calibration curve for **3p** is displayed below.

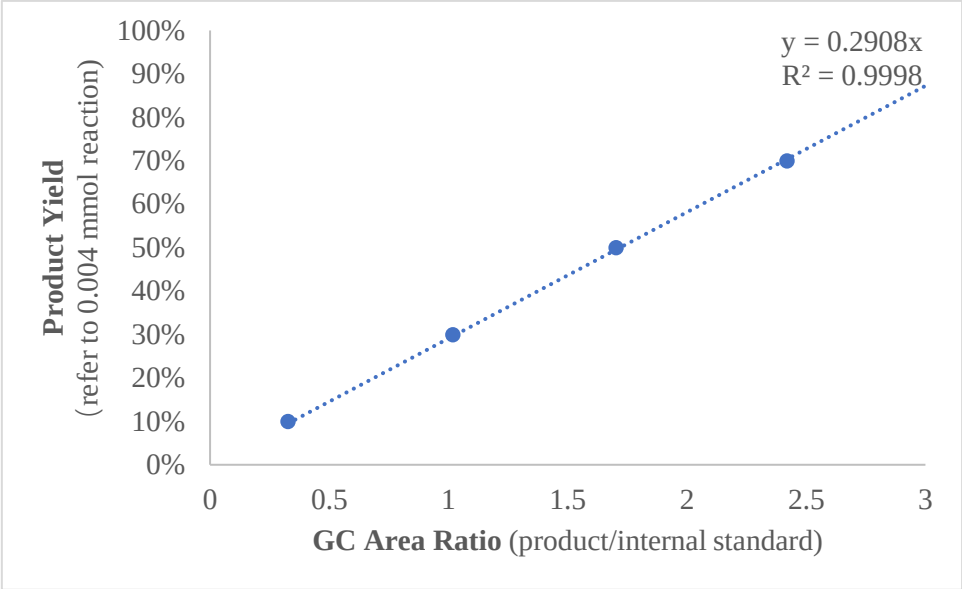

Enantiomeric excess was established by HPLC analysis using a Chiralpak AS-H column (HPLC: AS-H, 254 nm, *n*-hexane/isopropanol = 95:5, flow rate 0.5 mL/min, 30 °C, t_r (major) = 10.61 min, t_r (minor) = 12.40 min).

HPLC trace of *rac*-**3p**:

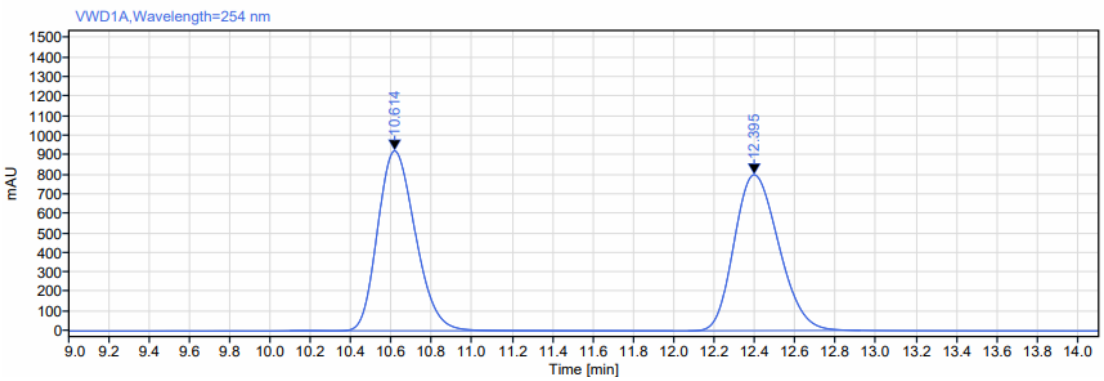

Signal: VWD1A,Wavelength=254 nm

RT [min]	Type	Area	Height	Area%
10.614	MB m	11994.93	921.80	49.50
12.395	MM m	12234.95	798.74	50.50
	Sum	24229.88		

HPLC trace of enantioenriched-**3p** obtained in a 0.004 mmol reaction:

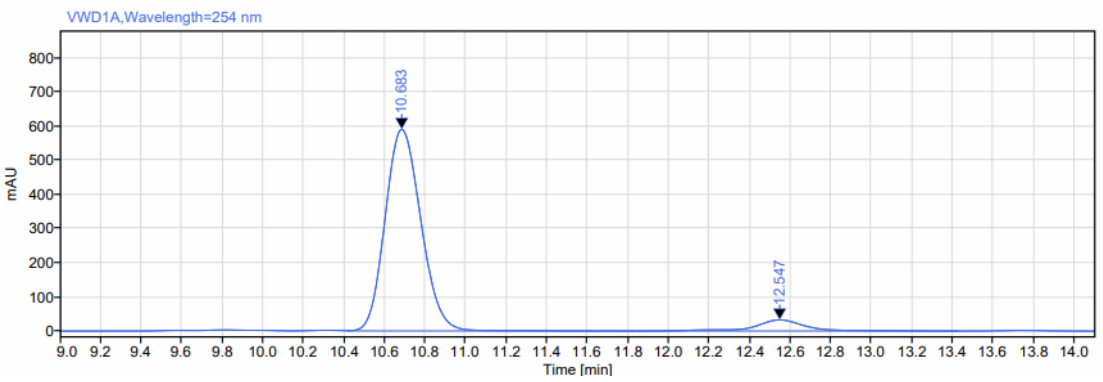

Signal: VWD1A,Wavelength=254 nm

RT [min]	Type	Area	Height	Area%
10.683	VB	7243.57	590.97	92.62
12.547	BB	576.94	32.67	7.38
	Sum	7820.51		

Rac-**3p** is a white solid (195 mg, 75%). The NMR spectra of *rac*-**3p** match the one previously reported[28].

^{1}H NMR (400 MHz, $CDCl_3$) δ 8.47 (s, 1H), 8.00 (dd, J = 8.6, 1.8 Hz, 1H), 7.88 (d, J = 8.0 Hz, 1H), 7.80 (dd, J = 8.5, 2.0 Hz, 2H), 7.57-7.44 (m, 2H), 7.37-7.31 (m, 2H), 7.32-7.24 (m, 2H), 7.22-7.13 (m, 1H), 4.84 (q, J = 6.8 Hz, 1H), 1.59 (d, J = 6.8 Hz, 3H).

^{13}C NMR (100 MHz, $CDCl_3$) δ 200.2, 141.5, 135.3, 133.8, 132.4, 130.4, 129.6, 129.0, 128.3, 128.3, 127.7, 127.6, 126.9, 126.6, 124.5, 47.9, 19.5.

MS (EI, *m/z*) calcd. for $C_{19}H_{16}O$ $[M]^+$ 260.1, found: 260.1.

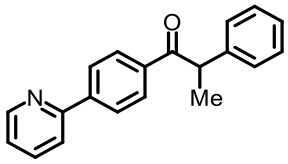

2-Phenyl-1-(4-(pyridin-2-yl)phenyl)propan-1-one (3q)

By using the typical procedure described in Section 4, the reaction of 4-(pyridin-2-yl)benzaldehyde **1q** (0.004 mmol) and ethylbenzene **2a** (0.016 mmol) catalysed by **RAT$_{CH}$** (2 mol%) afforded **3q** in 58% **GC yield** (average of duplicate runs), with a 95% ee.

GC calibration curve for **3q** is displayed below.

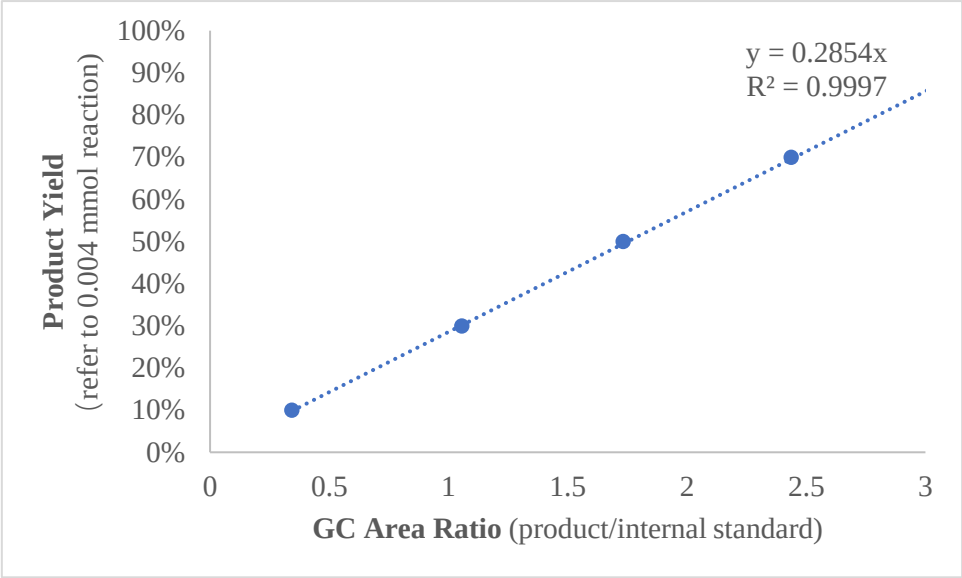

Enantiomeric excess was established by HPLC analysis using a Chiralpak AS-H column (HPLC: AS-H, 254 nm, *n*-hexane/isopropanol =85:15, flow rate 1.0 mL/min, 30 °C, t_r (major) = 13.59 min, t_r (minor) = 8.30 min).

HPLC trace of *rac*-**3q**:

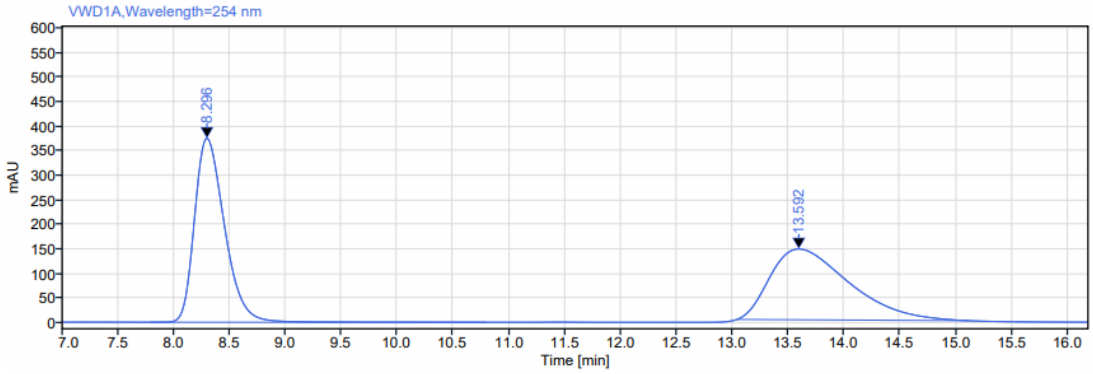

Signal: VWD1A,Wavelength=254 nm

RT [min]	Type	Area	Height	Area%
8.296	BB	6971.98	374.32	49.64
13.592	MM m	7074.35	144.03	50.36
	Sum	14046.33		

HPLC trace of enantioenriched-**3q** obtained in a 0.004 mmol reaction:

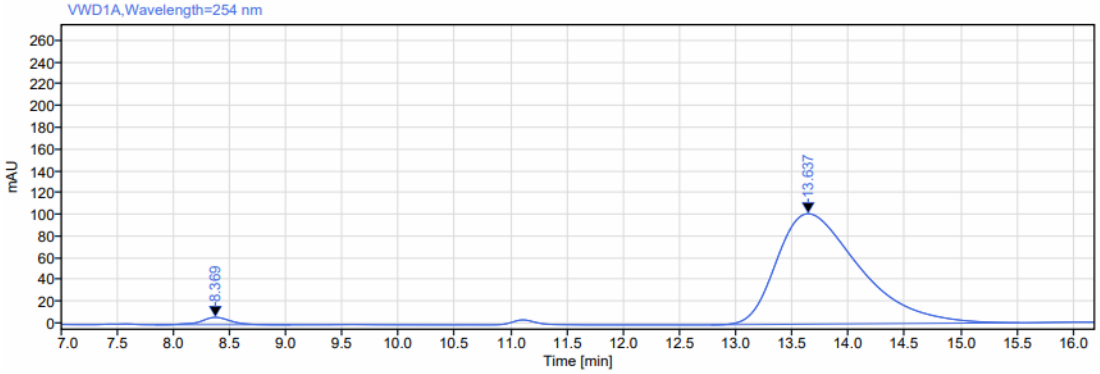

Signal: VWD1A,Wavelength=254 nm

RT [min]	Type	Area	Height	Area%
8.369	BB	124.94	6.83	2.35
13.637	BB	5181.00	101.60	97.65
	Sum	5305.95		

The reaction was scaled up to 0.1 mmol, which afforded 15.5 mg **3q**, corresponding to a 54% isolated yield with a 96% ee.

^{1}H NMR (400 MHz, $CDCl_3$) of enantioenriched-**3q** obtained in a 0.1 mmol reaction:

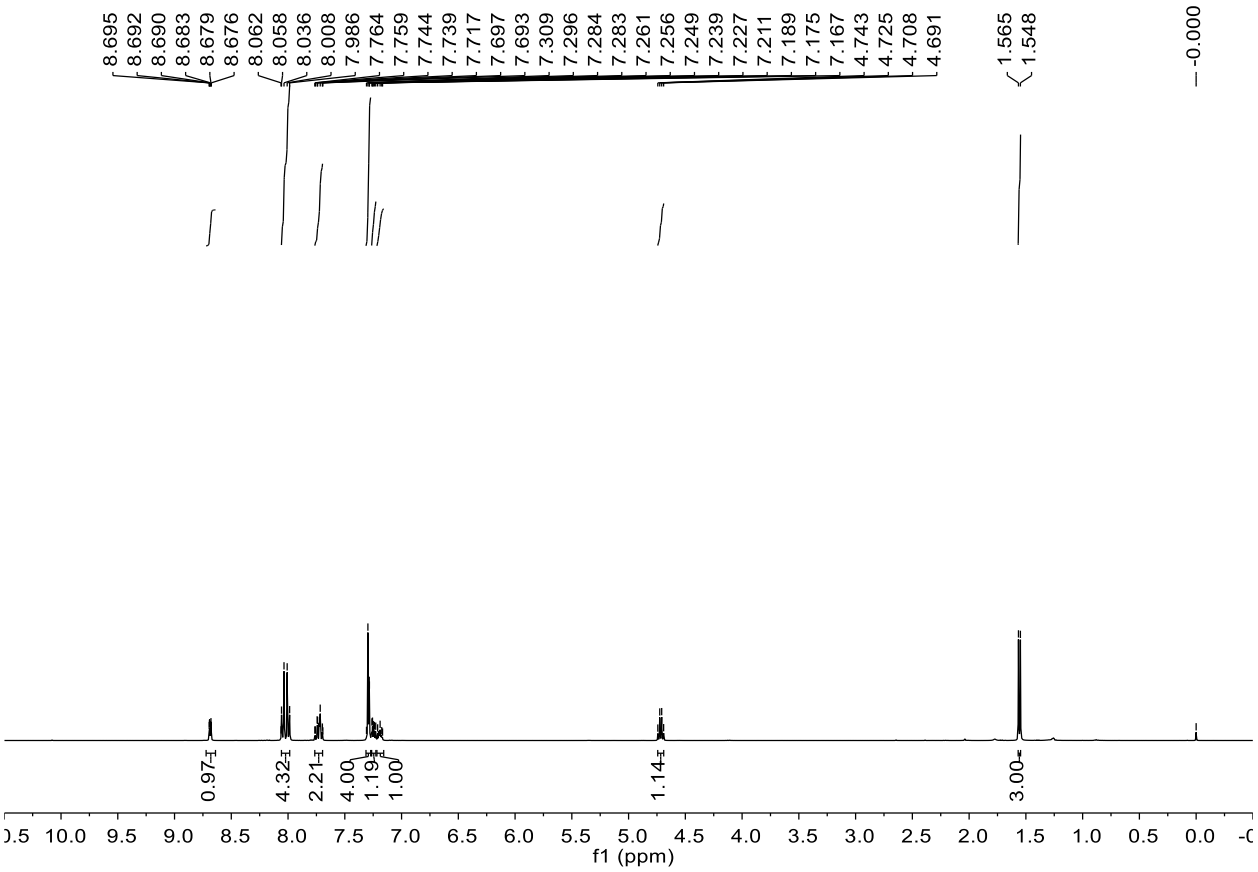

Enantiomeric excess was established by HPLC analysis using a Chiralpak AS-H column (HPLC: AS-H, 254 nm, *n*-hexane/isopropanol =85:15, flow rate 1.0 mL/min, 30 °C, t_r (major) = 14.16 min, t_r (minor) = 8.43 min).

HPLC trace of *rac*-**3q**:

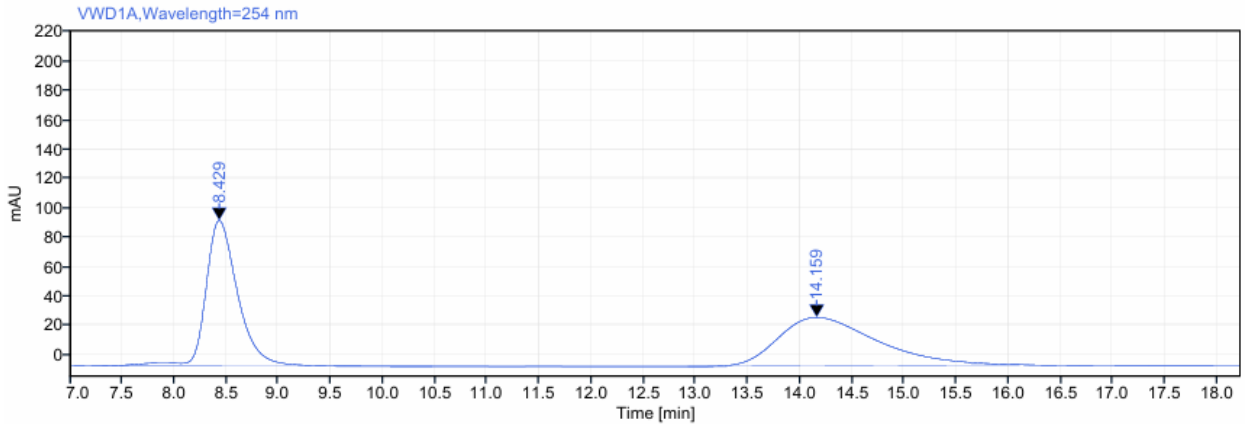

Signal: VWD1A,Wavelength=254 nm

RT [min]	Type	Area	Height	Area%
8.429	MB m	2128.08	99.20	49.60
14.159	BM m	2162.02	33.00	50.40
	Sum	4290.10		

HPLC trace of **3q** obtained in a 0.1 mmol reaction:

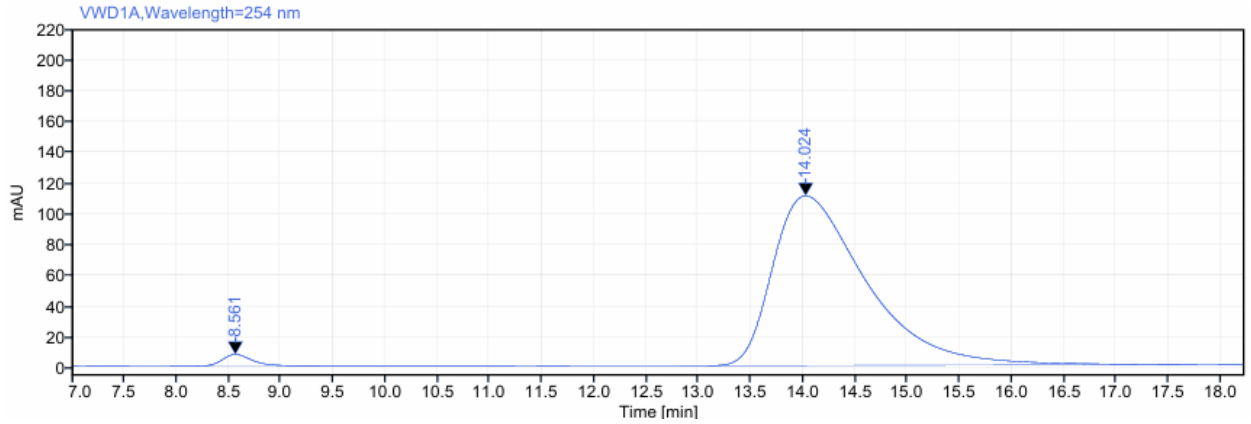

Signal: VWD1A,Wavelength=254 nm

RT [min]	Type	Area	Height	Area%
8.561	BB	142.67	7.41	2.04
14.024	BM m	6855.24	110.14	97.96
	Sum	6997.91		

Rac-**3q** is a white solid (82 mg, 29%).

^{1}H NMR (400 MHz, $CDCl_3$) δ 8.72-8.66 (m, 1H), 8.08-8.02 (m, 2H), 8.03-7.97 (m, 2H), 7.79-7.68 (m, 2H), 7.32-7.27 (m, 4H), 7.28-7.22 (m, 1H), 7.23-7.15 (m, 1H), 4.72 (q, J = 6.8 Hz, 1H), 1.56 (d, J = 6.8 Hz, 3H).

^{13}C NMR (100 MHz, $CDCl_3$) δ 199.9, 156.1, 149.8, 143.2, 141.4, 136.8, 136.5, 129.3, 129.0, 127.8, 126.91, 126.89, 122.8, 120.9, 48.1, 19.4.

HRMS (ESI, *m/z*) calcd. for $C_{20}H_{18}NO$ $[M+H]^+$ 288.1383, found: 288.1380.

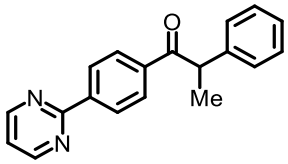

2-Phenyl-1-(4-(pyrimidin-2-yl)phenyl)propan-1-one (3r)

By using the typical procedure described in Section 4, the reaction of 4-(pyrimidin-2-yl)benzaldehyde **1r** (0.004 mmol) and ethylbenzene **2a** (0.016 mmol) catalysed by **RAT$_{CH}$** (2 mol%) afforded **3r** in 58% **GC yield** (average of duplicate runs), with a 92% ee.

GC calibration curve for **3r** is displayed below.

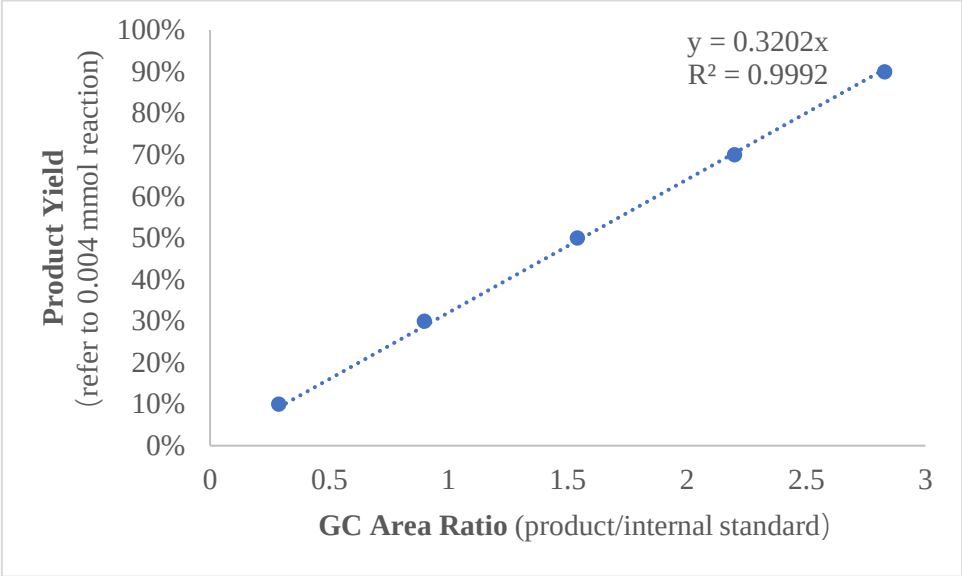

Enantiomeric excess was established by HPLC analysis using a Chiralpak AS-H column (HPLC: AS-H, 254 nm, *n*-hexane/isopropanol = 95:5, flow rate 0.5 mL/min, 30 °C, t_r (major) = 26.21 min, t_r (minor) = 23.11 min).

HPLC trace of *rac*-**3r**:

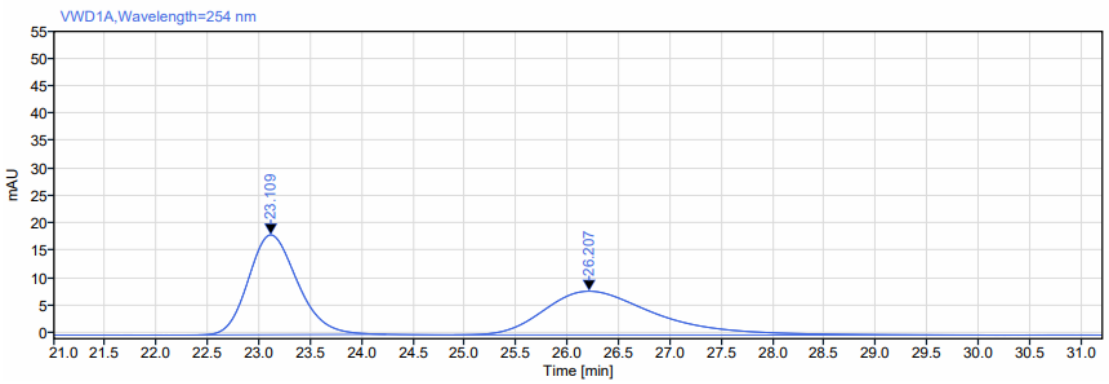

Signal: VWD1A,Wavelength=254 nm

RT [min]	Type	Area	Height	Area%
23.109	MM m	602.26	18.19	50.08
26.207	BB	600.43	7.98	49.92
	Sum	1202.69		

HPLC trace of enantioenriched-**3r** obtained in a 0.004 mmol reaction:

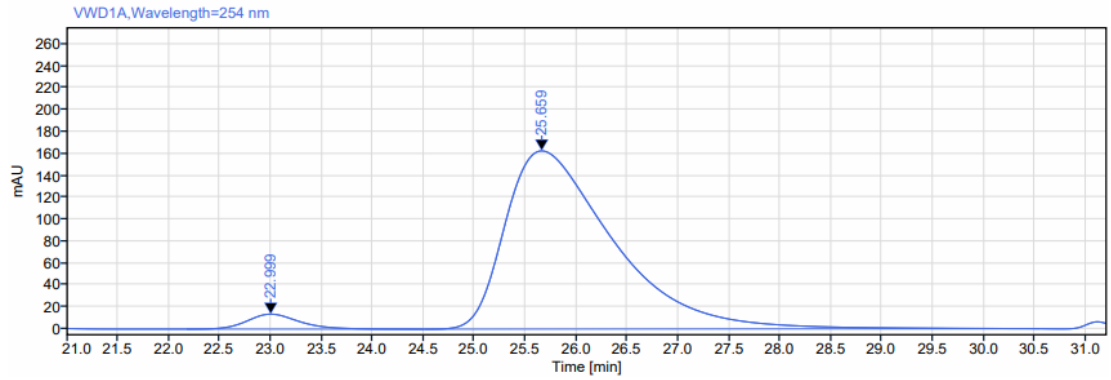

Signal: VWD1A,Wavelength=254 nm

RT [min]	Type	Area	Height	Area%
22.999	BB	489.14	13.69	3.92
25.659	BM m	11995.58	162.60	96.08
	Sum	12484.71		

Rac-**3r** is a white solid (150 mg, 52%).

^{1}H NMR (400 MHz, $CDCl_3$) δ 8.80 (d, J = 4.8 Hz, 2H), 8.48-8.41 (m, 2H), 8.09-8.02 (m, 2H), 7.32 -7.26 (m, 4H), 7.23-7.17 (m, 2H), 4.73 (q, J = 6.8 Hz, 1H), 1.56 (d, J = 6.9 Hz, 3H).

^{13}C NMR (100 MHz, $CDCl_3$) δ 200.1, 163.7, 157.3, 141.3, 138.0, 129.0, 128.98, 128.2, 127.8, 126.9, 119.6, 48.2, 19.4.

HRMS (ESI, *m/z*) calcd. for $C_{19}H_{17}N_2O$ $[M+H]^+$ 289.1335, found: 289.1332.

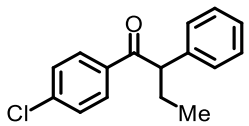

1-(4-Chlorophenyl)-2-phenylbutan-1-one (3s)

By using the typical procedure described in Section 4, the reaction of 4-chlorobenzaldehyde **1a** (0.004 mmol) and propylbenzene **2b** (0.016 mmol) catalysed by **RAT$_{CH}$** (2 mol%) afforded **3s** in 23% **GC yield** (average of duplicate runs), with a 92% ee.

GC calibration curve for **3s** is displayed below.

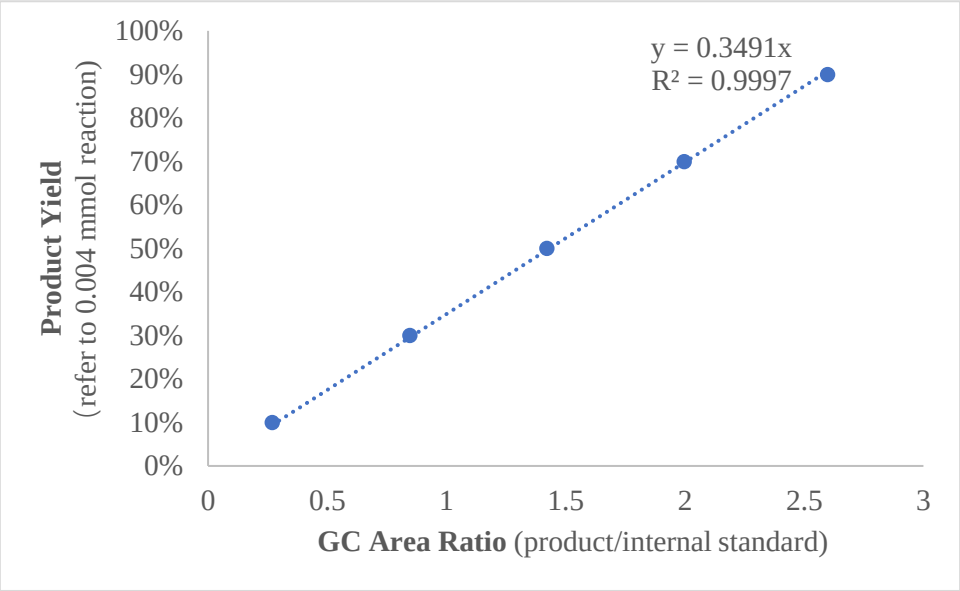

Enantiomeric excess was established by HPLC analysis using a Chiralcel OJ-H column (HPLC: OJ-H, 254 nm, *n*-hexane/isopropanol = 95:5, flow rate 0.5 mL/min, 30 °C, t_r (major) = 14.44 min, t_r (minor) = 16.42 min).

HPLC trace of *rac*-**3s**:

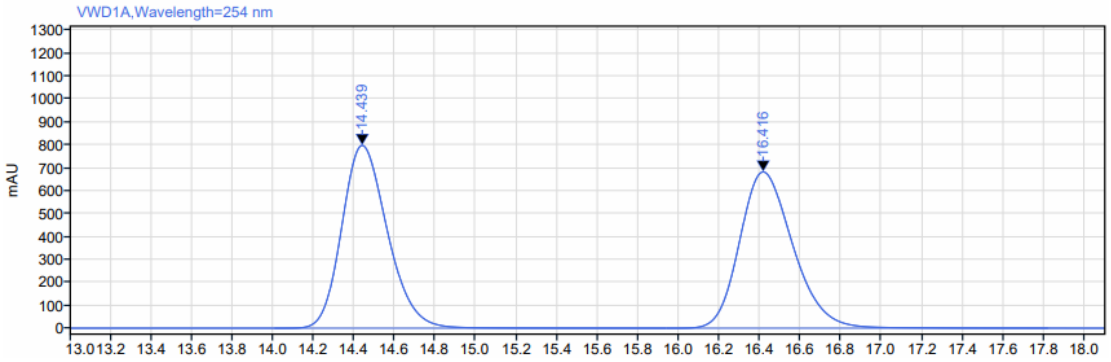

Signal: VWD1A,Wavelength=254 nm

RT [min]	Type	Area	Height	Area%
14.439	BB	12490.07	797.76	50.05
16.416	BM m	12467.27	681.93	49.95
	Sum	24957.34		

HPLC trace of enantioenriched-**3s** obtained in a 0.004 mmol reaction:

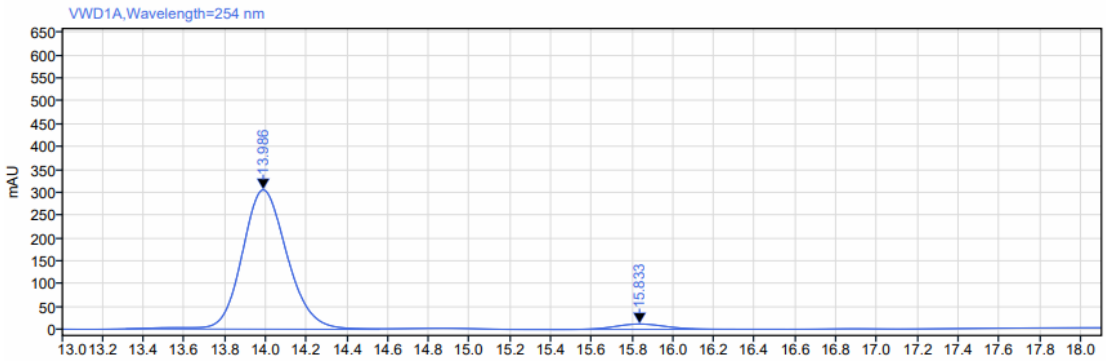

Signal: VWD1A,Wavelength=254 nm

RT [min]	Type	Area	Height	Area%
13.986	MV m	4696.42	304.85	95.90
15.833	BB	200.85	11.74	4.10
	Sum	4897.27		

Rac-**3s** is a colorless oil (514 mg, 62%). The NMR spectra of *rac*-**3s** match the one previously reported[28].

^{1}H NMR (400 MHz, $CDCl_3$) δ 7.92-7.85 (m, 2H), 7.37-7.28 (m, 2H), 7.27-7.25 (m, 3H), 7.20-7.16 (m, 1H), 4.36 (t, *J* = 7.2 Hz, 1H), 2.26-2.11 (m, 1H), 1.92-1.78 (m, 1H), 0.90 (t, *J* = 7.3 Hz, 3H).

^{13}C NMR (100 MHz, $CDCl_3$) δ 198.7, 139.3, 139.1, 135.2, 130.0, 128.9, 128.7, 128.1, 127.1, 55.6, 27.0, 12.2.

MS (EI, *m/z*) calcd. for $C_{16}H_{15}ClO$ $[M]^+$ 258.1, found: 258.1.

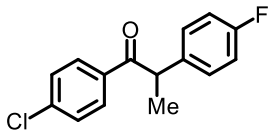

1-(4-Chlorophenyl)-2-(4-fluorophenyl)propan-1-one (3t)

By using the typical procedure described in Section 4, the reaction of 4-chlorobenzaldehyde **1a** (0.004 mmol) and 1-ethyl-4-fluorobenzene **2c** (0.016 mmol) catalysed by **RAT$_{CH}$** (2 mol%) afforded **3t** in 58% **GC yield** (average of duplicate runs), with a 93% ee.

GC calibration curve for **3t** is displayed below.

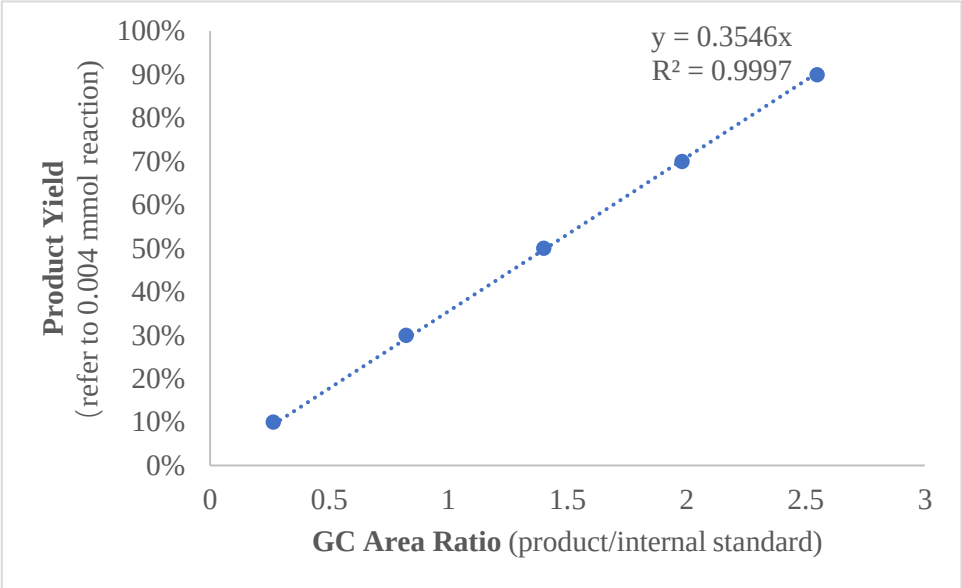

Enantiomeric excess was established by HPLC analysis using a Chiralpak AS-H column (HPLC: AS-H, 254 nm, *n*-hexane/isopropanol = 95:5, flow rate 0.5 mL/min, 30 °C, t_r (major) = 10.58 min, t_r (minor) = 14.41 min).

HPLC trace of *rac*-**3t**:

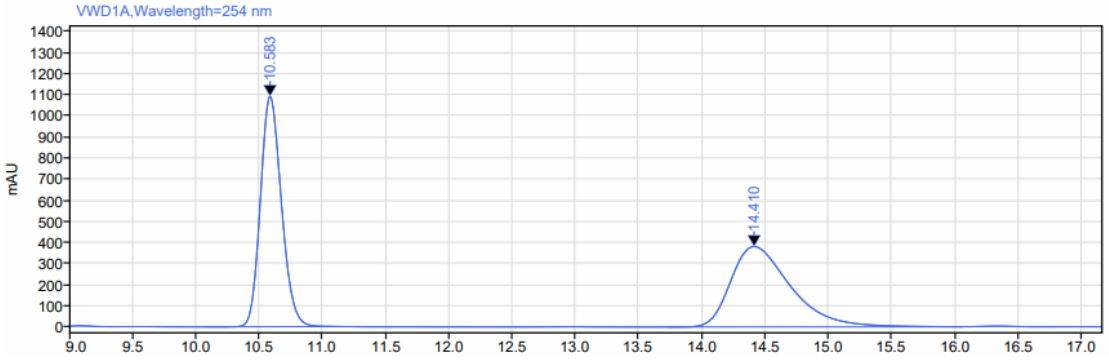

Signal: VWD1A,Wavelength=254 nm

RT [min]	Type	Area	Height	Area%
10.583	BM m	12629.43	1092.51	50.18
14.410	BV	12540.77	381.26	49.82
	Sum	25170.20		

HPLC trace of enantioenriched-**3t** obtained in a 0.004 mmol reaction:

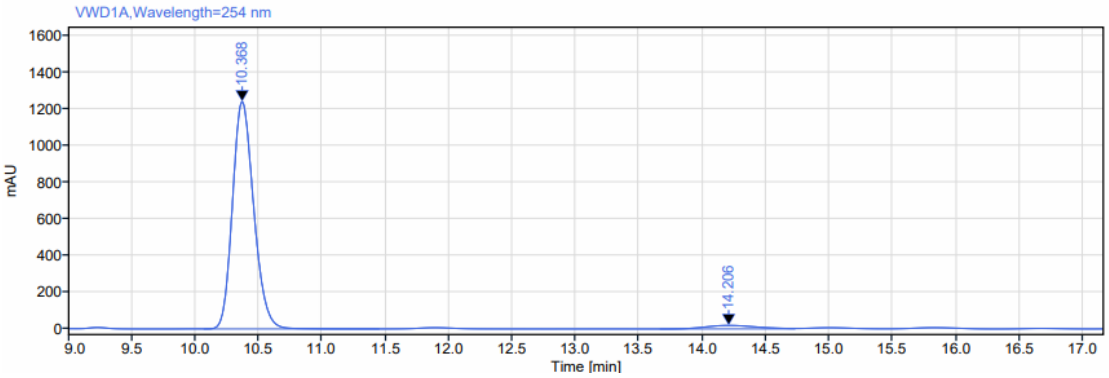

Signal: VWD1A,Wavelength=254 nm

RT [min]	Type	Area	Height	Area%
10.368	VB	14503.82	1242.33	96.38
14.206	BV	544.31	19.21	3.62
	Sum	15048.13		

Rac-**3t** is a colorless oil (264 mg, 60%).
^{1}H NMR (400 MHz, $CDCl_3$) δ 7.90-7.82 (m, 2H), 7.39-7.32 (m, 2H), 7.28-7.17 (m, 2H), 7.03-6.93 (m, 2H), 4.61 (q, J = 6.8 Hz, 1H), 1.51 (d, J = 6.9 Hz, 3H).
^{13}C NMR (100 MHz, $CDCl_3$) δ 198.9, 161.8 (d, J = 244.2 Hz), 139.3, 136.8 (d, J = 3.2 Hz), 134.5, 130.1, 129.2 (d, J = 8.1 Hz), 128.8, 116.0 (d, J = 21.3 Hz), 47.1, 19.5.
HRMS (ESI, *m/z*) calcd. for $C_{15}H_{13}ClFO$ $[M+H]^+$ 263.0633, found: 263.0631.

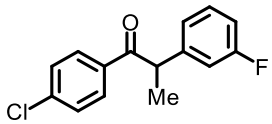

1-(4-Chlorophenyl)-2-(3-fluorophenyl)propan-1-one (3u)
By using the typical procedure described in Section 4, the reaction of 4-chlorobenzaldehyde **1a** (0.004 mmol) and 1-ethyl-3-fluorobenzene **2d** (0.016 mmol) catalysed by **RAT$_{CH}$** (2 mol%) afforded **3u** in 59% **GC yield** (average of duplicate runs), with a 93% ee.
GC calibration curve for **3u** is displayed below.

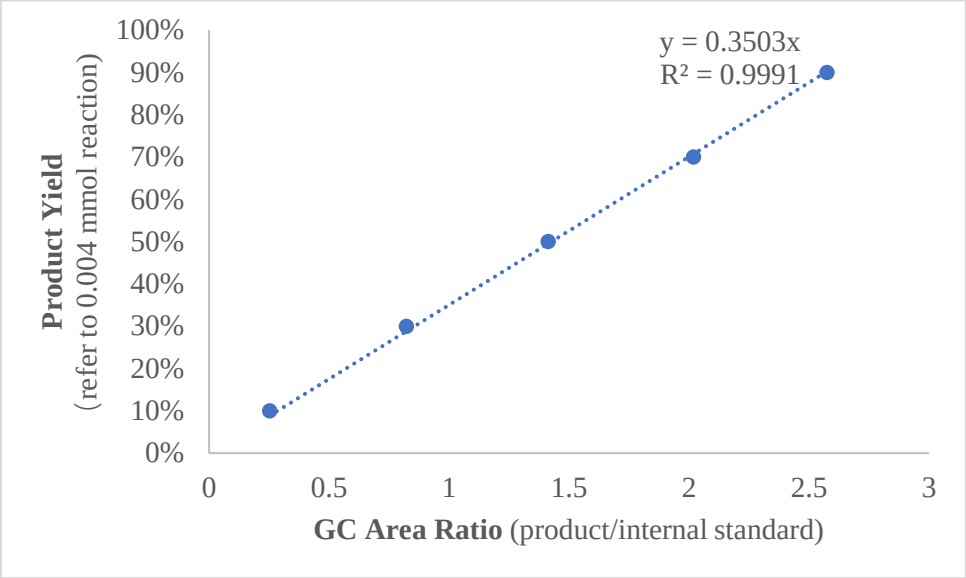

Enantiomeric excess was established by HPLC analysis using a Chiralpak AS-H column (HPLC: AS-H, 254 nm, *n*-hexane/isopropanol = 95:5, flow rate 0.5 mL/min, 30 °C, t_r (major) = 10.51 min, t_r (minor) = 11.91 min).

HPLC trace of *rac*-**3u**:

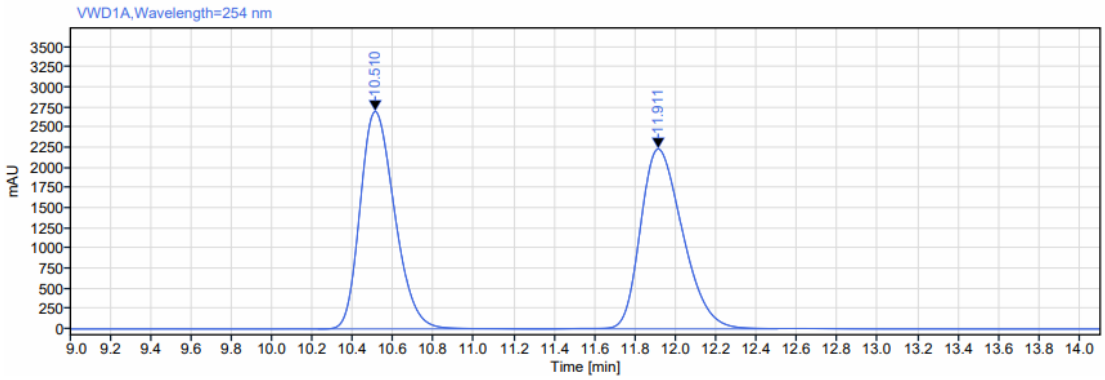

Signal: VWD1A,Wavelength=254 nm

RT [min]	Type	Area	Height	Area%
10.510	VB	32062.43	2698.96	49.72
11.911	BV	32422.80	2233.36	50.28
	Sum	64485.23		

HPLC trace of enantioenriched-**3u** obtained in a 0.004 mmol reaction:

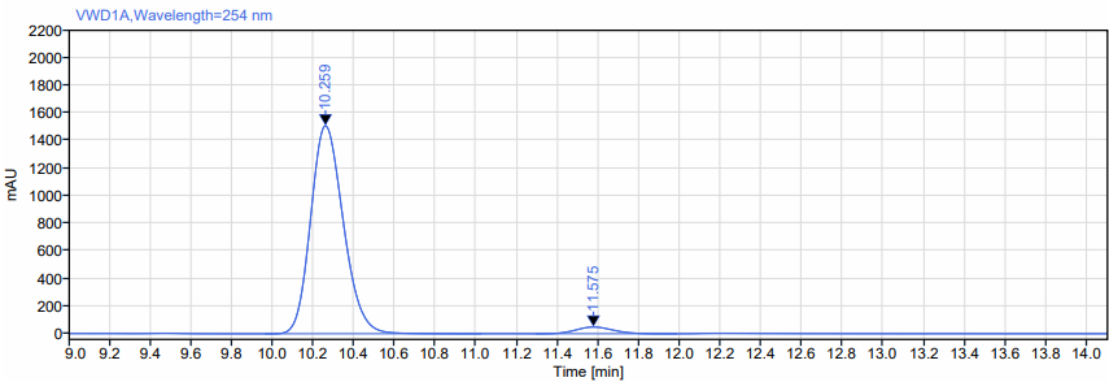

Signal: VWD1A,Wavelength=254 nm

RT [min]	Type	Area	Height	Area%
10.259	BB	16812.98	1507.67	96.43
11.575	BB	623.03	48.77	3.57
	Sum	17436.00		

Rac-**3u** is a colorless oil (168 mg, 64%).
^{1}H NMR (400 MHz, $CDCl_3$) δ 7.90-7.83 (m, 2H), 7.38-7.31 (m, 2H), 7.30-7.20 (m, 1H), 7.07-7.00 (m, 1H), 7.01-6.94 (m, 1H), 6.94-6.85 (m, 1H), 4.62 (q, J = 6.8 Hz, 1H), 1.52 (d, J = 6.8 Hz, 3H).
^{13}C NMR (100 MHz, $CDCl_3$) δ 198.4, 163.0 (d, J = 245.4 Hz), 143.5 (d, J = 7.2 Hz), 139.4, 134.5, 130.5 (d, J = 8.1 Hz), 130.1, 128.8, 123.4 (d, J = 2.9 Hz), 114.6 (d, J = 21.5 Hz), 114.0 (d, J = 21.1 Hz), 47.5 (d, J = 1.7 Hz), 19.2.
HRMS (ESI, *m/z*) calcd. for $C_{15}H_{13}ClFO$ $[M+H]^+$ 263.0633, found: 263.0630.

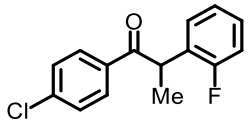

1-(4-Chlorophenyl)-2-(2-fluorophenyl)propan-1-one (3v)
By using the typical procedure described in Section 4, the reaction of 4-chlorobenzaldehyde **1a** (0.004 mmol) and 1-ethyl-2-fluorobenzene **2e** (0.016 mmol) catalysed by **RAT$_{CH}$** (2 mol%) afforded **3v** in 43% **GC yield** (average of duplicate runs), with a 95% ee.

GC calibration curve for **3v** is displayed below.

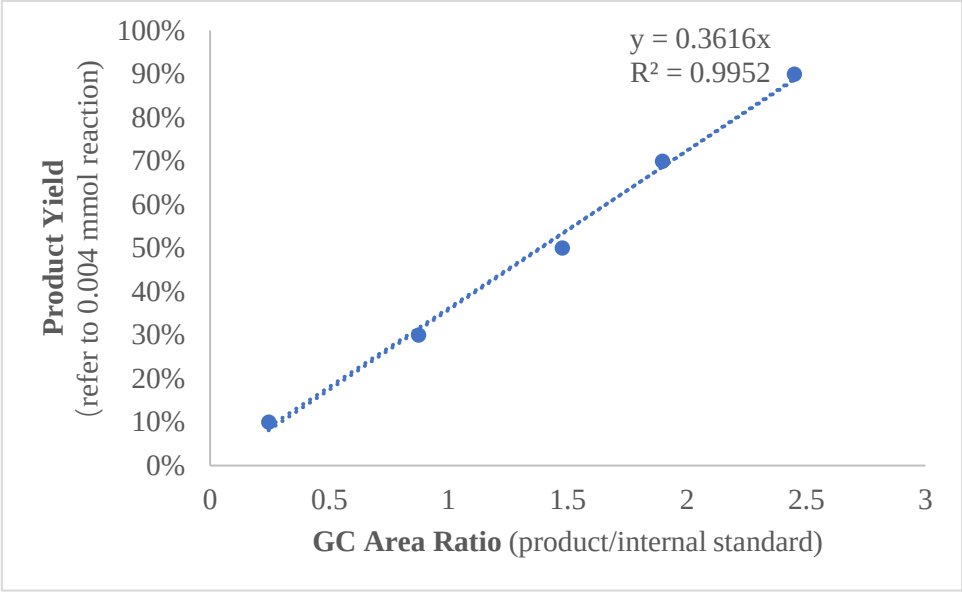

Enantiomeric excess was established by HPLC analysis using a Chiralpak AS-H column (HPLC: AS-H, 254 nm, *n*-hexane/isopropanol = 95:5, flow rate 0.5 mL/min, 30 °C, t_r (major) = 8.32 min, t_r (minor) = 9.30 min).

HPLC trace of *rac*-**3v**:

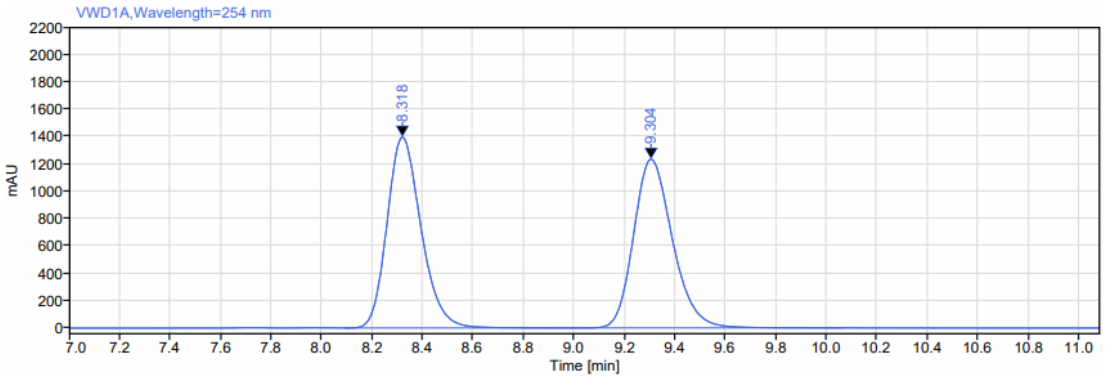

Signal: VWD1A,Wavelength=254 nm

RT [min]	Type	Area	Height	Area%
8.318	VB	13102.53	1397.38	49.82
9.304	BM m	13199.38	1234.44	50.18
	Sum	26301.91		

HPLC trace of enantioenriched-**3v** obtained in a 0.004 mmol reaction:

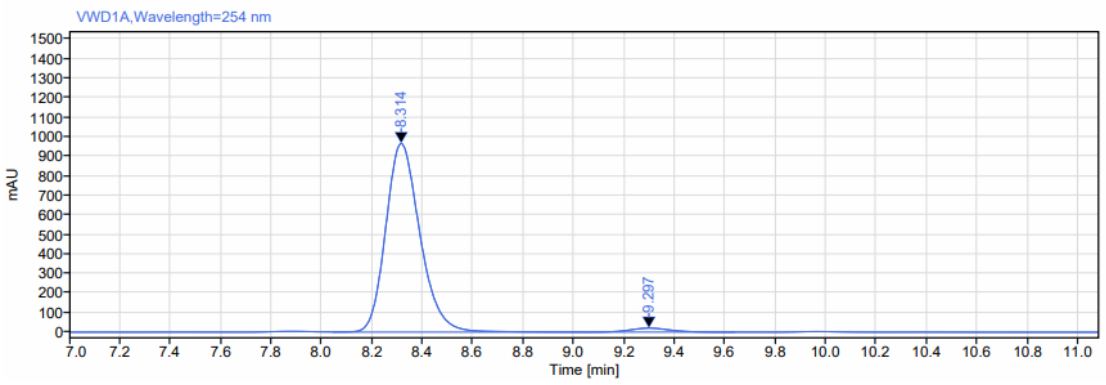

Signal: VWD1A,Wavelength=254 nm

RT [min]	Type	Area	Height	Area%
8.314	VV	9131.47	966.92	97.56
9.297	VB	227.94	20.59	2.44
	Sum	9359.41		

Rac-**3v** is a colorless oil (121 mg, 77%).
^{1}H NMR (400 MHz, $CDCl_3$) δ 7.92-7.85 (m, 2H), 7.39-7.32 (m, 2H), 7.24-7.12 (m, 2H), 7.10-7.01 (m, 2H), 4.96 (q, J = 6.8 Hz, 1H), 1.51 (d, J = 6.8 Hz, 3H).
^{13}C NMR (100 MHz, $CDCl_3$) δ 198.6, 159.6 (d, J = 243.4 Hz), 139.4, 134.3, 129.9, 128.9,128.8 (d, J = 8.3 Hz), 128.7 (d, J = 3.8 Hz), 128.0 (d, J = 15.3 Hz), 124.7 (d, J = 3.5 Hz), 115.7 (d, J = 22.4 Hz), 39.6 (d, J = 2.3 Hz), 17.9.
HRMS (ESI, *m/z*) calcd. for $C_{15}H_{13}ClFO$ $[M+H]^+$ 263.0633, found: 263.0631.

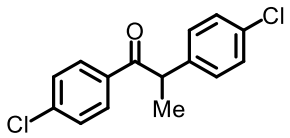

1,2-Bis(4-chlorophenyl)propan-1-one (3w)
By using the typical procedure described in Section 4, the reaction of 4-chlorobenzaldehyde **1a** (0.004 mmol) and 1-chloro-4-ethylbenzene **2f** (0.016 mmol) catalysed by **RAT$_{CH}$** (2 mol%) afforded **3w** in 54% **GC yield** (average of duplicate runs), with a 94% ee.

GC calibration curve for **3w** is displayed below.

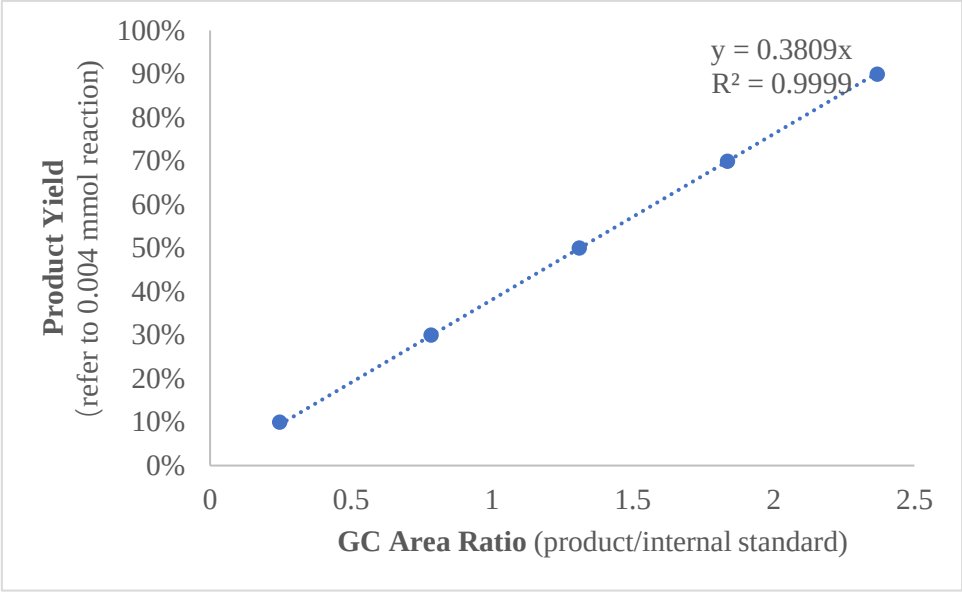

Enantiomeric excess was established by HPLC analysis using a Chiralpak AS-H column (HPLC: AS-H, 254 nm, *n*-hexane/isopropanol = 95:5, flow rate 0.5 mL/min, 30 °C, t_r (major) = 11.22 min, t_r (minor) = 12.82 min).

HPLC trace of *rac*-**3w**:

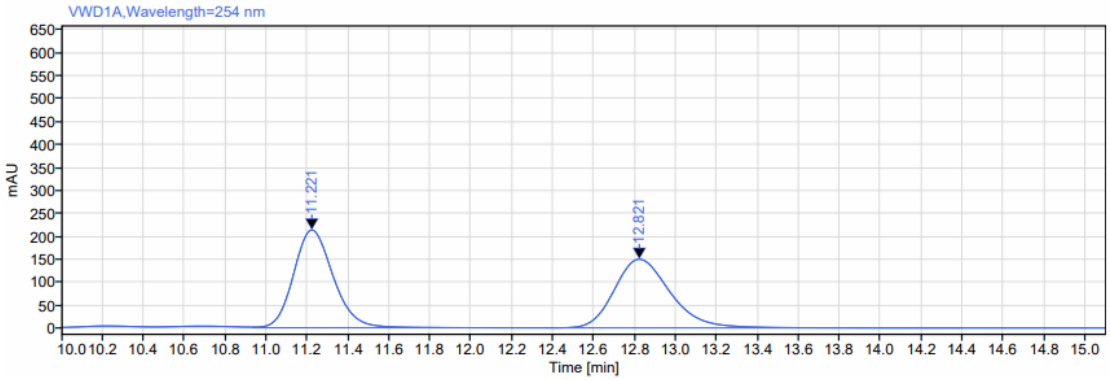

Signal: VWD1A,Wavelength=254 nm

RT [min]	Type	Area	Height	Area%
11.221	VM m	2850.85	212.94	50.10
12.821	BM m	2839.36	149.53	49.90
	Sum	5690.21		

HPLC trace of enantioenriched-**3w** obtained in a 0.004 mmol reaction:

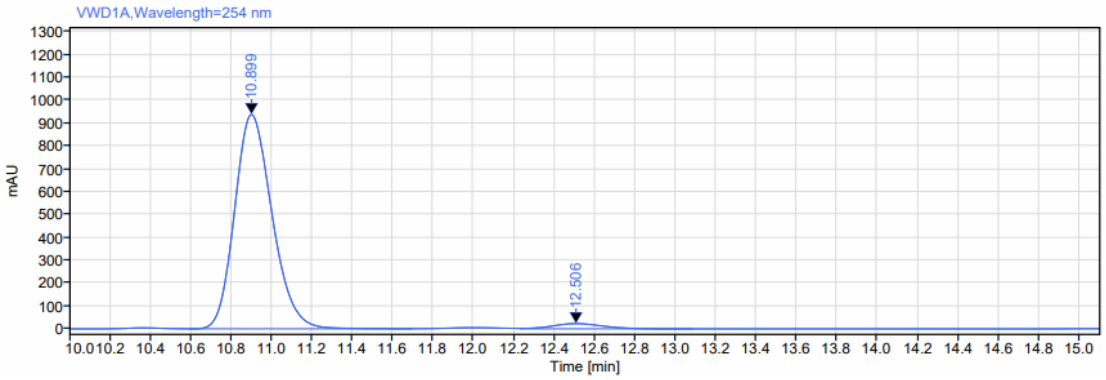

Signal: VWD1A,Wavelength=254 nm

RT [min]	Type	Area	Height	Area%
10.899	BV	12106.90	938.90	96.79
12.506	VM m	400.96	22.97	3.21
	Sum	12507.86		

Rac-**3w** is a pale-yellow oil (154 mg, 68%). The NMR spectra of *rac*-**3w** match the one previously reported[37].

^{1}H NMR (400 MHz, $CDCl_3$) δ 7.89-7.81 (m, 2H), 7.40-7.32 (m, 2H), 7.30-7.23 (m, 2H), 7.22-7.16 (m, 2H), 4.60 (q, J = 6.8 Hz, 1H), 1.51 (d, J = 6.9 Hz, 3H).

^{13}C NMR (100 MHz, $CDCl_3$) δ 198.7, 139.6, 139.4, 134.5, 133.0, 130.1, 129.2, 129.0, 128.9, 47.3, 19.3.

MS (EI, *m/z*) calcd. for $C_{15}H_{12}Cl_2O$ $[M]^+$ 278.0, found: 278.0.

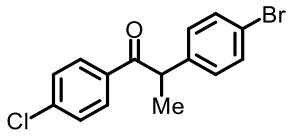

2-(4-Bromophenyl)-1-(4-chlorophenyl)propan-1-one (3x)

By using the typical procedure described in Section 4, the reaction of 4-chlorobenzaldehyde **1a** (0.004 mmol) and 1-bromo-4-ethylbenzene **2g** (0.016 mmol) catalysed by **RAT$_{CH}$** (2 mol%) afforded **3x** in 54% **GC yield** (average of duplicate runs), with a 93% ee.

GC calibration curve for **3x** is displayed below.

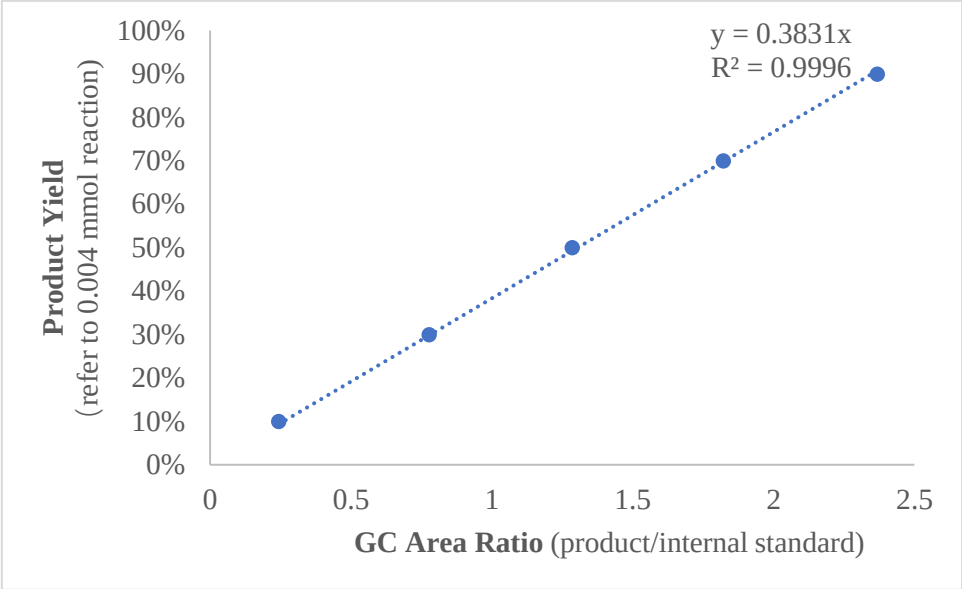

Enantiomeric excess was established by HPLC analysis using a Chiralpak AS-H column (HPLC: AS-H, 254 nm, *n*-hexane/isopropanol = 95:5, flow rate 0.5 mL/min, 30 °C, t_r (major) = 11.69 min, t_r (minor) = 13.37 min).

HPLC trace of *rac*-**3x**:

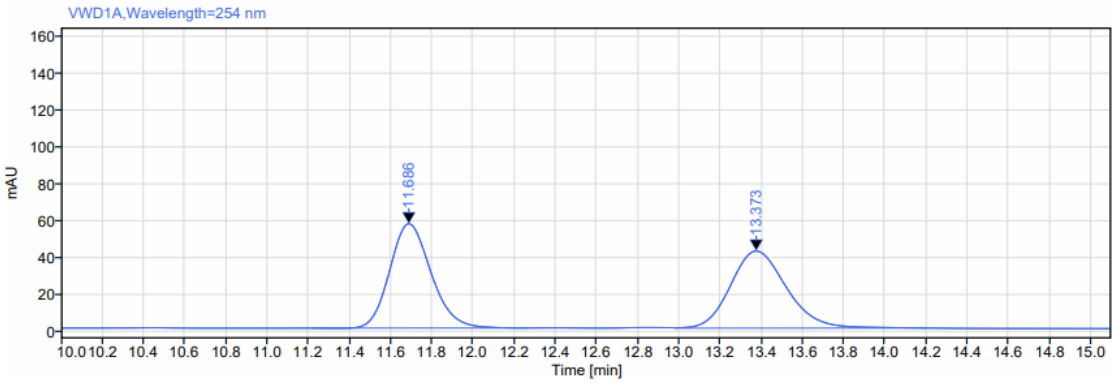

Signal: VWD1A,Wavelength=254 nm

RT [min]	Type	Area	Height	Area%
11.686	MB m	788.25	56.60	49.92
13.373	VM m	790.79	41.84	50.08
	Sum	1579.03		

HPLC trace of enantioenriched-**3x** obtained in a 0.004 mmol reaction:

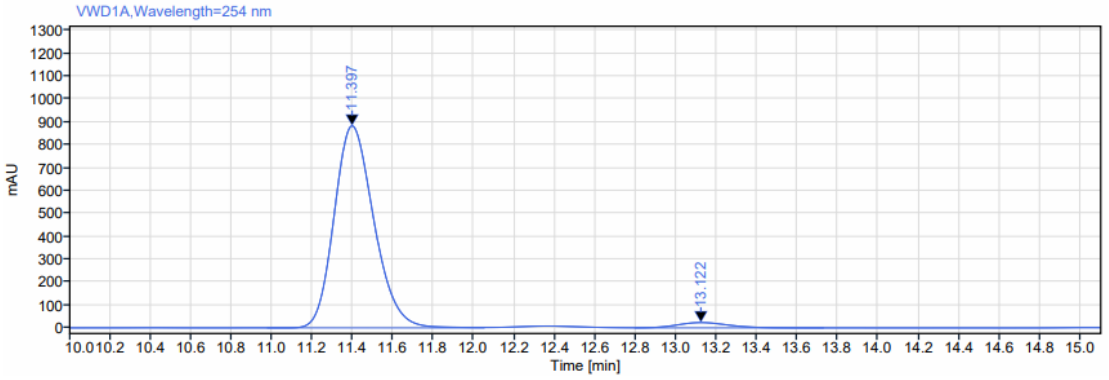

Signal: VWD1A,Wavelength=254 nm

RT [min]	Type	Area	Height	Area%
11.397	MV m	12082.50	883.66	96.70
13.122	VM m	412.53	23.39	3.30
	Sum	12495.03		

Rac-**3x** is a pale-yellow oil (1.12 g, 77%).
^{1}H NMR (400 MHz, $CDCl_3$) δ 7.89-7.81 (m, 2H), 7.46-7.38 (m, 2H), 7.40-7.32 (m, 2H), 7.17-7.09 (m, 2H), 4.58 (q, J = 6.8 Hz, 1H), 1.50 (d, J = 6.9 Hz, 3H).
^{13}C NMR (100 MHz, $CDCl_3$) δ 198.6, 140.1, 139.4, 134.5, 132.2, 130.1, 129.4, 128.9, 121.1, 47.3, 19.3.
HRMS (ESI, *m/z*) calcd. for $C_{15}H_{13}BrClO$ $[M+H]^+$ 322.9833, found: 322.9831.

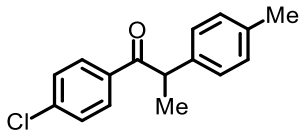

1-(4-Chlorophenyl)-2-(*p*-tolyl)propan-1-one (3y)
By using the typical procedure described in Section 4, the reaction of 4-chlorobenzaldehyde **1a** (0.004 mmol) and 1-ethyl-4-methylbenzene **2h** (0.016 mmol) catalysed by **RAT$_{CH}$** (2 mol%) afforded **3y** in 52% **GC yield** (average of duplicate runs), with a 91% ee.

GC calibration curve for **3y** is displayed below.

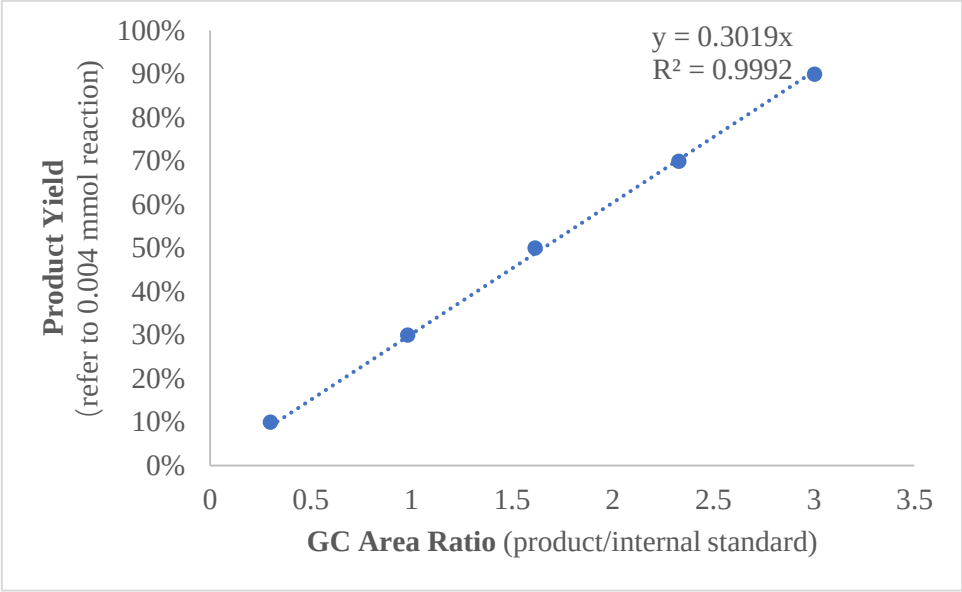

Enantiomeric excess was established by HPLC analysis using a Chiralcel OJ-H column (HPLC: OJ-H, 254 nm, *n*-hexane/isopropanol = 95:5, flow rate 0.5 mL/min, 30 °C, t_r (major) = 15.49 min, t_r (minor) = 18.22 min).

HPLC trace of *rac*-**3y**:

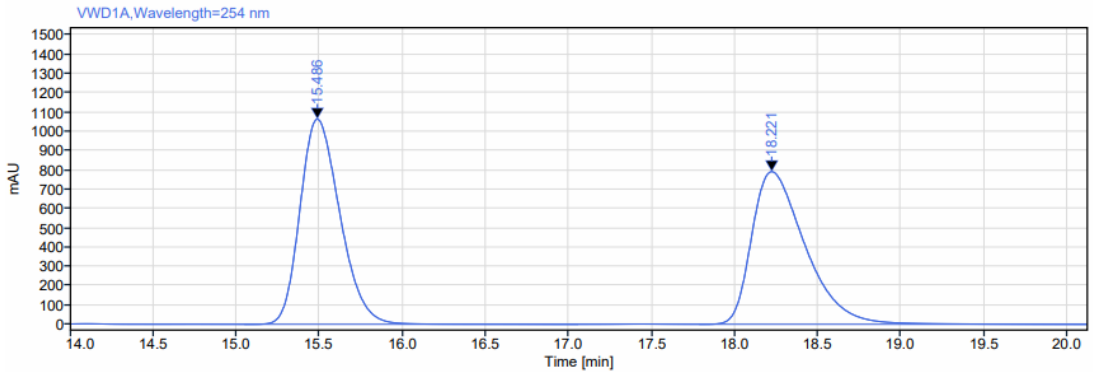

Signal: VWD1A,Wavelength=254 nm

RT [min]	Type	Area	Height	Area%
15.486	BB	17776.24	1064.16	50.03
18.221	VB	17756.58	791.59	49.97
	Sum	35532.82		

HPLC trace of enantioenriched-**3y** obtained in a 0.004 mmol reaction:

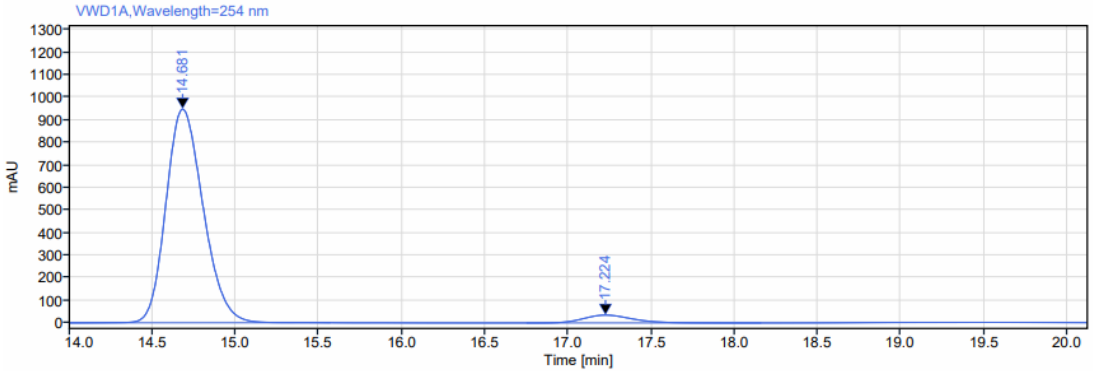

Signal: VWD1A,Wavelength=254 nm

RT [min]	Type	Area	Height	Area%
14.681	BM m	14781.99	948.64	95.41
17.224	BB	711.45	34.81	4.59
	Sum	15493.44		

Rac-**3y** is a colorless oil (201 mg, 78%). The NMR spectra of *rac*-**3y** match the one previously reported[38].

^{1}H NMR (400 MHz, $CDCl_3$) δ 7.90-7.84 (m, 2H), 7.36-7.28 (m, 2H), 7.11 (q, J = 8.0 Hz, 4H), 4.57 (q, J = 6.8 Hz, 1H), 2.27 (s, 3H), 1.50 (d, J = 6.8 Hz, 3H).

^{13}C NMR (100 MHz, $CDCl_3$) δ 199.1, 139.0, 138.1, 136.7, 134.8, 130.1, 129.8, 128.7, 127.5, 47.6, 21.0, 19.4.

MS (EI, *m/z*) calcd. for $C_{16}H_{15}ClO$ $[M]^+$ 258.1, found: 258.1.

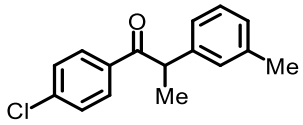

1-(4-Chlorophenyl)-2-(*m*-tolyl)propan-1-one (3z)

By using the typical procedure described in Section 4, the reaction of 4-chlorobenzaldehyde **1a** (0.004 mmol) and 1-ethyl-3-methylbenzene **2i** (0.016 mmol) catalysed by **RAT$_{CH}$** (2 mol%) afforded **3z** in 58% **GC yield** (average of duplicate runs), with a 91% ee.

GC calibration curve for **3z** is displayed below.

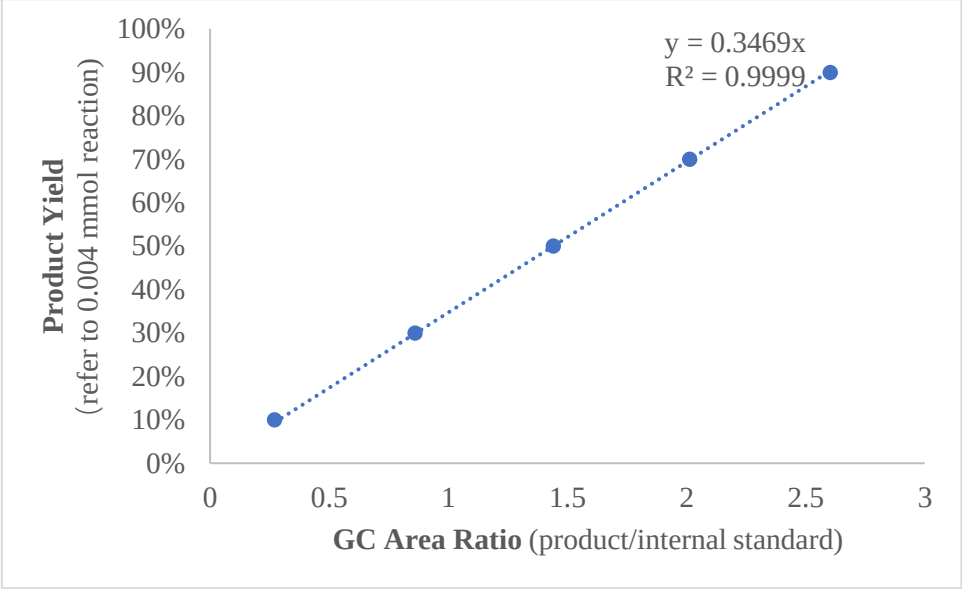

Enantiomeric excess was established by HPLC analysis using a Chiralcel OJ-H column (HPLC: OJ-H, 254 nm, *n*-hexane/isopropanol = 95:5, flow rate 0.5 mL/min, 30 °C, t_r (major) = 13.43 min, t_r (minor) = 15.40 min).

HPLC trace of *rac*-**3z**:

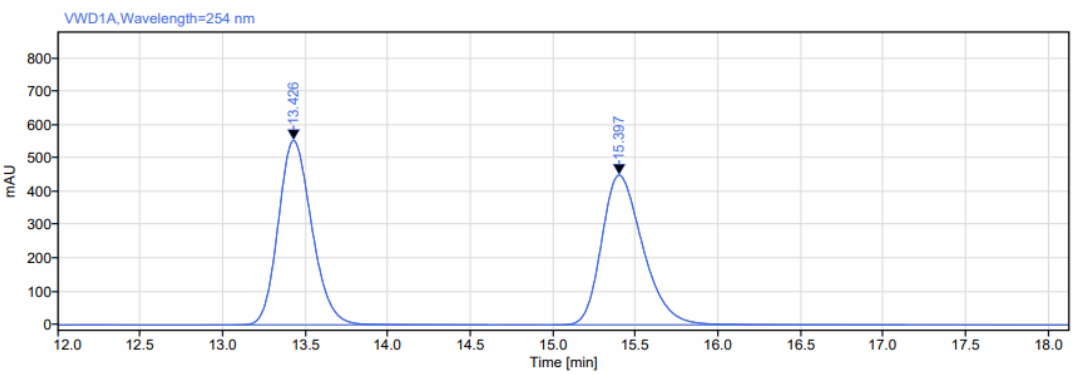

Signal: VWD1A,Wavelength=254 nm

RT [min]	Type	Area	Height	Area%
13.426	BB	7831.10	554.20	50.03
15.397	BB	7821.75	450.03	49.97
	Sum	15652.85		

HPLC trace of enantioenriched-**3z** obtained in a 0.004 mmol reaction:

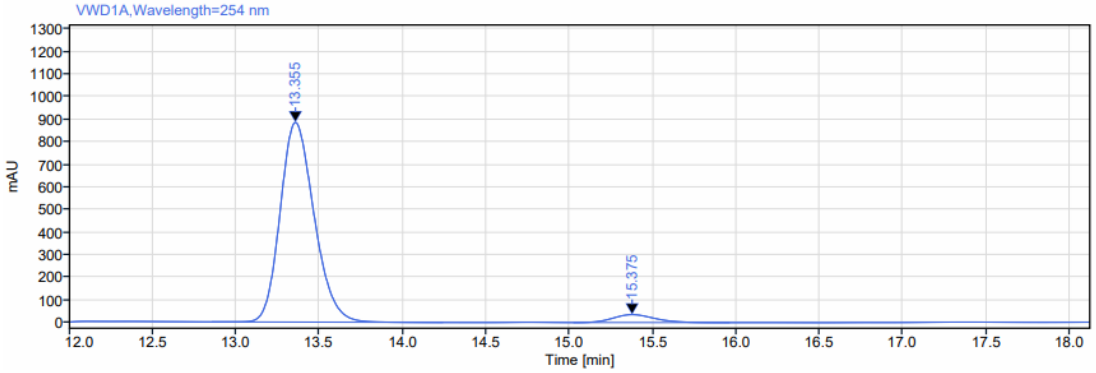

Signal: VWD1A,Wavelength=254 nm

RT [min]	Type	Area	Height	Area%
13.355	BB	12549.40	884.78	95.38
15.375	BB	607.18	35.18	4.62
	Sum	13156.58		

Rac-**3z** is a colorless oil (890 mg, 86%).
^{1}H NMR (400 MHz, $CDCl_3$) δ 7.91-7.84 (m, 2H), 7.37-7.30 (m, 2H), 7.22-7.14 (m, 1H), 7.07-6.99 (m, 3H), 4.57 (q, J = 6.8 Hz, 1H), 2.30 (s, 3H), 1.50 (d, J = 6.8 Hz, 3H).
^{13}C NMR (100 MHz, $CDCl_3$) δ 199.1, 141.1, 139.1, 138.8, 134.8, 130.2, 128.9, 128.7, 128.2, 127.8, 124.8, 48.0, 21.4, 19.4.
HRMS (ESI, *m/z*) calcd. for $C_{16}H_{16}ClO$ $[M+H]^+$ 259.0884, found: 259.0881.

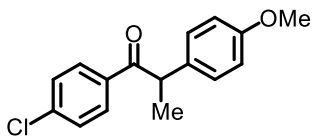

1-(4-Chlorophenyl)-2-(4-methoxyphenyl)propan-1-one (3aa)
By using the typical procedure described in Section 4, the reaction of 4-chlorobenzaldehyde **1a** (0.004 mmol) and 1-ethyl-4-methoxybenzene **2j** (0.016 mmol) catalysed by **RAT$_{CH}$** (2 mol%) afforded **3aa**

in 60% **GC yield** (average of duplicate runs), with a 87% ee.

GC calibration curve for **3aa** is displayed below.

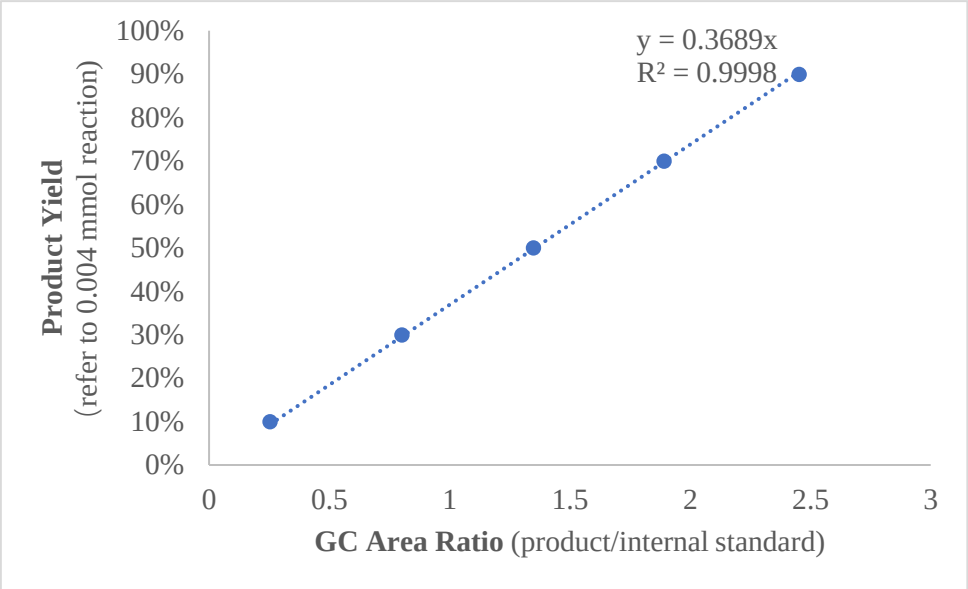

Enantiomeric excess was established by HPLC analysis using a Chiralpak AD-3 column (HPLC: AD-3, 254 nm, *n*-hexane/isopropanol = 95:5, flow rate 0.5 mL/min, 30 °C, t_r (major) = 18.82 min, t_r (minor) = 22.57 min).

HPLC trace of *rac*-**3aa**:

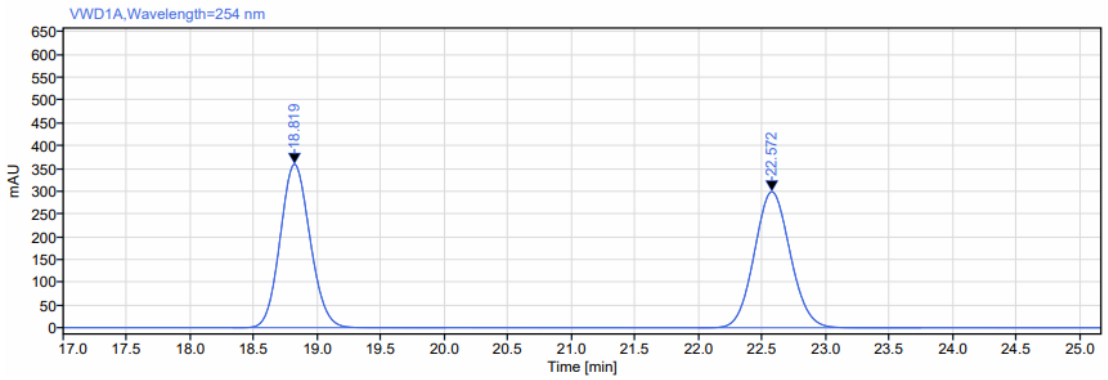

Signal: VWD1A,Wavelength=254 nm

RT [min]	Type	Area	Height	Area%
18.819	BB	5855.46	358.78	50.02
22.572	BB	5851.68	298.48	49.98
	Sum	11707.14		

HPLC trace of enantioenriched-**3aa** obtained in a 0.004 mmol reaction:

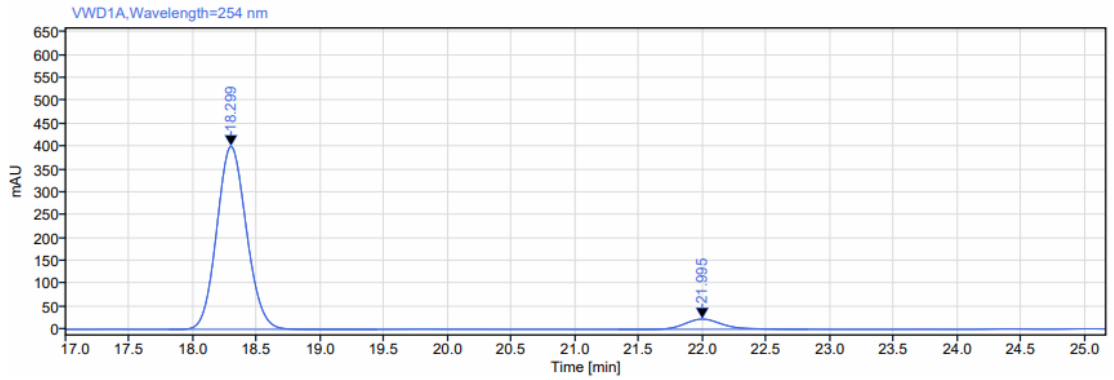

Signal: VWD1A,Wavelength=254 nm

RT [min]	Type	Area	Height	Area%
18.299	BB	6468.90	400.32	93.39
21.995	BM m	458.17	22.40	6.61
	Sum	6927.07		

Rac-**3aa** is a colorless oil (198 mg, 72%). The NMR spectra of *rac*-**3aa** match the one previously reported[39].

^{1}H NMR (400 MHz, $CDCl_3$) δ 7.91-7.83 (m, 2H), 7.37-7.30 (m, 2H), 7.20-7.12 (m, 2H), 6.86-6.79 (m, 2H), 4.56 (q, J = 6.8 Hz, 1H), 3.75 (s, 3H), 1.49 (d, J = 6.8 Hz, 3H).

^{13}C NMR (100 MHz, $CDCl_3$) δ 199.2, 158.6, 139.0, 134.8, 133.1, 130.2, 128.74, 128.69, 114.5, 55.2, 47.2, 19.4.

MS (EI, *m/z*) calcd. for $C_{16}H_{15}ClO_2$ $[M]^+$ 274.1, found: 274.1.

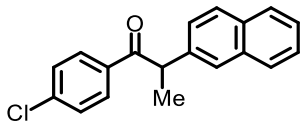

1-(4-Chlorophenyl)-2-(naphthalen-2-yl)propan-1-one (3ab)

By using the typical procedure described in Section 4, the reaction of 4-chlorobenzaldehyde **1a** (0.004 mmol) and ethylbenzene **2k** (0.016 mmol) catalysed by **RAT$_{CH}$** (2 mol%) afforded **3ab** in 26% **GC yield** (average of duplicate runs), with a 85% ee.

GC calibration curve for **3ab** is displayed below.

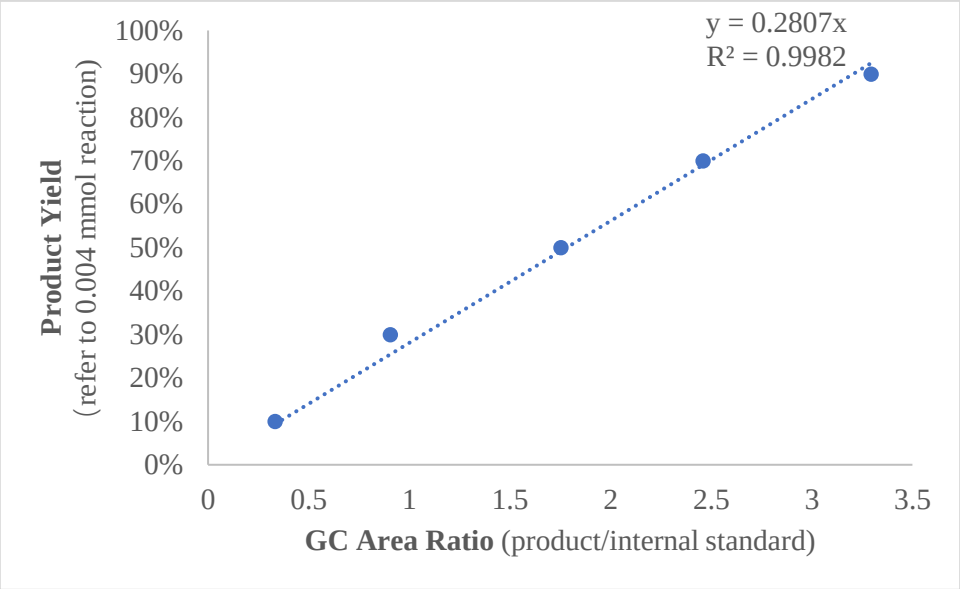

Enantiomeric excess was established by HPLC analysis using a Chiralpak AS-H column (HPLC: AS-H, 254 nm, *n*-hexane/isopropanol = 95:5, flow rate 0.5 mL/min, 30 °C, t_r (major) = 11.75 min, t_r (minor) = 13.57 min).

HPLC trace of *rac*-**3ab**:

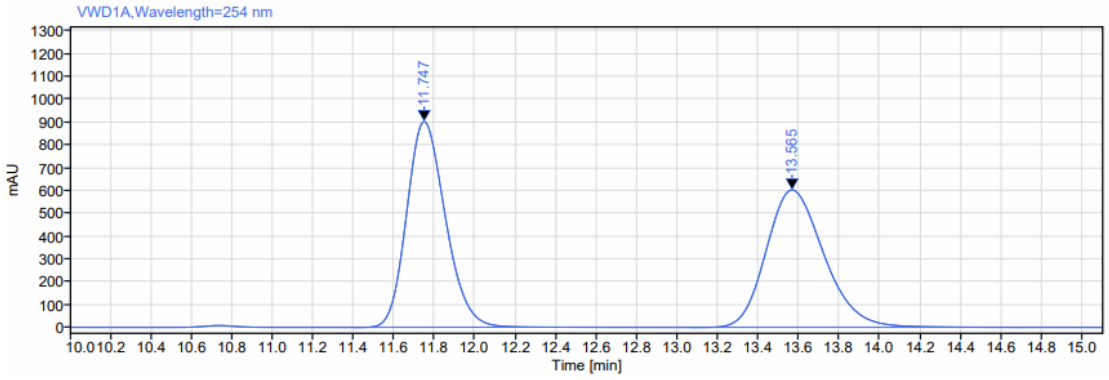

Signal: VWD1A,Wavelength=254 nm

RT [min]	Type	Area	Height	Area%
11.747	BM m	11996.01	902.27	50.09
13.565	MM m	11952.43	602.63	49.91
	Sum	23948.44		

HPLC trace of enantioenriched-**3ab** obtained in a 0.004 mmol reaction:

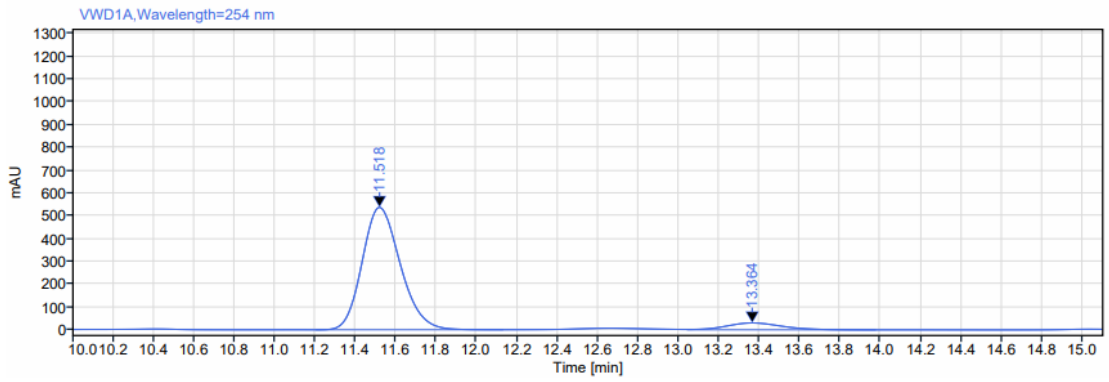

Signal: VWD1A,Wavelength=254 nm

RT [min]	Type	Area	Height	Area%
11.518	BB	7056.39	537.29	92.54
13.364	VB	568.47	30.11	7.46
	Sum	7624.86		

Rac-**3ab** is a white solid (259 mg, 59%). The NMR spectra of *rac*-**3ab** match the one previously reported[40].

^{1}H NMR (400 MHz, $CDCl_3$) δ 7.94-7.87 (m, 2H), 7.82-7.73 (m, 3H), 7.68 (d, J = 1.8 Hz, 1H), 7.47-7.40 (m, 2H), 7.38 (dd, J = 8.5, 1.9 Hz, 1H), 7.35-7.28 (m, 2H), 4.77 (q, J = 6.8 Hz, 1H), 1.60 (d, J = 6.8 Hz, 3H).

^{13}C NMR (100 MHz, $CDCl_3$) δ 199.0, 139.2, 138.7, 134.7, 133.7, 132.4, 130.2, 129.0, 128.8, 127.7, 127.6, 126.4, 126.3, 125.9, 125.7, 48.2, 19.4.

MS (EI, *m/z*) calcd. for $C_{19}H_{15}ClO$ $[M]^+$ 294.1, found: 294.1.

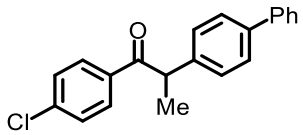

2-([1,1'-Biphenyl]-4-yl)-1-(4-chlorophenyl)propan-1-one (3ac)

By using the typical procedure described in Section 4, the reaction of 4-chlorobenzaldehyde **1a** (0.004 mmol) and 4-ethyl-1,1'-biphenyl **2l** (0.016 mmol) catalysed by **RAT$_{CH}$** (2 mol%) afforded **3ac** in 23% **GC yield** (average of duplicate runs), with a 80% ee.

GC calibration curve for **3ac** is displayed below.

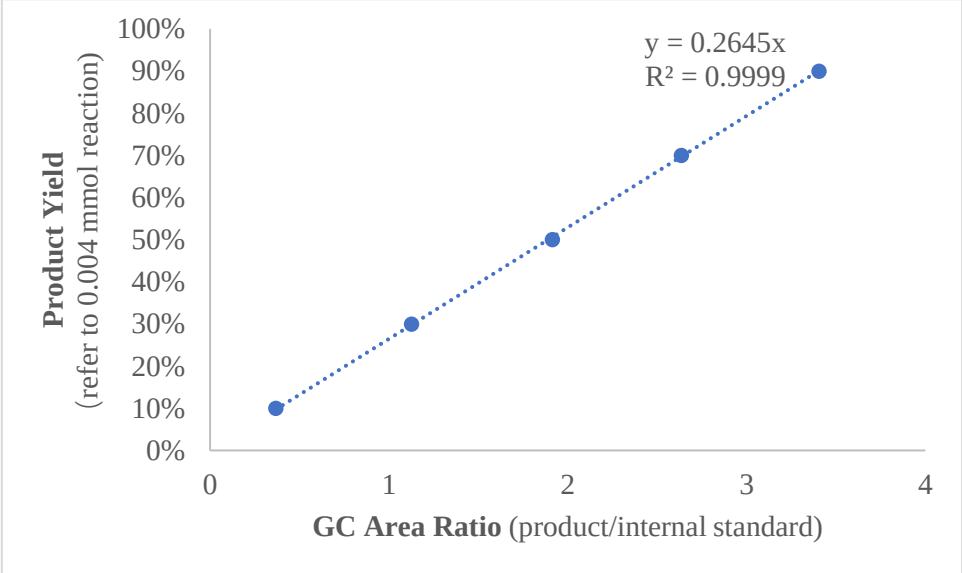

Enantiomeric excess was established by HPLC analysis using a Chiralpak AS-H column (HPLC: AS-H, 254 nm, *n*-hexane/isopropanol = 95:5, flow rate 0.5 mL/min, 30 °C, t_r (major) = 11.31 min, t_r (minor) = 12.61 min).

HPLC trace of *rac*-**3ac**:

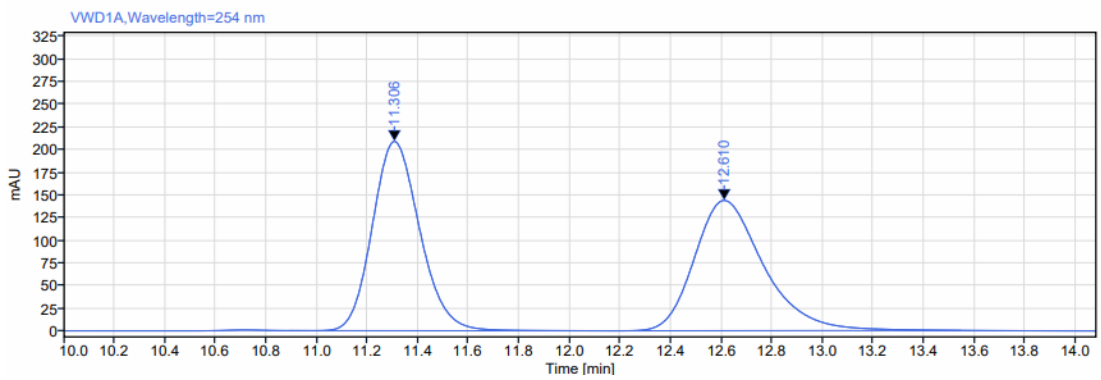

Signal: VWD1A,Wavelength=254 nm

RT [min]	Type	Area	Height	Area%
11.306	MB m	2719.84	208.86	49.86
12.610	BM m	2735.13	143.78	50.14
	Sum	5454.97		

HPLC trace of enantioenriched-**3ac** obtained in a 0.004 mmol reaction:

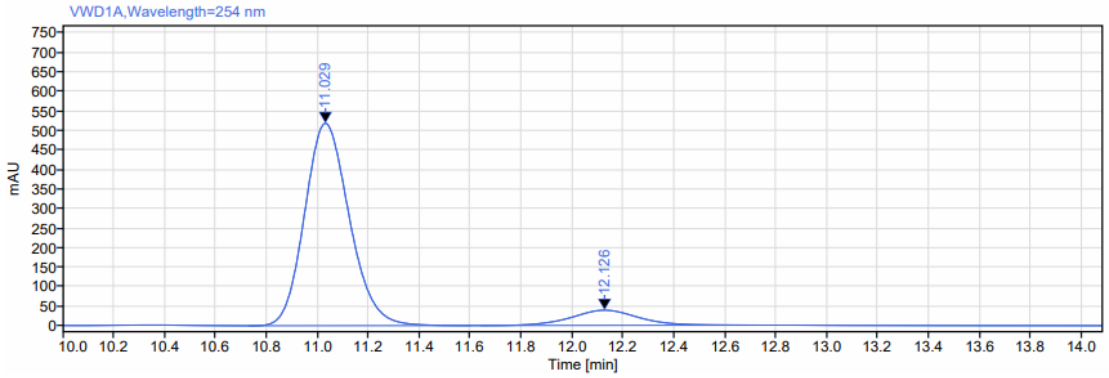

Signal: VWD1A,Wavelength=254 nm

RT [min]	Type	Area	Height	Area%
11.029	BB	6334.50	518.48	89.88
12.126	BB	713.47	38.83	10.12
	Sum	7047.97		

Rac-**3ac** is a white solid (564 mg, 88%).

^{1}H NMR (400 MHz, $CDCl_3$) δ 7.94-7.86 (m, 2H), 7.56-7.48 (m, 4H), 7.44-7.27 (m, 7H), 4.65 (q, J = 6.8 Hz, 1H), 1.56 (d, J = 6.9 Hz, 3H).

^{13}C NMR (100 MHz, $CDCl_3$) δ 199.0, 140.5, 140.1, 140.0, 139.2, 134.7, 130.2, 128.8, 128.7, 128.1, 127.8, 127.3, 127.0, 47.6, 19.4.

HRMS (ESI, *m/z*) calcd. for $C_{21}H_{18}ClO$ $[M+H]^+$ 321.1041, found: 321.1041.

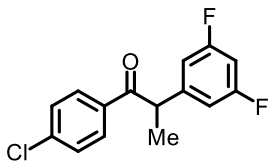

1-(4-Chlorophenyl)-2-(3,5-difluorophenyl)propan-1-one (3ad)

By using the typical procedure described in Section 4, the reaction of 4-chlorobenzaldehyde **1a** (0.004 mmol) and 1-ethyl-3,5-difluorobenzene **2m** (0.016 mmol) catalysed by **RAT$_{CH}$** (2 mol%) afforded

3ad in 45% **GC yield** (average of duplicate runs), with a 89% ee.

GC calibration curve for **3ad** is displayed below.

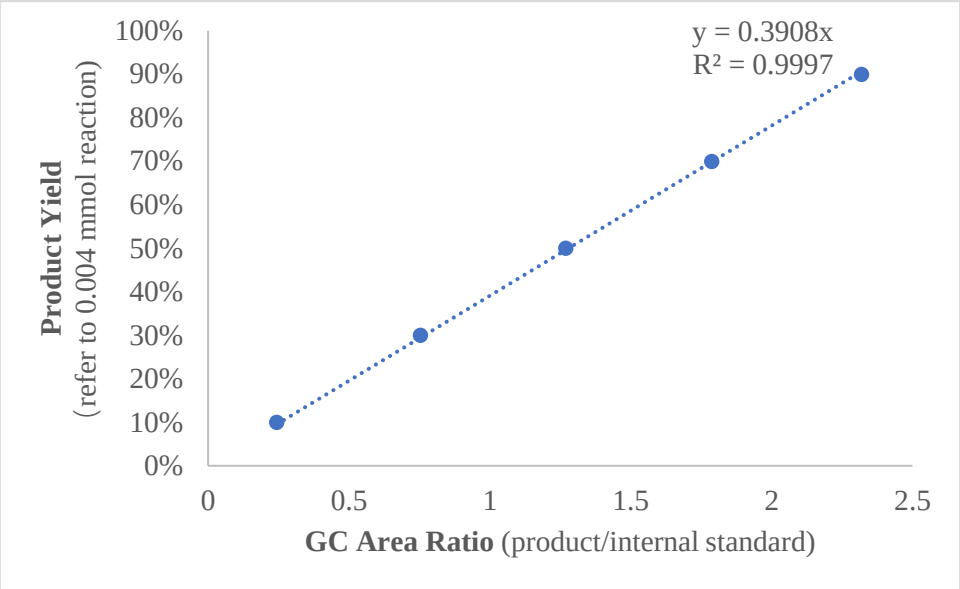

Enantiomeric excess was established by HPLC analysis using a Chiralcel OJ-3 column (HPLC: OJ-3, 254 nm, *n*-hexane/isopropanol = 95:5, flow rate 0.5 mL/min, 30 °C, t_r (major) = 14.69 min, t_r (minor) = 18.00 min).

HPLC trace of *rac*-**3ad**:

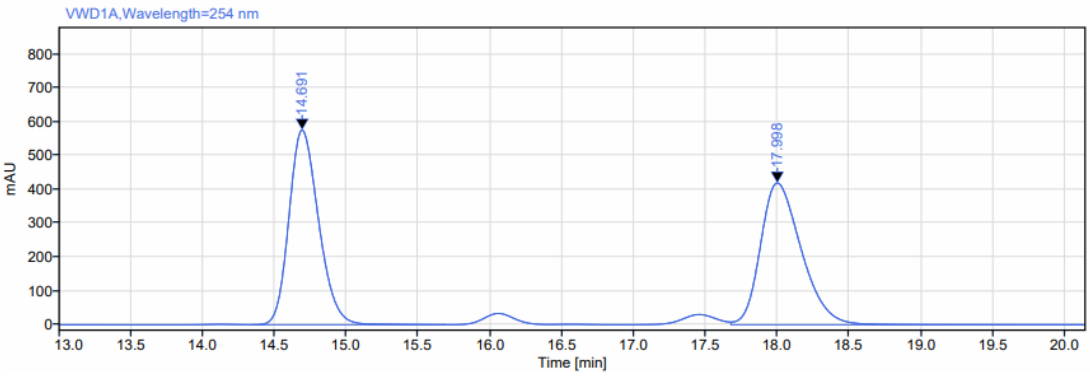

Signal: VWD1A,Wavelength=254 nm

RT [min]	Type	Area	Height	Area%
14.691	VB	8266.09	576.42	49.94
17.998	VB	8285.81	419.57	50.06
	Sum	16551.90		

HPLC trace of enantioenriched-**3ad** obtained in a 0.004 mmol reaction:

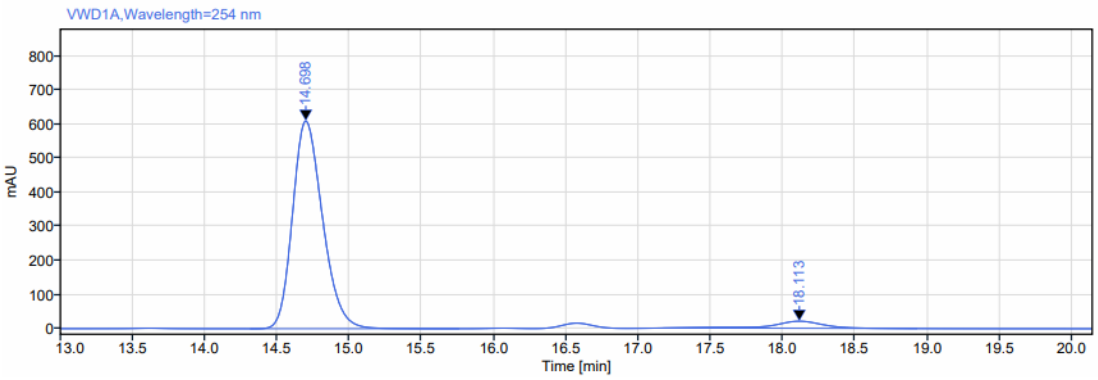

Signal: VWD1A,Wavelength=254 nm

RT [min]	Type	Area	Height	Area%
14.698	BB	8817.32	609.92	94.38
18.113	MM m	525.16	20.84	5.62
	Sum	9342.48		

Rac-**3ad** is a pale-yellow oil (223 mg, 69%).
^{1}H NMR (400 MHz, $CDCl_3$) δ 7.90-7.83 (m, 2H), 7.43-7.35 (m, 2H), 6.84-6.75 (m, 2H), 6.71-6.61 (m, 1H), 4.60 (q, J = 6.8 Hz, 1H), 1.52 (d, J = 6.9 Hz, 3H).
^{13}C NMR (100 MHz, $CDCl_3$) δ 197.7, 163.3 (dd , J = 248.0, 12.9 Hz), 144.7 (t , J = 8.8 Hz), 139.7, 134.2, 130.0, 129.0, 110.7 (dd , J = 18.4 Hz, 7.1 Hz), 102.7 (t , J = 25.1 Hz), 47.3 (t , J = 1.9 Hz), 19.1.
HRMS (ESI, *m/z*) calcd. for $C_{15}H_{12}ClF_2O$ $[M+H]^+$ 281.0539, found: 281.0539.

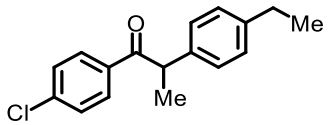

1-(4-Chlorophenyl)-2-(4-ethylphenyl)propan-1-one (3ae)
By using the typical procedure described in Section 4, the reaction of 4-chlorobenzaldehyde **1a** (0.004 mmol) and 1,4-diethylbenzene **2n** (0.016 mmol) catalysed by **RAT$_{CH}$** (2 mol%) afforded **3ae** in 59% **GC yield** (average of duplicate runs), with a 83% ee.

GC calibration curve for **3ae** is displayed below.

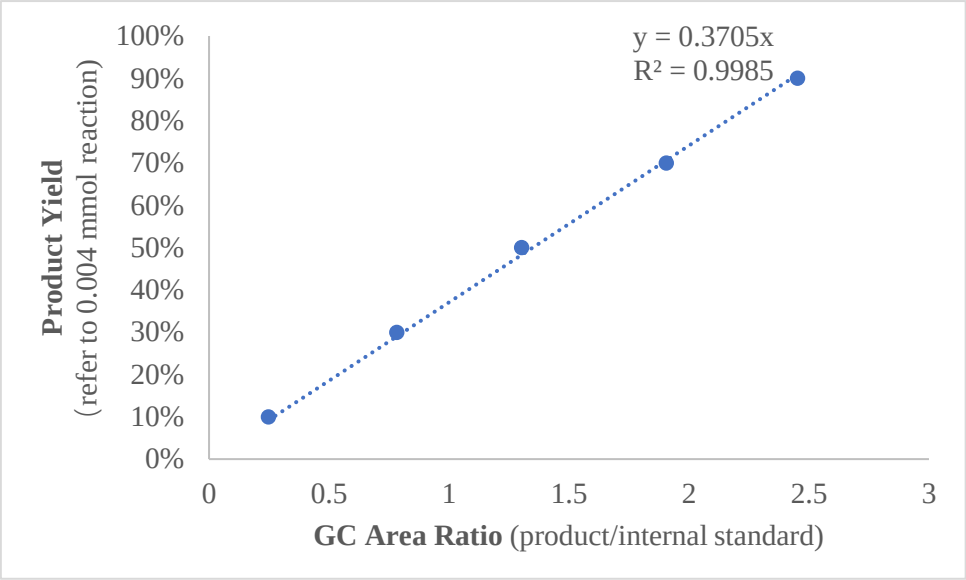

Enantiomeric excess was established by HPLC analysis using a Chiralpak AS-H column (HPLC: AS-H, 254 nm, *n*-hexane/isopropanol = 95:5, flow rate 0.5 mL/min, 30 °C, t_r (major) = 8.40 min, t_r (minor) = 8.82 min).

HPLC trace of *rac*-**3ae**:

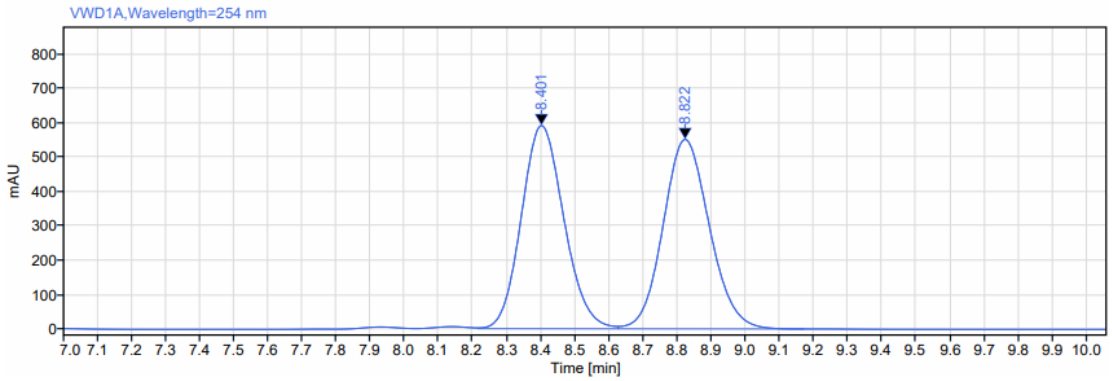

Signal: VWD1A,Wavelength=254 nm

RT [min]	Type	Area	Height	Area%
8.401	VV	5123.89	591.61	49.64
8.822	VB	5198.98	551.62	50.36
	Sum	10322.87		

HPLC trace of enantioenriched-**3ae** obtained in a 0.004 mmol reaction:

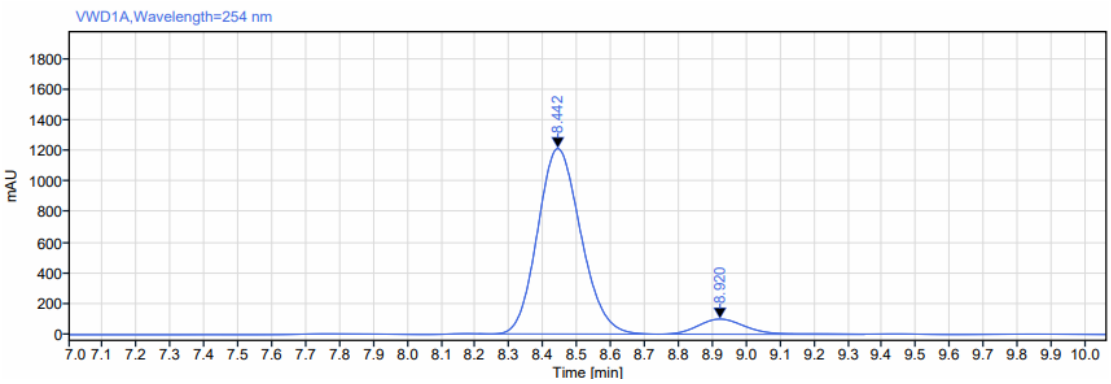

Signal: VWD1A,Wavelength=254 nm

RT [min]	Type	Area	Height	Area%
8.442	MM m	10722.69	1211.23	91.58
8.920	MV m	985.93	99.10	8.42
	Sum	11708.62		

Rac-**3ae** is a colorless oil (105 mg, 48%).
^{1}H NMR (400 MHz, $CDCl_3$) δ 7.91-7.84 (m, 2H), 7.36-7.29 (m, 2H), 7.19-7.09 (m, 4H), 4.58 (q, *J* = 6.8 Hz, 1H), 2.58 (q, *J* = 7.6 Hz, 2H), 1.50 (d, *J* = 6.8 Hz, 3H), 1.19 (t, *J* = 7.6 Hz, 3H).
^{13}C NMR (100 MHz, $CDCl_3$) δ 199.1, 142.9, 139.0, 138.3, 134.8, 130.2, 128.7, 128.5, 127.5, 47.6, 28.3, 19.4, 15.3.
HRMS (ESI, *m/z*) calcd. for $C_{17}H_{18}ClO$ $[M+H]^+$ 273.1041, found: 273.1037.

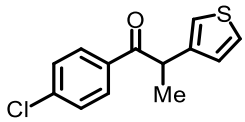

1-(4-Chlorophenyl)-2-(thiophen-3-yl)propan-1-one (3af)
By using the typical procedure described in Section 4, the reaction of 4-chlorobenzaldehyde **1a** (0.004 mmol) and 3-ethylthiophene **2o** (0.016 mmol) catalysed by **RAT$_{CH}$** (2 mol%) afforded **3af** in 74% **GC yield** (average of duplicate runs), with a 85% ee.

GC calibration curve for **3af** is displayed below.

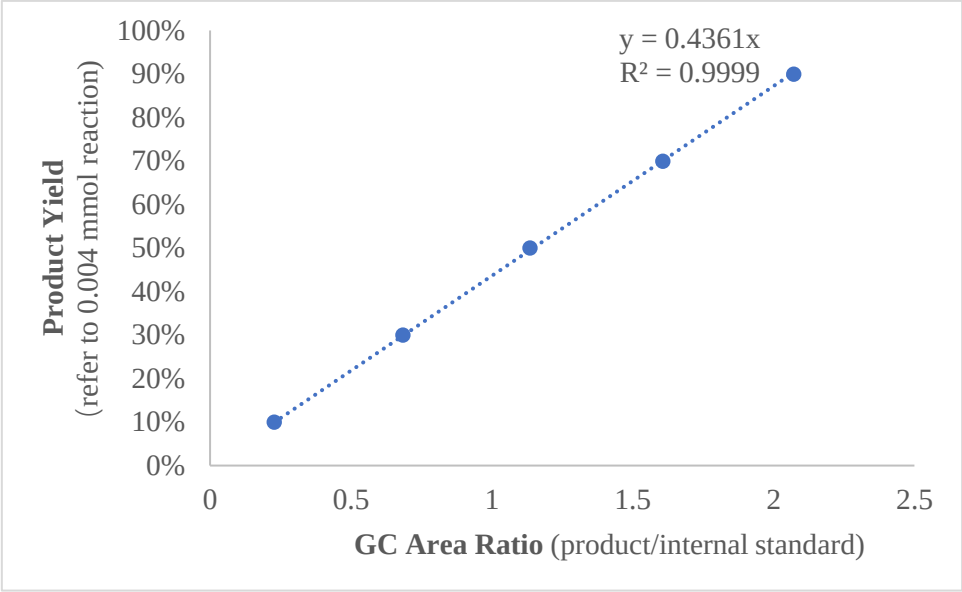

Enantiomeric excess was established by HPLC analysis using a Chiralcel OJ-H column (HPLC: OJ-H, 254 nm, *n*-hexane/isopropanol = 95:5, flow rate 0.5 mL/min, 30 °C, t_r (major) = 22.23 min, t_r (minor) = 27.89 min).

HPLC trace of *rac*-**3af**:

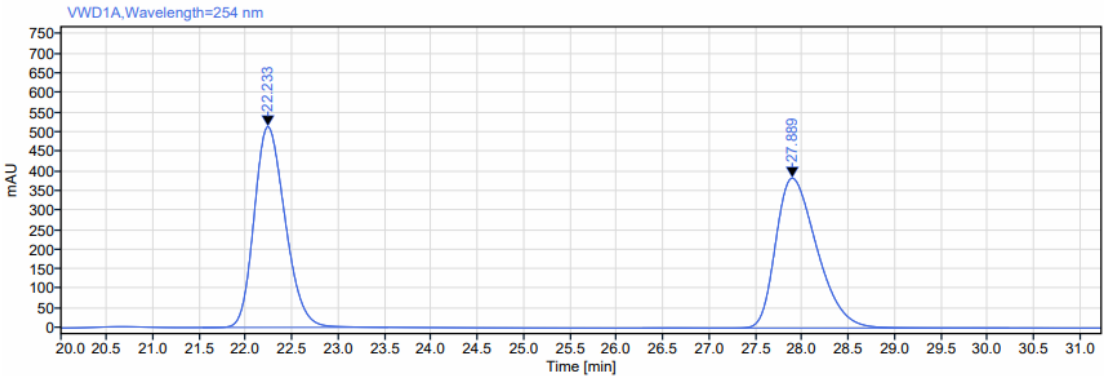

Signal: VWD1A,Wavelength=254 nm

RT [min]	Type	Area	Height	Area%
22.233	MM m	11901.19	512.65	50.17
27.889	MB m	11822.45	382.88	49.83
	Sum	23723.63		

HPLC trace of enantioenriched-**3af** obtained in a 0.004 mmol reaction:

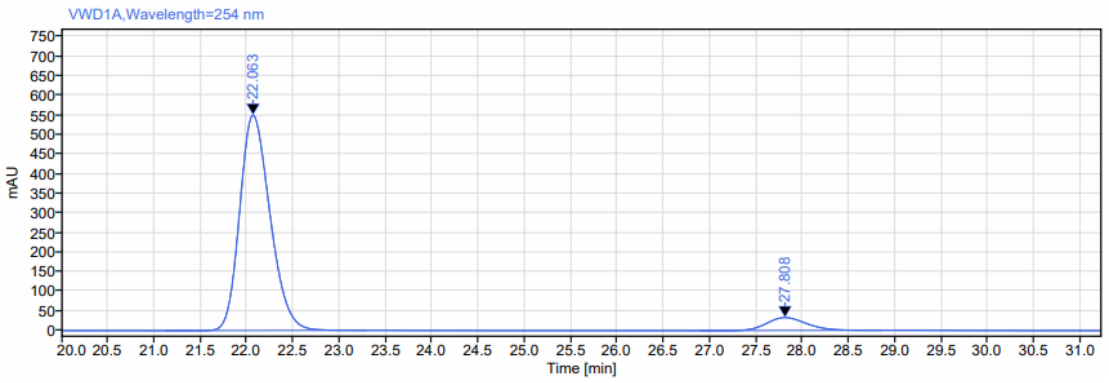

Signal: VWD1A,Wavelength=254 nm

RT [min]	Type	Area	Height	Area%
22.063	BM m	12533.40	550.14	92.67
27.808	BM m	990.85	33.07	7.33
	Sum	13524.24		

The reaction was scaled up to 0.1 mmol, which afforded 18.0 mg **3af** in 72% isolated yield with a 82% ee.

^{1}H NMR (400 MHz, $CDCl_3$) of enantioenriched-**3af** obtained in a 0.1 mmol reaction:

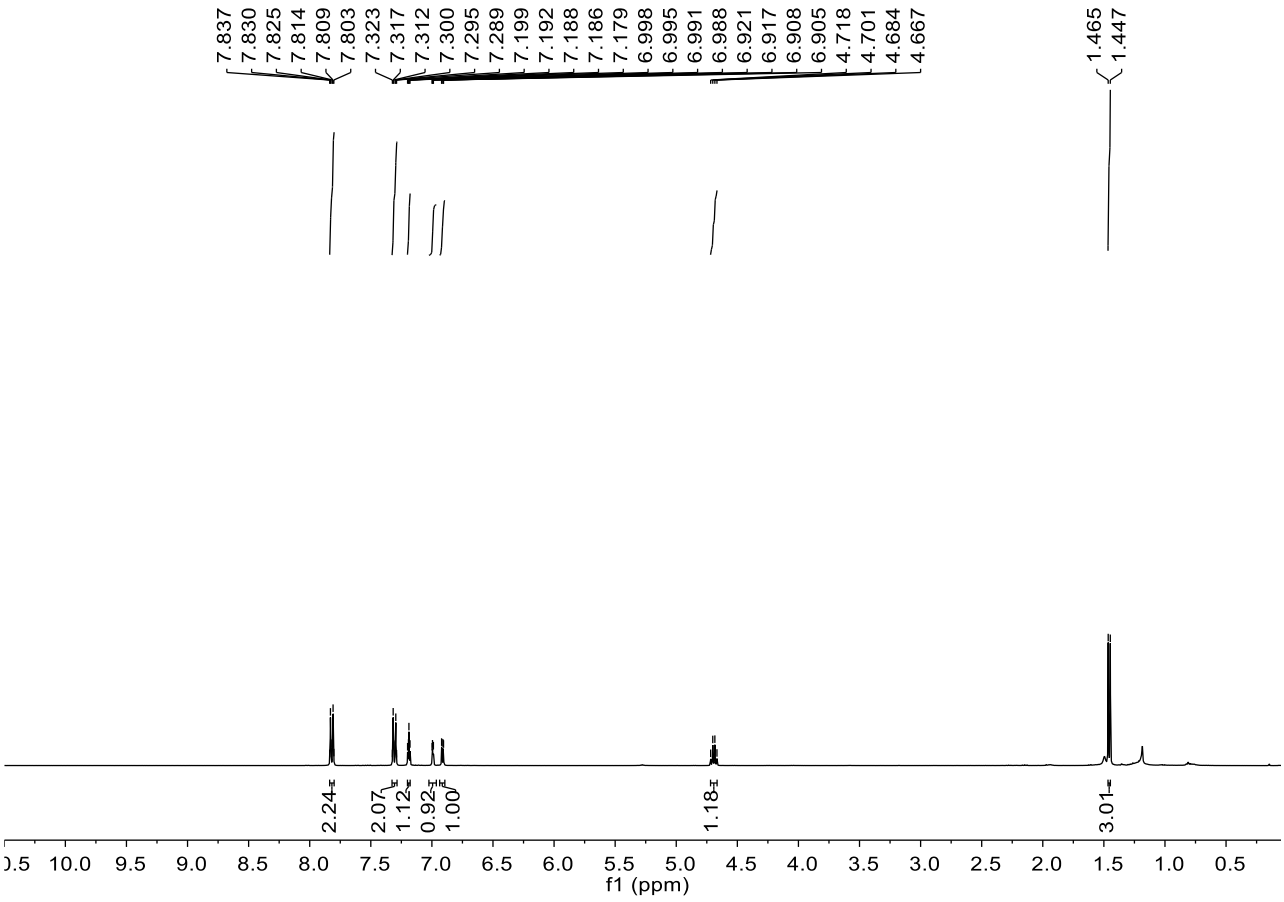

Enantiomeric excess was established by HPLC analysis using a Chiralcel OJ-H column (HPLC: OJ-H, 254 nm, *n*-hexane/isopropanol = 95:5, flow rate 0.5 mL/min, 30 °C, t_r (major) = 22.12 min, t_r (minor) = 27.32 min).

HPLC trace of *rac*-**3af**:

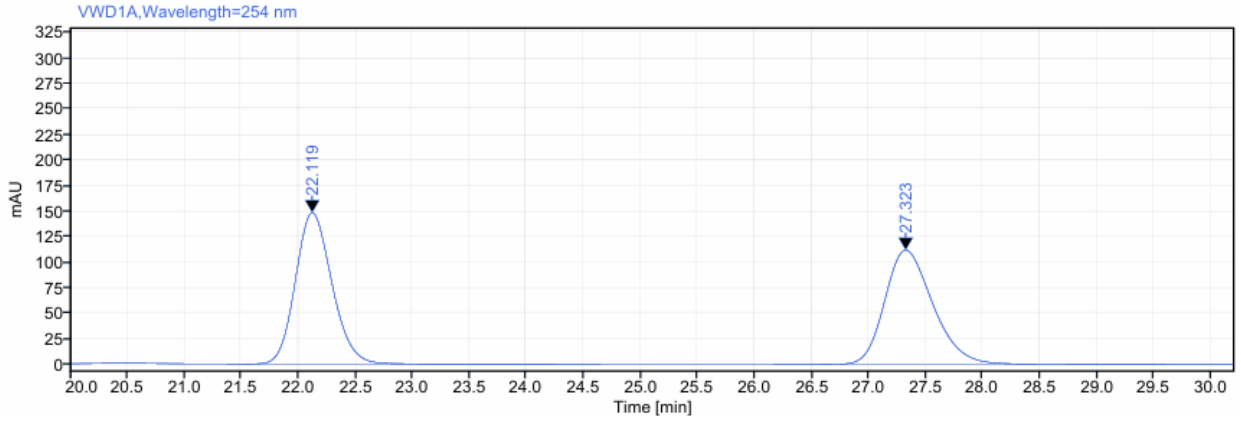

Signal: VWD1A,Wavelength=254 nm

RT [min]	Type	Area	Height	Area%
22.119	BB	3287.96	148.09	50.07
27.323	BB	3278.33	111.72	49.93
	Sum	6566.29		

HPLC trace of **3af** obtained in a 0.1 mmol reaction:

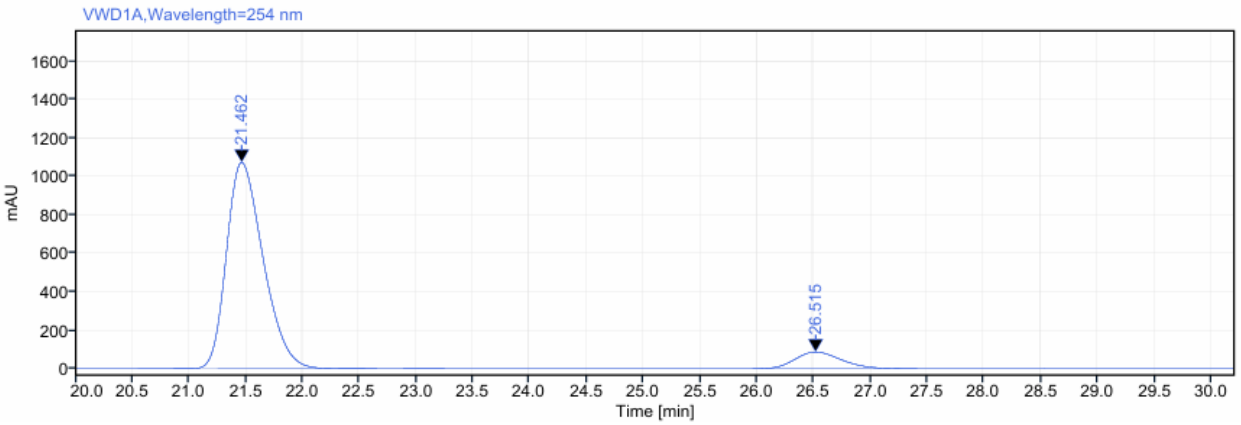

Signal: VWD1A,Wavelength=254 nm

RT [min]	Type	Area	Height	Area%
21.462	BM m	24148.50	1074.48	90.81
26.515	MM m	2445.07	86.84	9.19
	Sum	26593.57		

Rac-**3af** is a white solid (168 mg, 78%).

^{1}H NMR (400 MHz, $CDCl_3$) δ 7.93-7.85 (m, 2H), 7.41-7.34 (m, 2H), 7.29-7.23 (m, 1H), 7.06 (dd, *J* = 3.0, 1.3 Hz, 1H), 6.98 (dd, *J* = 4.9, 1.3 Hz, 1H), 4.76 (q, *J* = 6.9 Hz, 1H), 1.53 (d, *J* = 6.8 Hz, 3H).

^{13}C NMR (100 MHz, $CDCl_3$) δ 198.8, 141.1, 139.3, 134.6, 130.1, 128.8, 126.9, 126.3, 121.5, 43.0, 18.8.

HRMS (ESI, *m/z*) calcd. for $C_{13}H_{12}ClOS$ $[M+H]^+$ 251.0292, found: 251.0291.

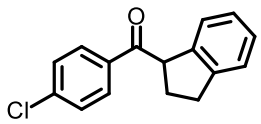

1-(4-Chlorophenyl)-2-(2,3-dihydro-1*H*-inden-1-yl)propan-1-one (3ag)

By using the typical procedure described in Section 4, the reaction of 4-chlorobenzaldehyde **1a** (0.004 mmol) and 2,3-dihydro-1H-indene **2p** (0.016 mmol) catalysed by **RAT2** (2 mol%) afforded **3ag** in 49% **GC yield** (average of duplicate runs), with a 34% ee.

GC calibration curve for **3ag** is displayed below.

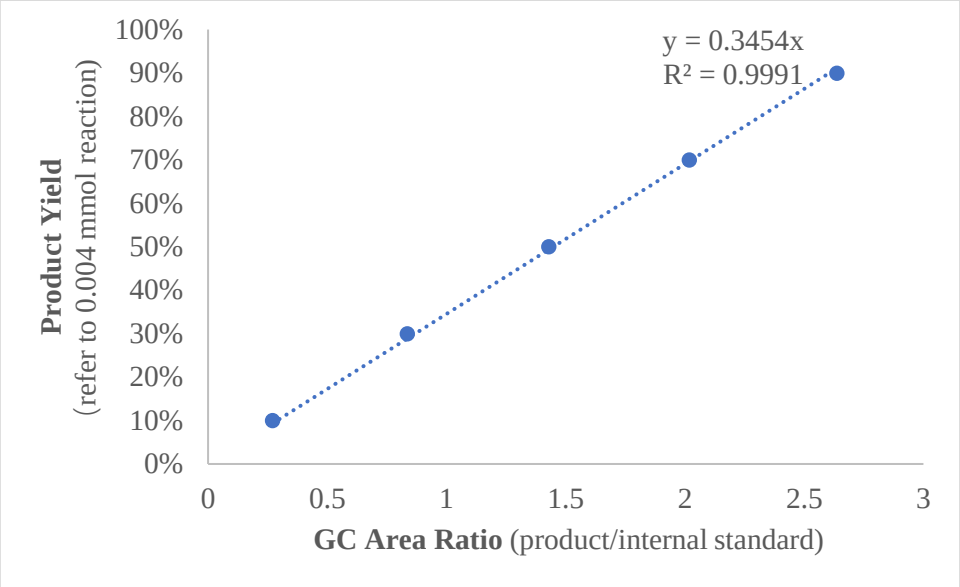

Enantiomeric excess was established by HPLC analysis using a Chiralpak AS-H column (HPLC: AS-H, 254 nm, *n*-hexane/isopropanol = 95:5, flow rate 0.5 mL/min, 30 °C, t_r (major) = 12.10 min, t_r (minor) = 14.73 min).

HPLC trace of *rac*-**3ag**:

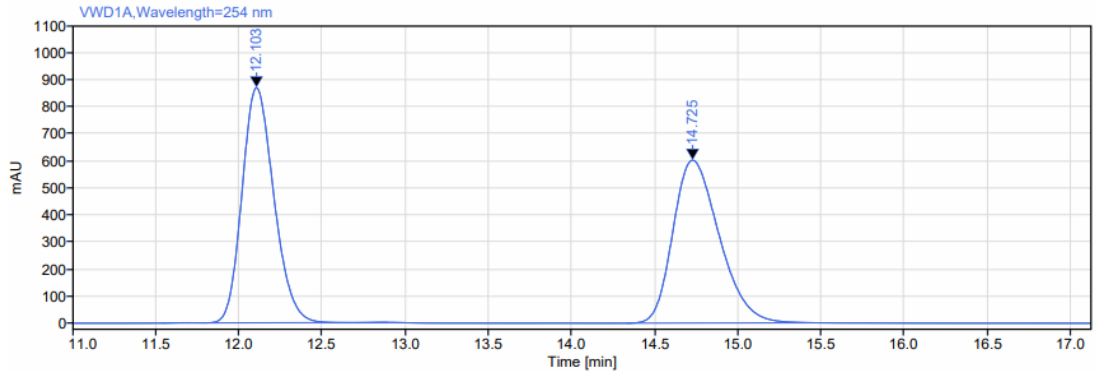

Signal: VWD1A,Wavelength=254 nm

RT [min]	Type	Area	Height	Area%
12.103	MM m	11558.18	868.48	49.88
14.725	MM m	11614.04	601.70	50.12
	Sum	23172.22		

HPLC trace of enantioenriched-**3ag** obtained in a 0.004 mmol reaction:

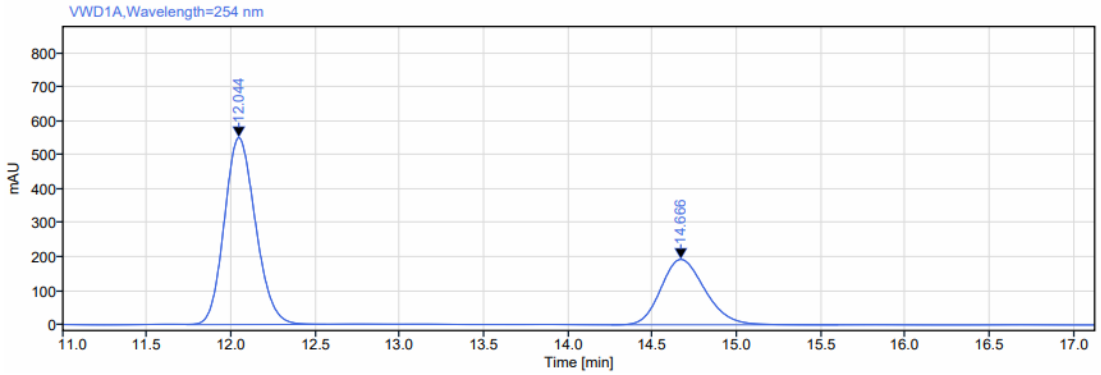

Signal: VWD1A,Wavelength=254 nm

RT [min]	Type	Area	Height	Area%
12.044	VV	7094.98	550.61	66.98
14.666	BB	3498.39	192.73	33.02
	Sum	10593.37		

Rac-**3ag** is a white solid (956 mg, 73%). The NMR spectra of *rac*-**3ag** match the one previously reported[41].

^{1}H NMR (400 MHz, $CDCl_3$) δ 8.02-7.94 (m, 2H), 7.51-7.44 (m, 2H), 7.28-7.24 (m, 1H), 7.23-7.15 (m, 1H), 7.14-7.06 (m, 1H), 7.03 (d, J = 7.6 Hz, 1H), 4.97 (t, J = 7.5 Hz, 1H), 3.21-3.09 (m, 1H), 3.06-2.94 (m, 1H), 2.55-2.37 (m, 2H).

^{13}C NMR (100 MHz, $CDCl_3$) δ 199.1, 144.5, 141.1, 139.6, 135.3, 130.3, 129.0, 127.4, 126.3, 124.88, 124.86, 52.5, 31.9, 29.5.

MS (EI, *m/z*) calcd. for $C_{16}H_{13}ClO$ $[M]^+$ 256.0, found: 256.0.

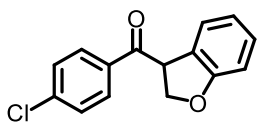

1-(4-Chlorophenyl)-2-(2,3-dihydrobenzofuran-3-yl)propan-1-one (3ah)

By using the typical procedure described in Section 4, the reaction of 4-chlorobenzaldehyde **1a** (0.004

mmol) and 2,3-dihydrobenzofuran **2q** (0.016 mmol) catalysed by **RAT$_{CH}$** (2 mol%) afforded **3ah** in 43% **GC yield** (average of duplicate runs), with a 0% ee.

GC calibration curve for **3ah** is displayed below.

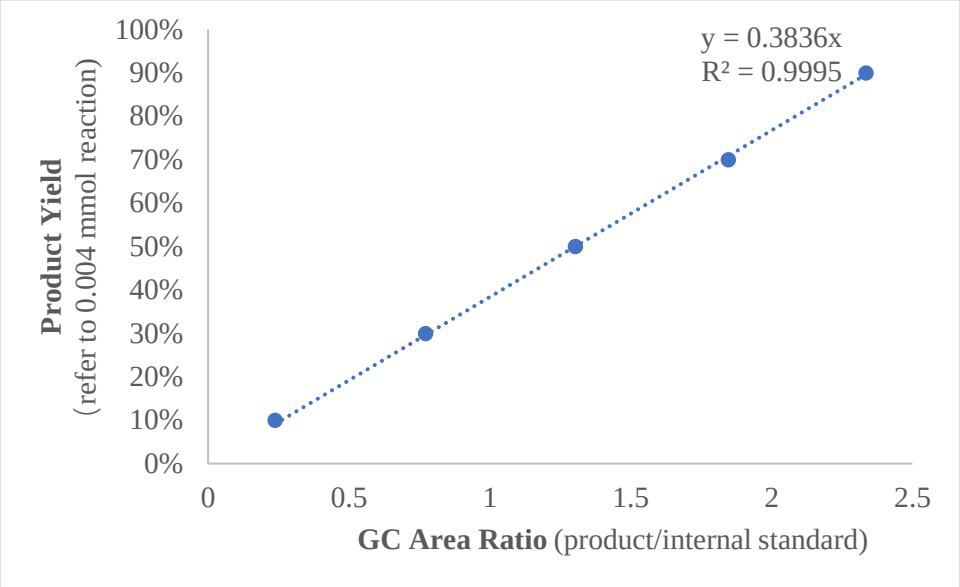

Enantiomeric excess was established by HPLC analysis using a Chiralpak AS-H column (HPLC: AS-H, 254 nm, *n*-hexane/isopropanol = 95:5, flow rate 0.5 mL/min, 30 °C, t_{r1} = 21.02 min, t_{r2} = 27.63 min).

HPLC trace of *rac*-**3ah**:

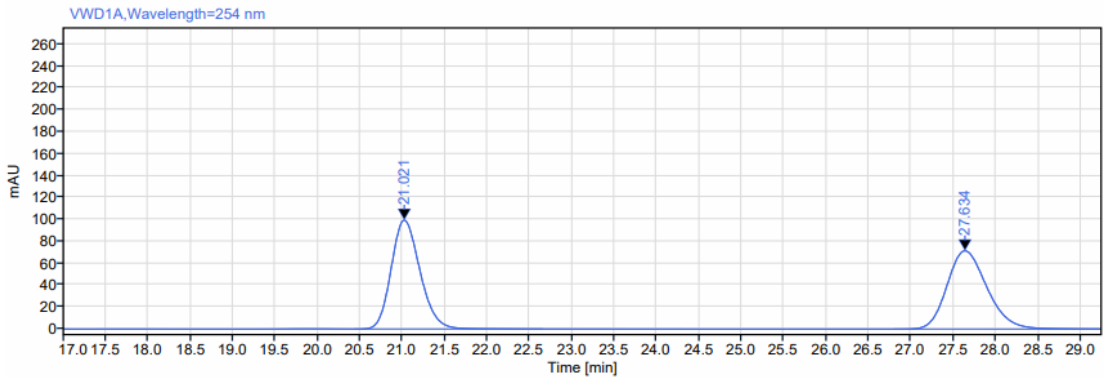

Signal: VWD1A,Wavelength=254 nm

RT [min]	Type	Area	Height	Area%
21.021	BB	2350.96	99.46	50.02
27.634	BB	2349.31	71.50	49.98
	Sum	4700.27		

HPLC trace of enantioenriched-**3ah** obtained in a 0.004 mmol reaction:

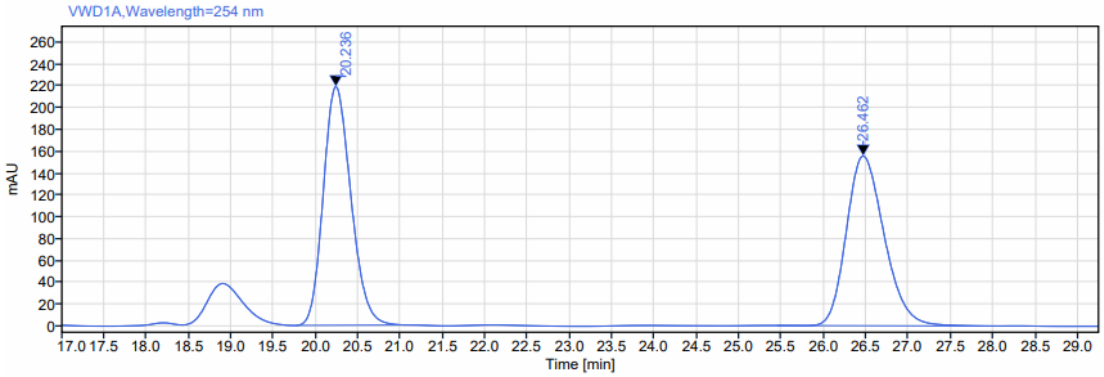

Signal: VWD1A,Wavelength=254 nm

RT [min]	Type	Area	Height	Area%
20.236	MM m	4950.54	218.30	50.67
26.462	MM m	4820.30	155.30	49.33
	Sum	9770.84		

Rac-**3ah** is a pale-red solid (529 mg, 66%).

^{1}H NMR (400 MHz, $CDCl_3$) δ 8.02-7.95 (m, 2H), 7.56-7.49 (m, 2H), 7.20-7.12 (m, 1H), 6.95 (d, J = 7.5 Hz, 1H), 6.86 (d, J = 8.0 Hz, 1H), 6.81-6.73 (m, 1H), 5.22 (dd, J = 2.3, 1.6 Hz, 1H), 5.10 (dd, J = 9.0, 6.4 Hz, 1H), 4.8 (t, J = 9.2 Hz, 1H).

^{13}C NMR (100 MHz, $CDCl_3$) δ 195.1, 160.1, 140.3, 134.4, 130.4, 129.5, 129.3, 125.0, 124.6, 120.5, 110.3, 72.4, 49.5.

HRMS (ESI, *m/z*) calcd. for $C_{15}H_{12}ClO_2$ $[M+H]^+$ 259.0520, found: 259.0519.

9. NMR Spectra of Racemic Standards

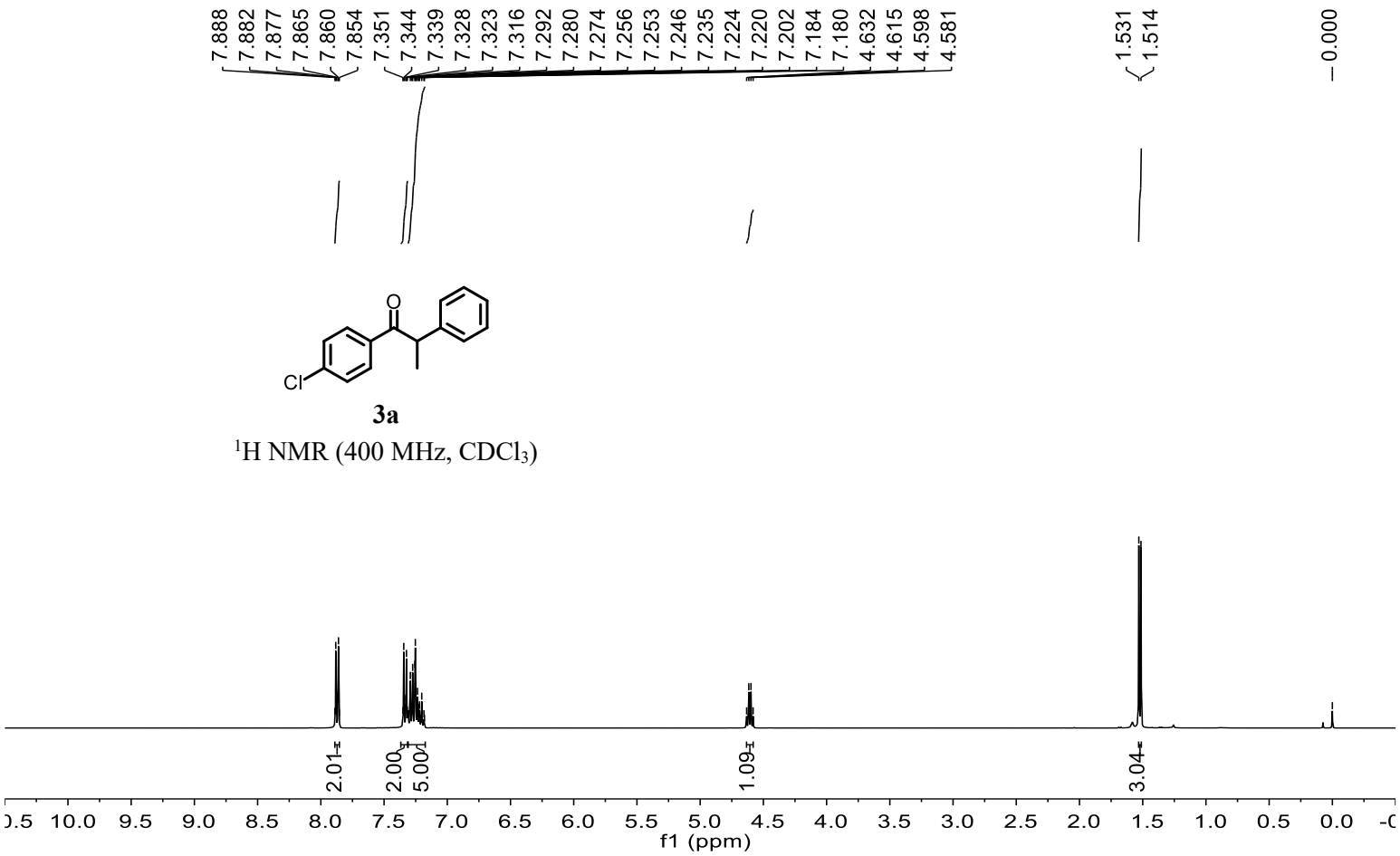

3a

^{1}H NMR (400 MHz, $CDCl_3$)

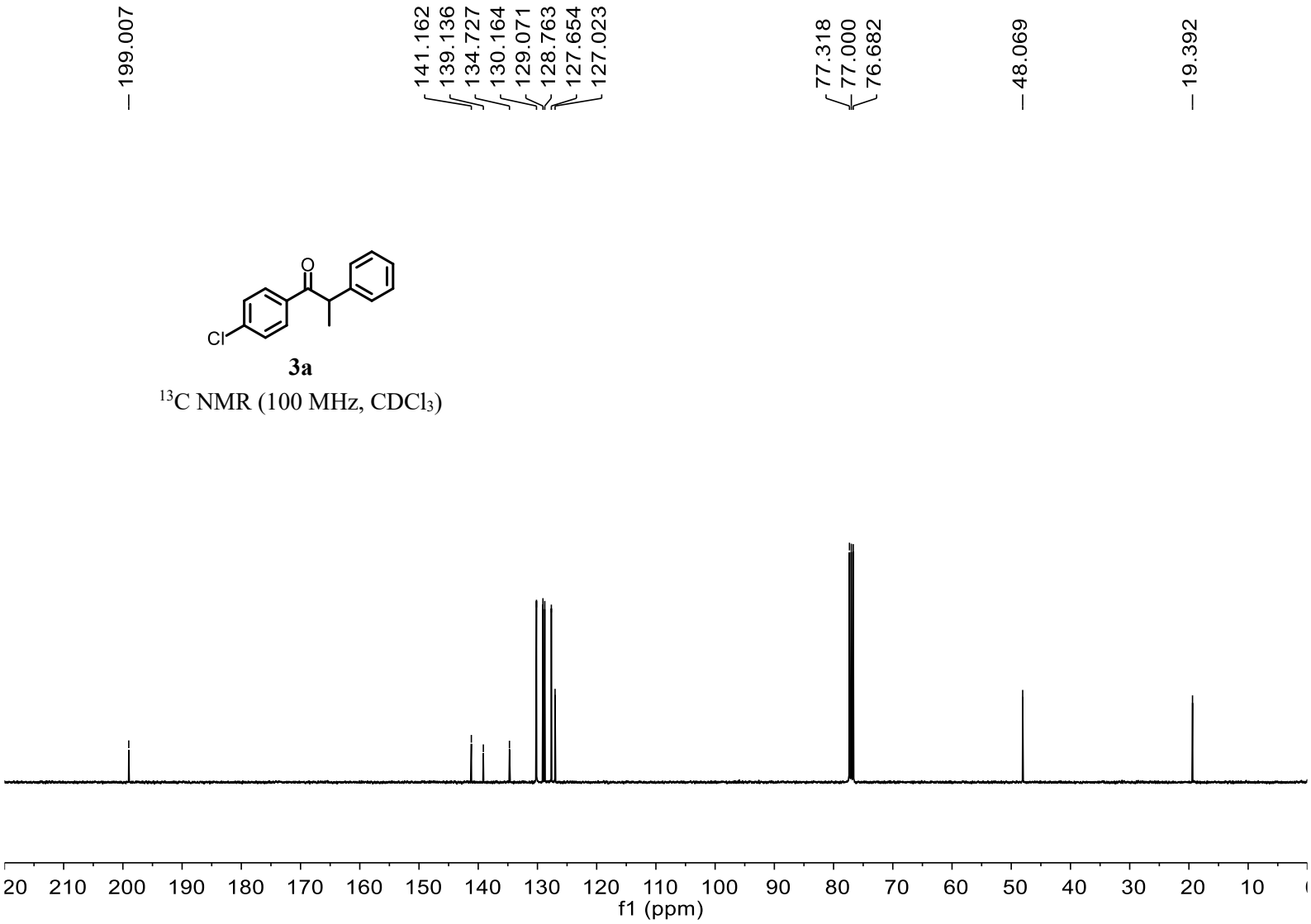

3a

^{13}C NMR (100 MHz, $CDCl_3$)

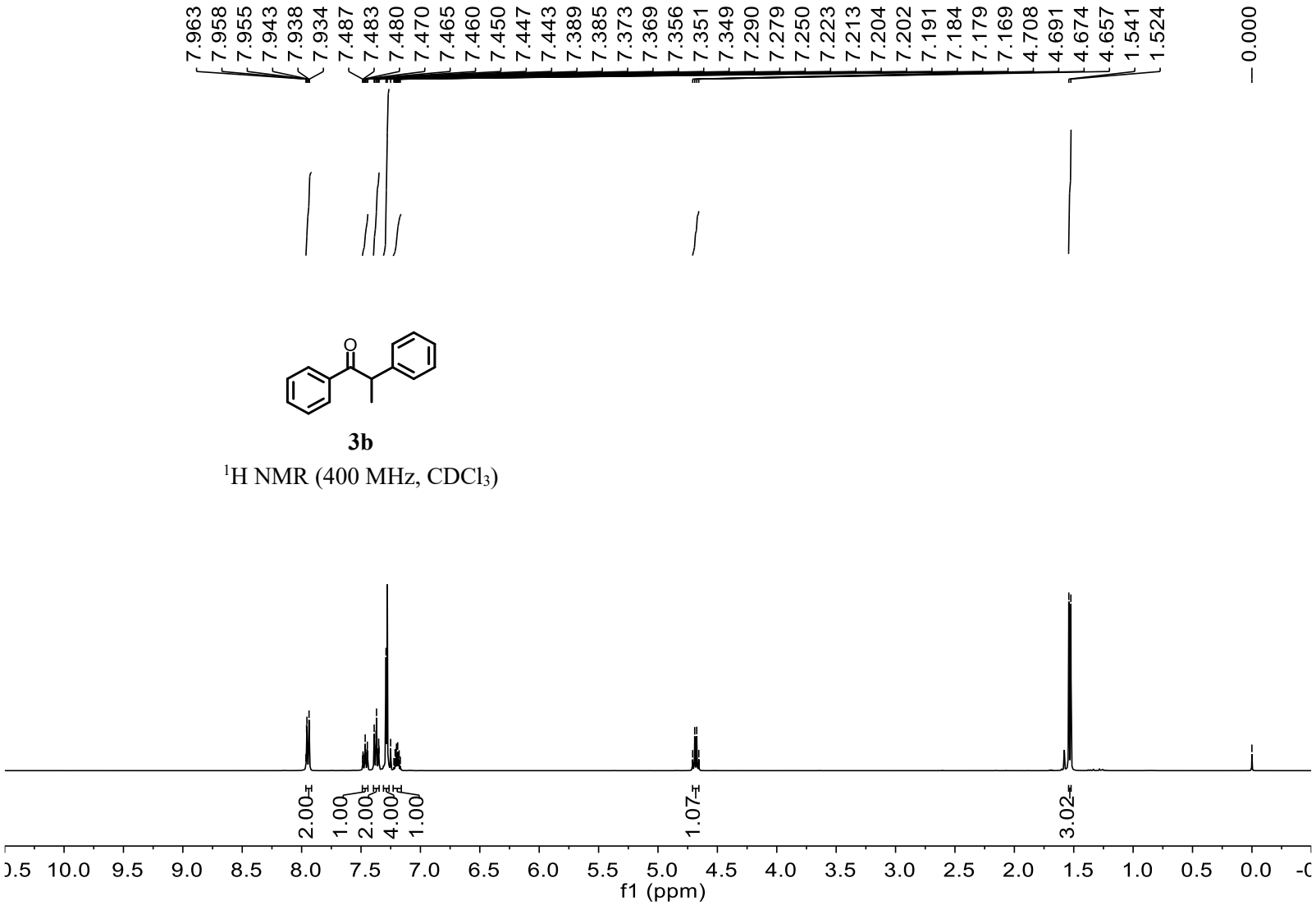

3b

^{1}H NMR (400 MHz, $CDCl_3$)

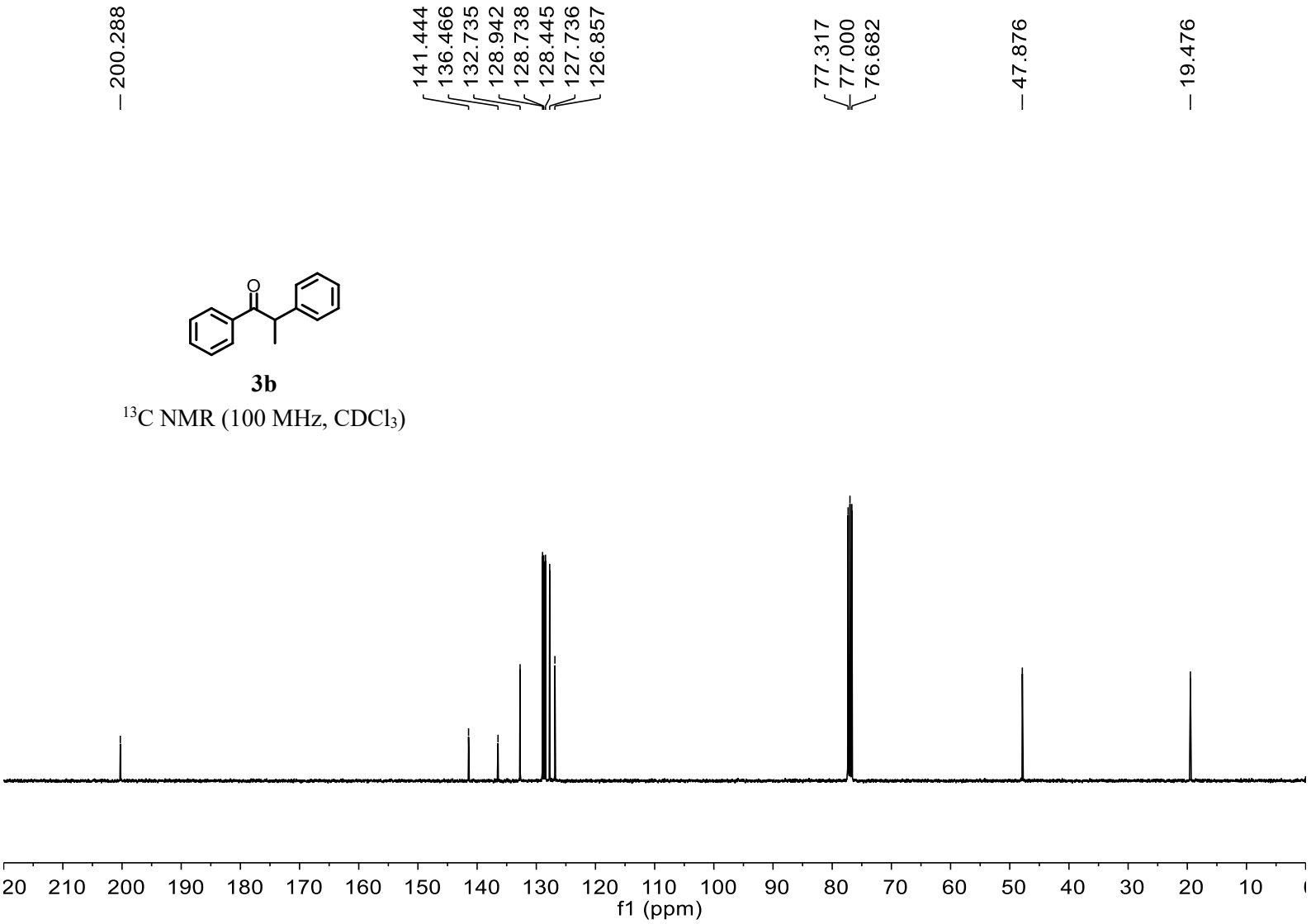

3b

^{13}C NMR (100 MHz, $CDCl_3$)

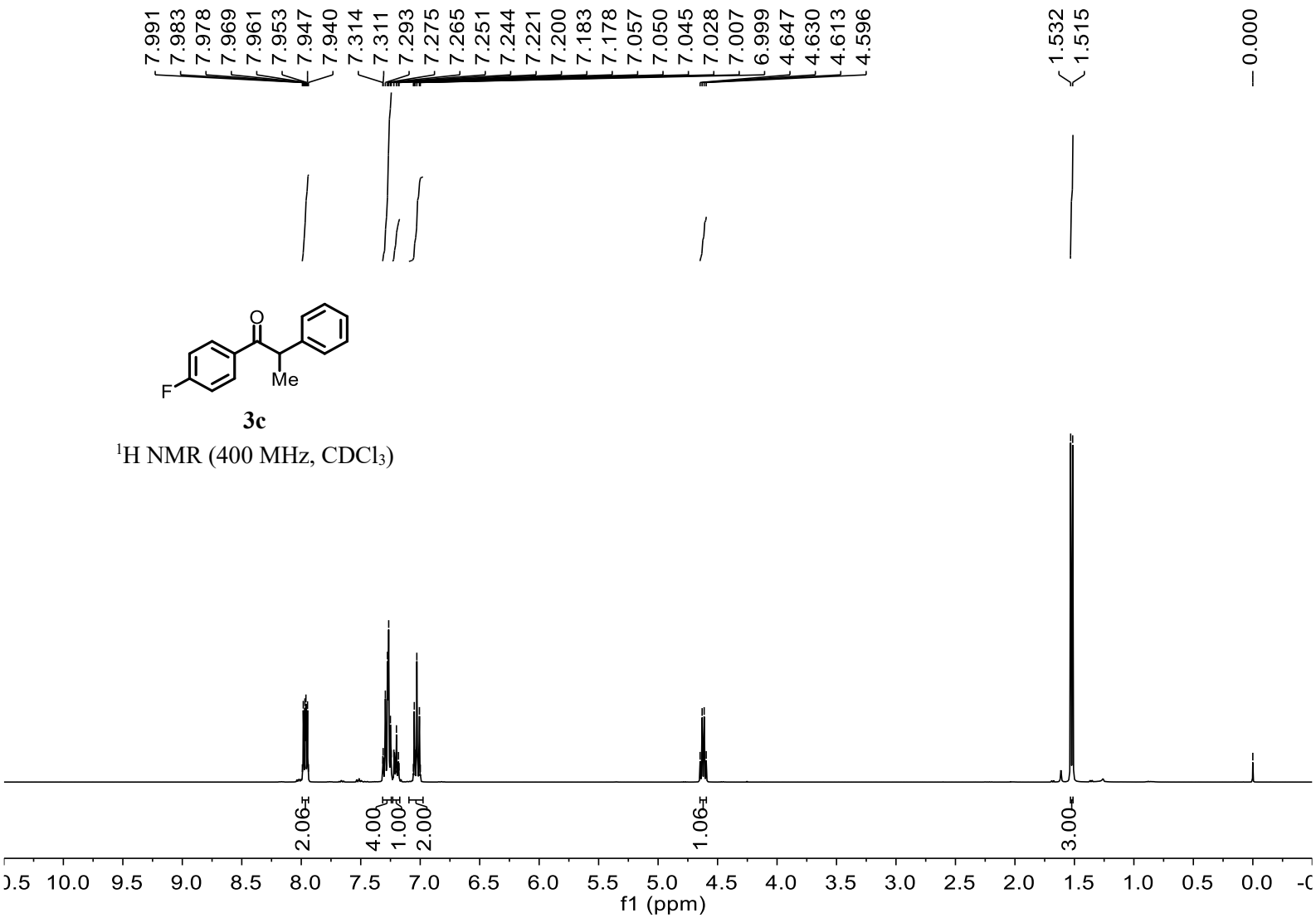

3c

^{1}H NMR (400 MHz, $CDCl_3$)

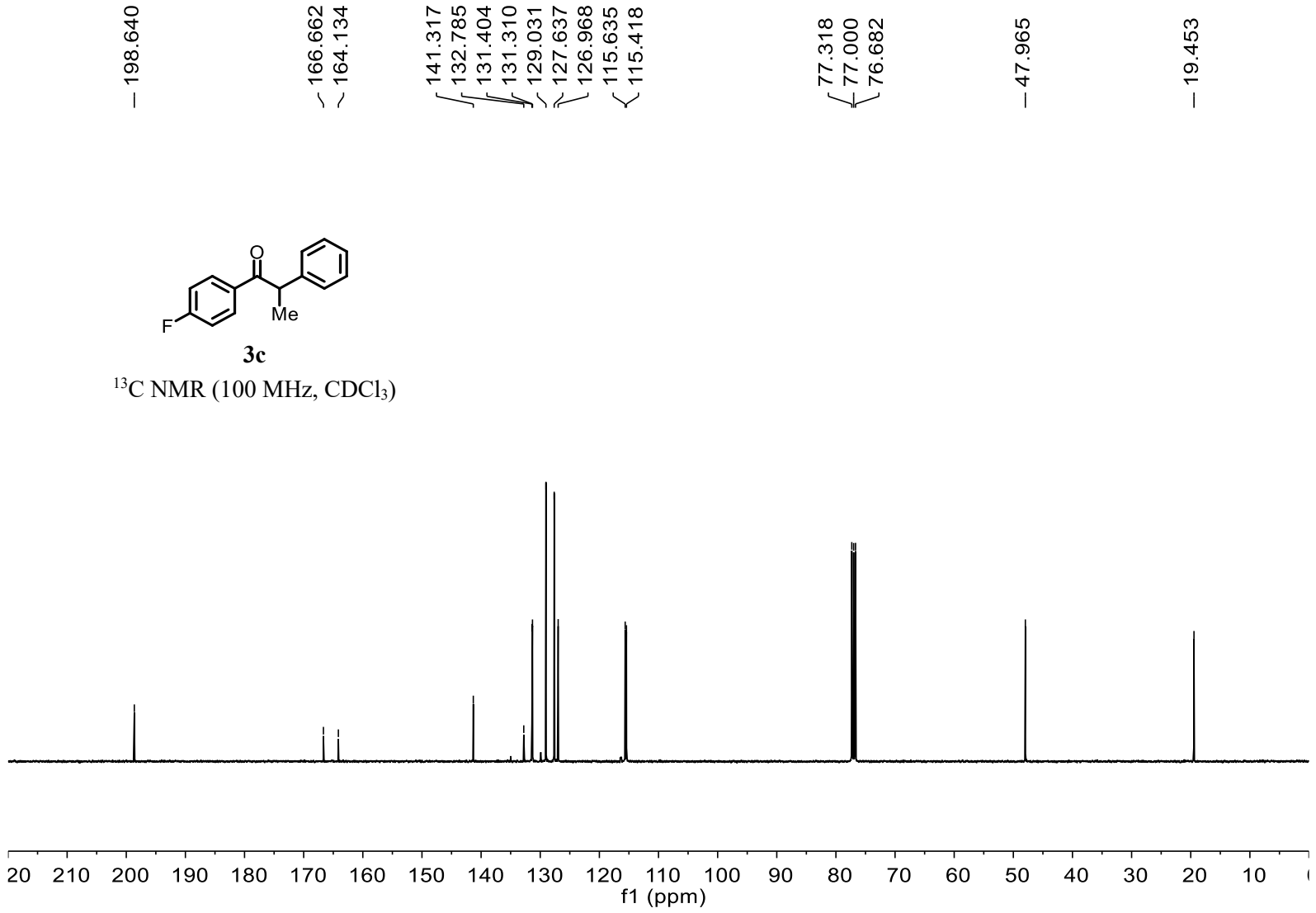

3c

^{13}C NMR (100 MHz, $CDCl_3$)

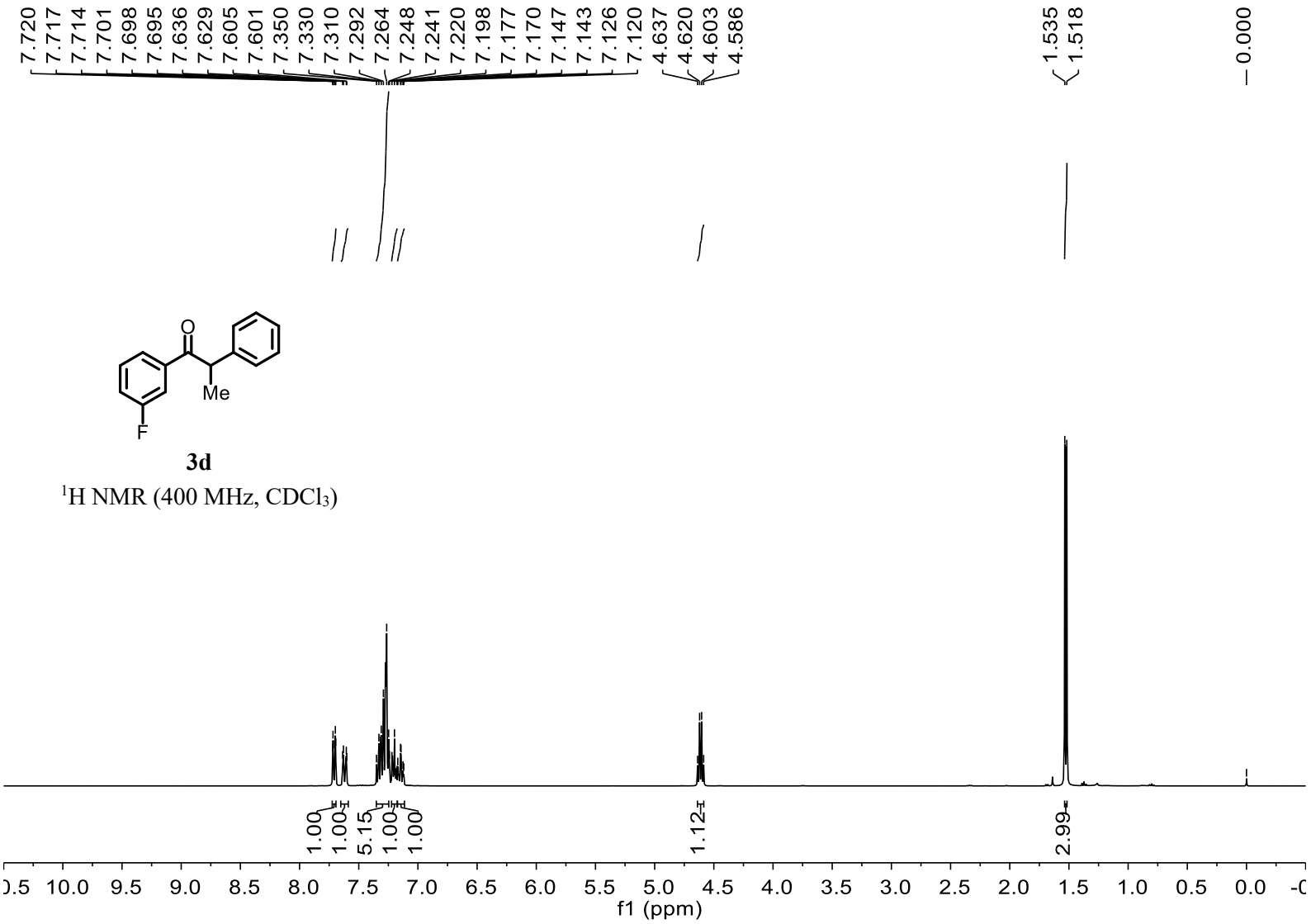

3d

^{1}H NMR (400 MHz, $CDCl_3$)

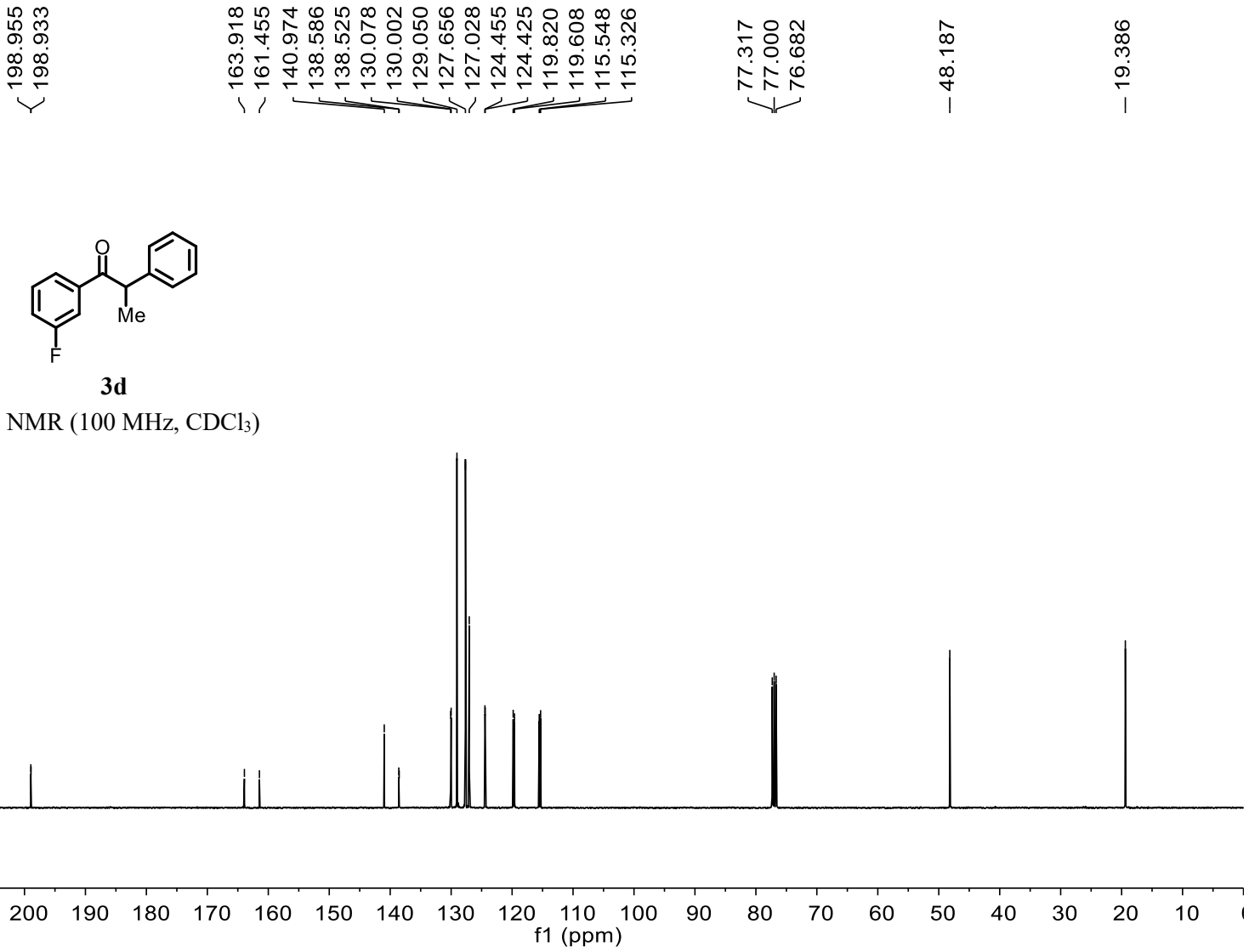

3d

^{13}C NMR (100 MHz, $CDCl_3$)

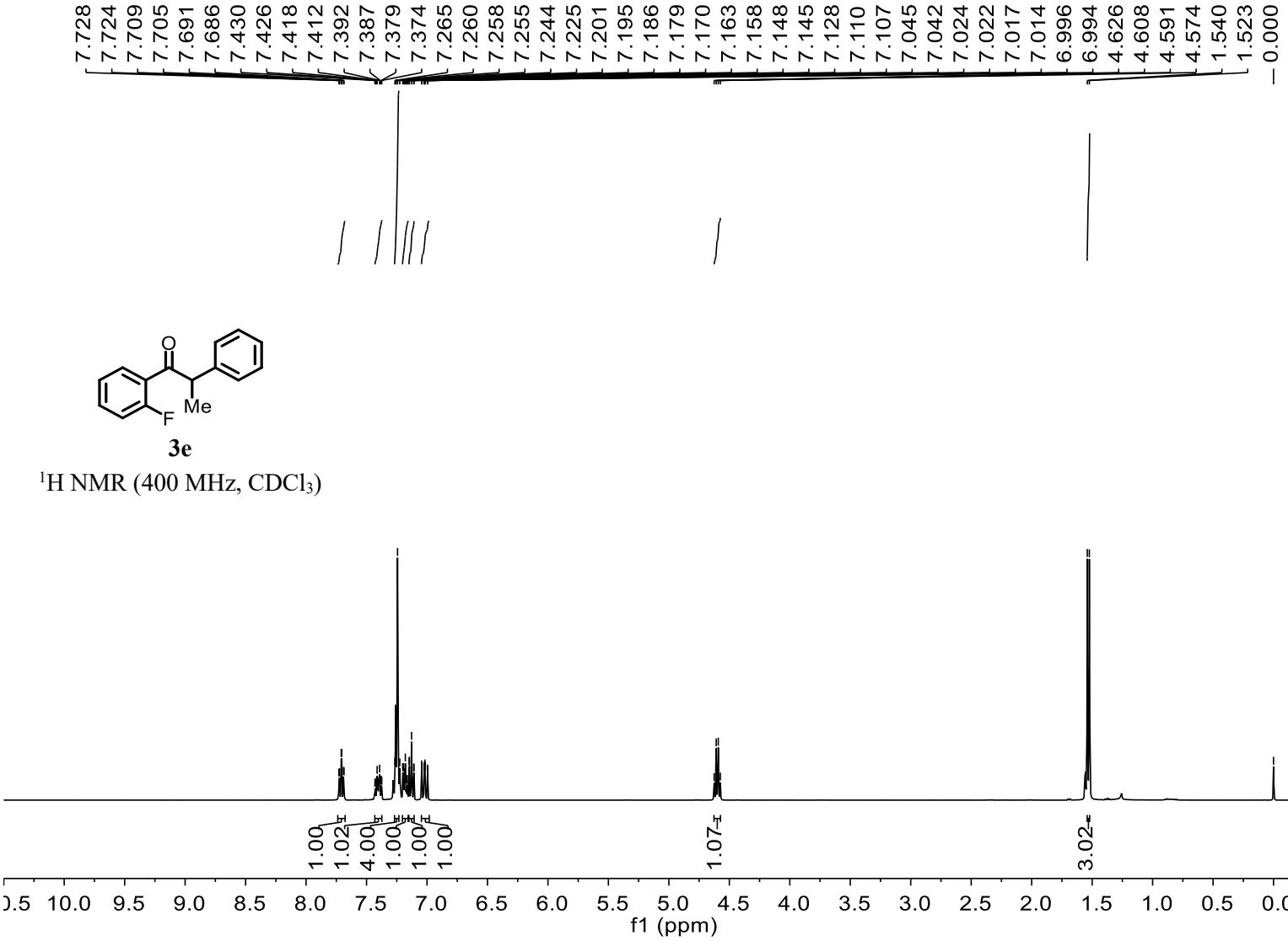

3e

^{1}H NMR (400 MHz, $CDCl_3$)

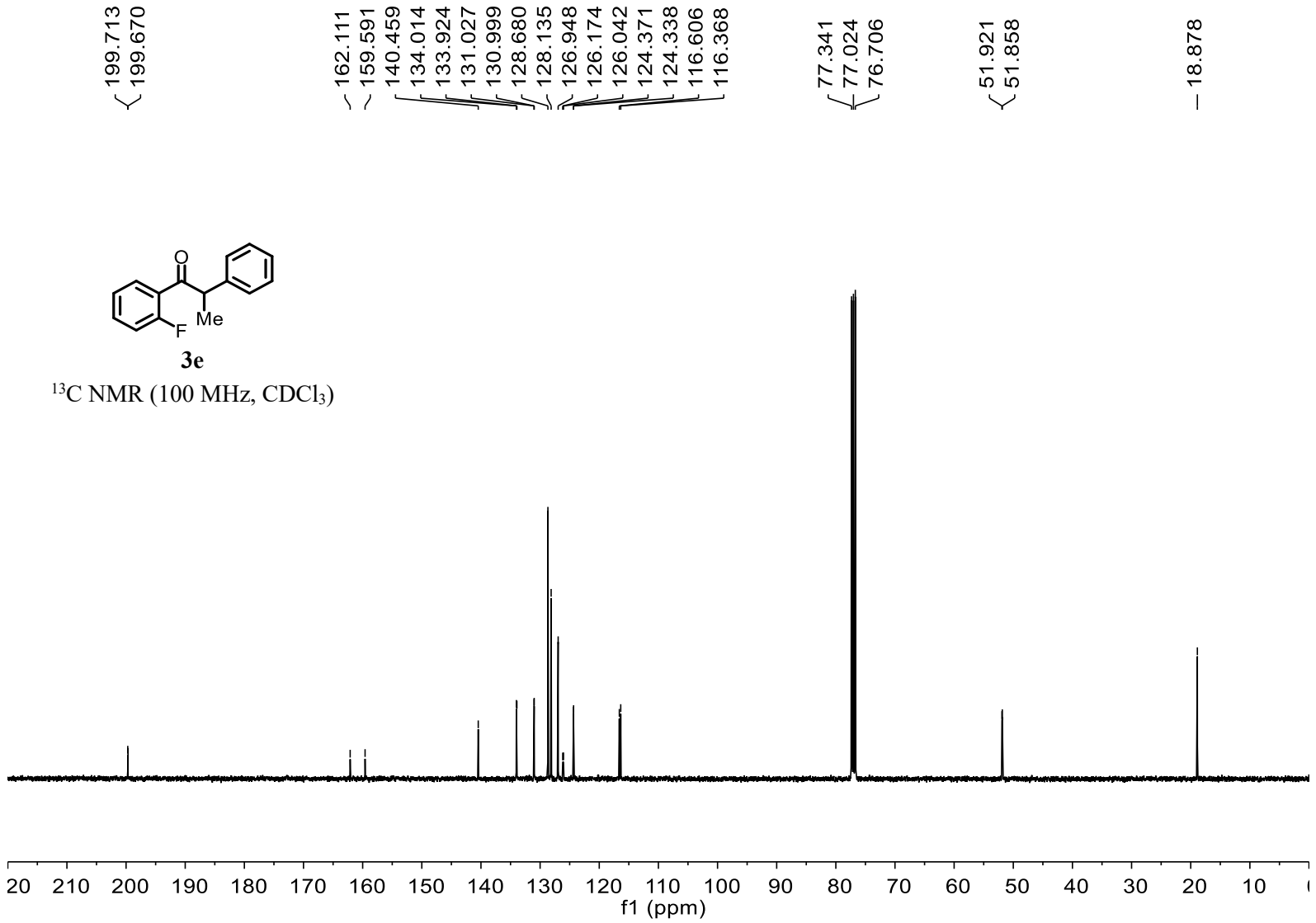

3e

^{13}C NMR (100 MHz, $CDCl_3$)

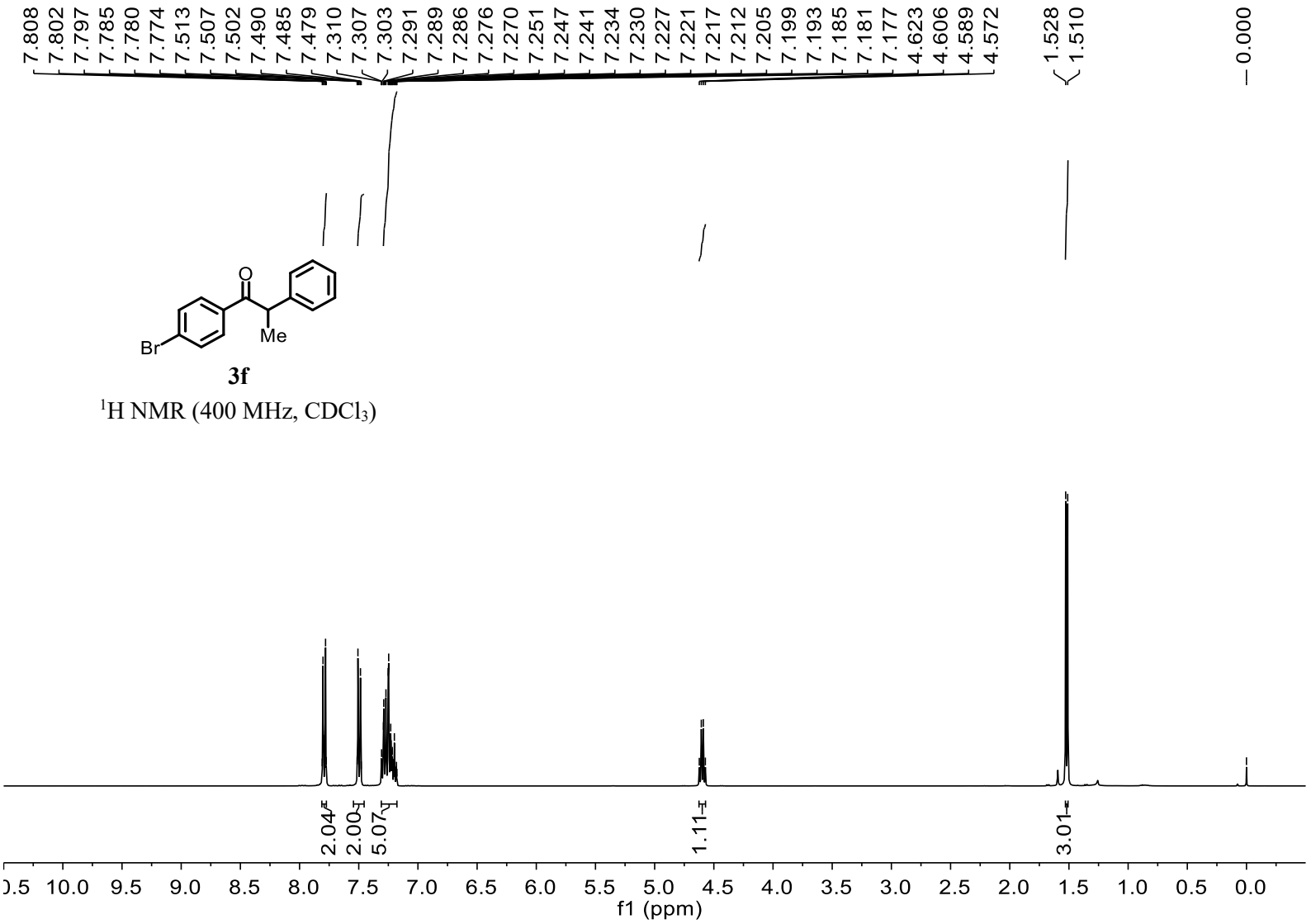

3f

^{1}H NMR (400 MHz, $CDCl_3$)

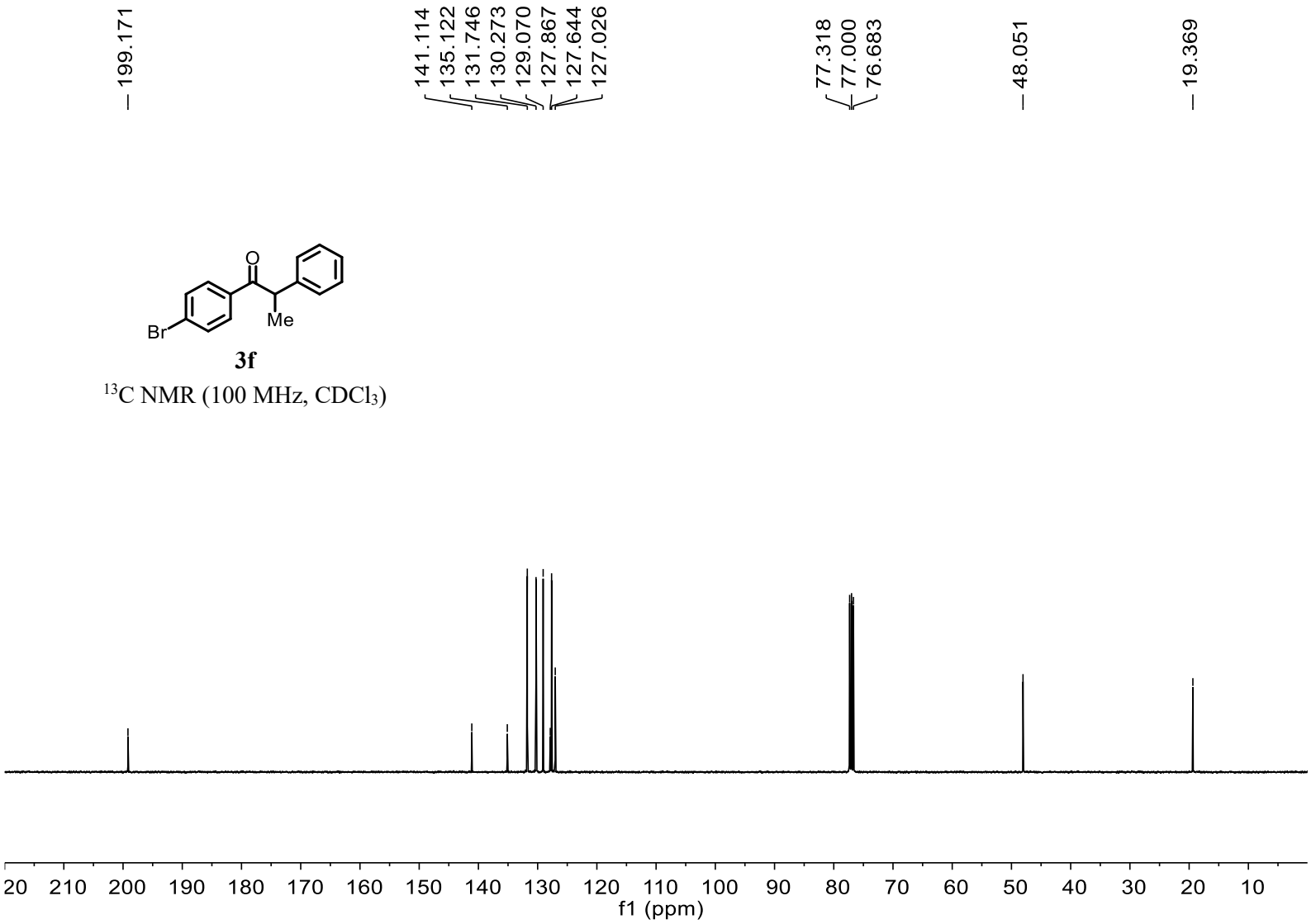

3f

^{13}C NMR (100 MHz, $CDCl_3$)

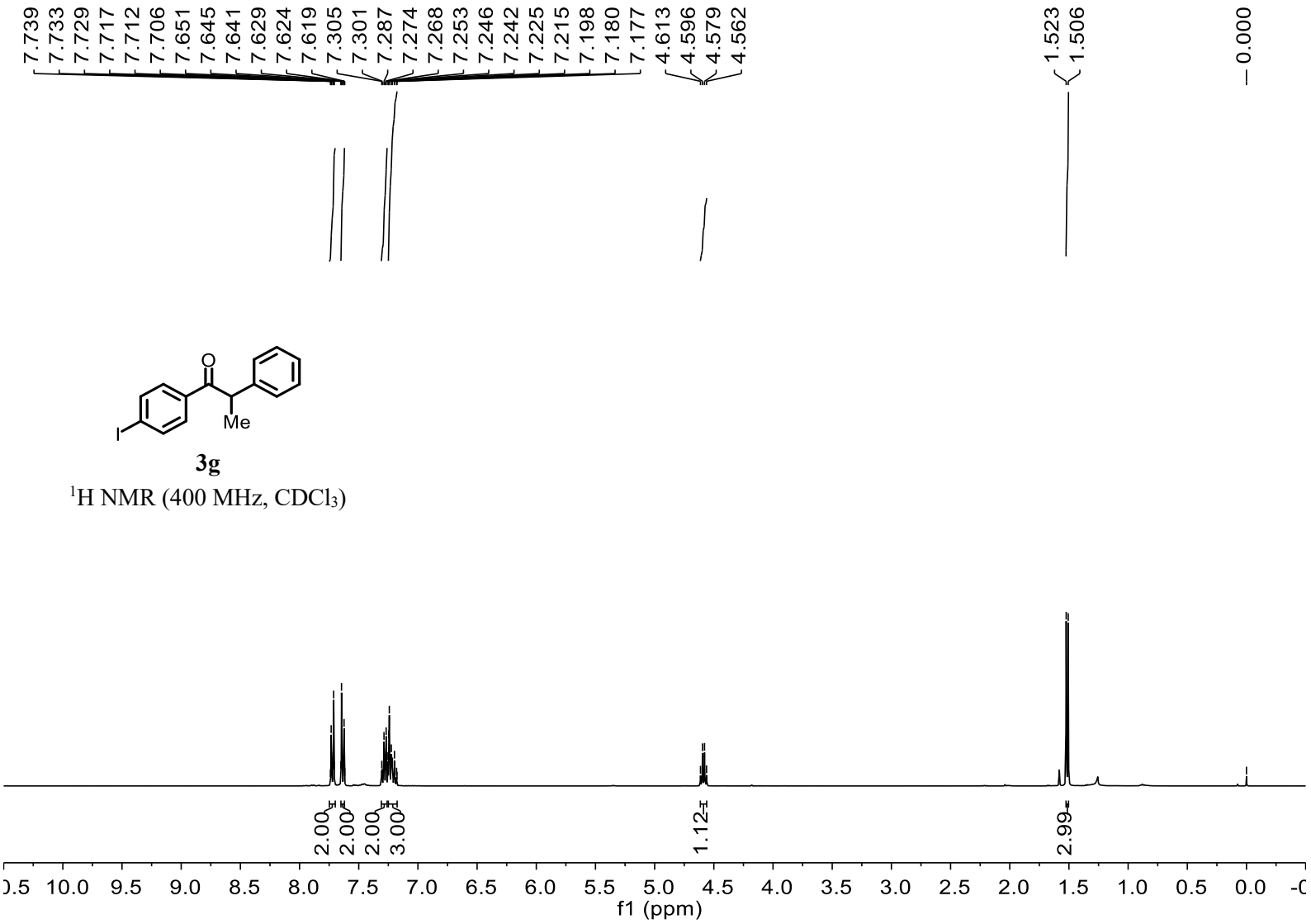

3g

^{1}H NMR (400 MHz, $CDCl_3$)

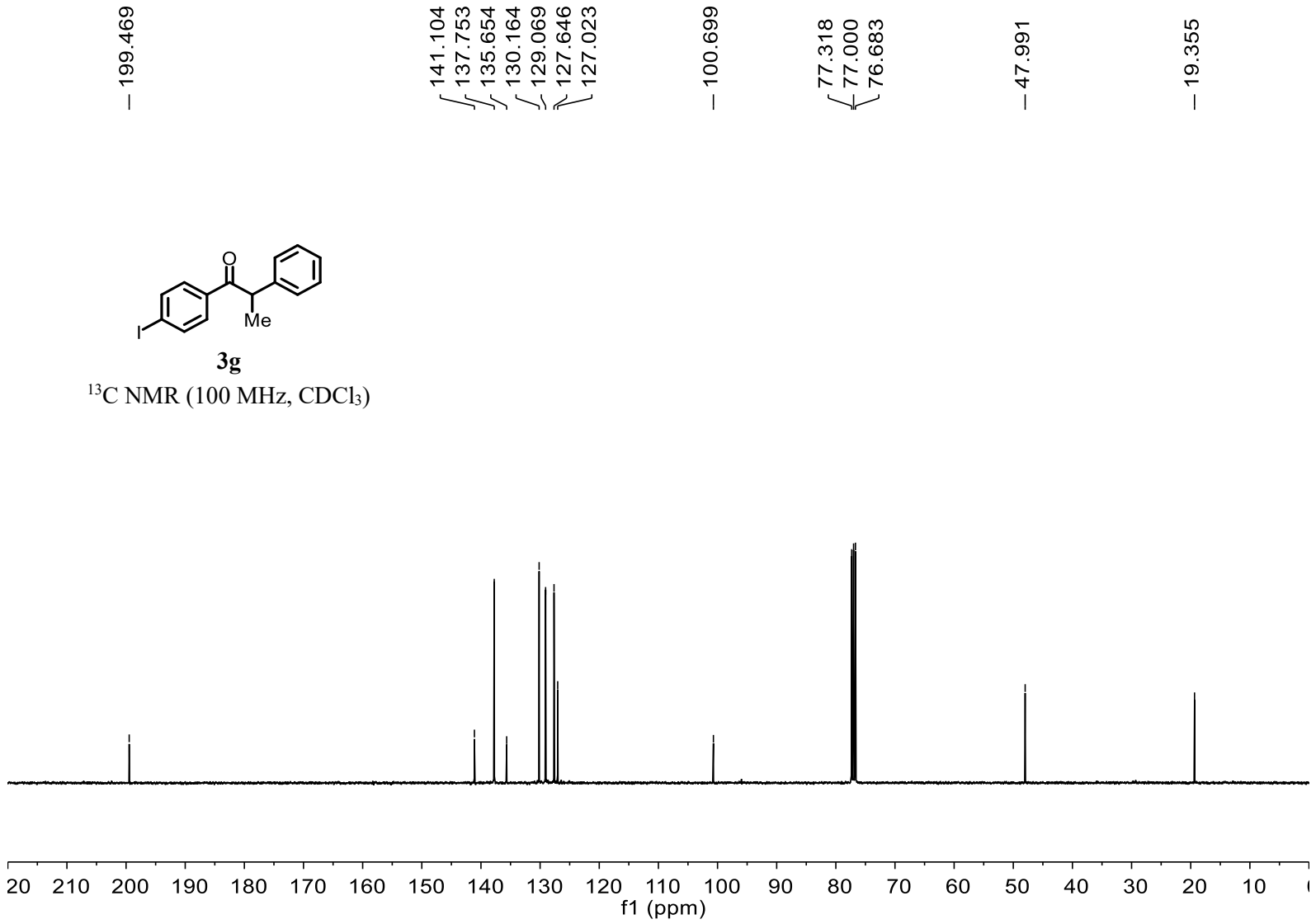

3g

^{13}C NMR (100 MHz, $CDCl_3$)

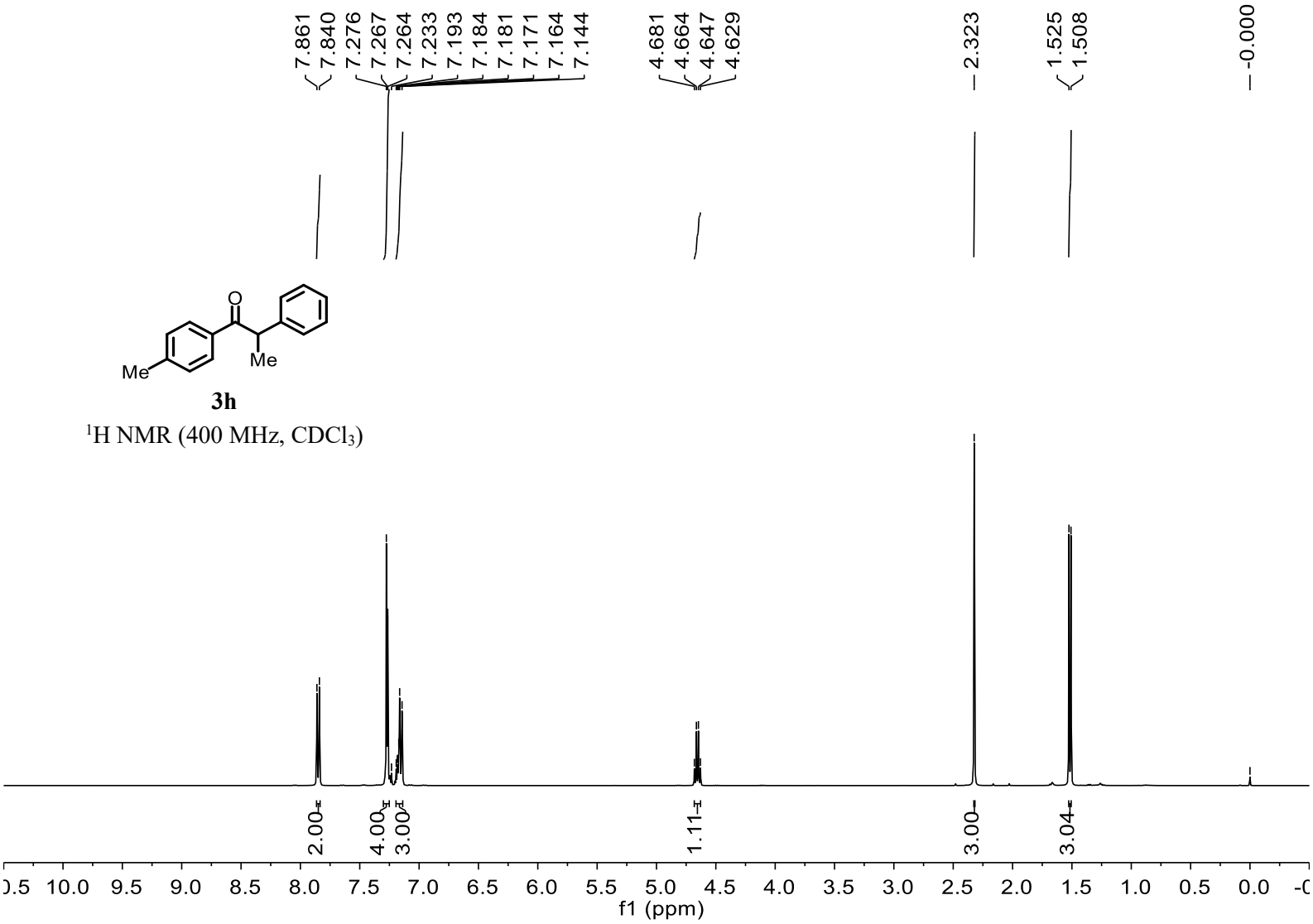

3h

^{1}H NMR (400 MHz, $CDCl_3$)

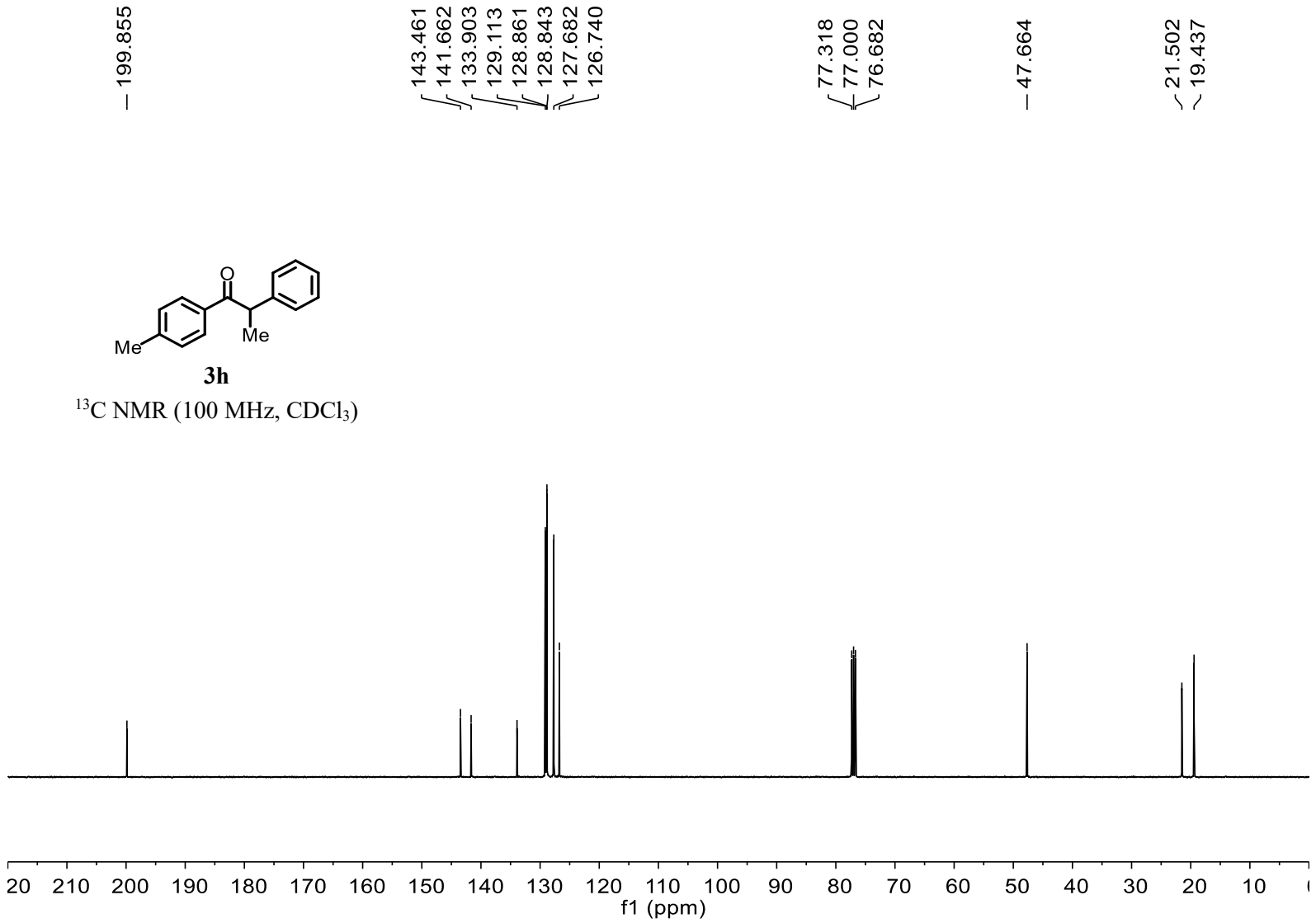

3h

^{13}C NMR (100 MHz, $CDCl_3$)

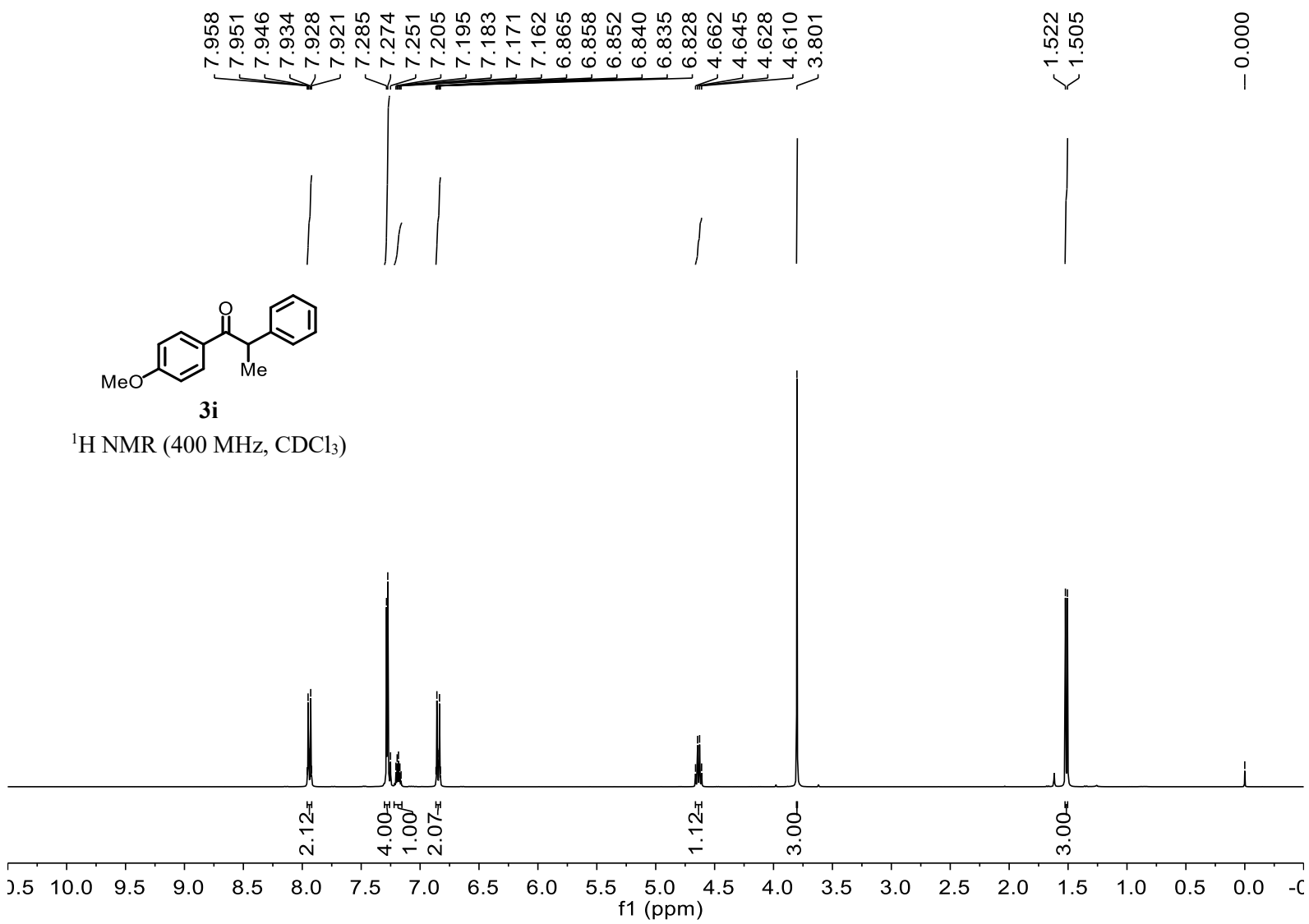

3i

^{1}H NMR (400 MHz, $CDCl_3$)

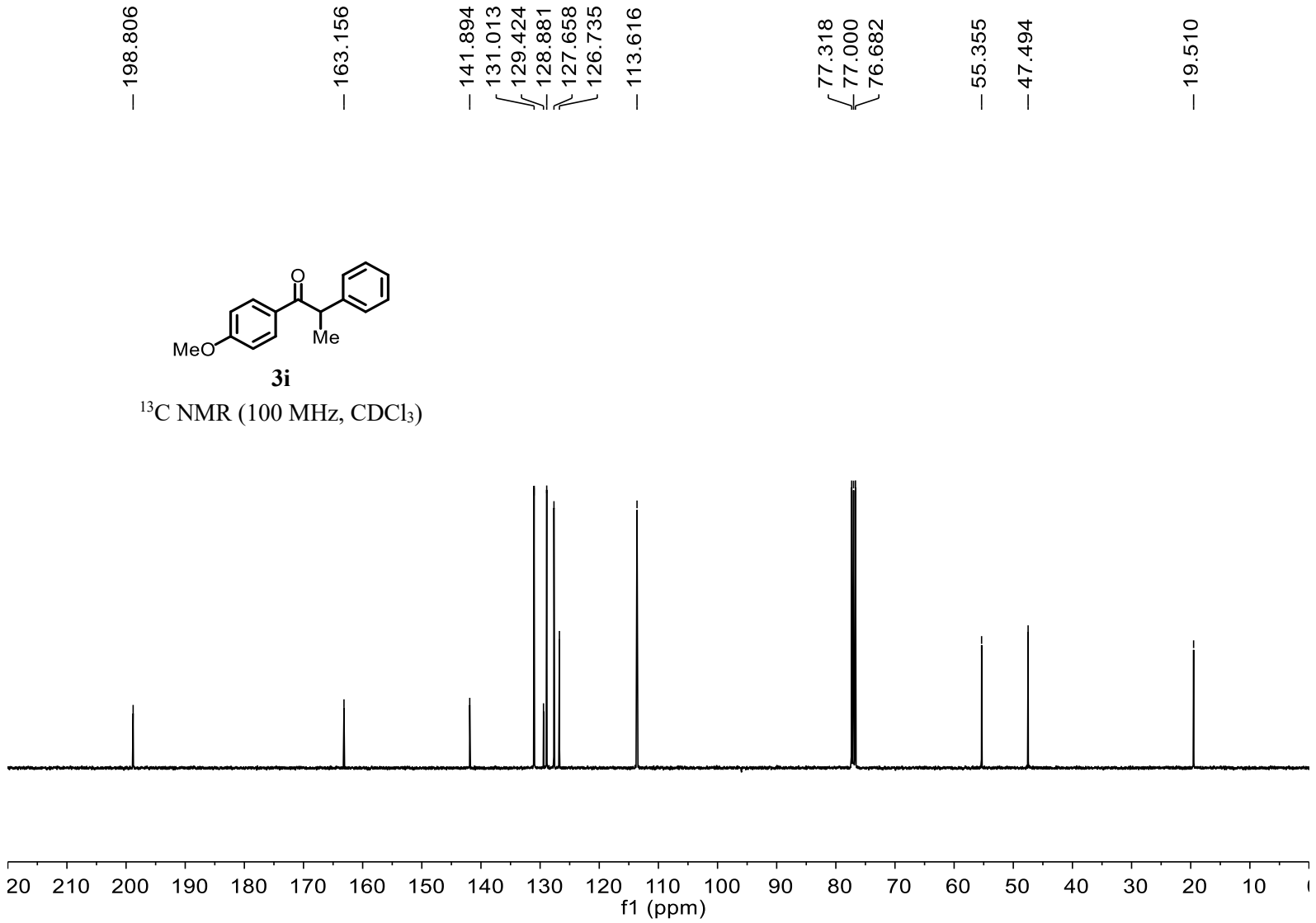

3i

^{13}C NMR (100 MHz, $CDCl_3$)

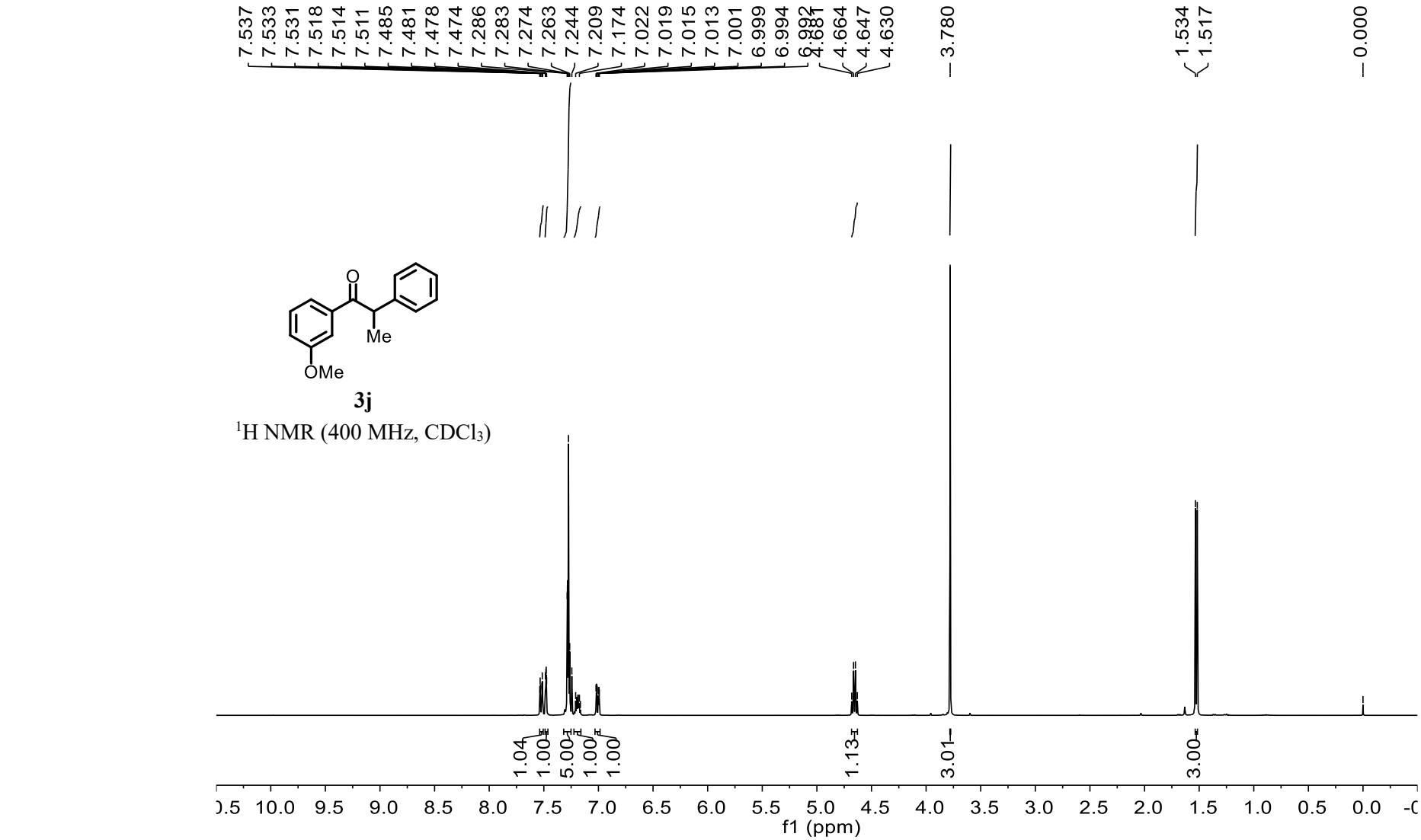

3j

^{1}H NMR (400 MHz, $CDCl_3$)

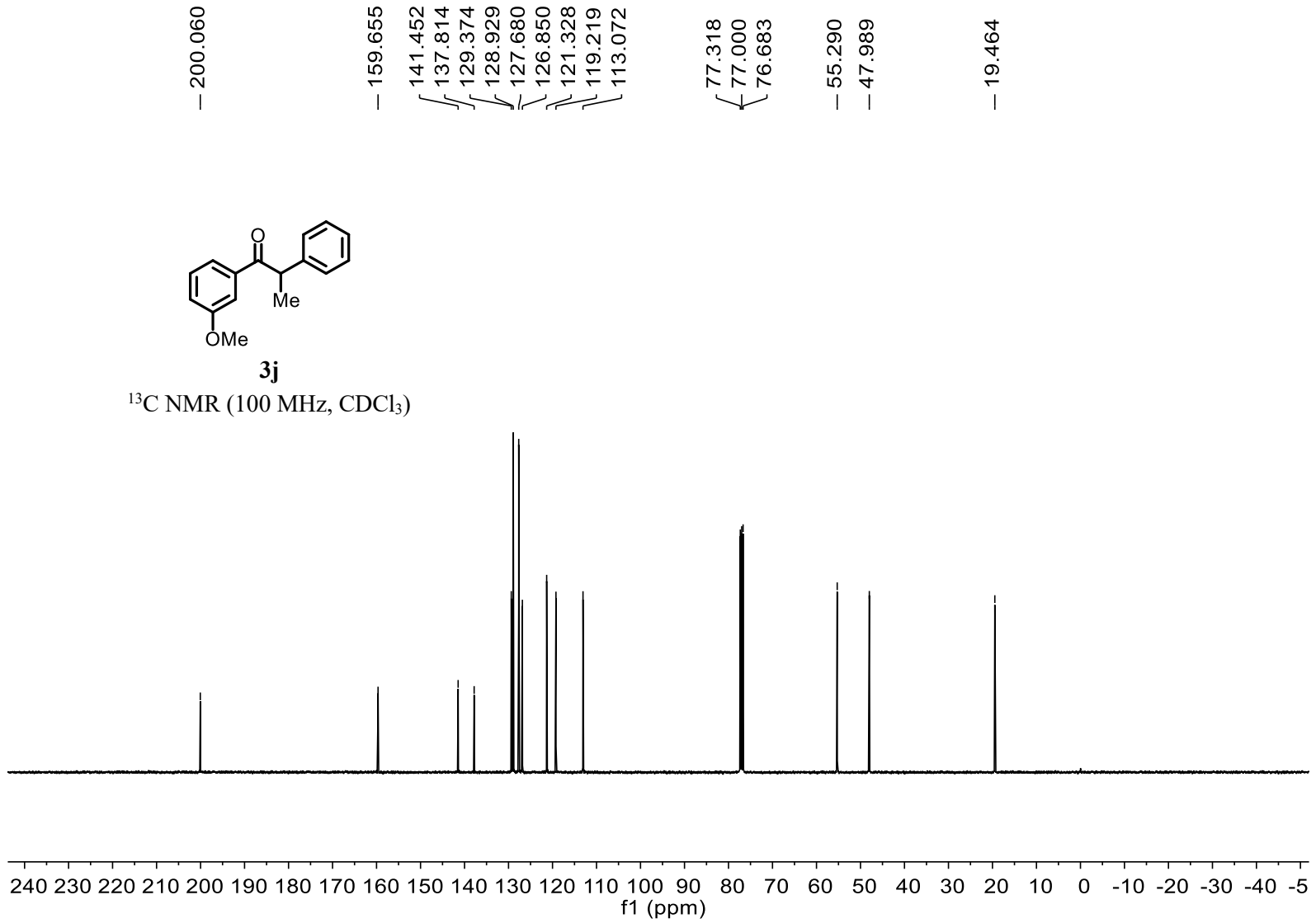

3j

^{13}C NMR (100 MHz, $CDCl_3$)

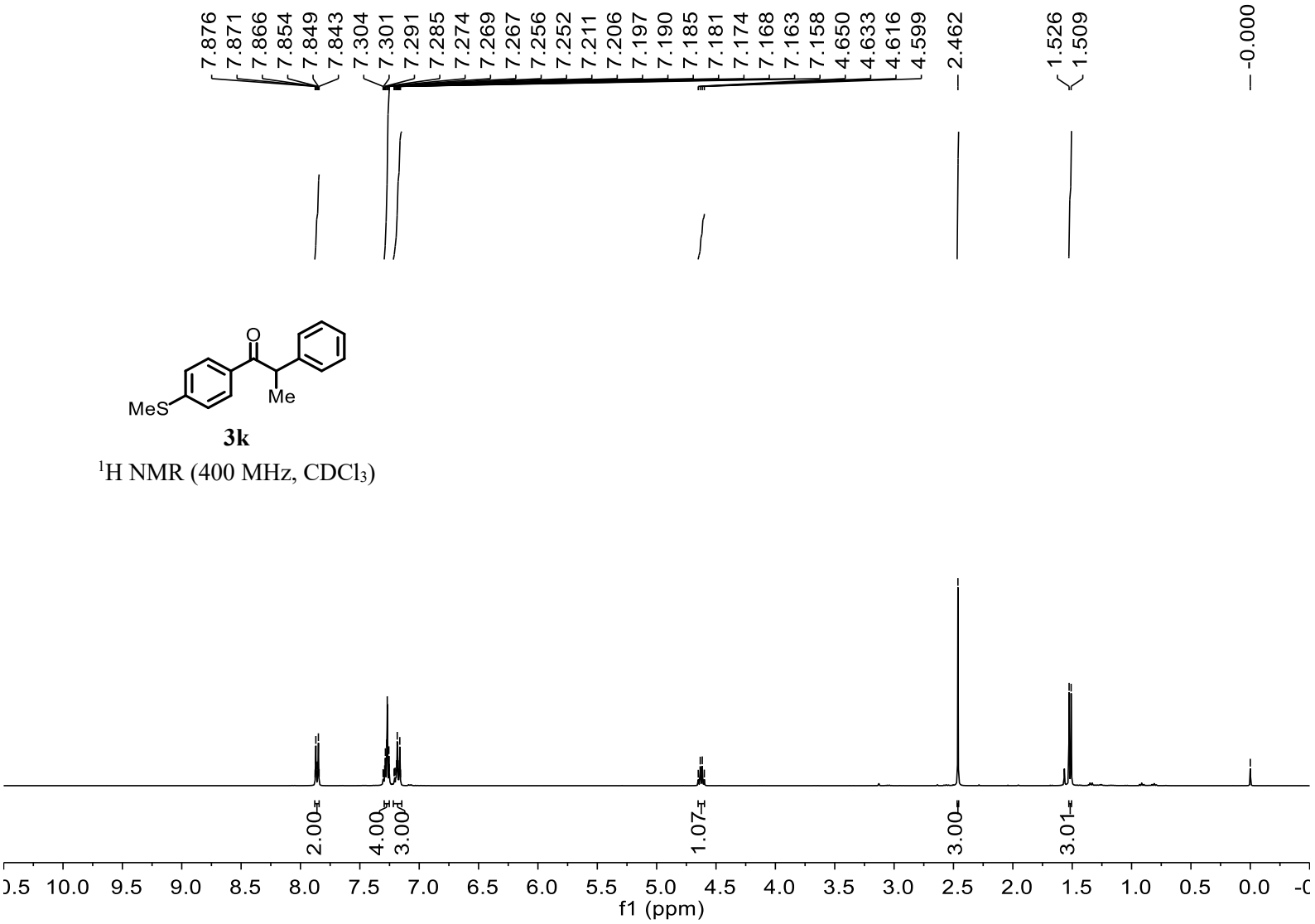

3k

^{1}H NMR (400 MHz, $CDCl_3$)

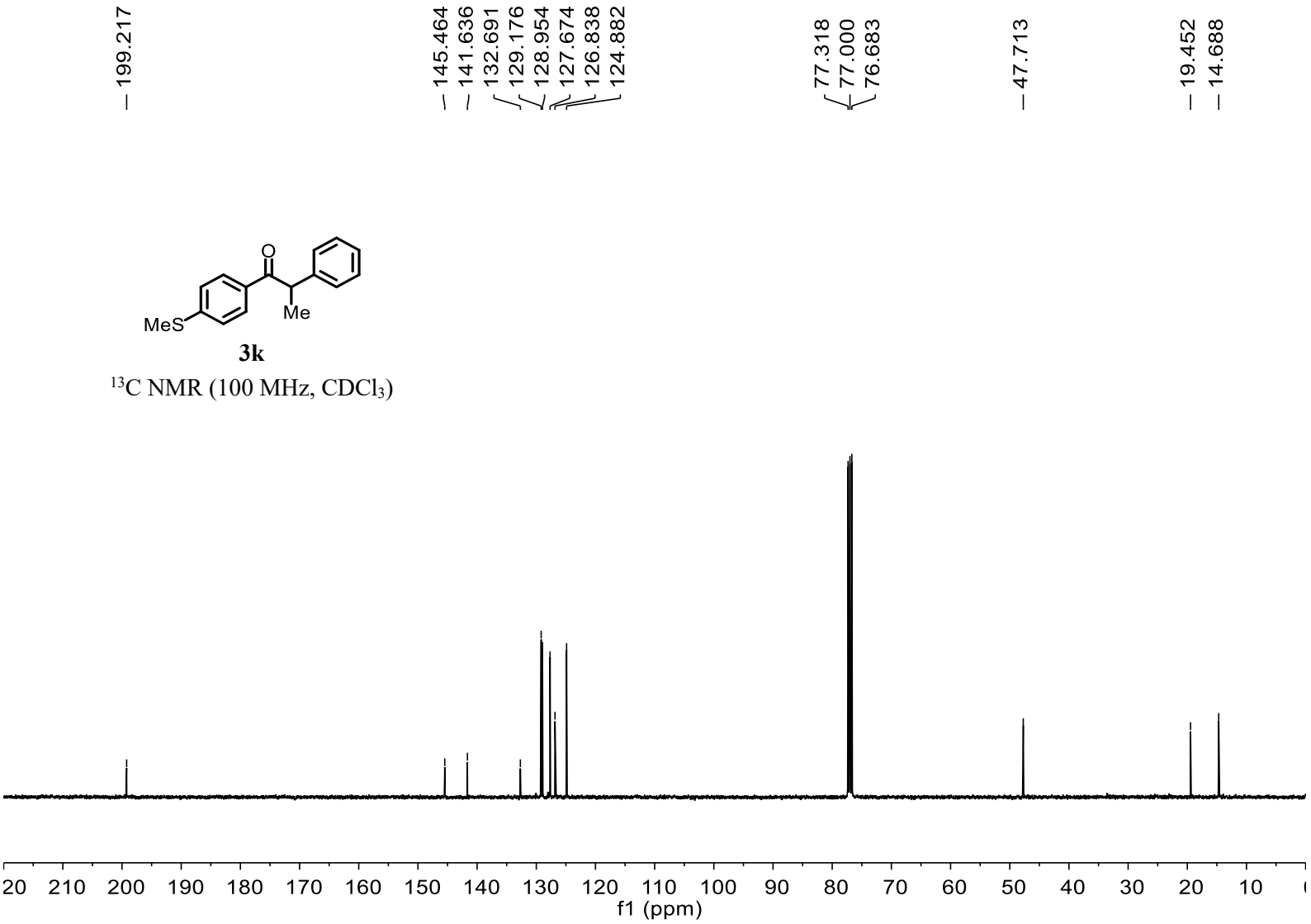

3k

^{13}C NMR (100 MHz, $CDCl_3$)

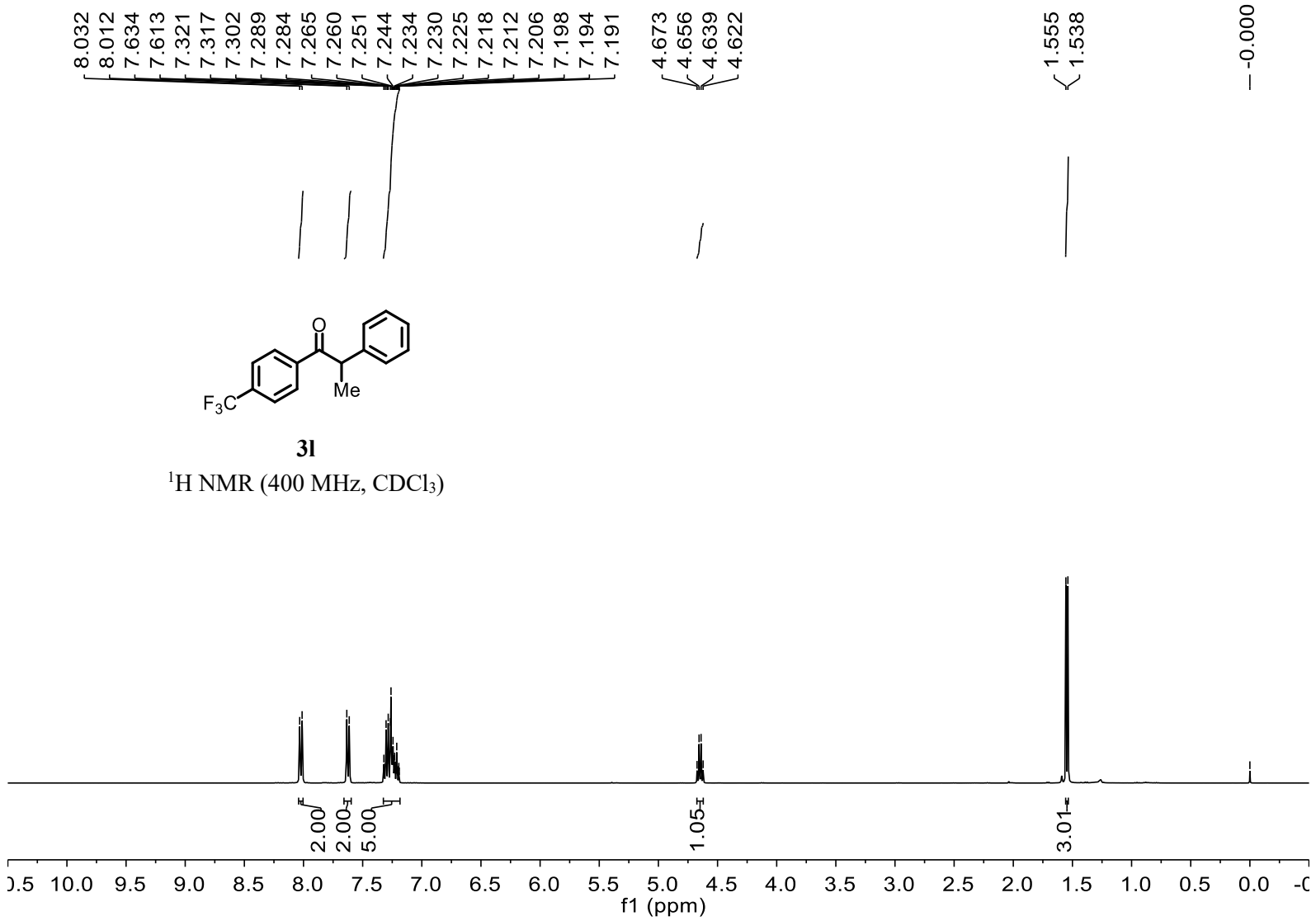

3l

^{1}H NMR (400 MHz, $CDCl_3$)

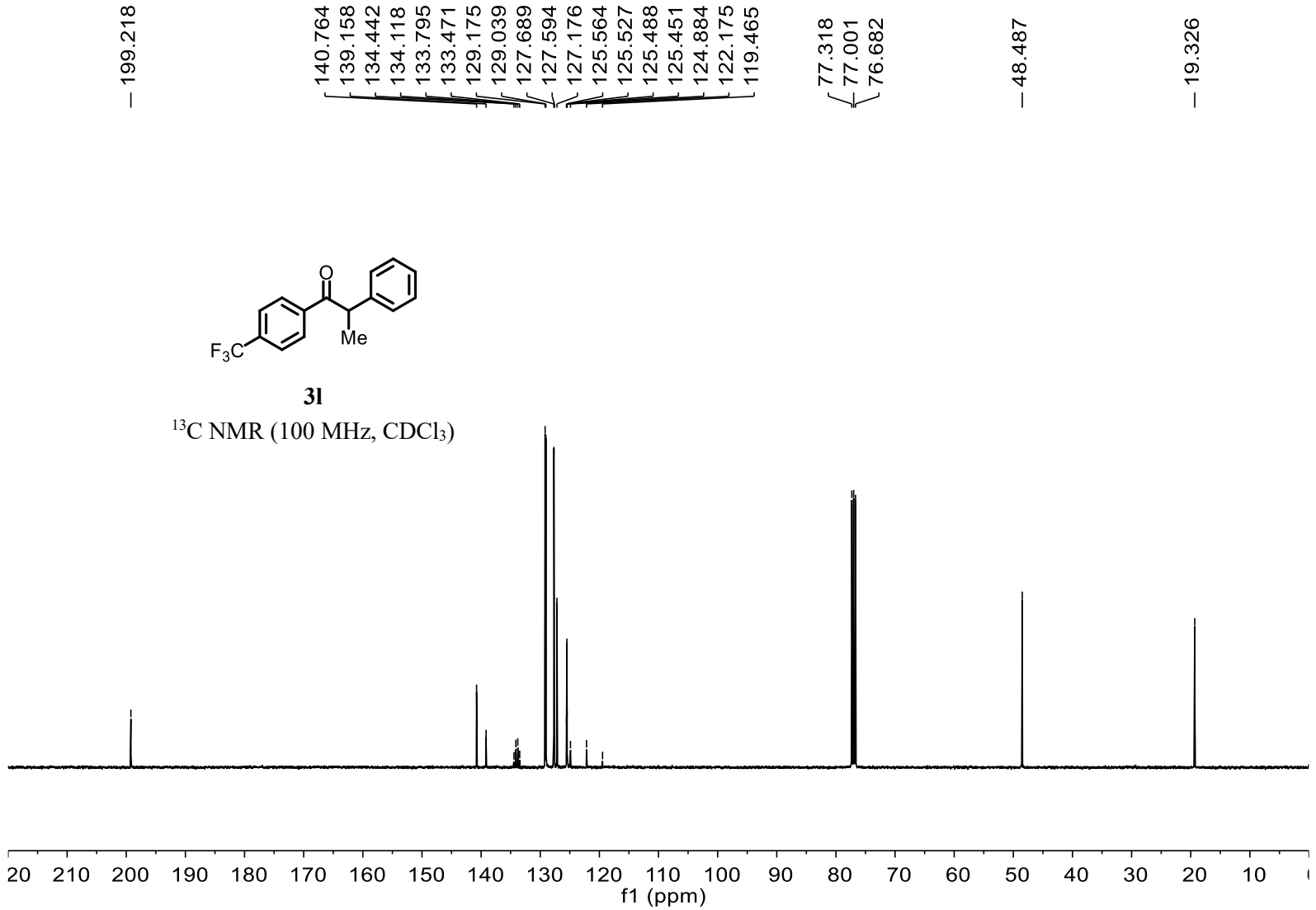
199.218
140.764
139.158
134.442
134.118
133.795
133.471
129.175
129.039
127.689
127.594
127.176
125.564
125.527
125.488
125.451
124.884
122.175
119.465
77.318
77.001
76.682
48.487
19.326
O
Me
F3C
3l
13C NMR (100 MHz, CDCl3)
20 210 200 190 180 170 160 150 140 130 120 110 100 90 80 70 60 50 40 30 20 10
f1 (ppm)

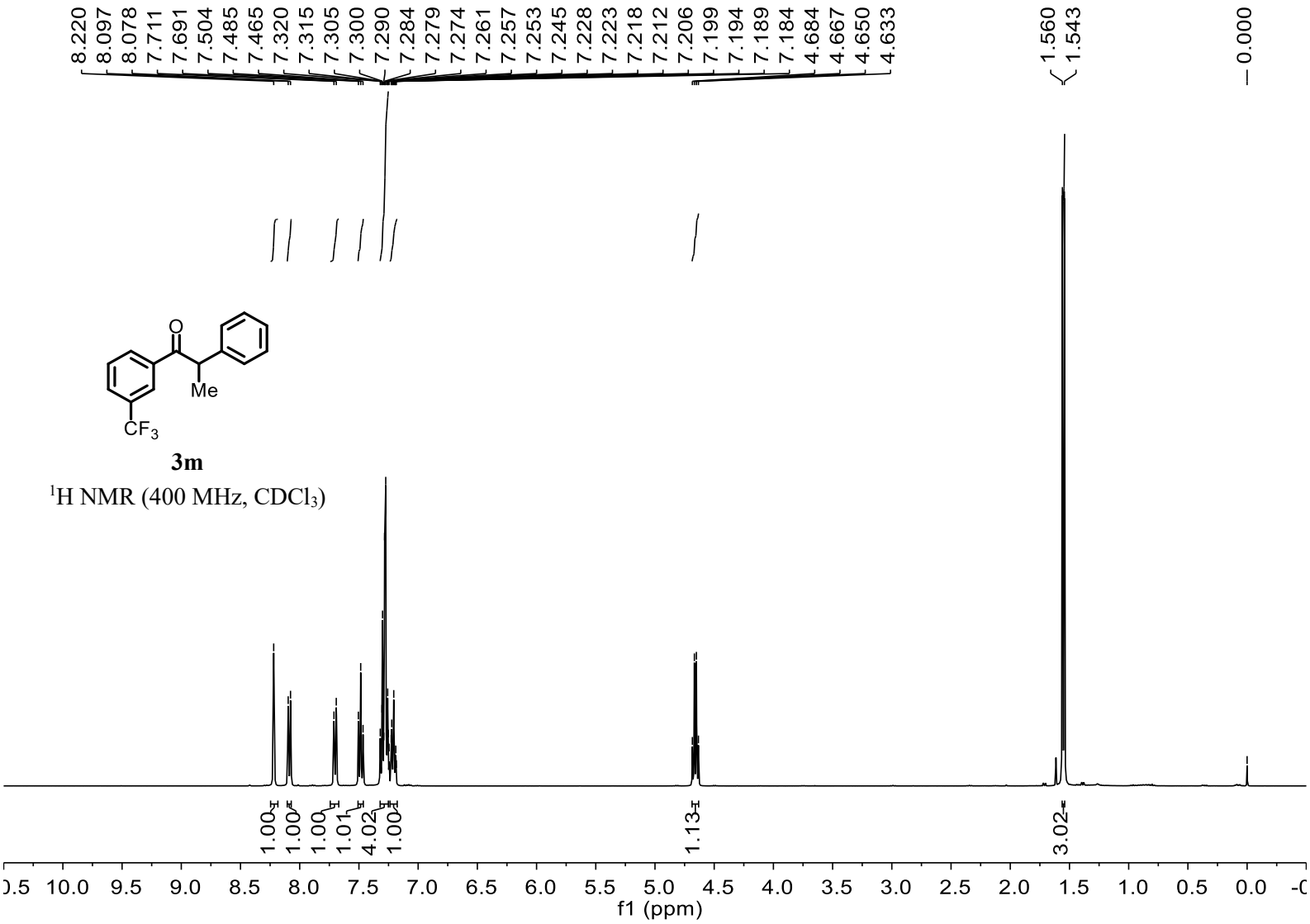

3m

^{1}H NMR (400 MHz, $CDCl_3$)

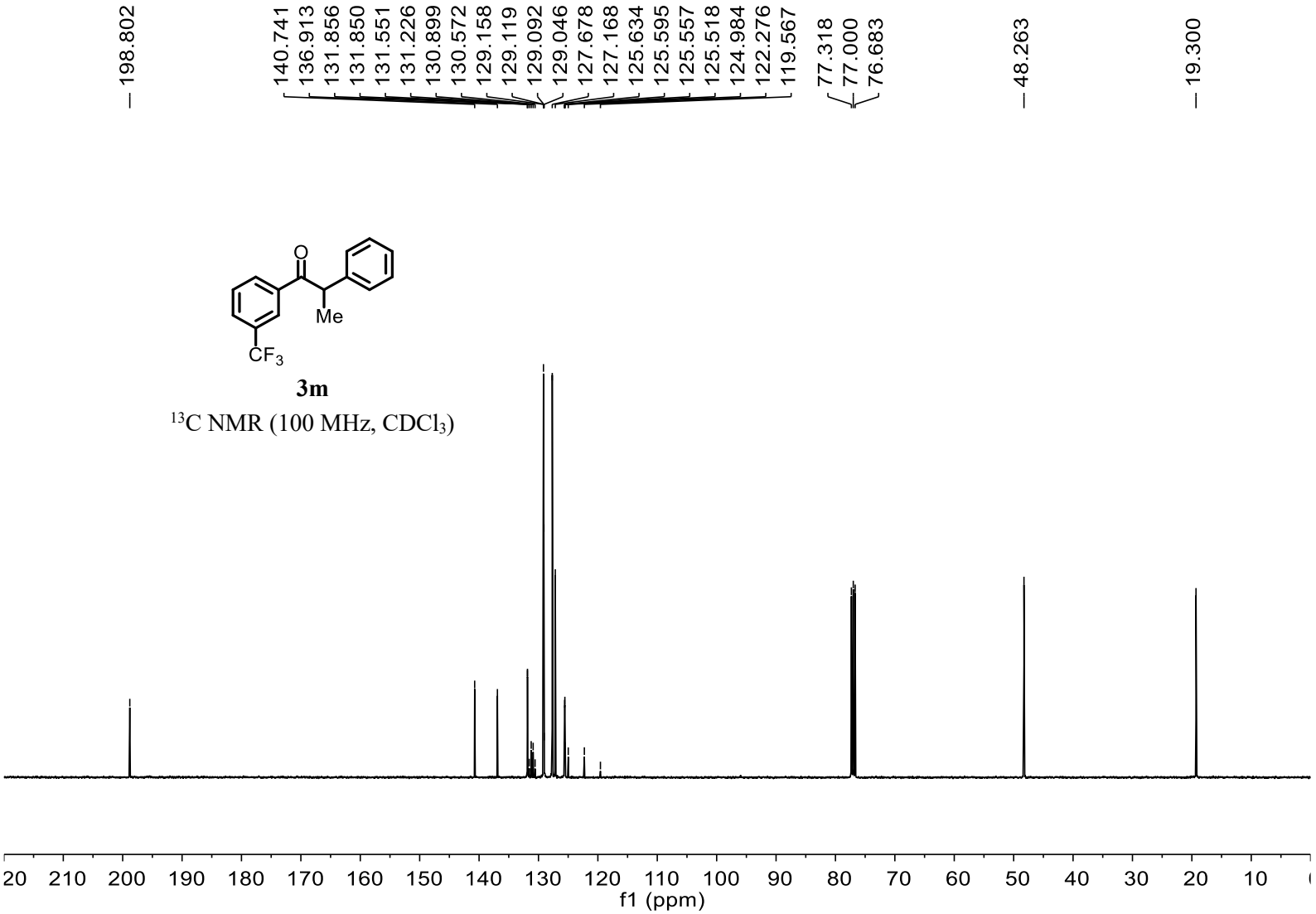

3m

^{13}C NMR (100 MHz, $CDCl_3$)

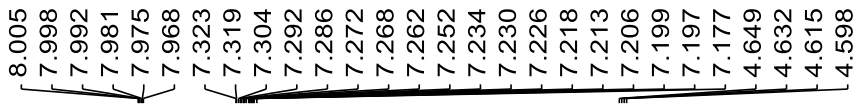

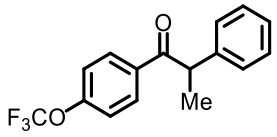

3n

^{1}H NMR (400 MHz, $CDCl_3$)

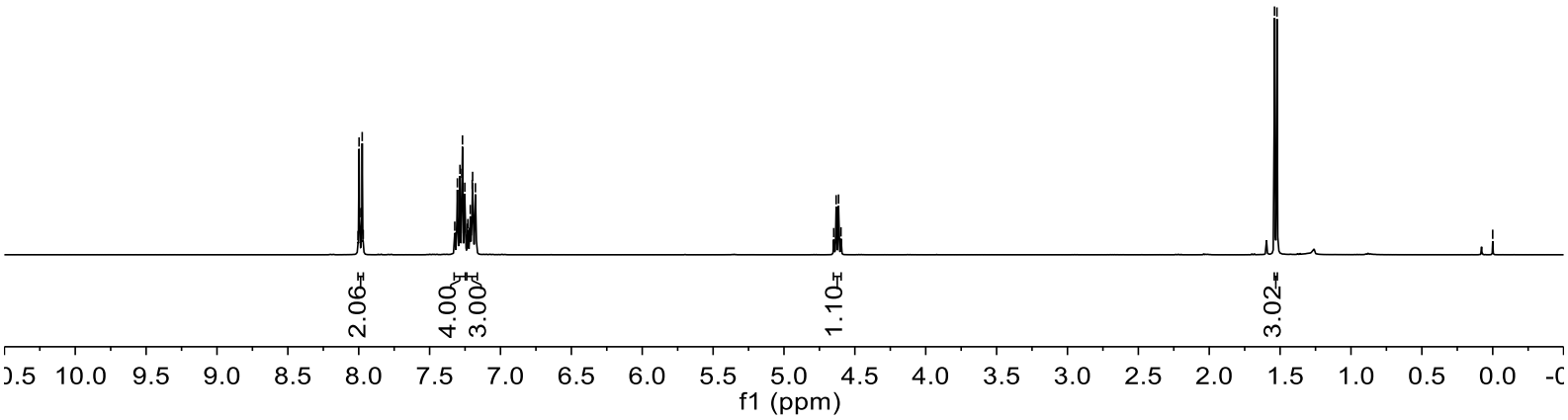

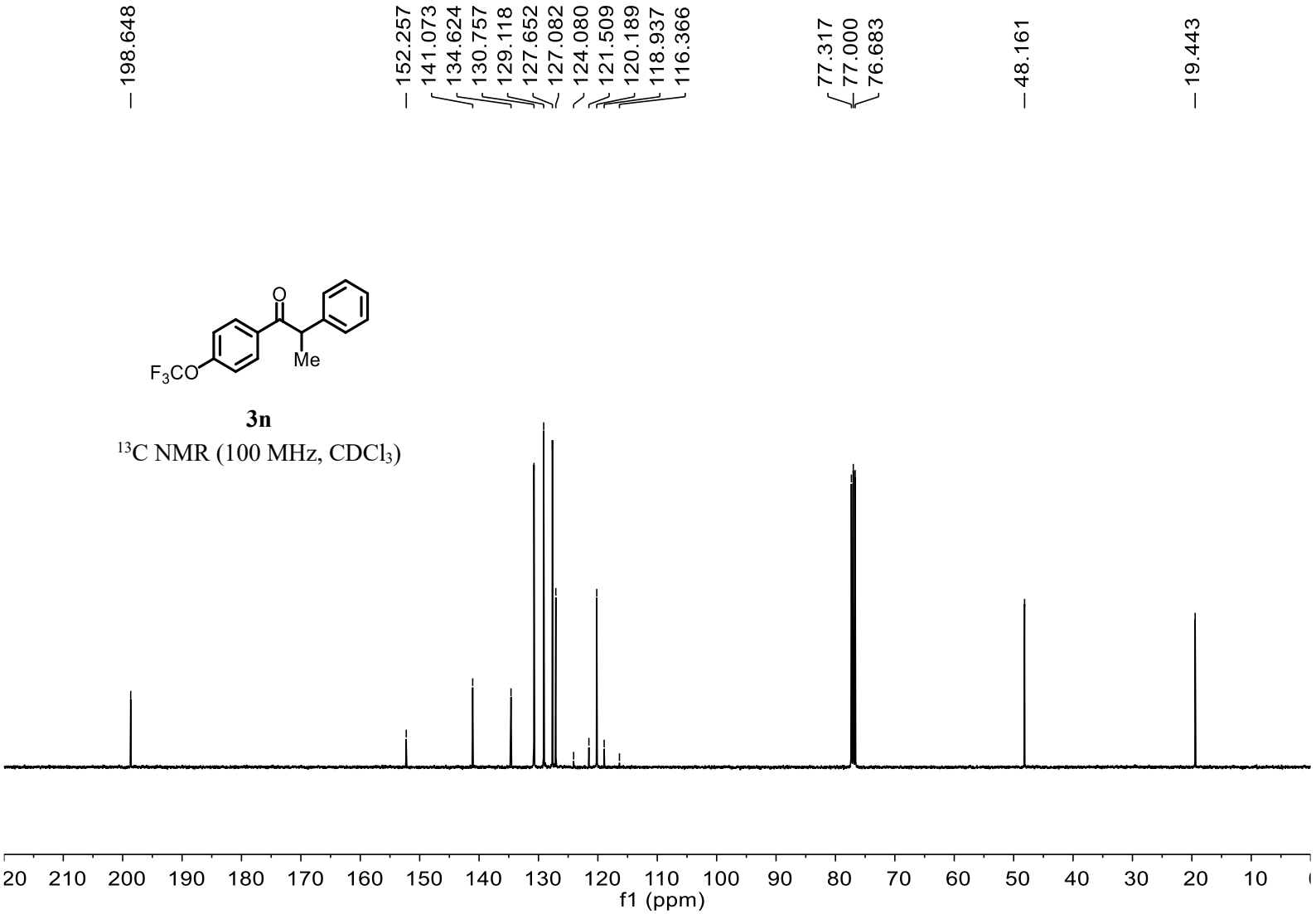

3n

^{13}C NMR (100 MHz, $CDCl_3$)

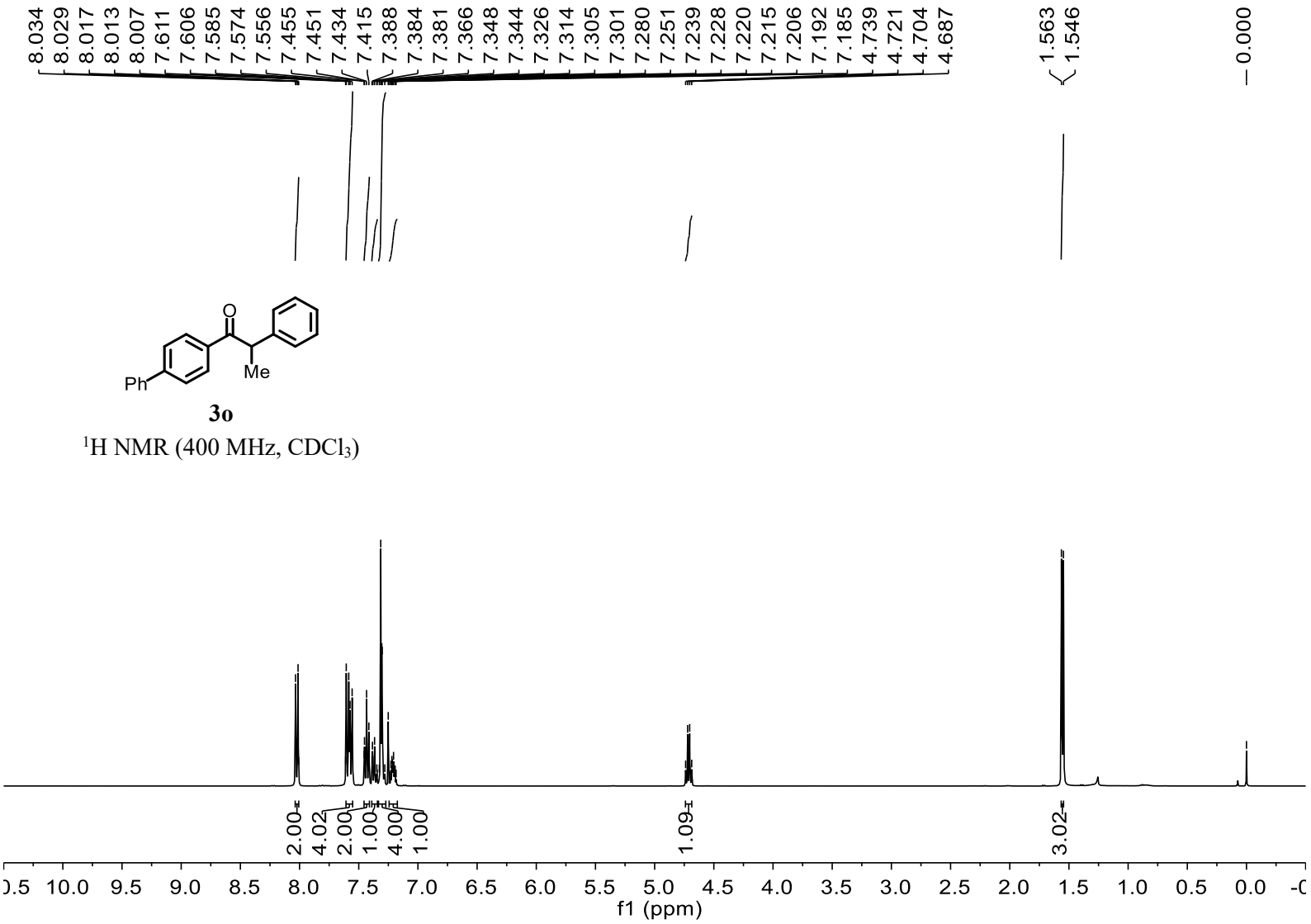

3o

^{1}H NMR (400 MHz, $CDCl_3$)

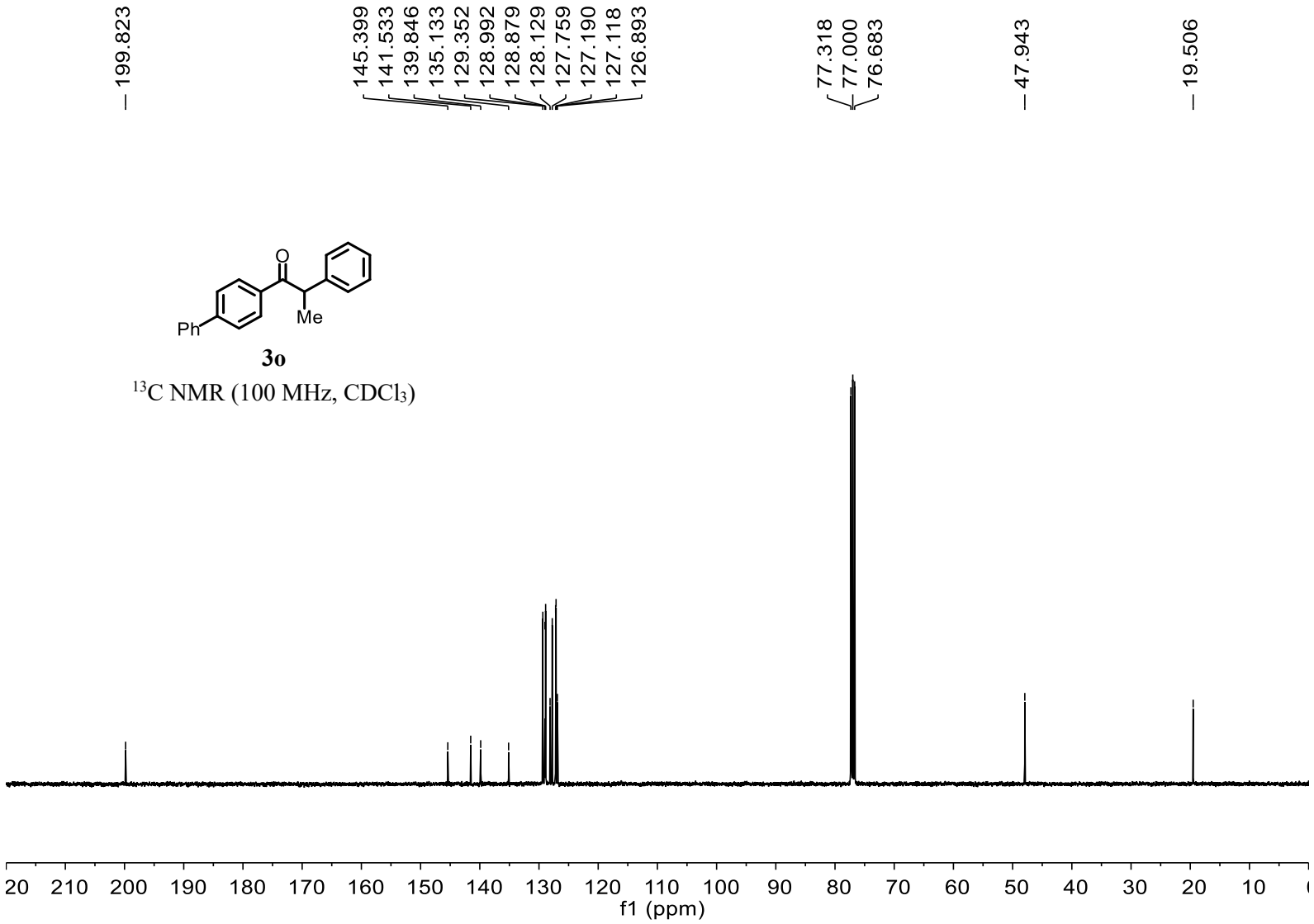

3o

^{13}C NMR (100 MHz, $CDCl_3$)

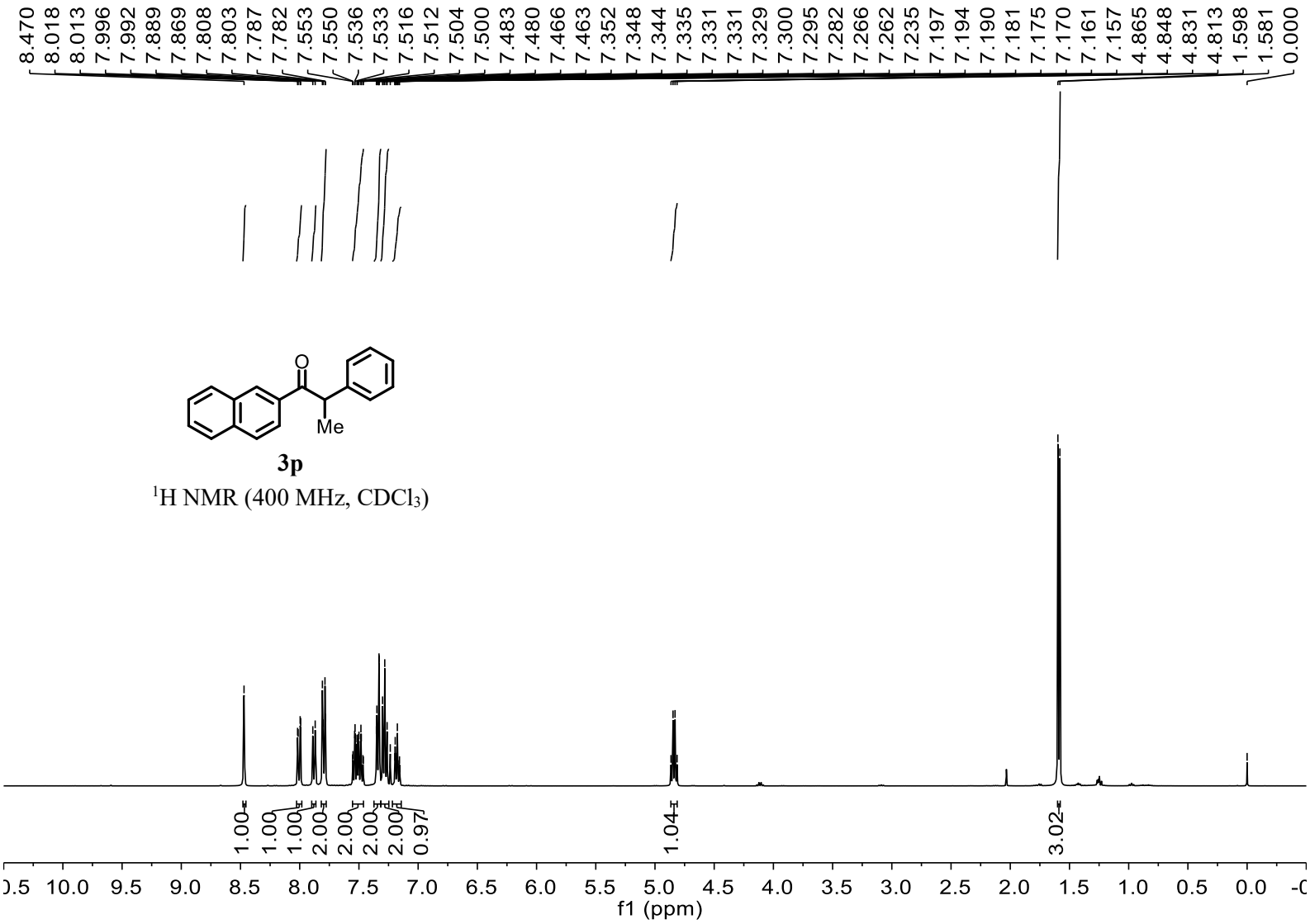

3p

^{1}H NMR (400 MHz, $CDCl_3$)

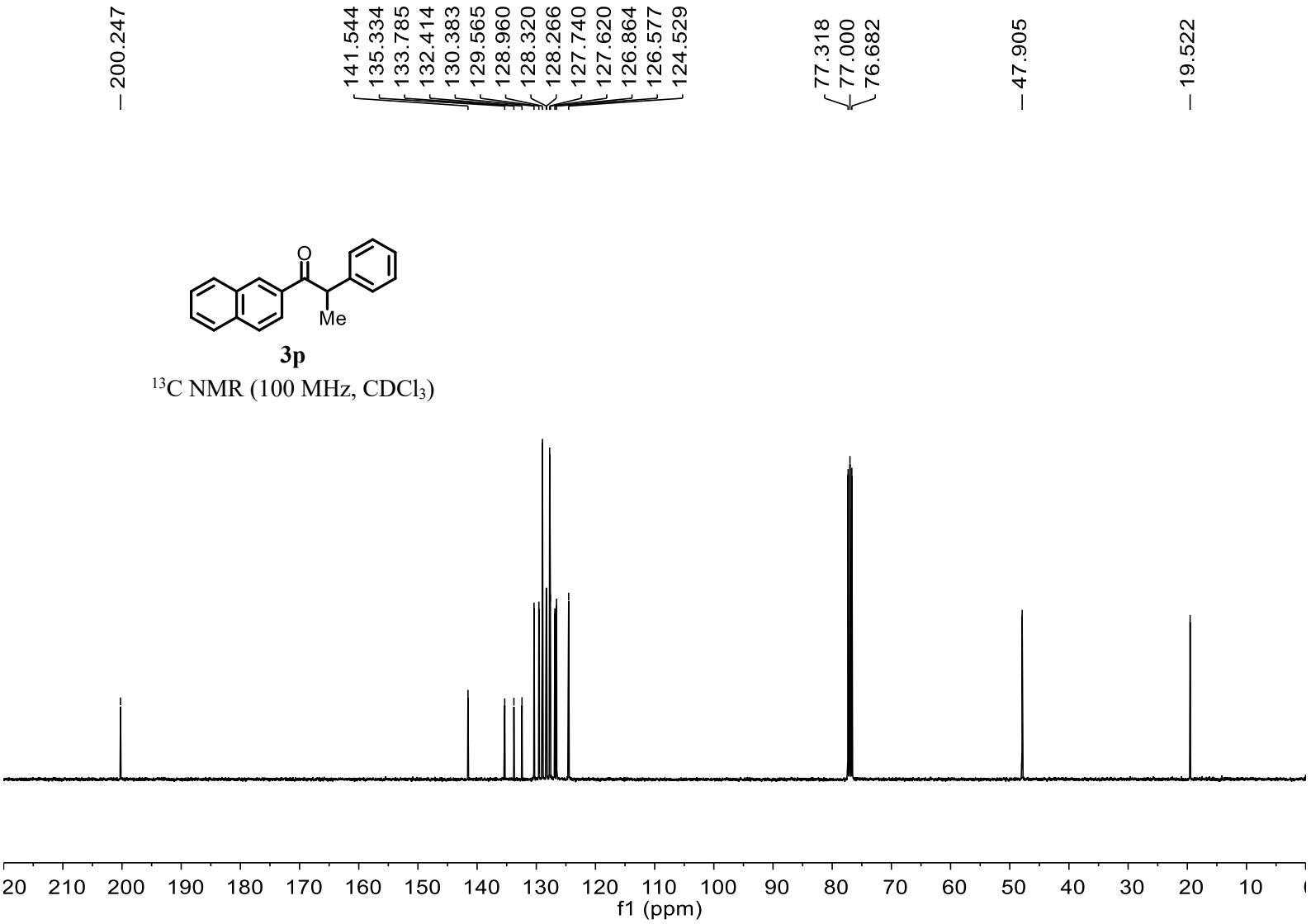

3p

^{13}C NMR (100 MHz, $CDCl_3$)

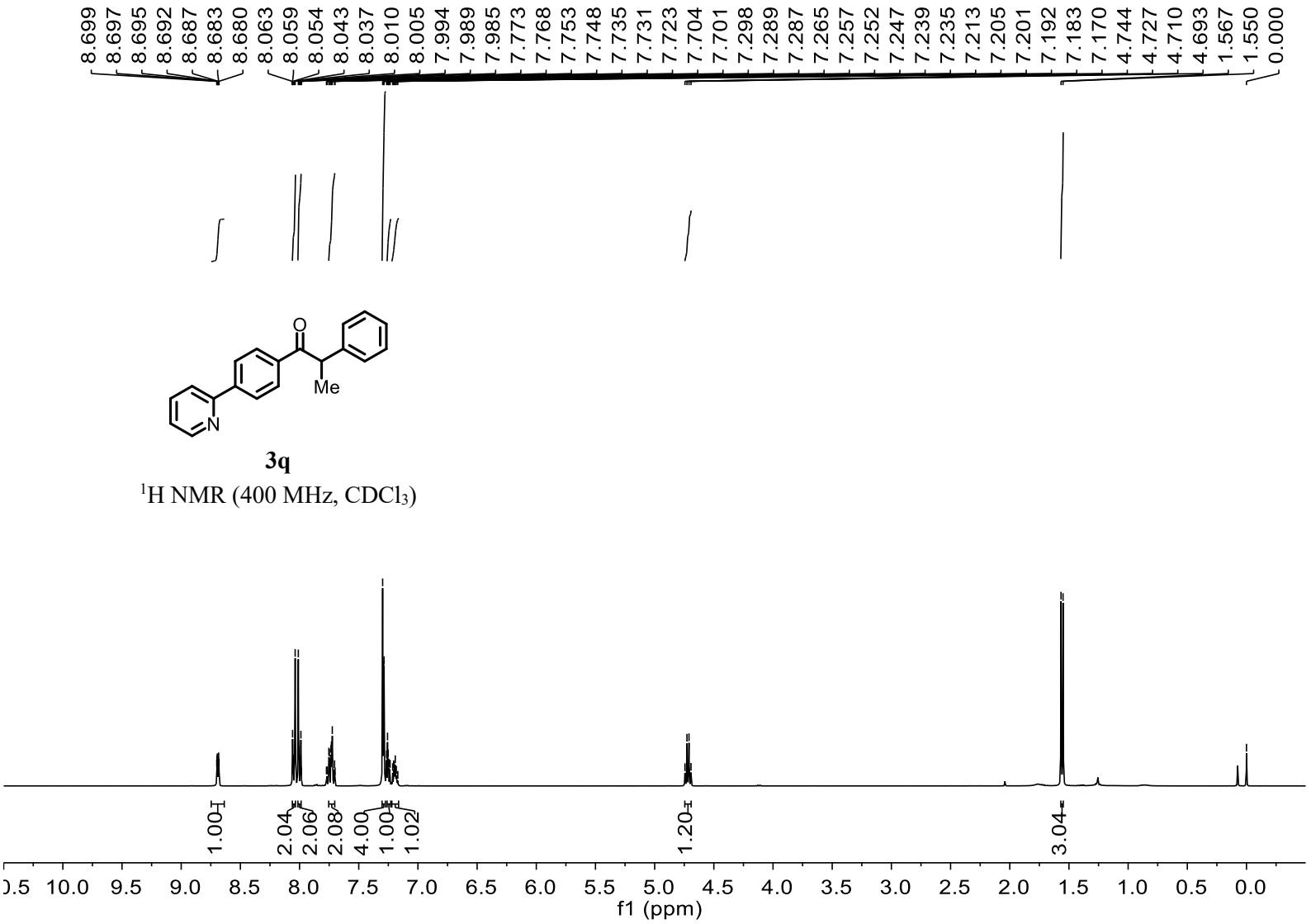

3q

^{1}H NMR (400 MHz, $CDCl_3$)

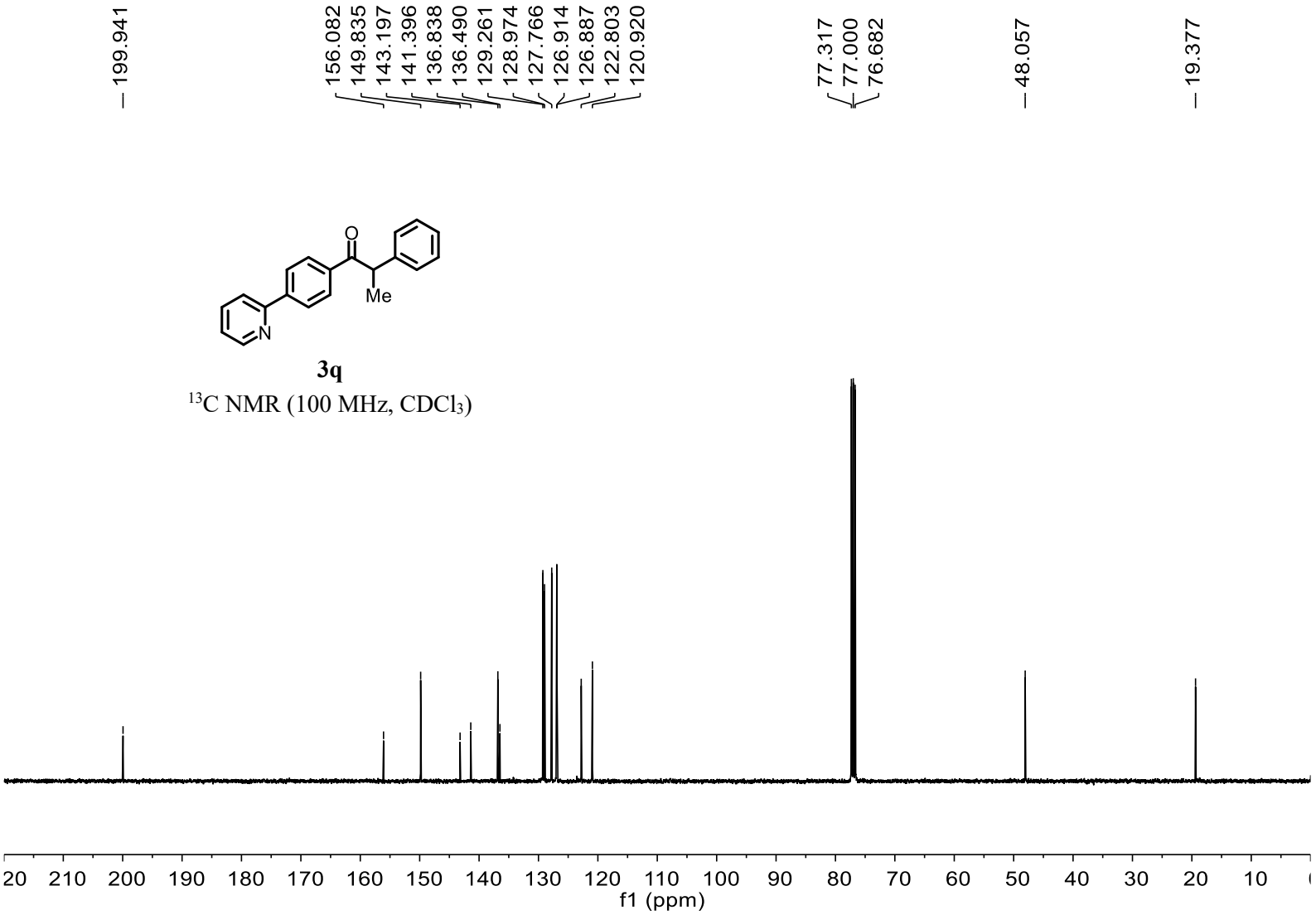

3q

^{13}C NMR (100 MHz, $CDCl_3$)

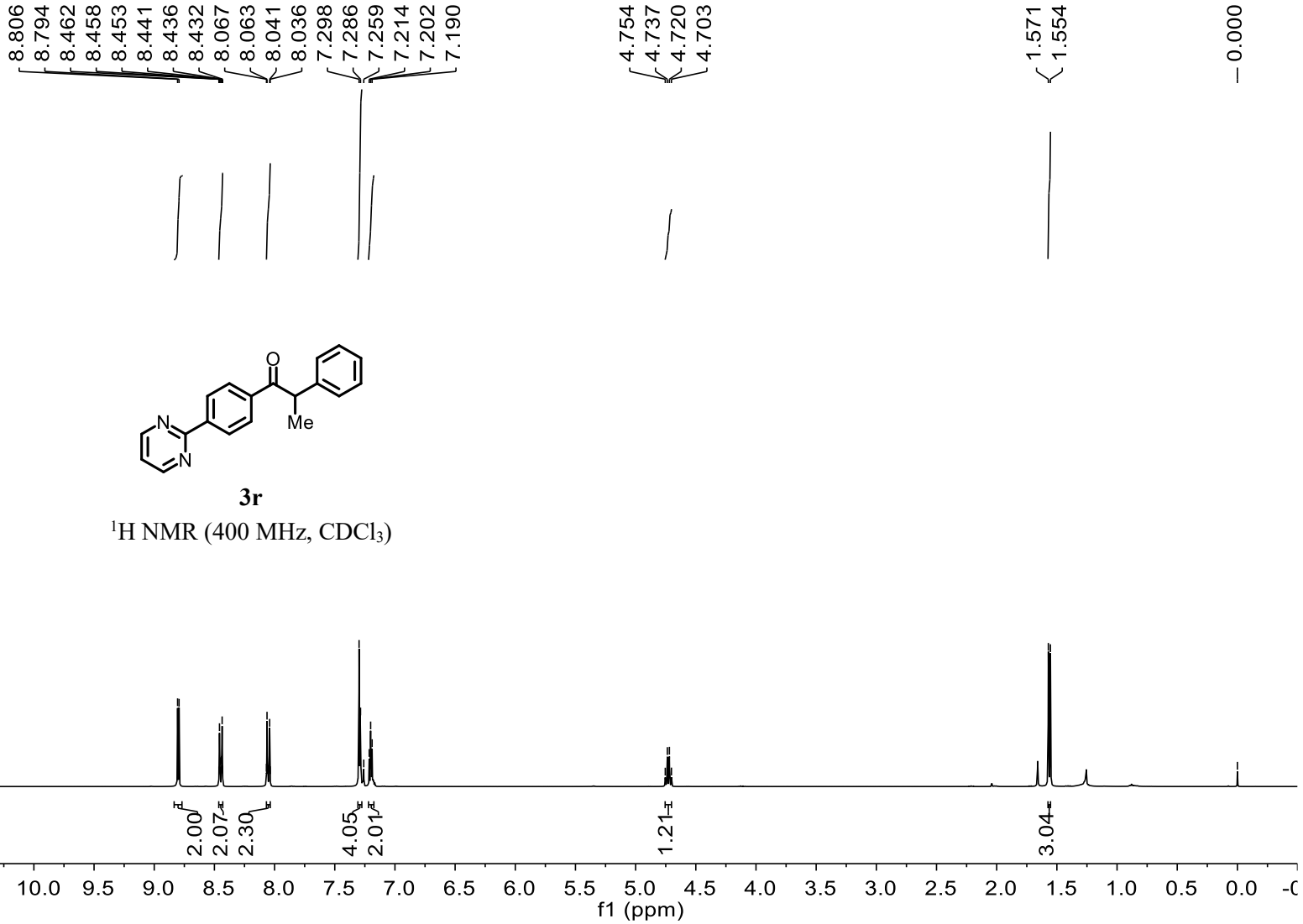

3r

^{1}H NMR (400 MHz, $CDCl_3$)

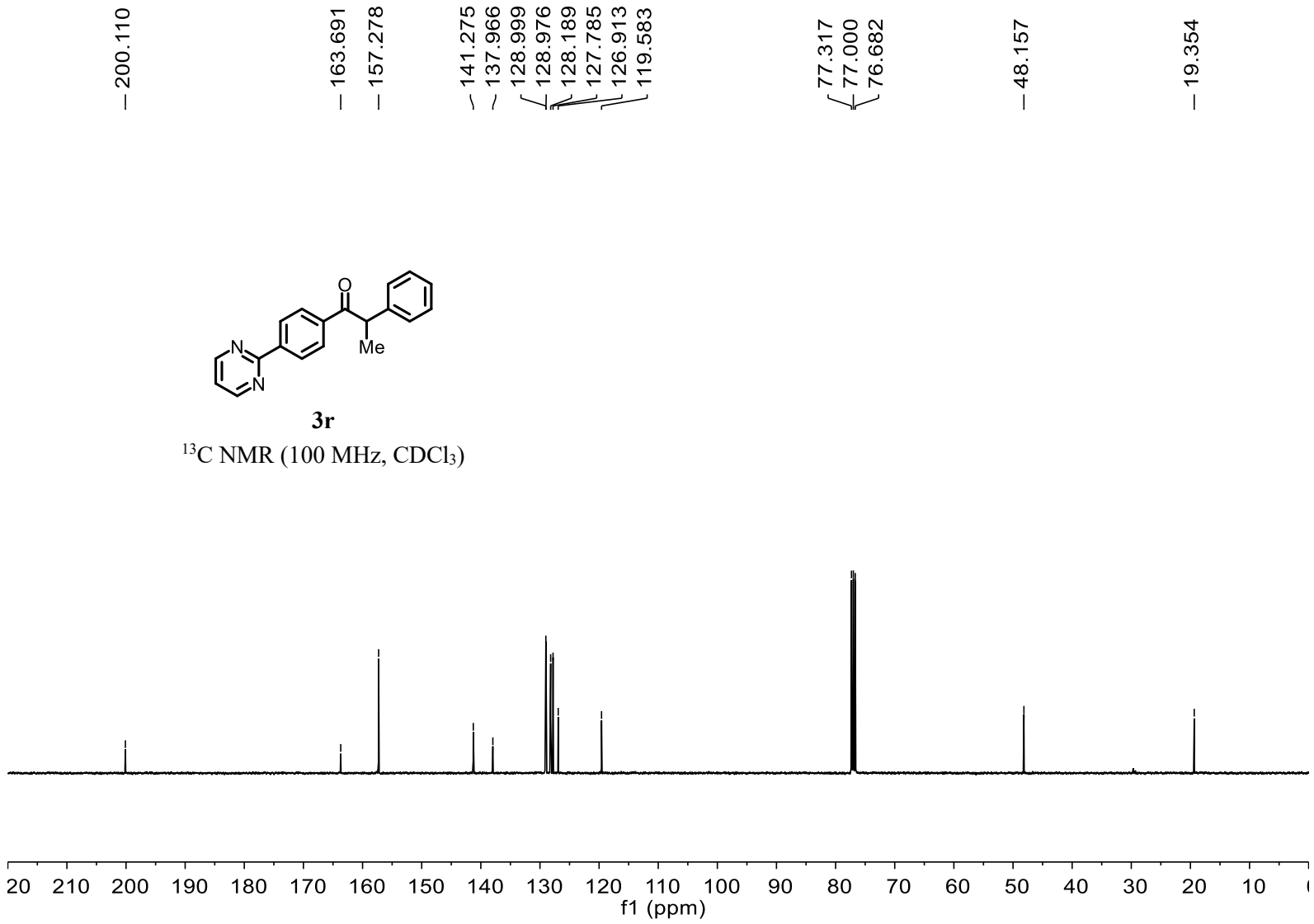

3r

^{13}C NMR (100 MHz, $CDCl_3$)

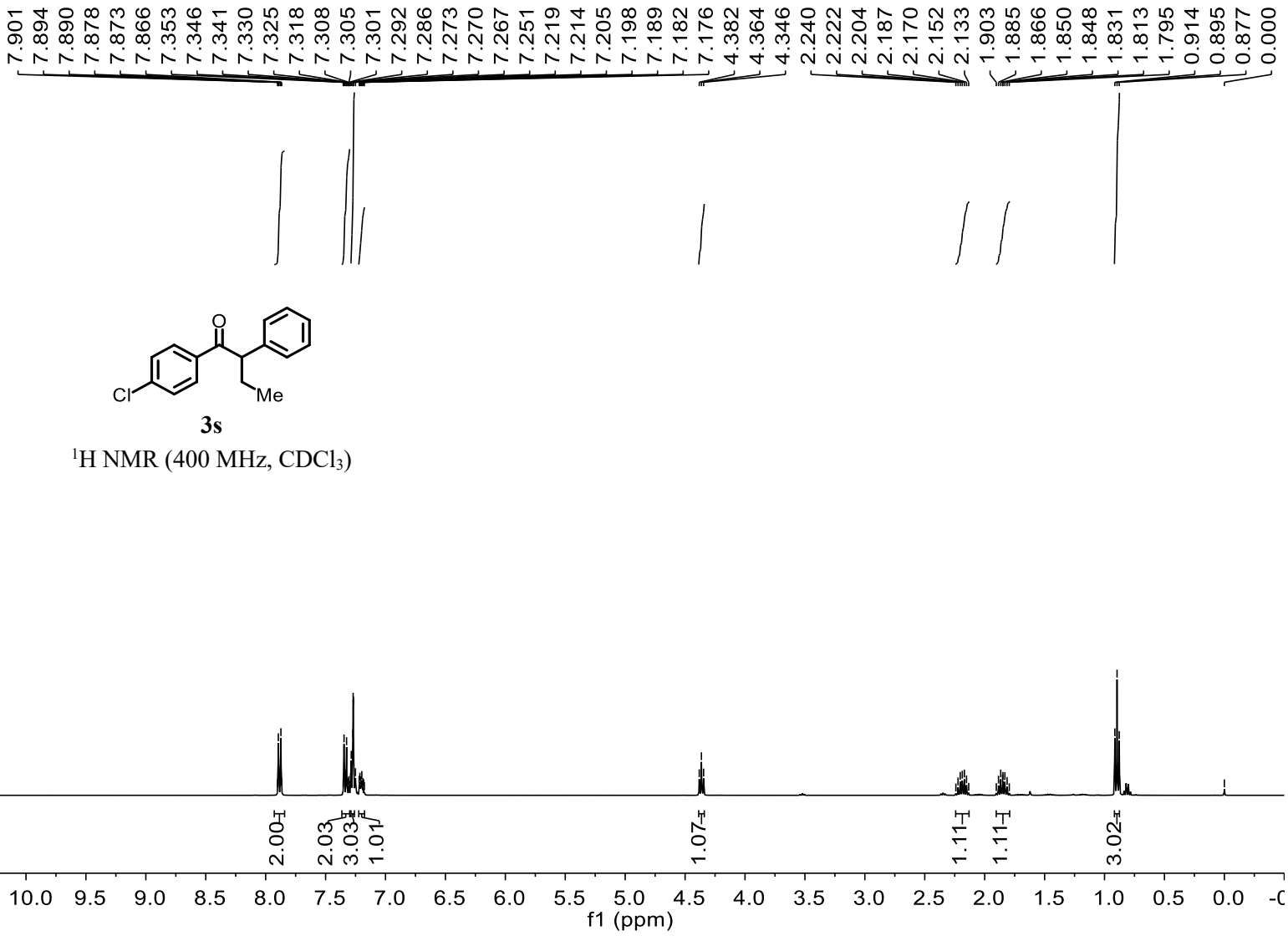

3s

^{1}H NMR (400 MHz, $CDCl_3$)

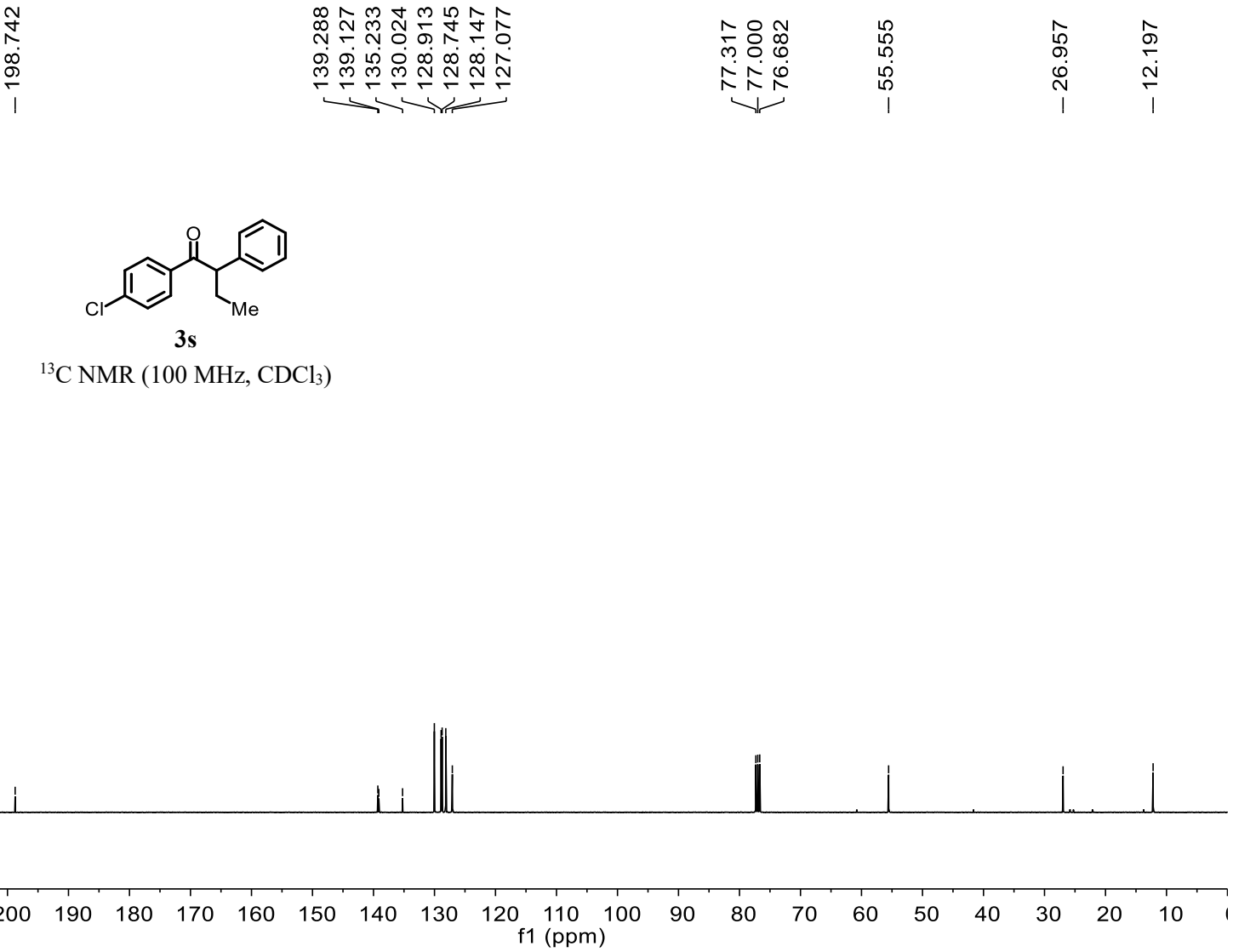

3s

^{13}C NMR (100 MHz, $CDCl_3$)

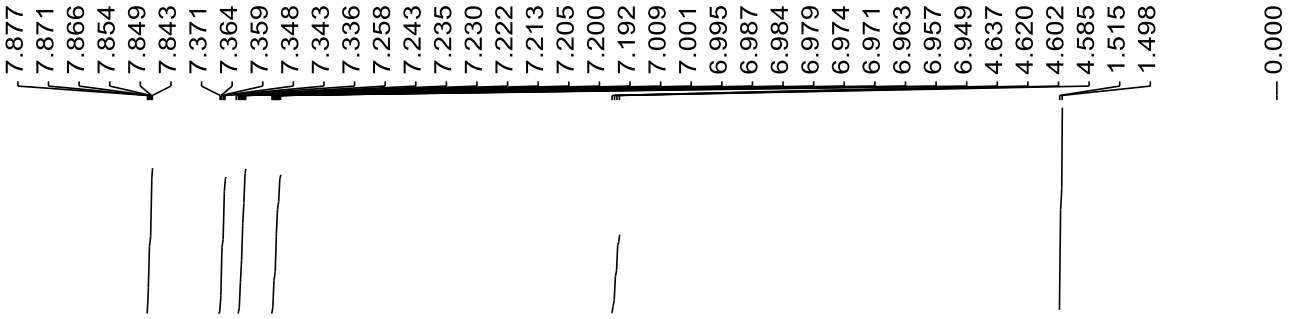

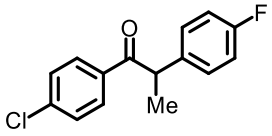

3t

^{1}H NMR (400 MHz, $CDCl_3$)

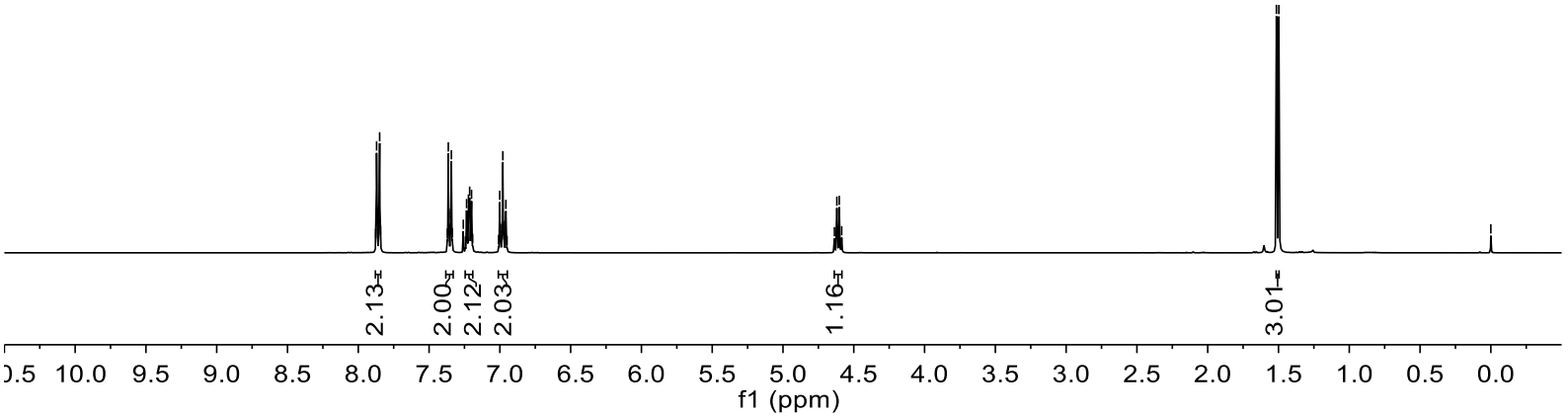

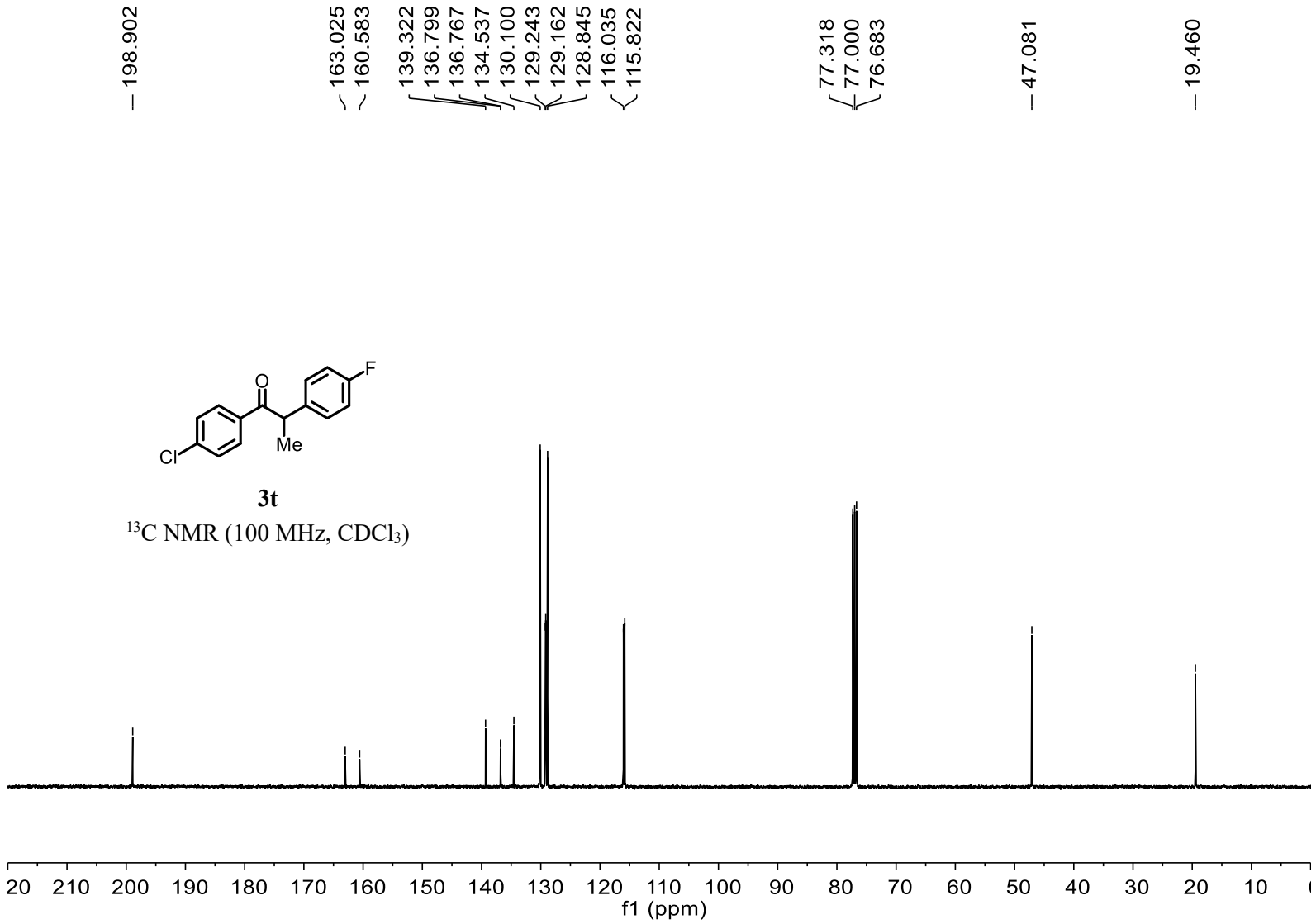

3t

^{13}C NMR (100 MHz, $CDCl_3$)

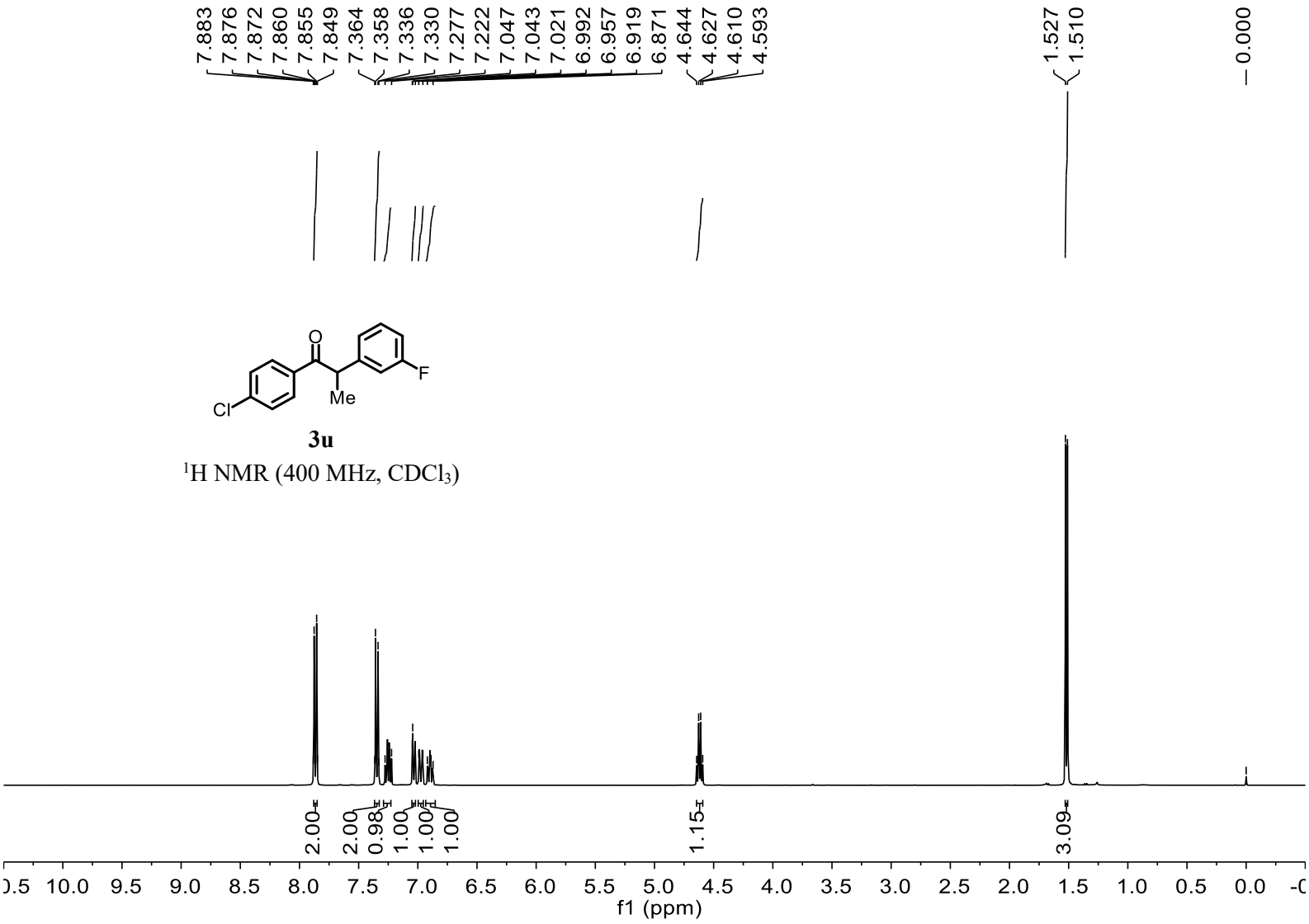

3u

^{1}H NMR (400 MHz, $CDCl_3$)

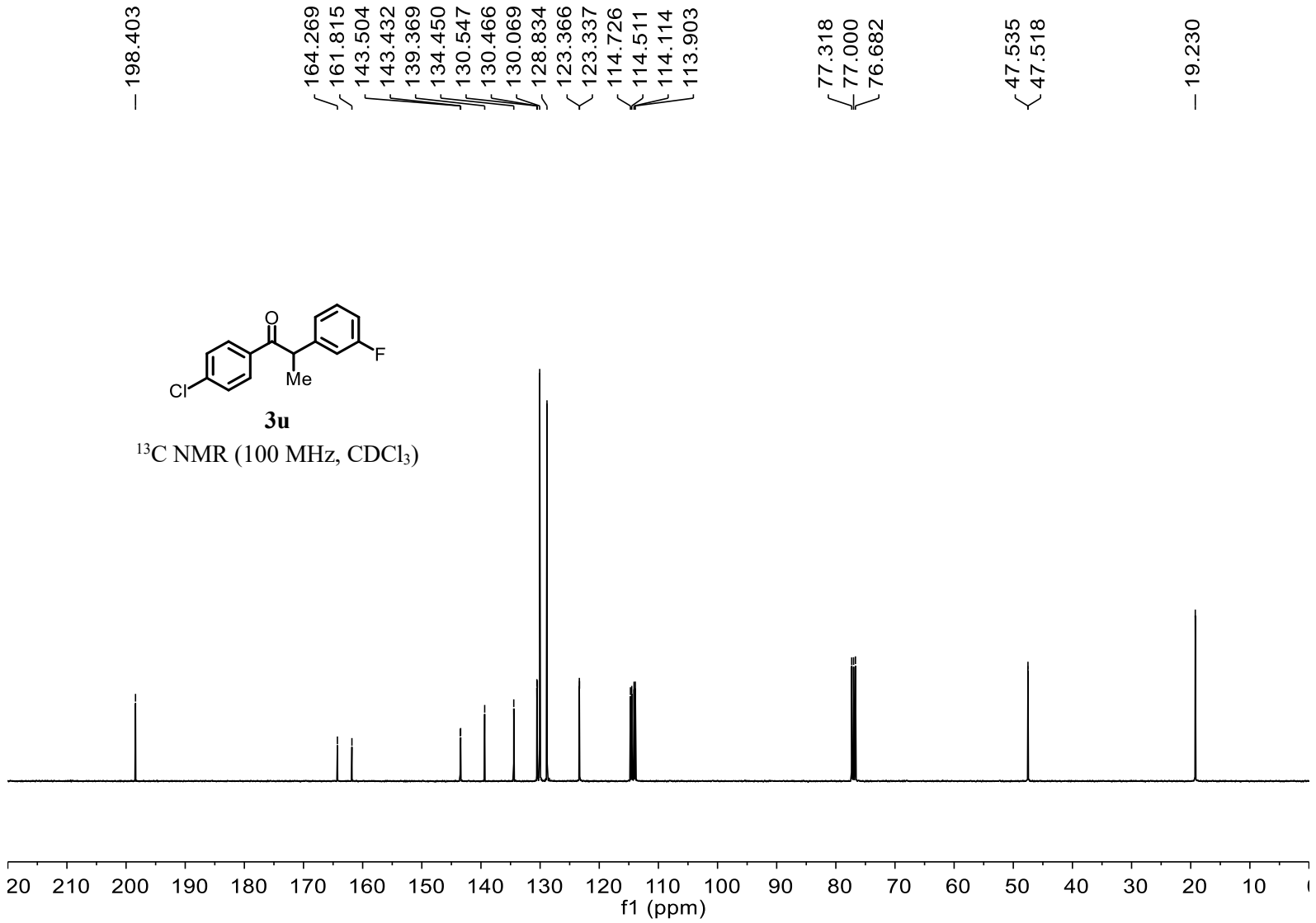
198.403
164.269
161.815
143.504
143.432
139.369
134.450
130.547
130.466
130.069
128.834
123.366
123.337
114.726
114.511
114.114
113.903
77.318
77.000
76.682
47.535
47.518
19.230
O
F
Cl
Me
3u
13C NMR (100 MHz, CDCl3)
20 210 200 190 180 170 160 150 140 130 120 110 100 90 80 70 60 50 40 30 20 10
f1 (ppm)

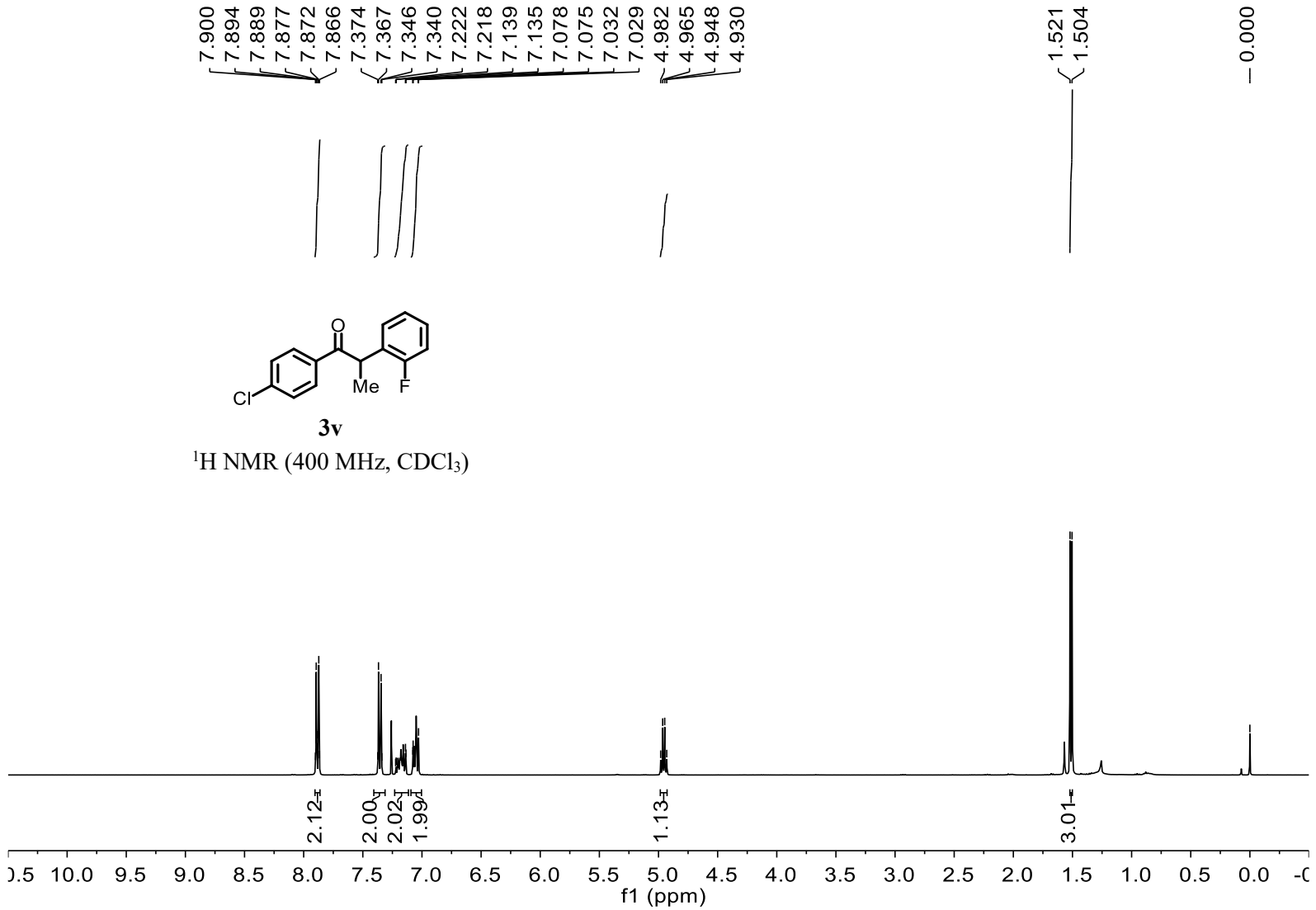

3v

^{1}H NMR (400 MHz, $CDCl_3$)

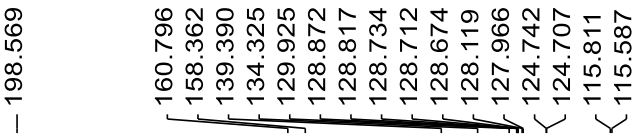

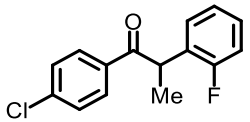

3v

^{13}C NMR (100 MHz, $CDCl_3$)

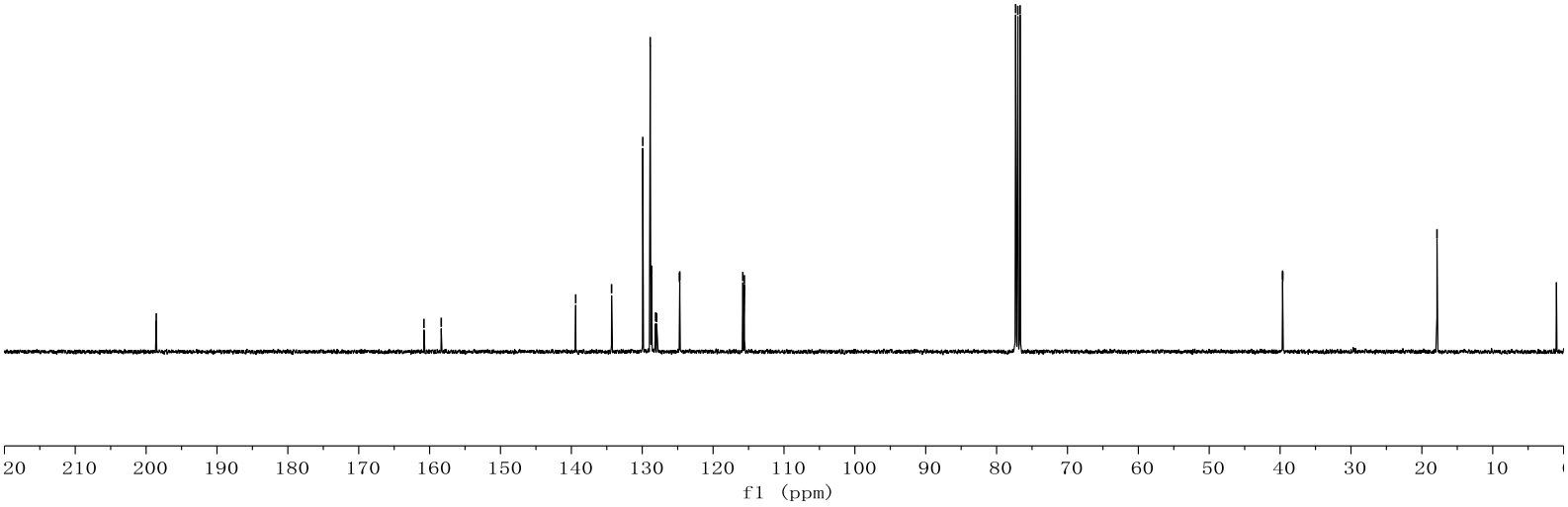

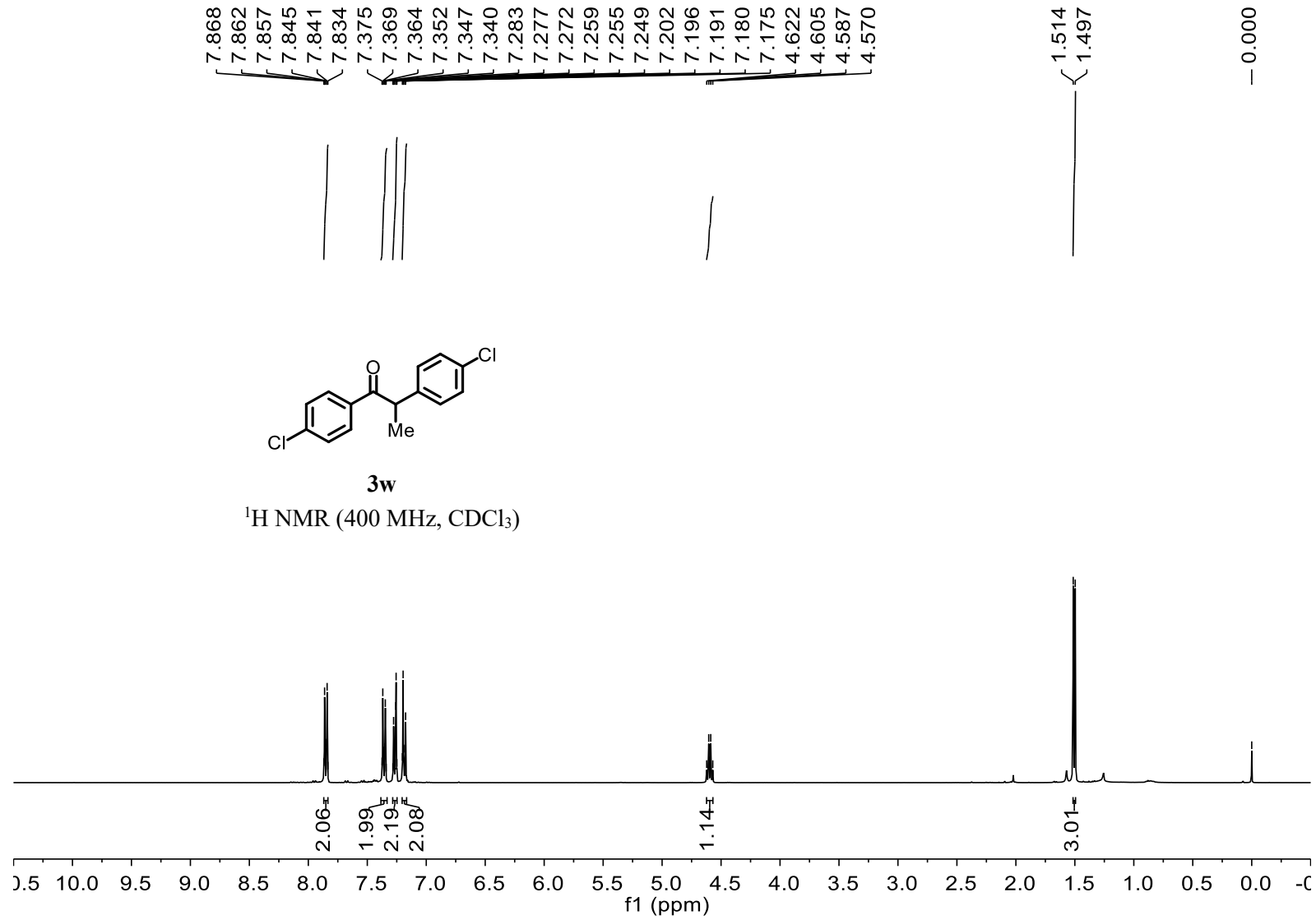

3w

^{1}H NMR (400 MHz, $CDCl_3$)

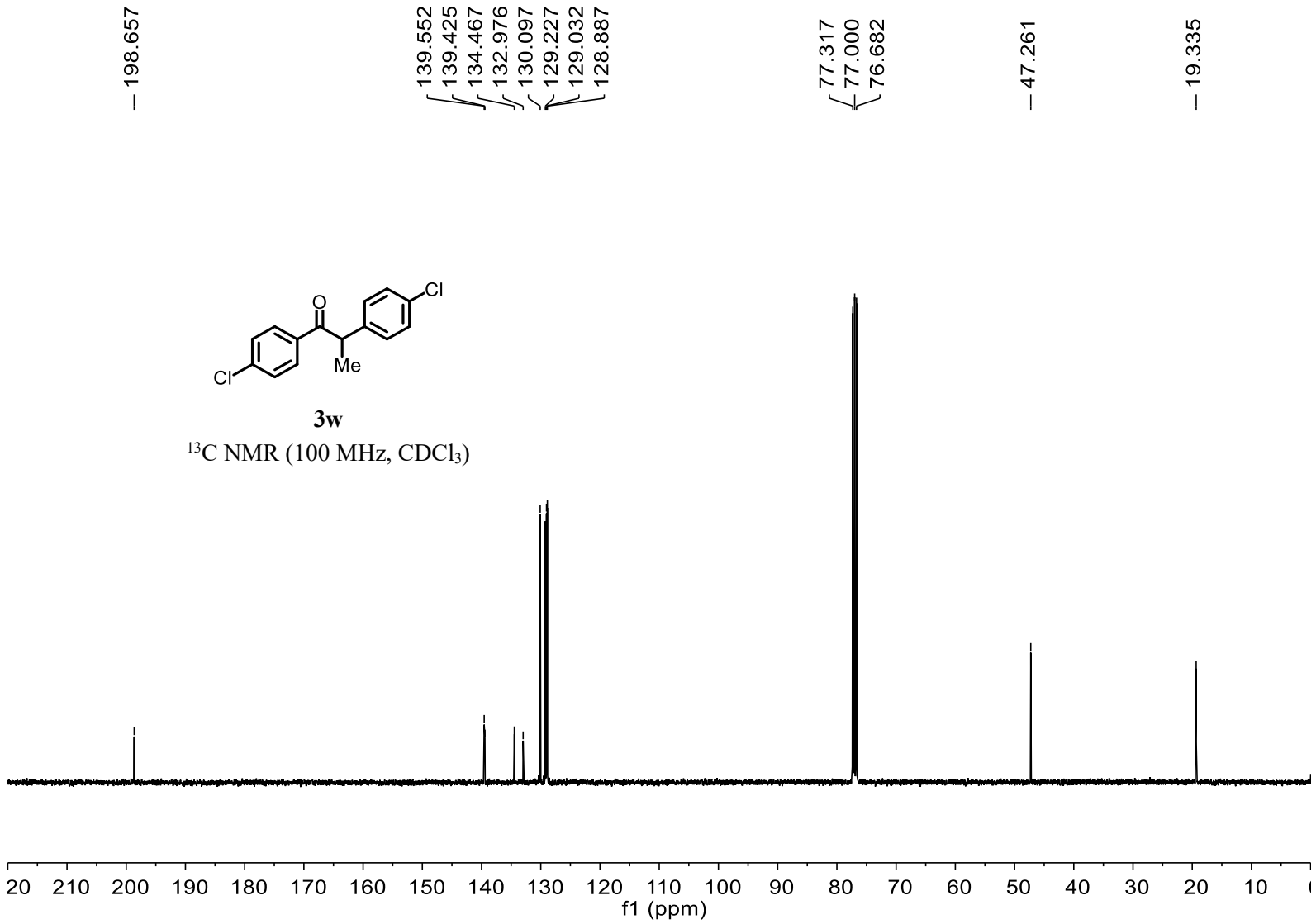

3w

^{13}C NMR (100 MHz, $CDCl_3$)

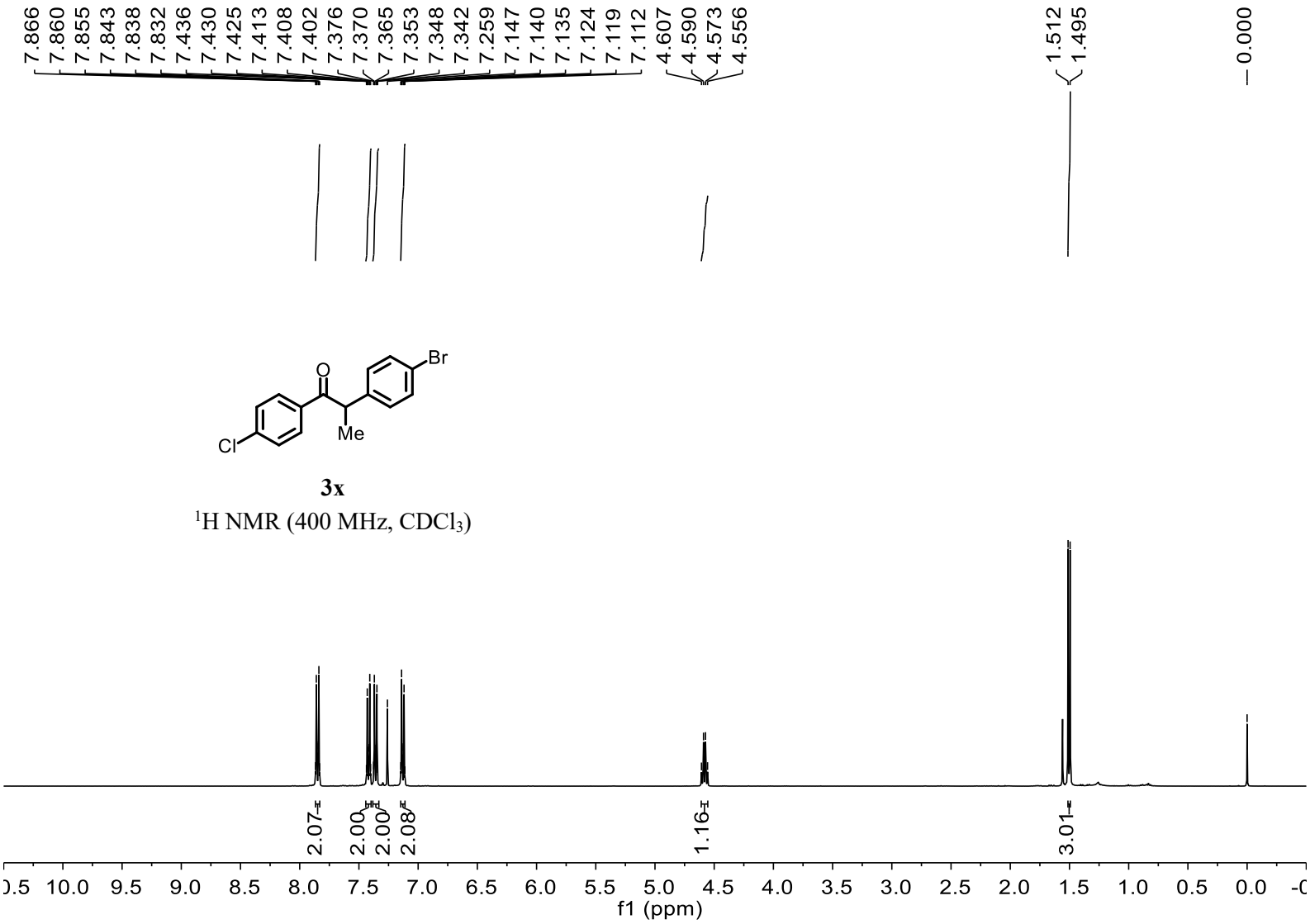

3x

^{1}H NMR (400 MHz, $CDCl_3$)

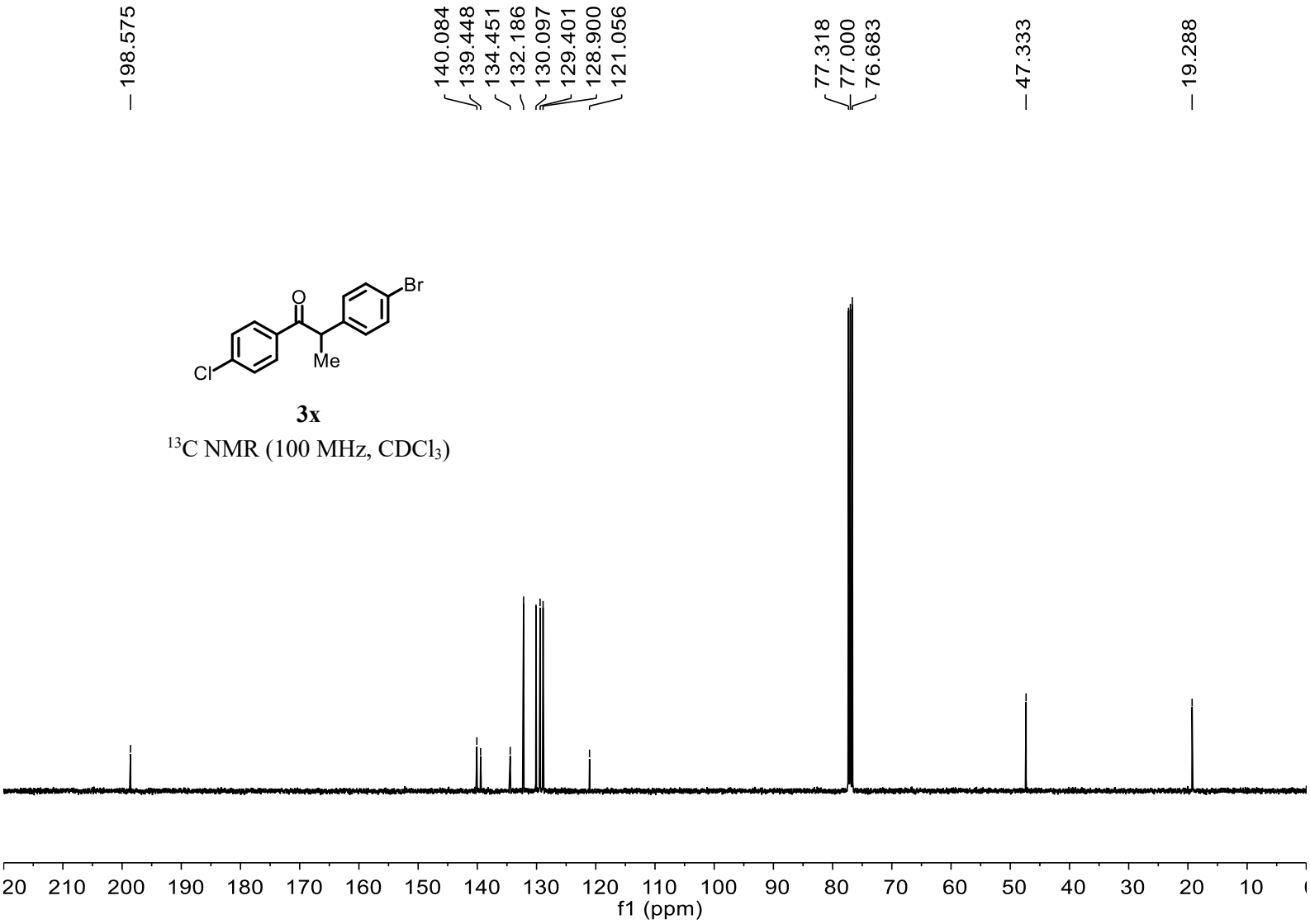

3x

^{13}C NMR (100 MHz, $CDCl_3$)

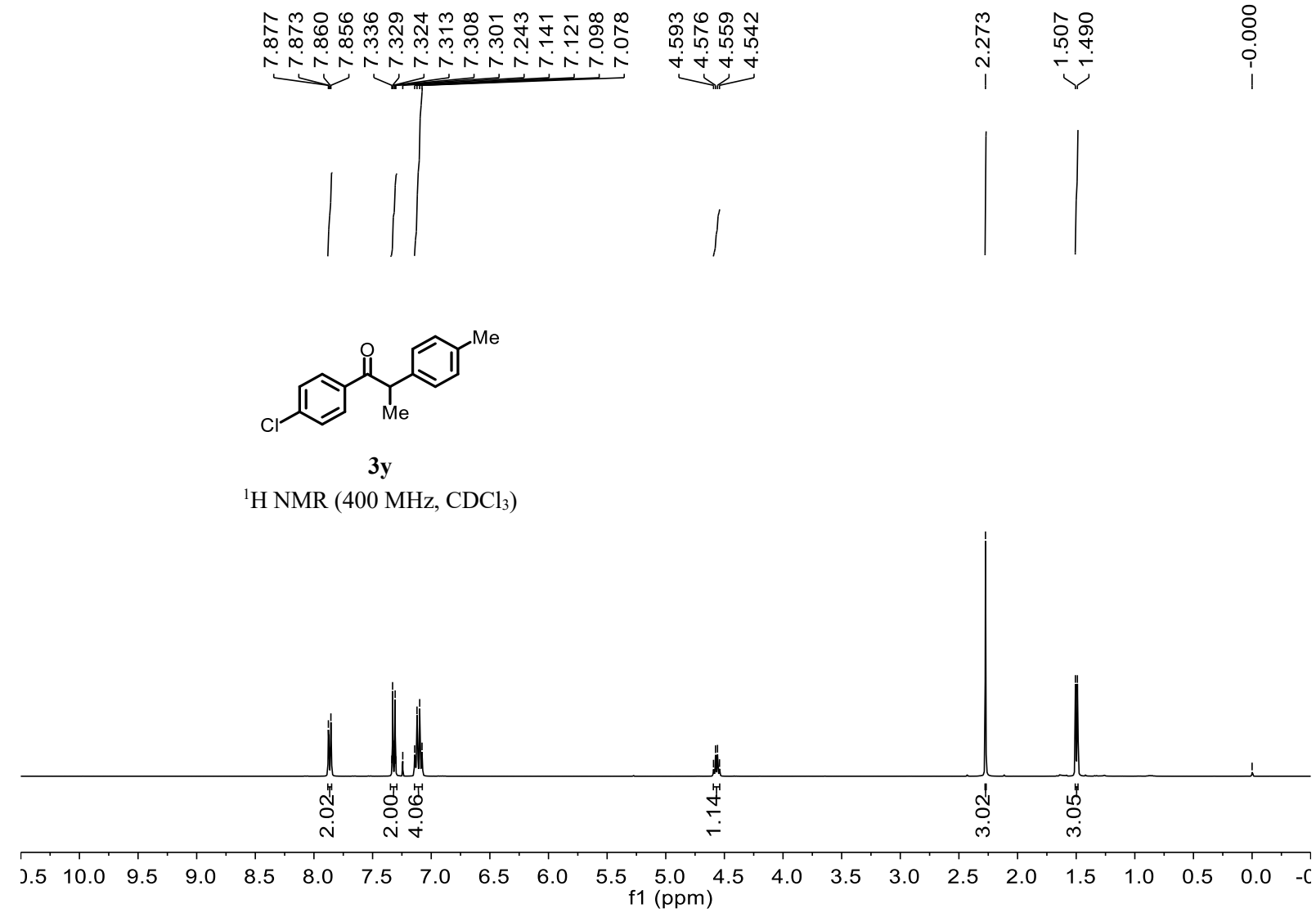

3y

^{1}H NMR (400 MHz, $CDCl_3$)

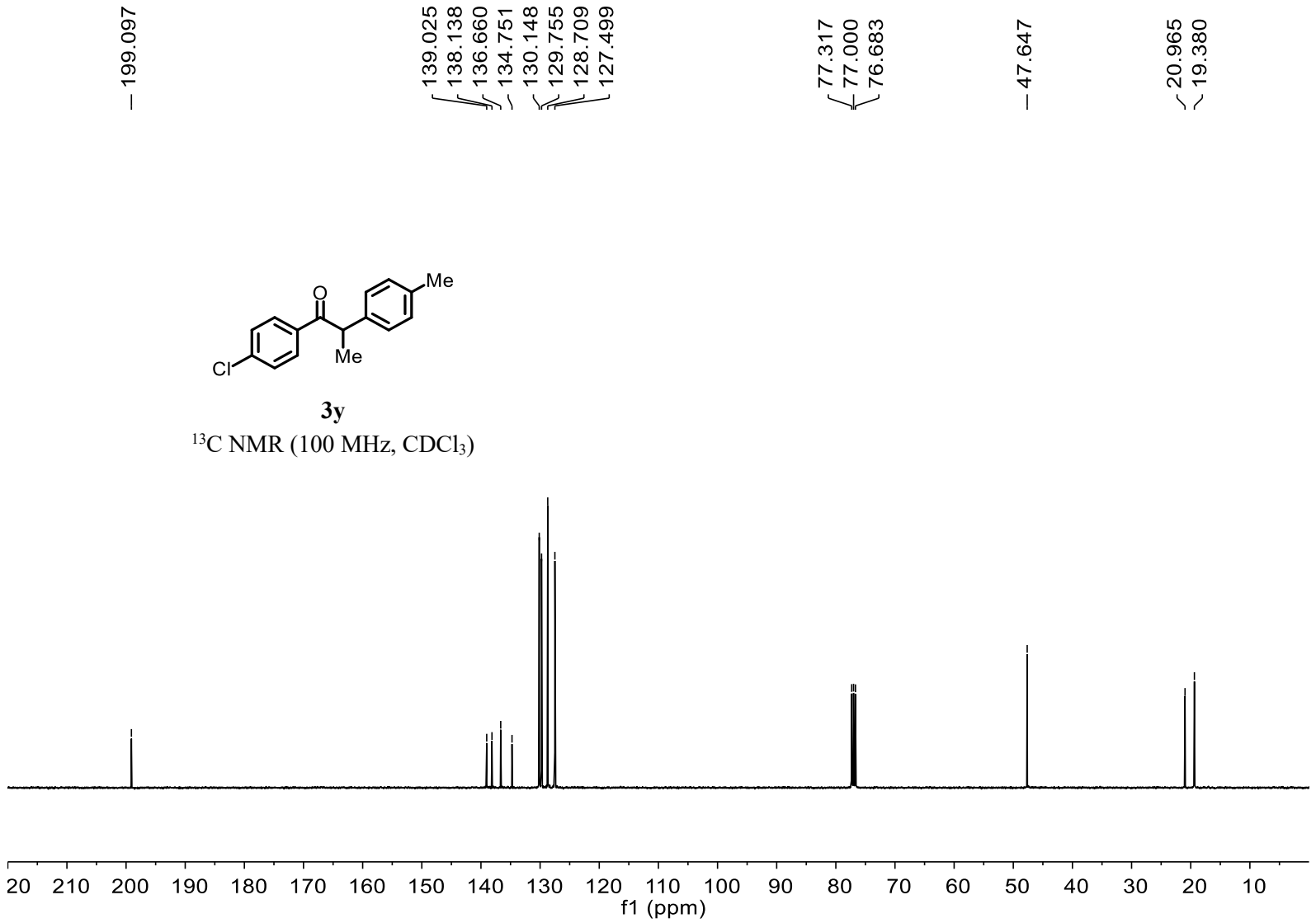

3y

^{13}C NMR (100 MHz, $CDCl_3$)

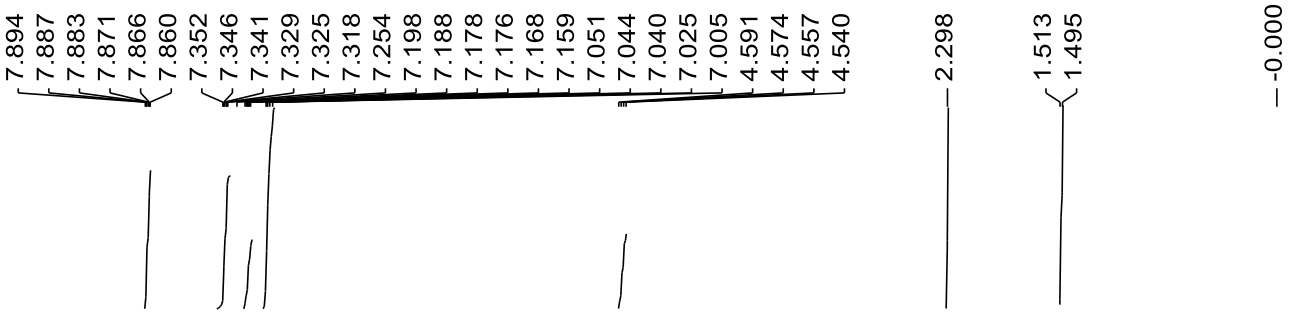

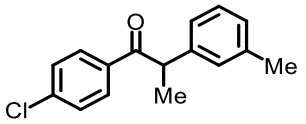

3z

^{1}H NMR (400 MHz, $CDCl_3$)

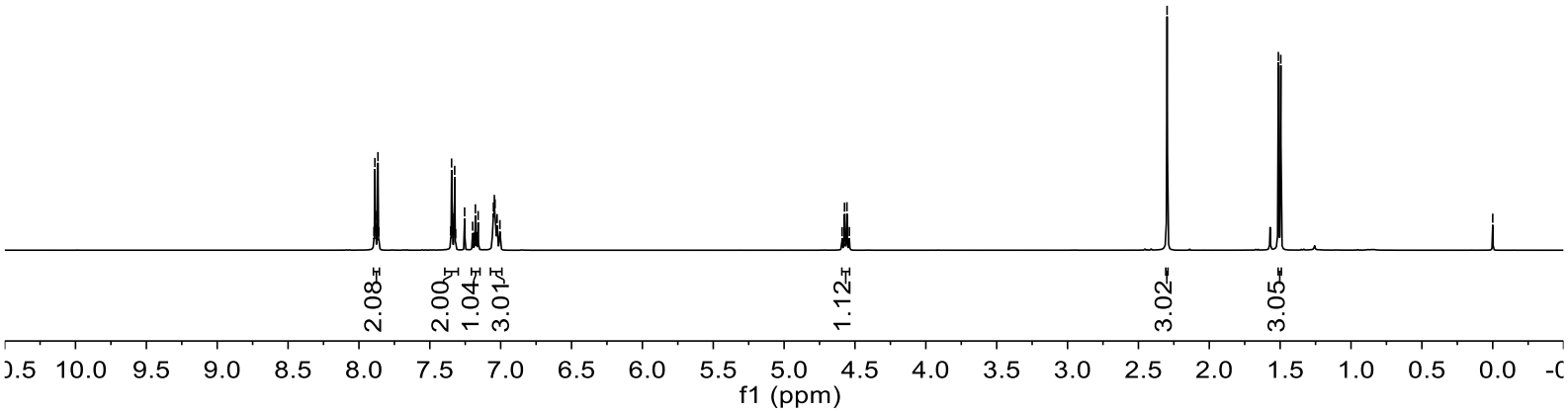

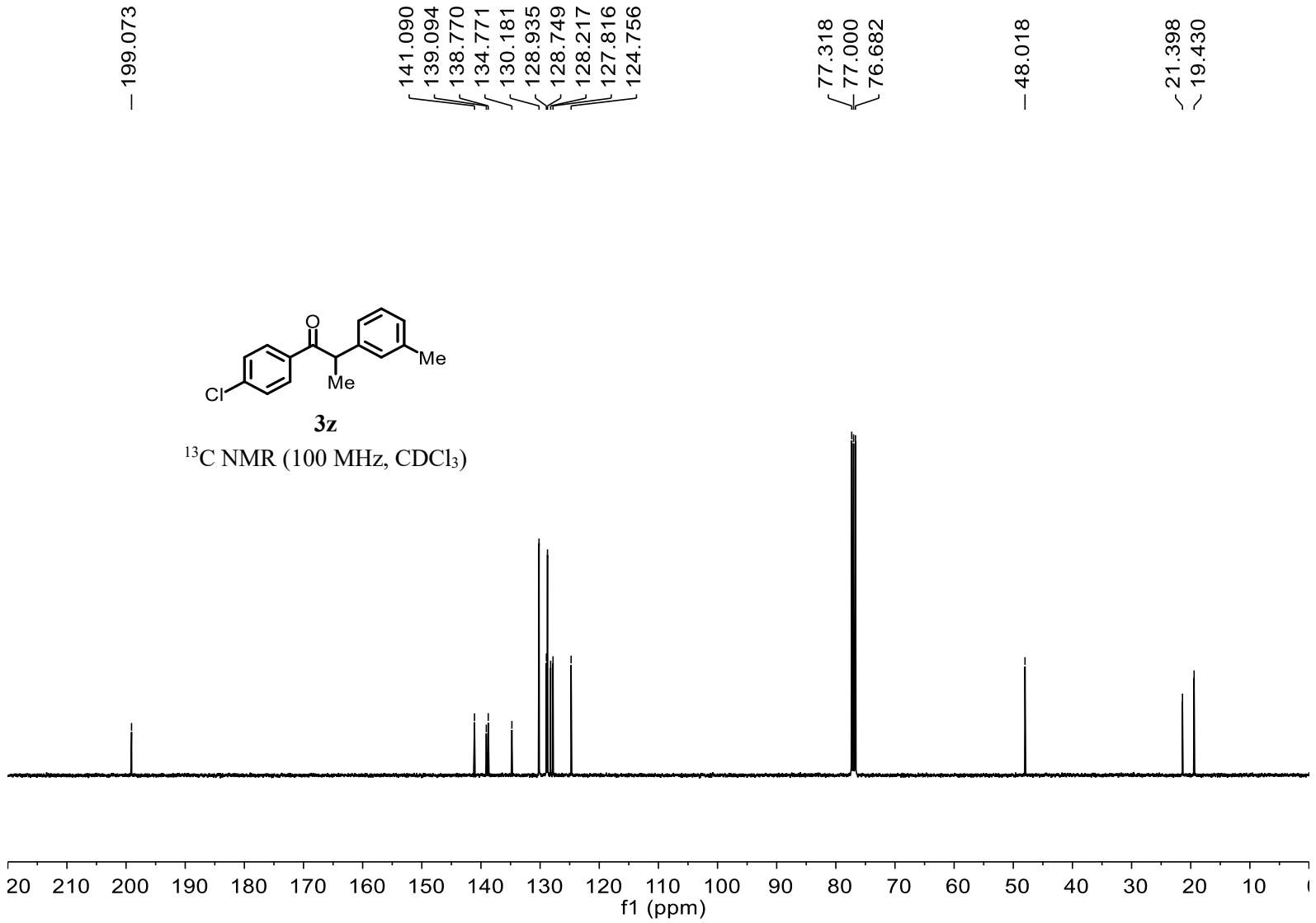
199.073
141.090
139.094
138.770
134.771
130.181
128.935
128.749
128.217
127.816
124.756
77.318
77.000
76.682
48.018
21.398
19.430
O
Me
Me
Cl
3z
13C NMR (100 MHz, CDCl3)
20 210 200 190 180 170 160 150 140 130 120 110 100 90 80 70 60 50 40 30 20 10
f1 (ppm)

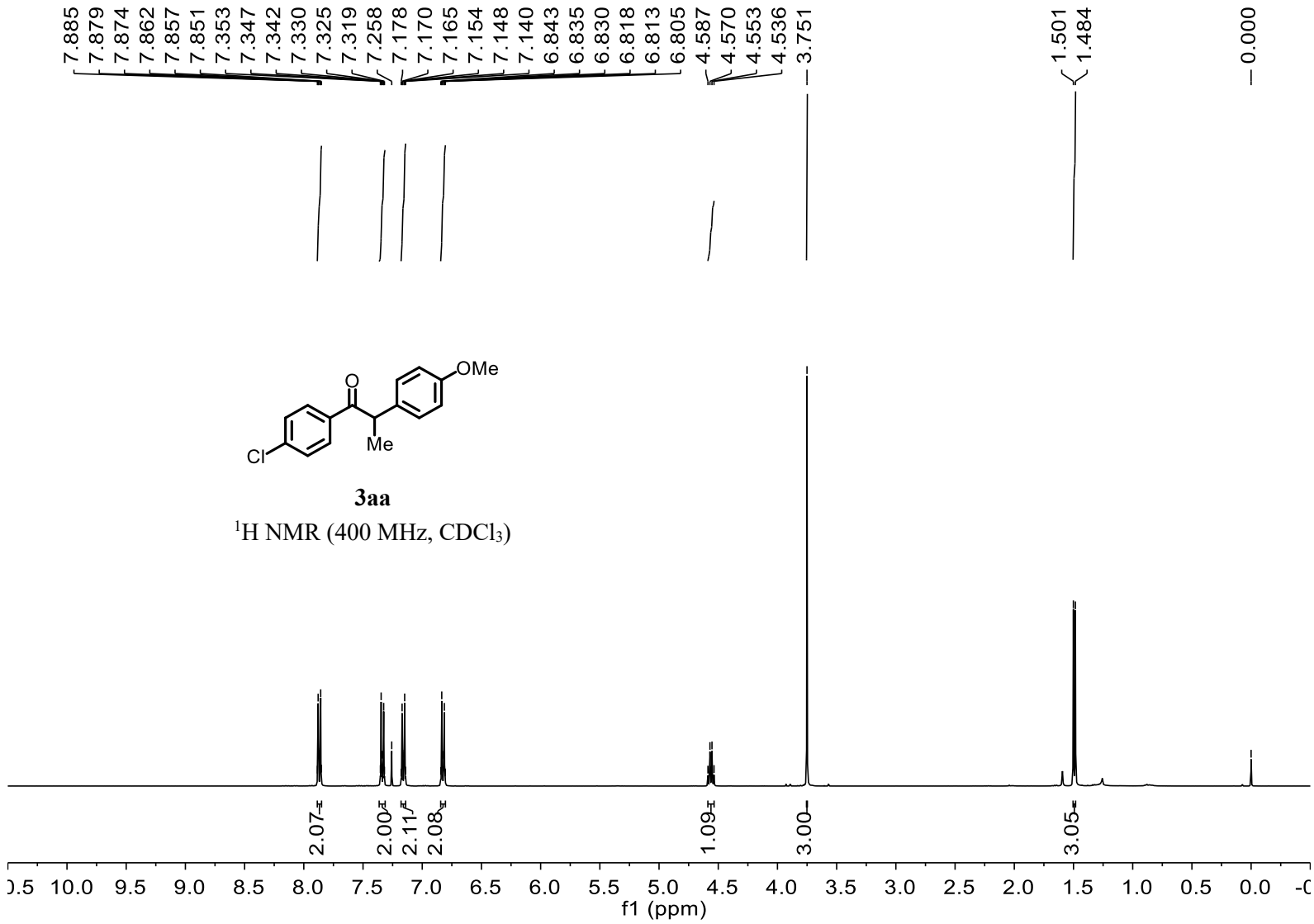

3aa

^{1}H NMR (400 MHz, $CDCl_3$)

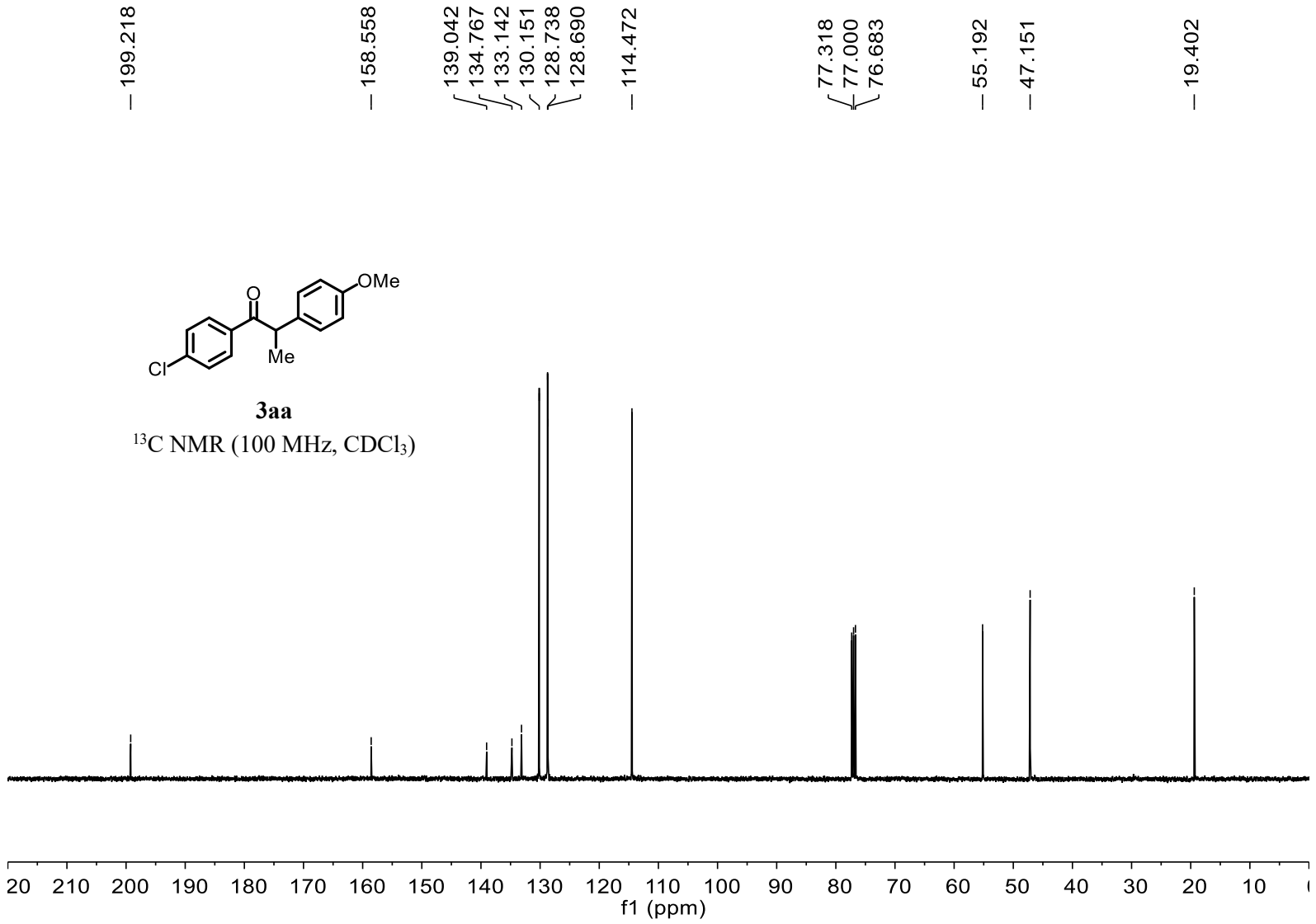
199.218
158.558
139.042
134.767
133.142
130.151
128.738
128.690
114.472
77.318
77.000
76.683
55.192
47.151
19.402
OMe
O
Me
Cl
3aa
13C NMR (100 MHz, CDCl3)
20 210 200 190 180 170 160 150 140 130 120 110 100 90 80 70 60 50 40 30 20 10
f1 (ppm)

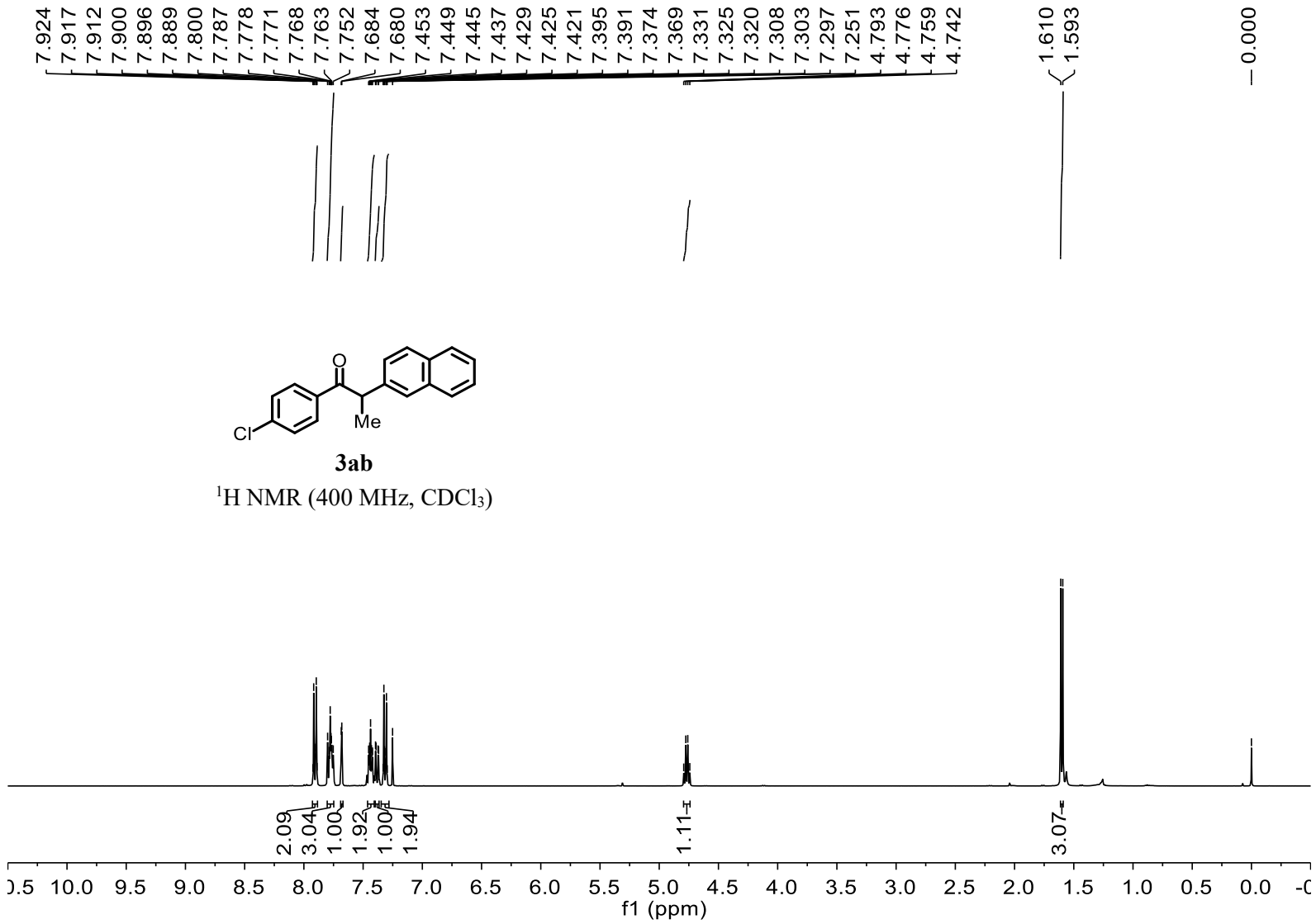

3ab

^{1}H NMR (400 MHz, $CDCl_3$)

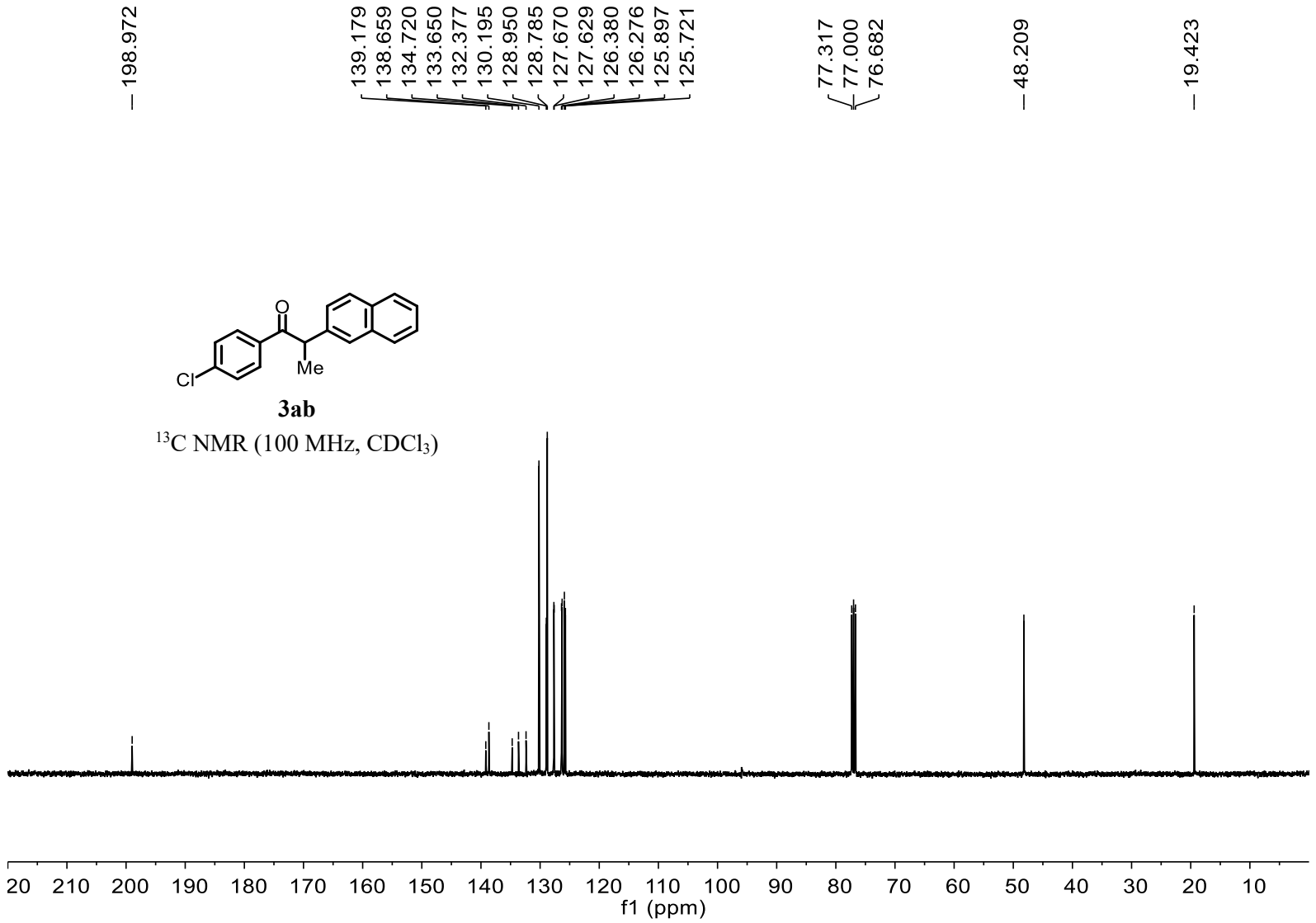
198.972
139.179
138.659
134.720
133.650
132.377
130.195
128.950
128.785
127.670
127.629
126.380
126.276
125.897
125.721
77.317
77.000
76.682
48.209
19.423
O
Cl
Me
3ab
13C NMR (100 MHz, CDCl3)
20 210 200 190 180 170 160 150 140 130 120 110 100 90 80 70 60 50 40 30 20 10
f1 (ppm)

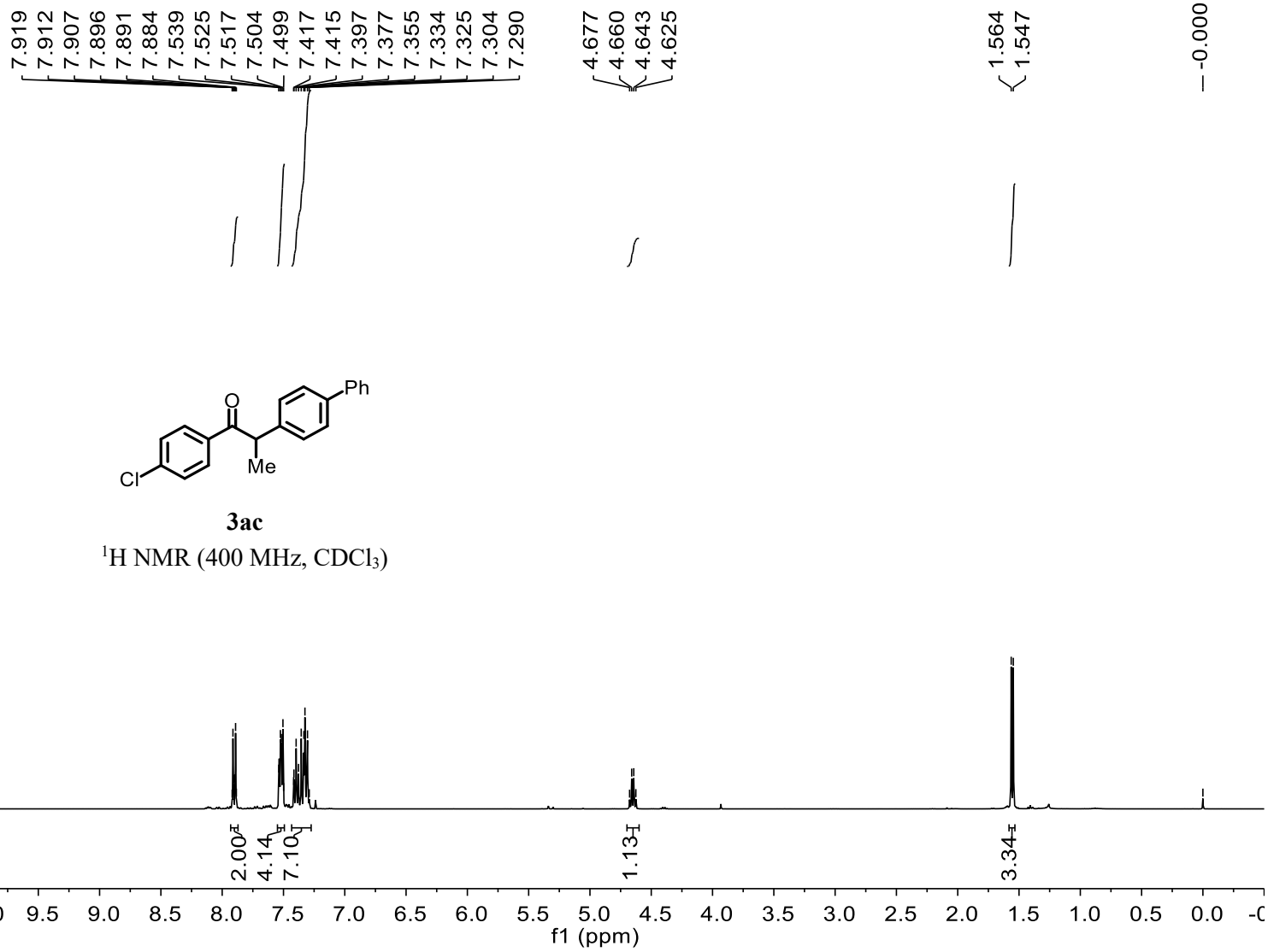

3ac

^{1}H NMR (400 MHz, $CDCl_3$)

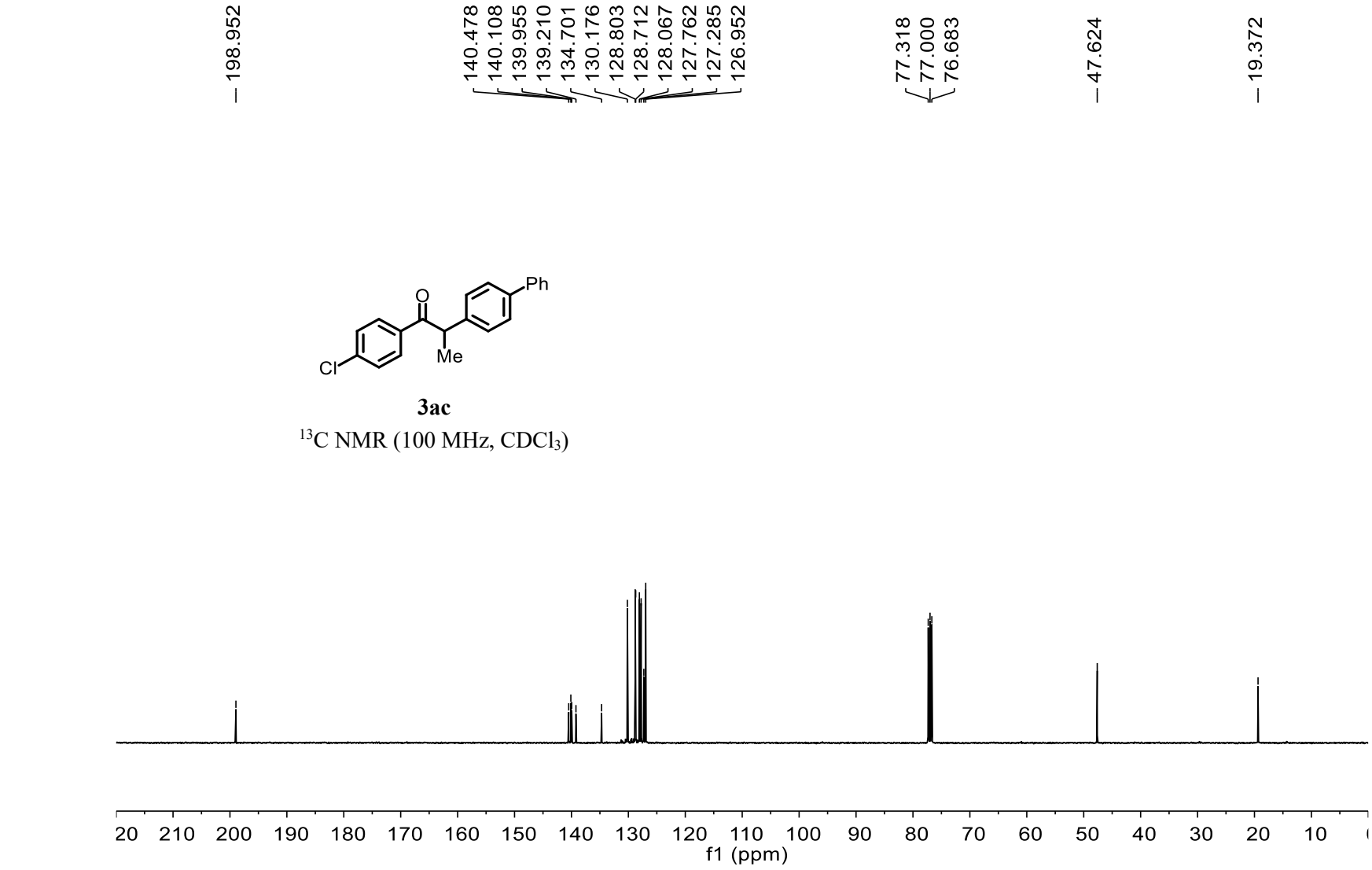

3ac

^{13}C NMR (100 MHz, $CDCl_3$)

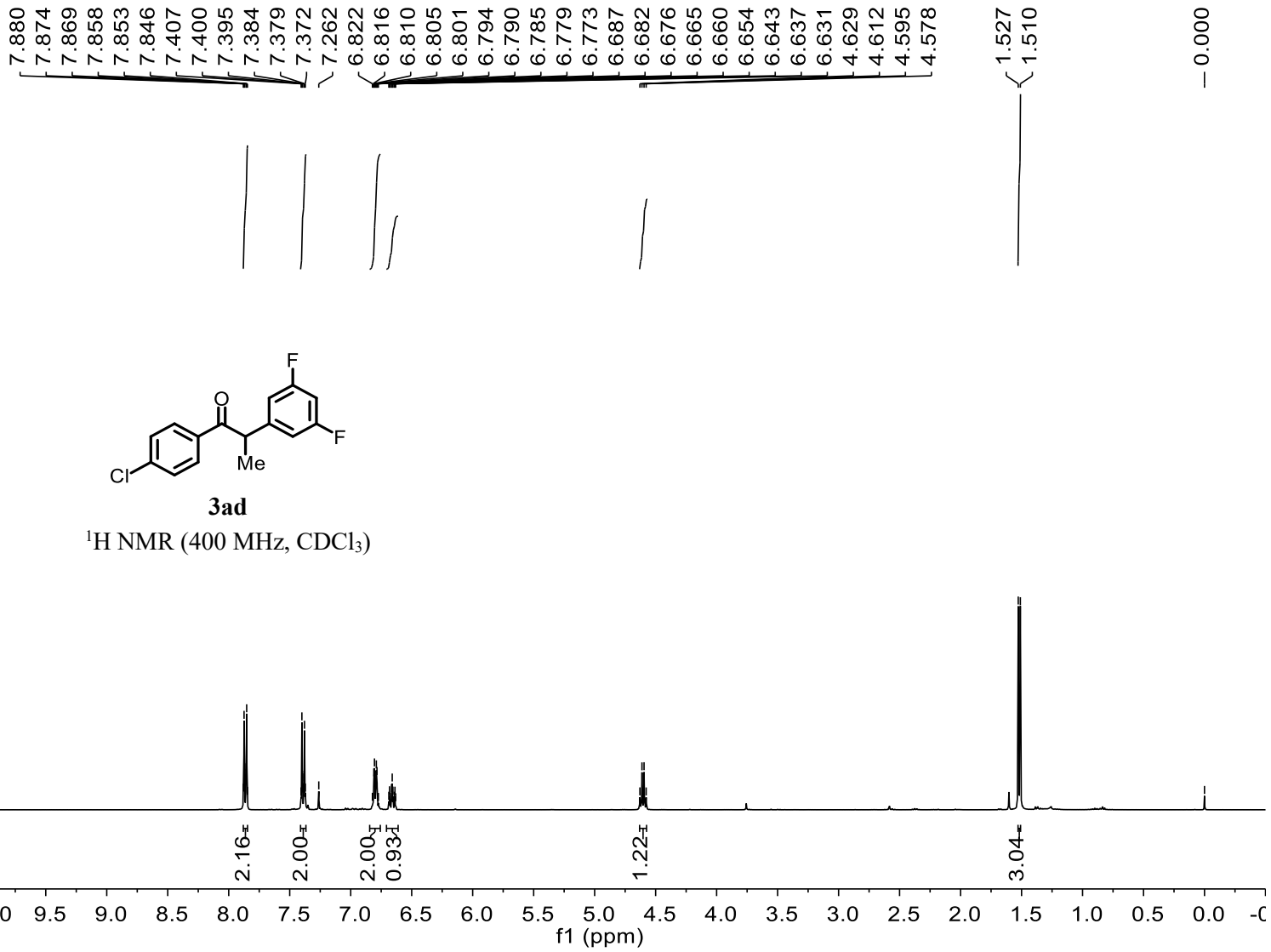

3ad

^{1}H NMR (400 MHz, $CDCl_3$)

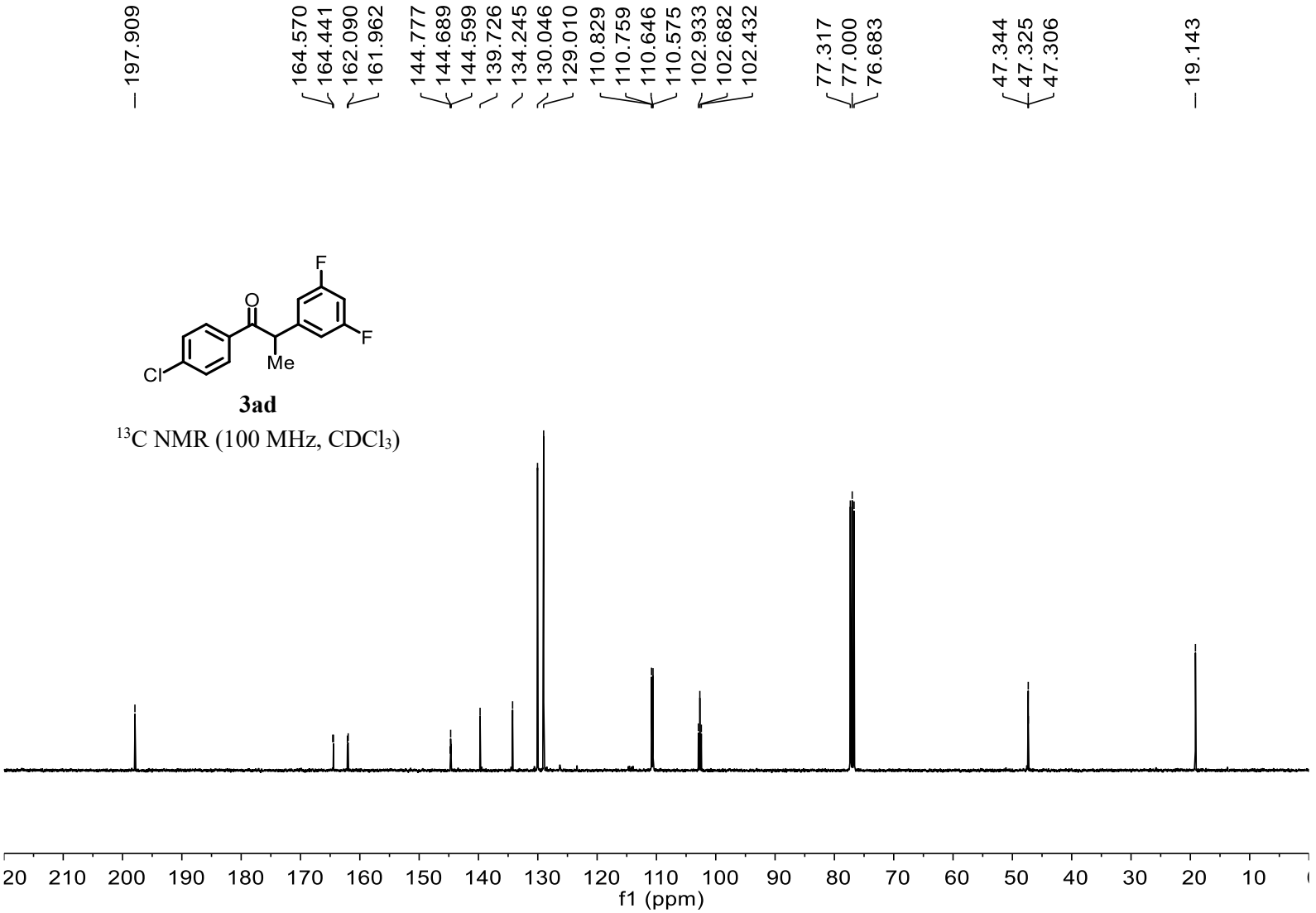

3ad

^{13}C NMR (100 MHz, $CDCl_3$)

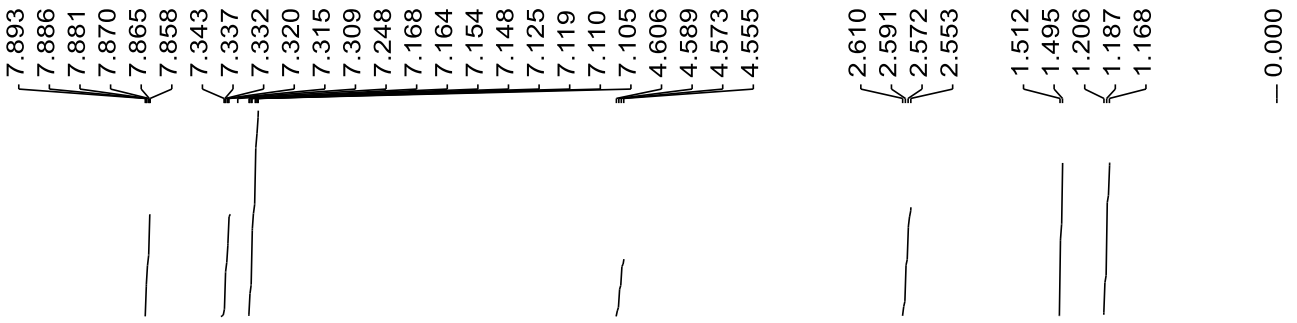

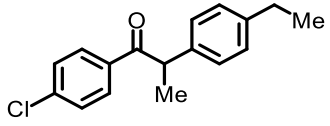

3ae

^{1}H NMR (400 MHz, $CDCl_3$)

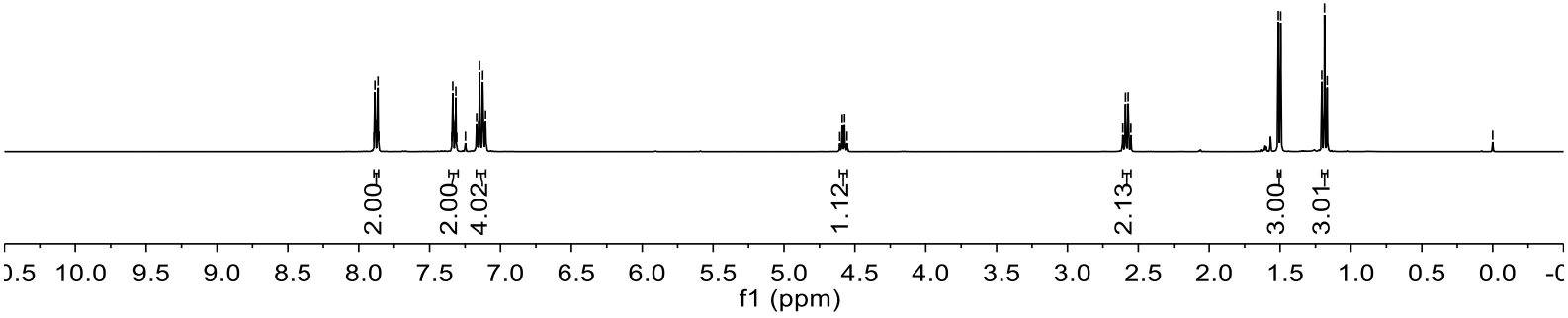

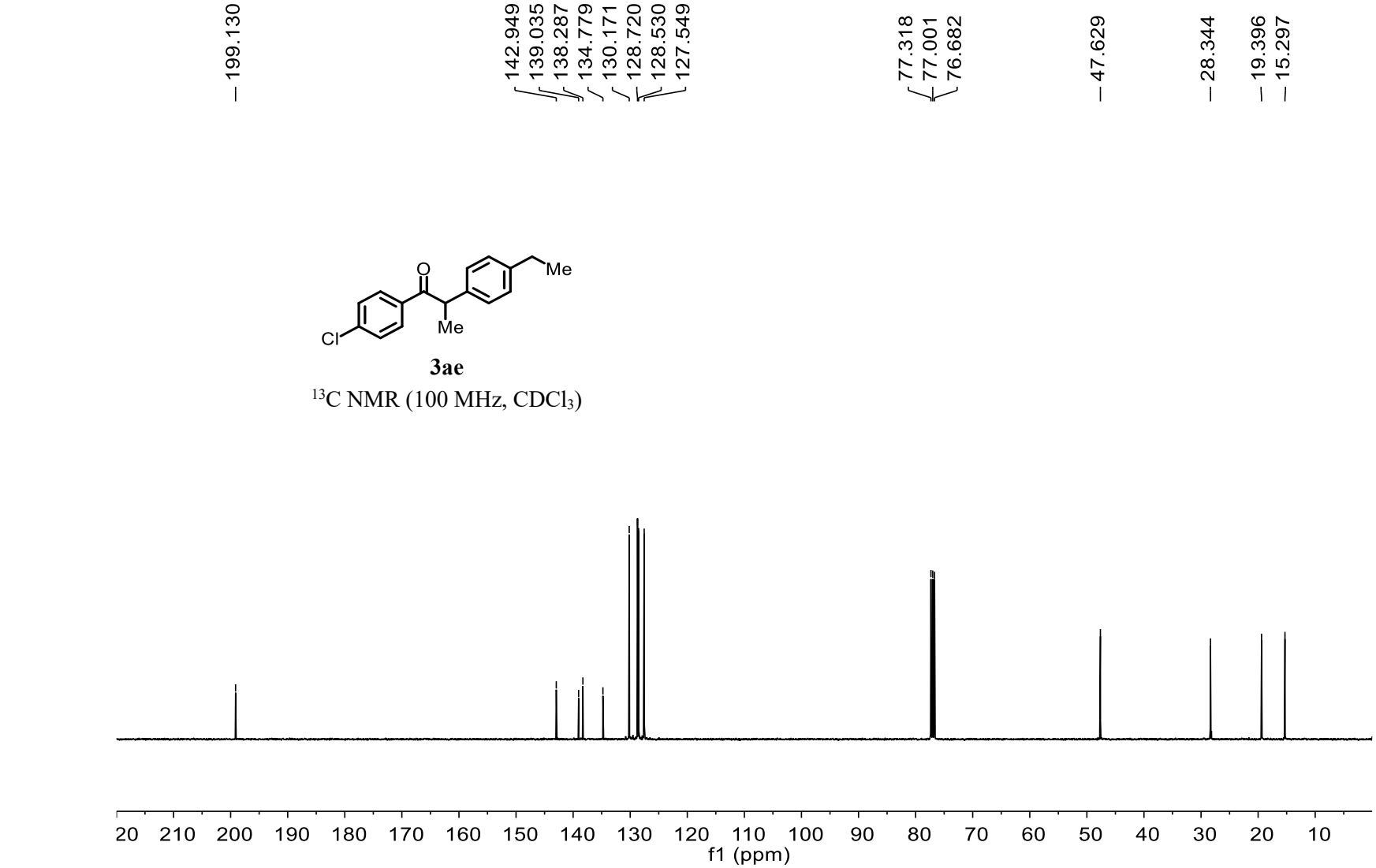

3ae

^{13}C NMR (100 MHz, $CDCl_3$)

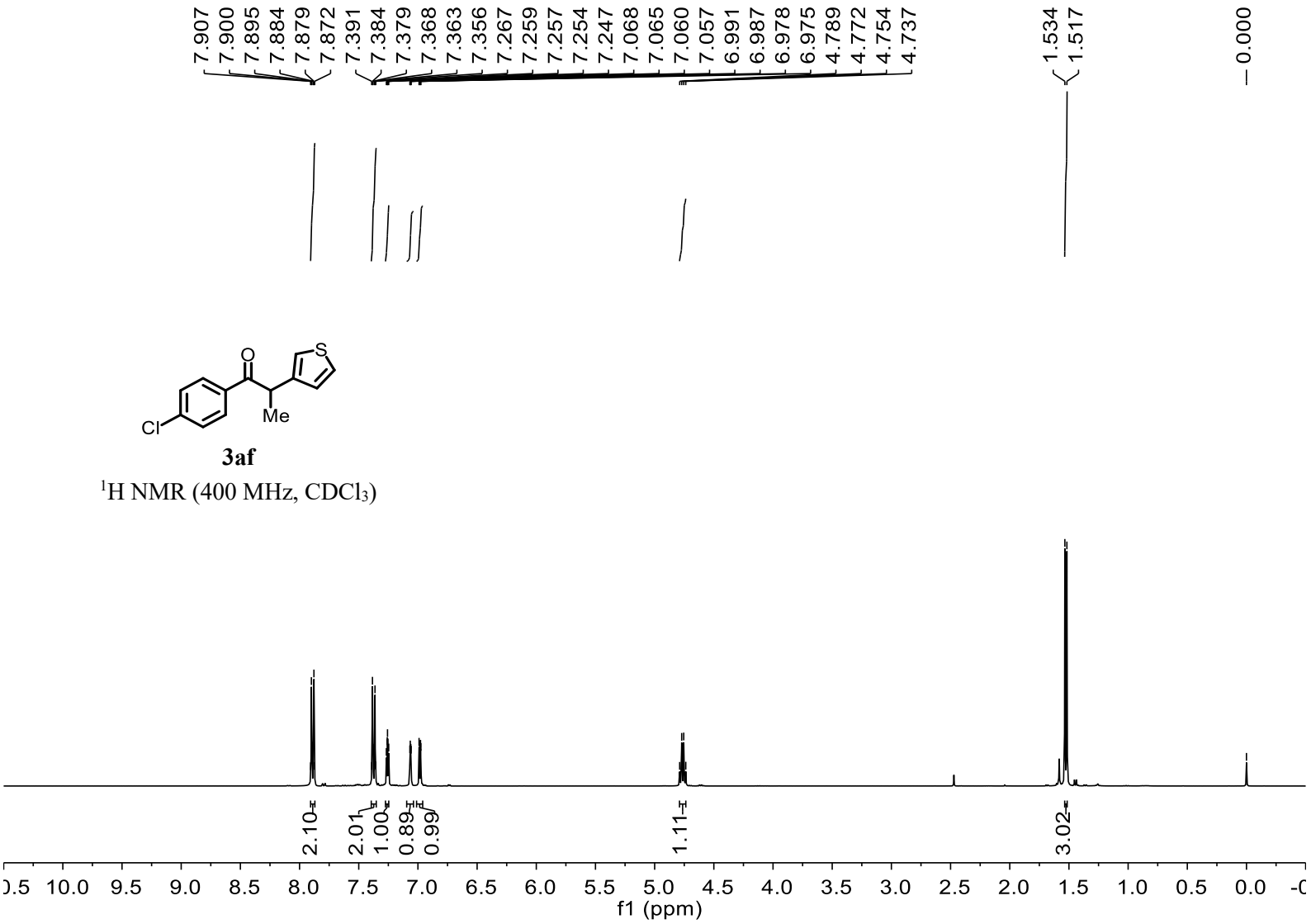

3af

^{1}H NMR (400 MHz, $CDCl_3$)

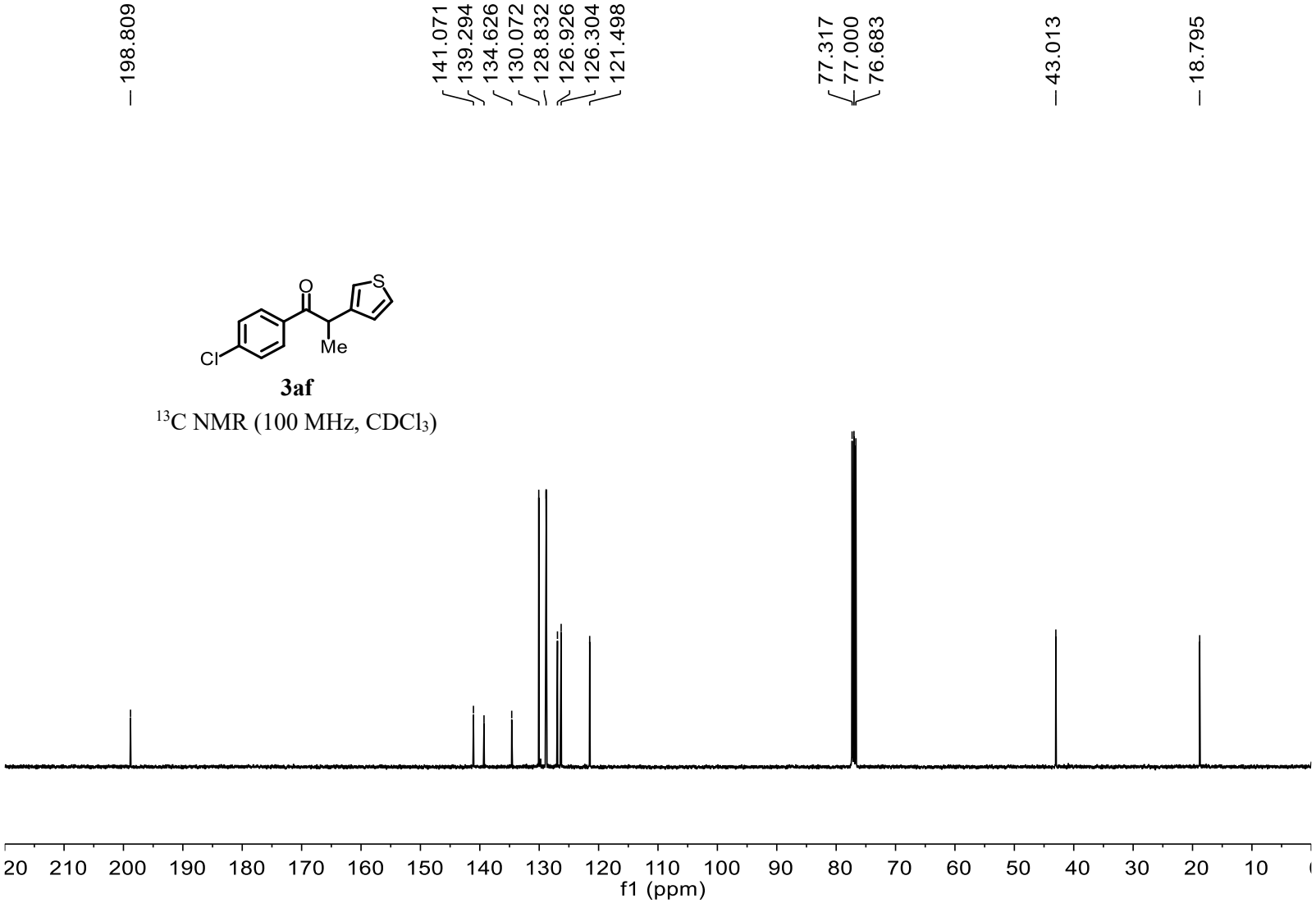

3af

^{13}C NMR (100 MHz, $CDCl_3$)

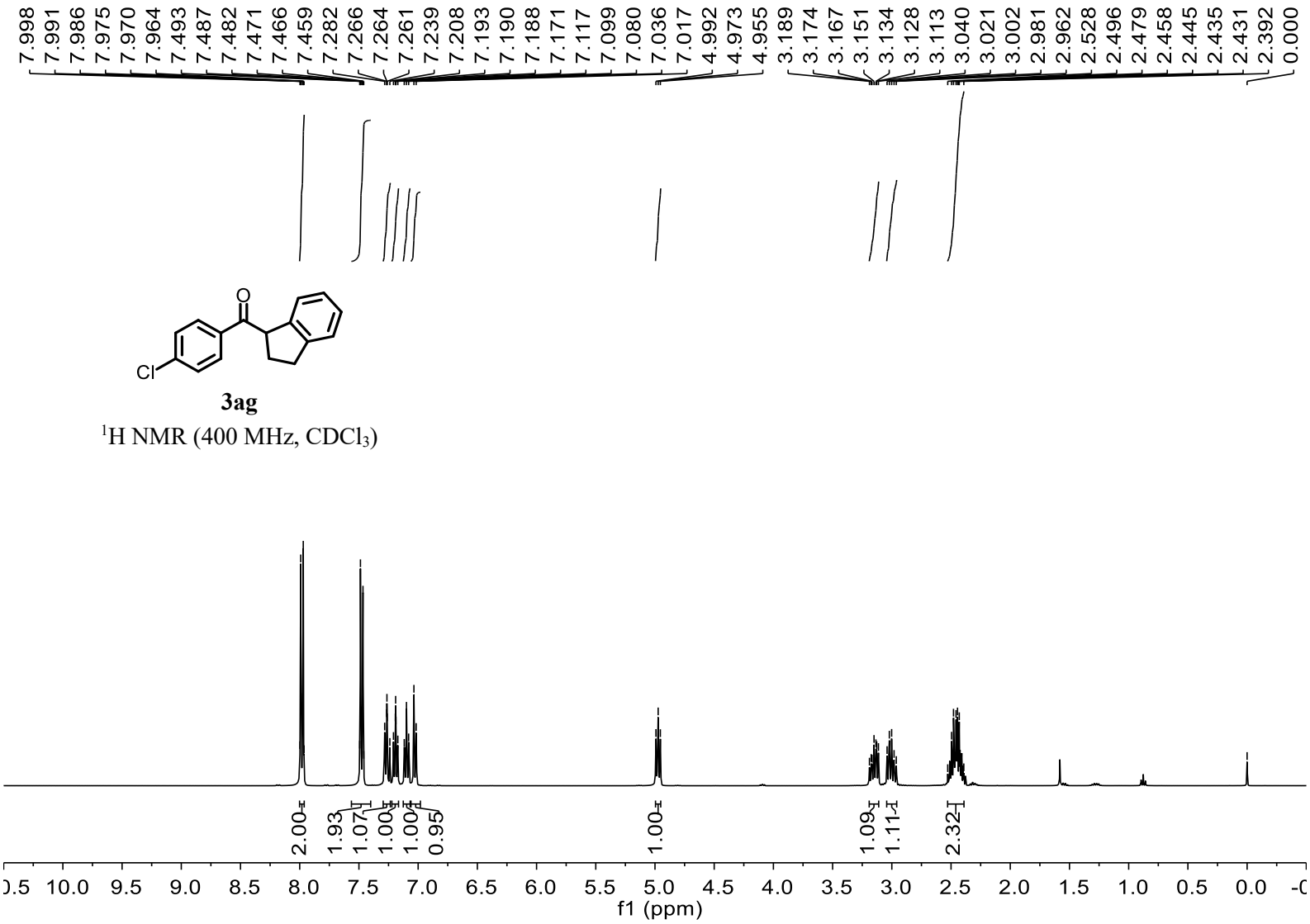

3ag

^{1}H NMR (400 MHz, $CDCl_3$)

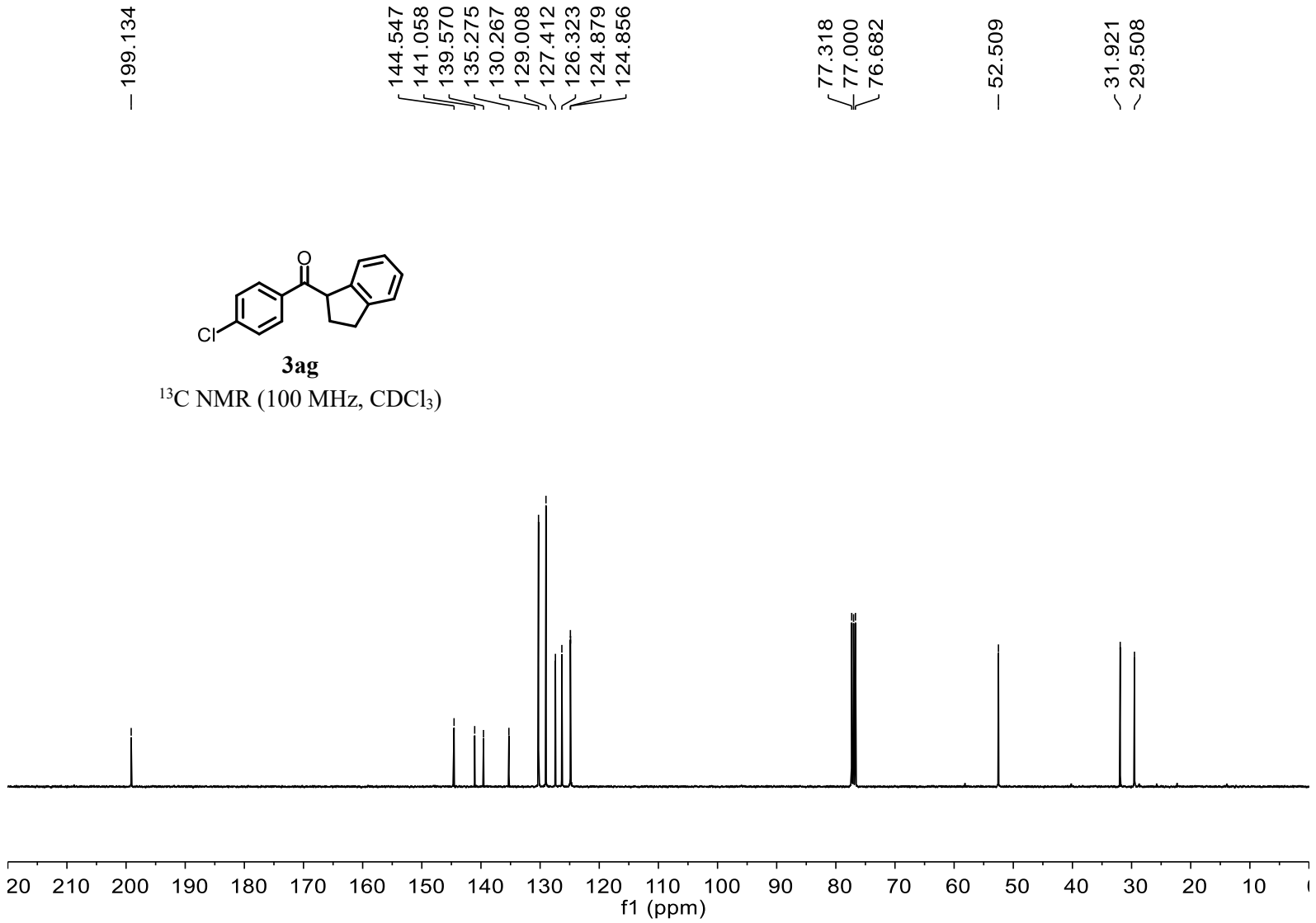

3ag

^{13}C NMR (100 MHz, $CDCl_3$)

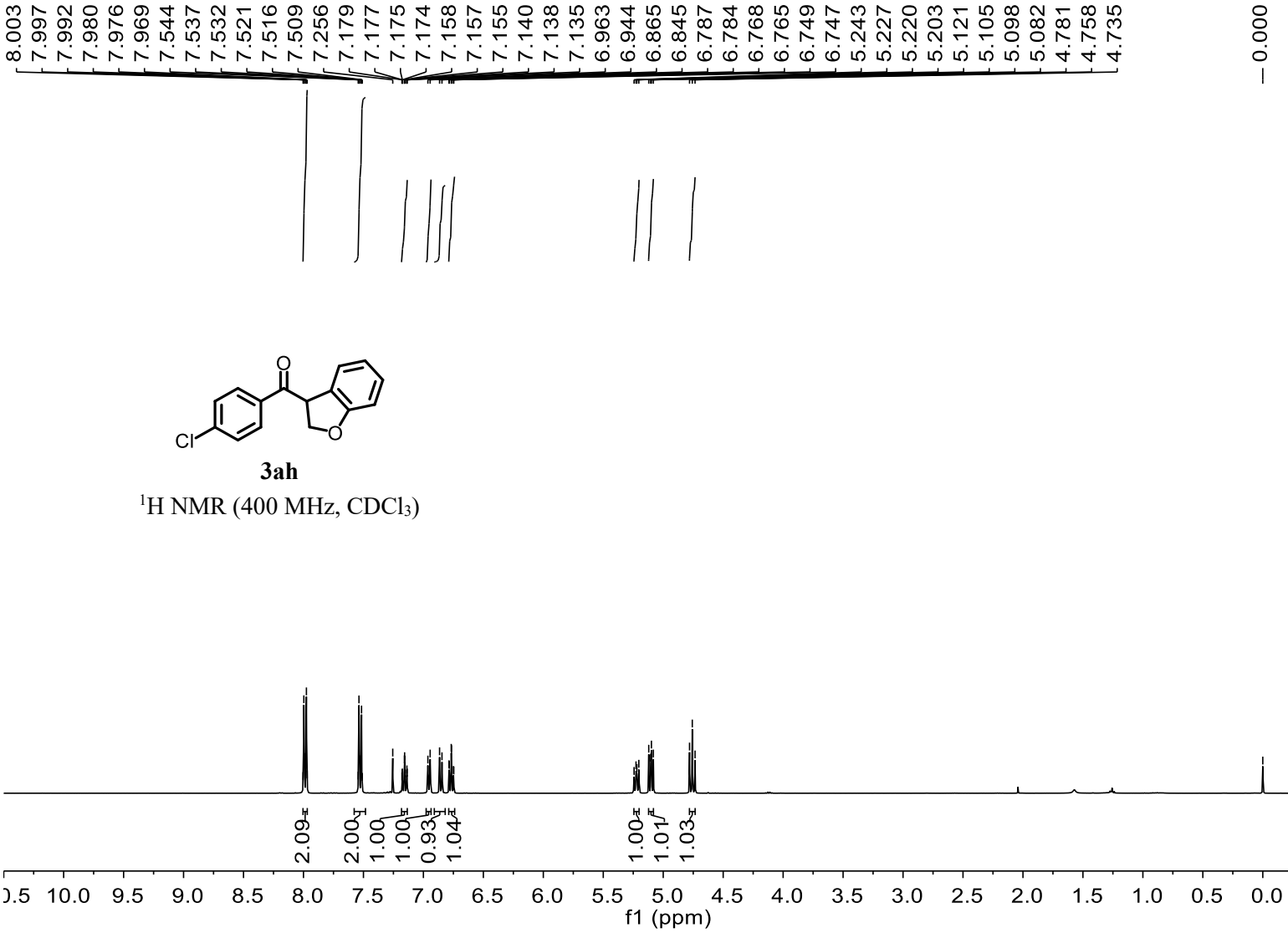

3ah

^{1}H NMR (400 MHz, $CDCl_3$)

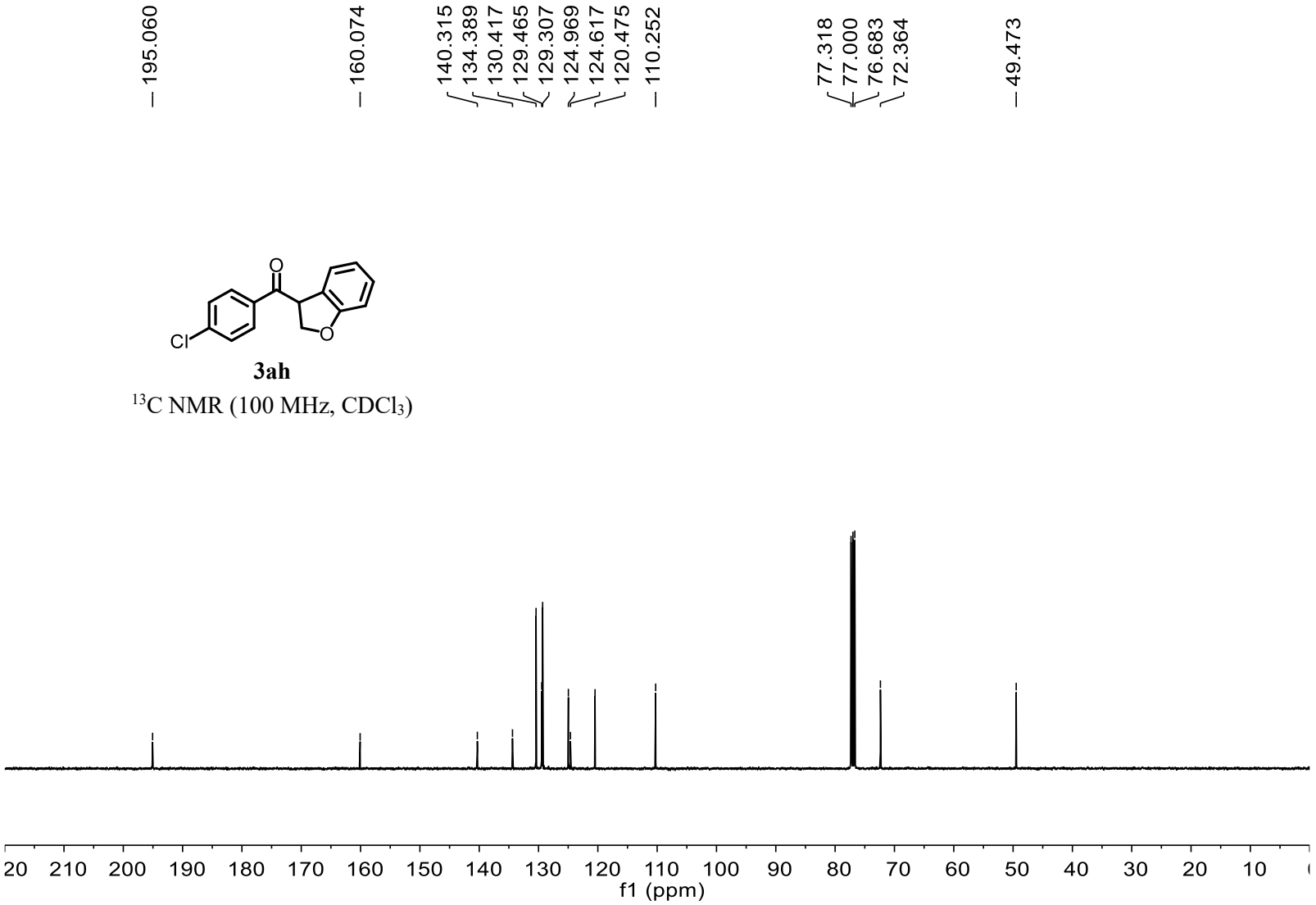

3ah

^{13}C NMR (100 MHz, $CDCl_3$)

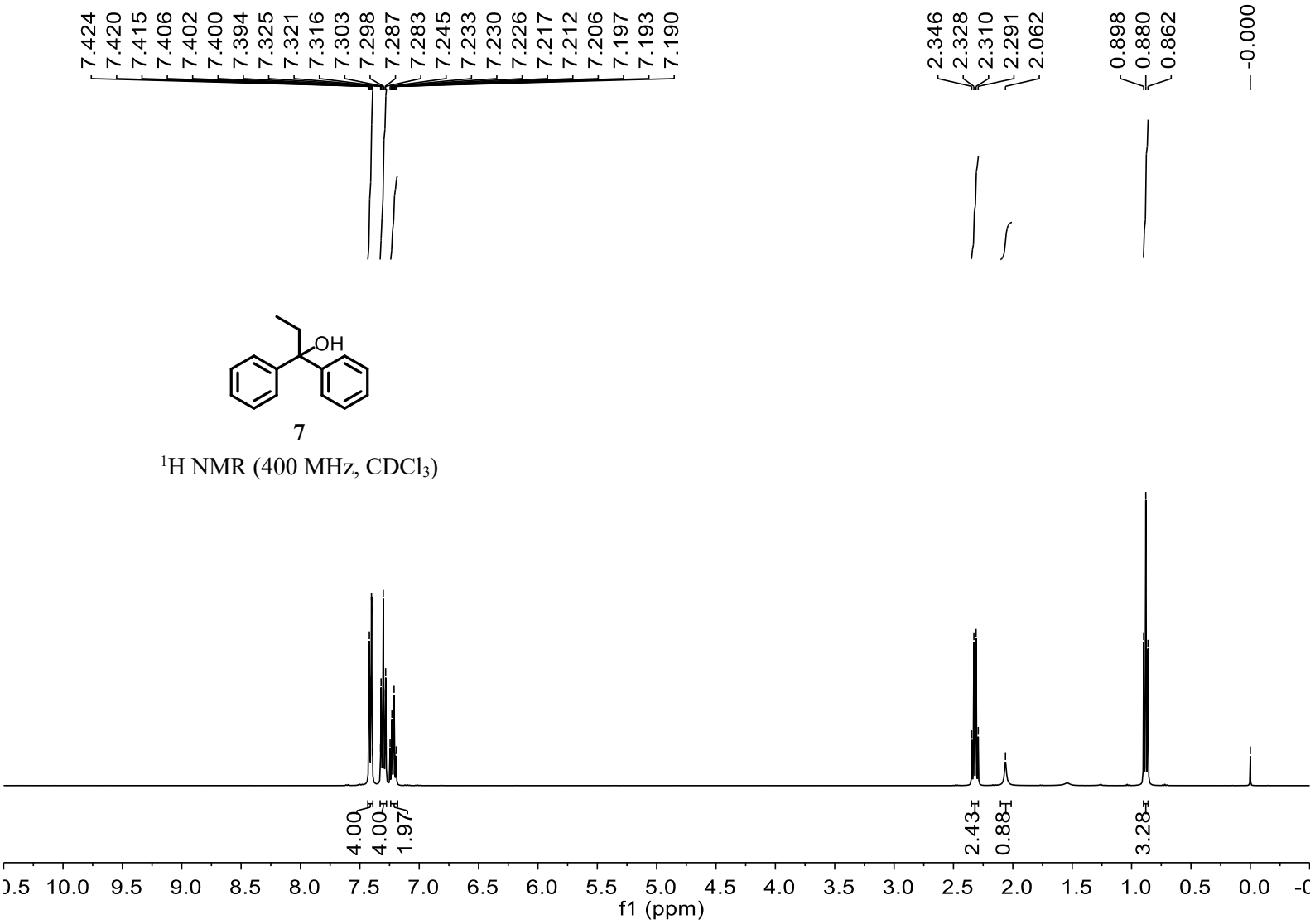

7

^{1}H NMR (400 MHz, $CDCl_3$)

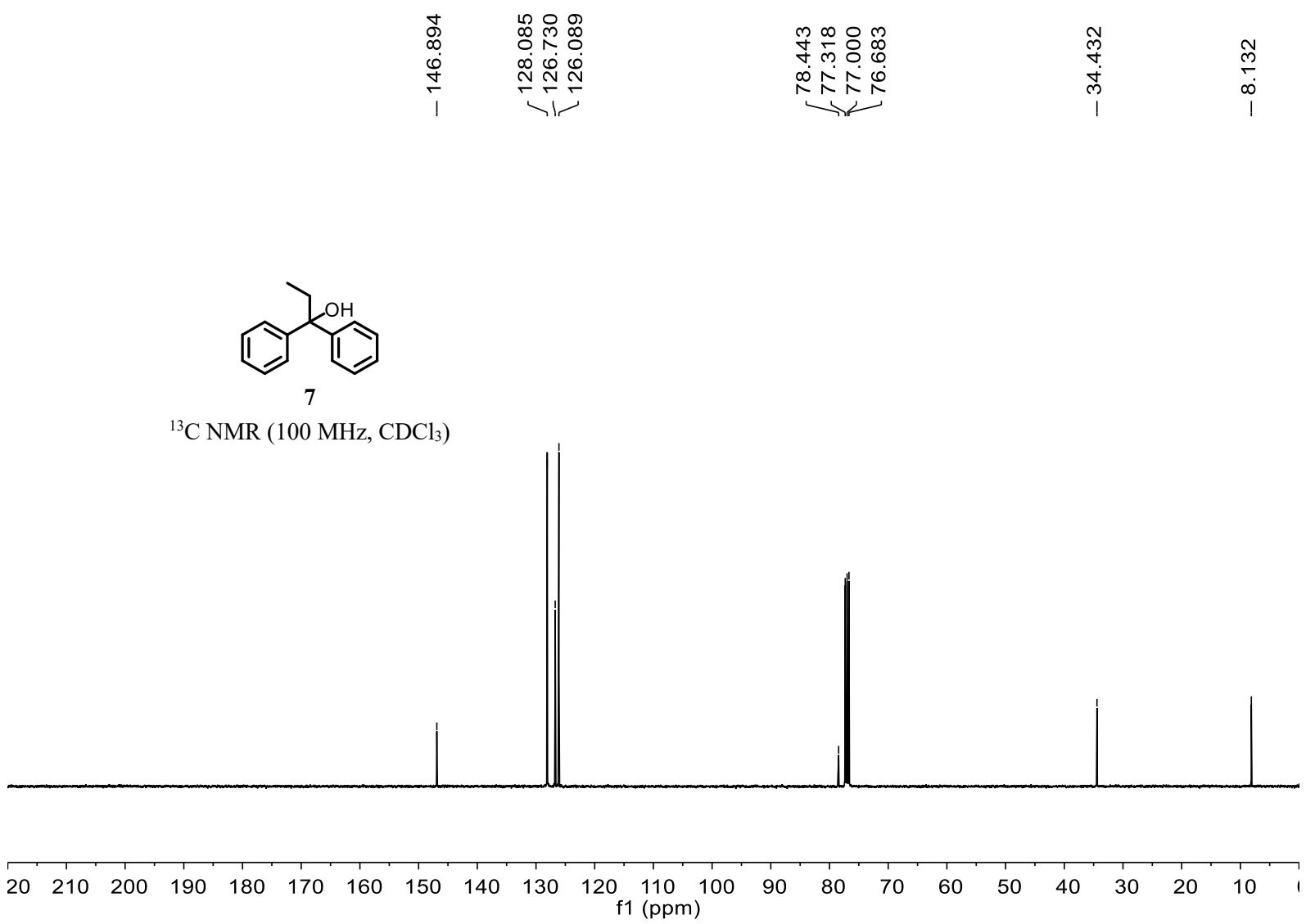
146.894
128.085
126.730
126.089
78.443
77.318
77.000
76.683
34.432
8.132
OH
7
13C NMR (100 MHz, CDCl3)
20 210 200 190 180 170 160 150 140 130 120 110 100 90 80 70 60 50 40 30 20 10
f1 (ppm)

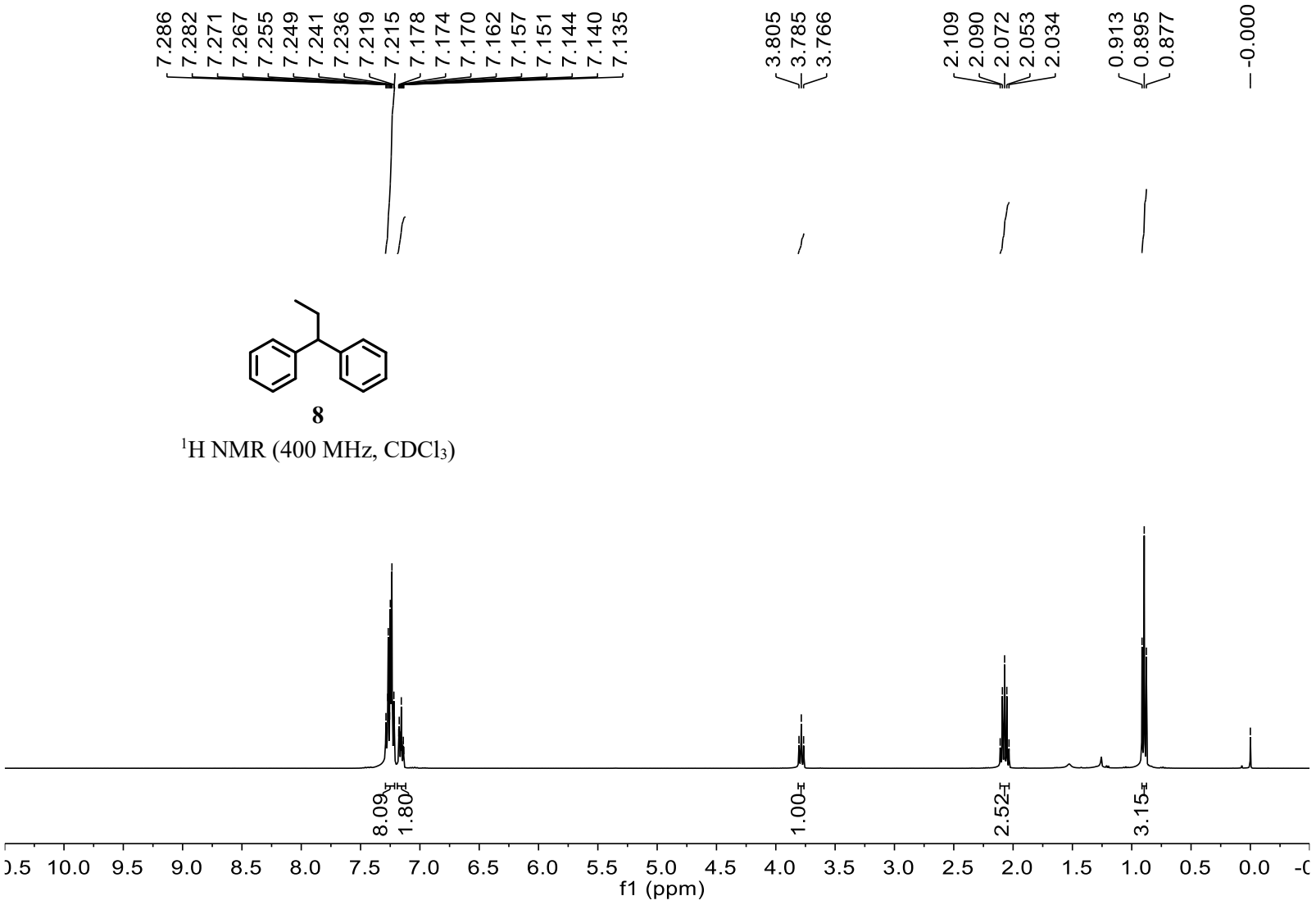

8

^{1}H NMR (400 MHz, $CDCl_3$)

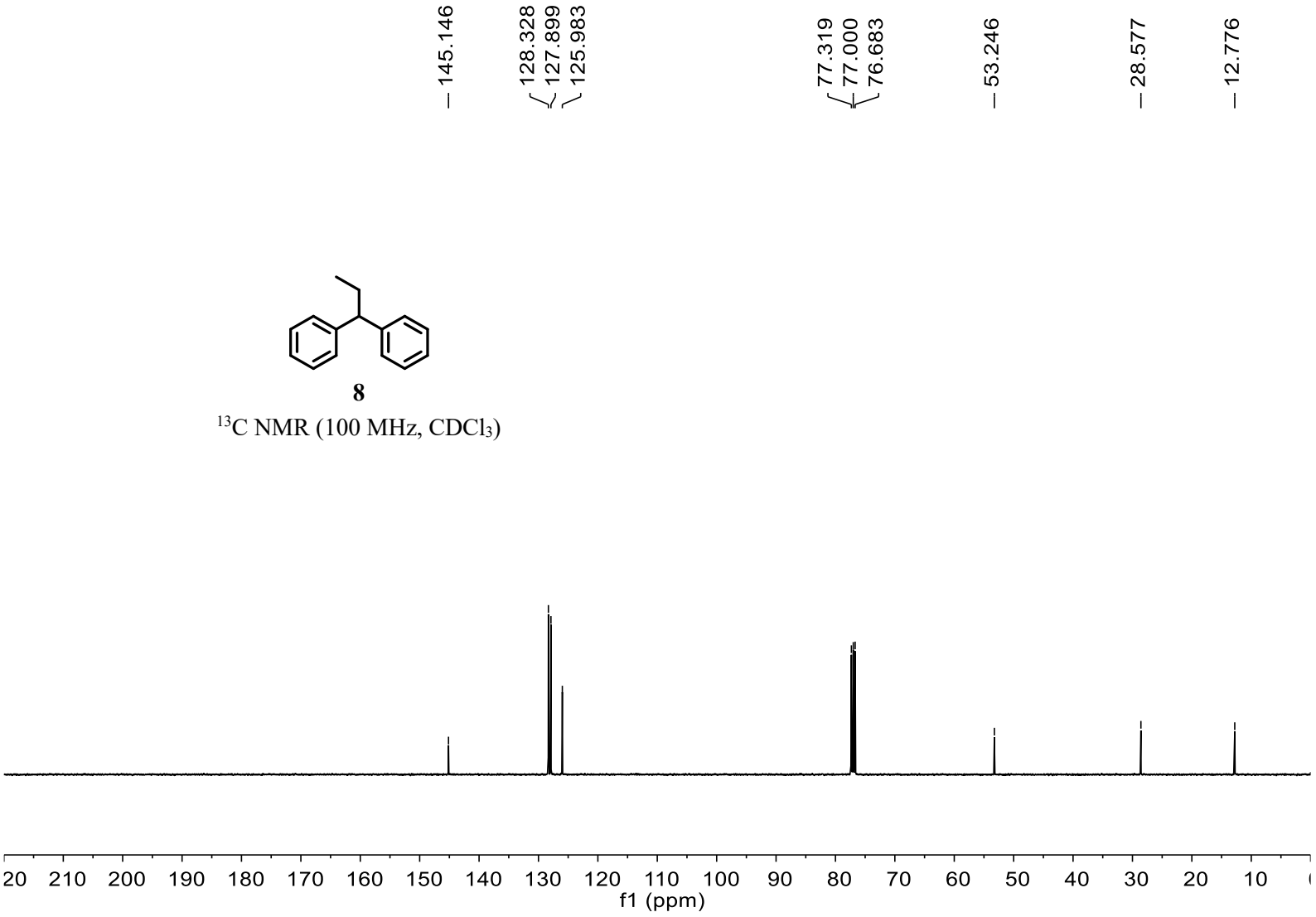

8

^{13}C NMR (100 MHz, $CDCl_3$)

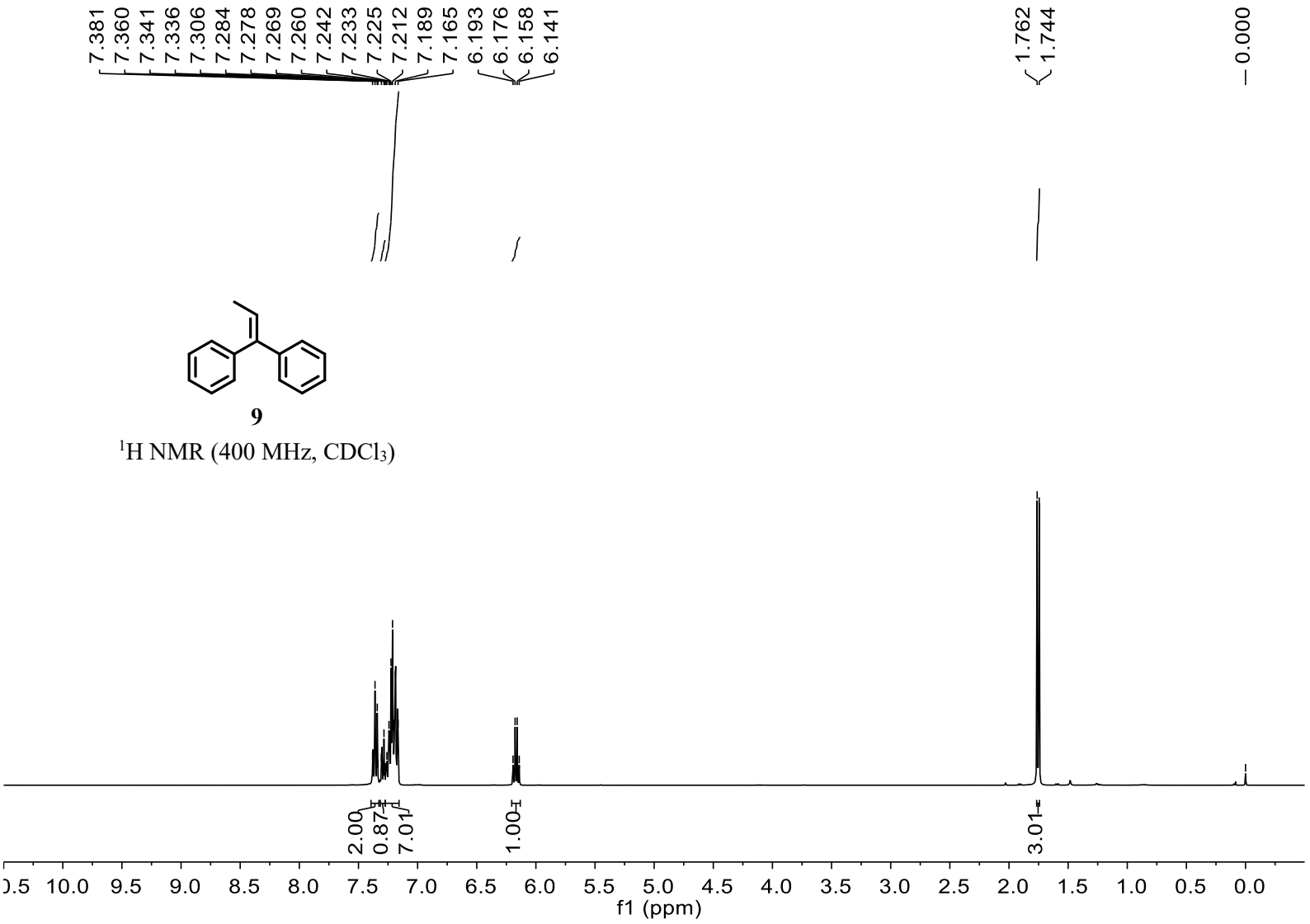

9

^{1}H NMR (400 MHz, $CDCl_3$)

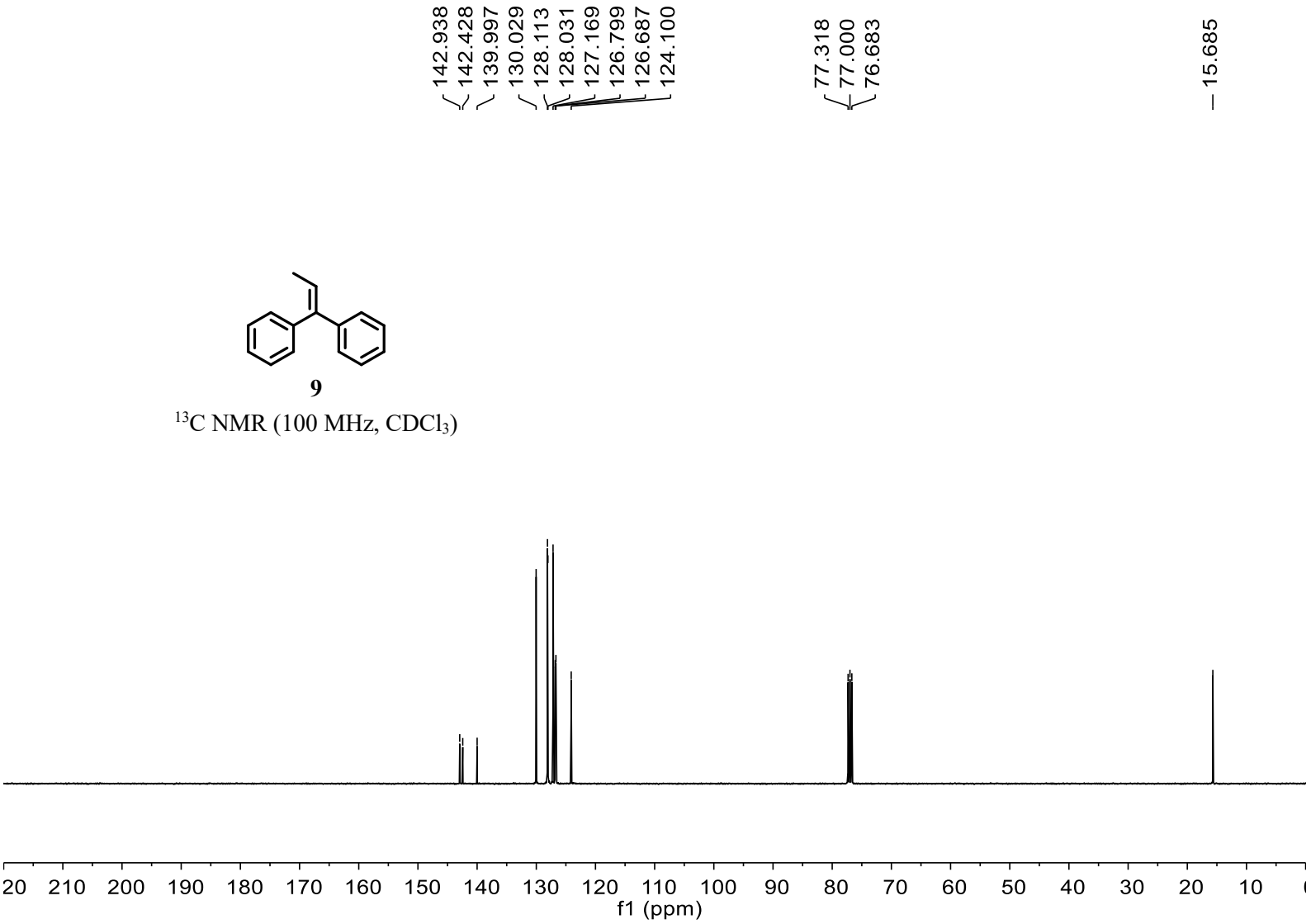

9

^{13}C NMR (100 MHz, $CDCl_3$)

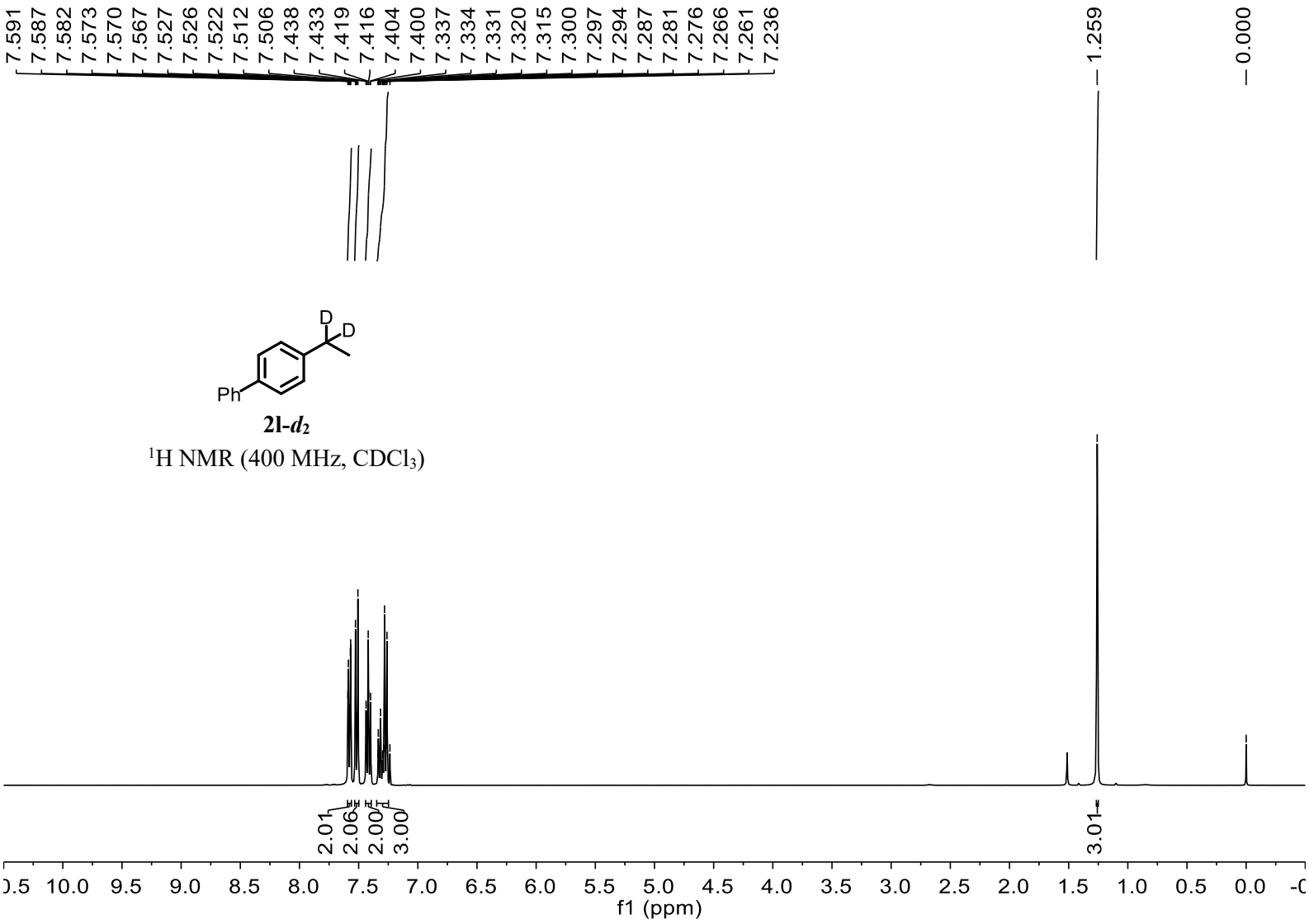

2l-d_2

^{1}H NMR (400 MHz, $CDCl_3$)

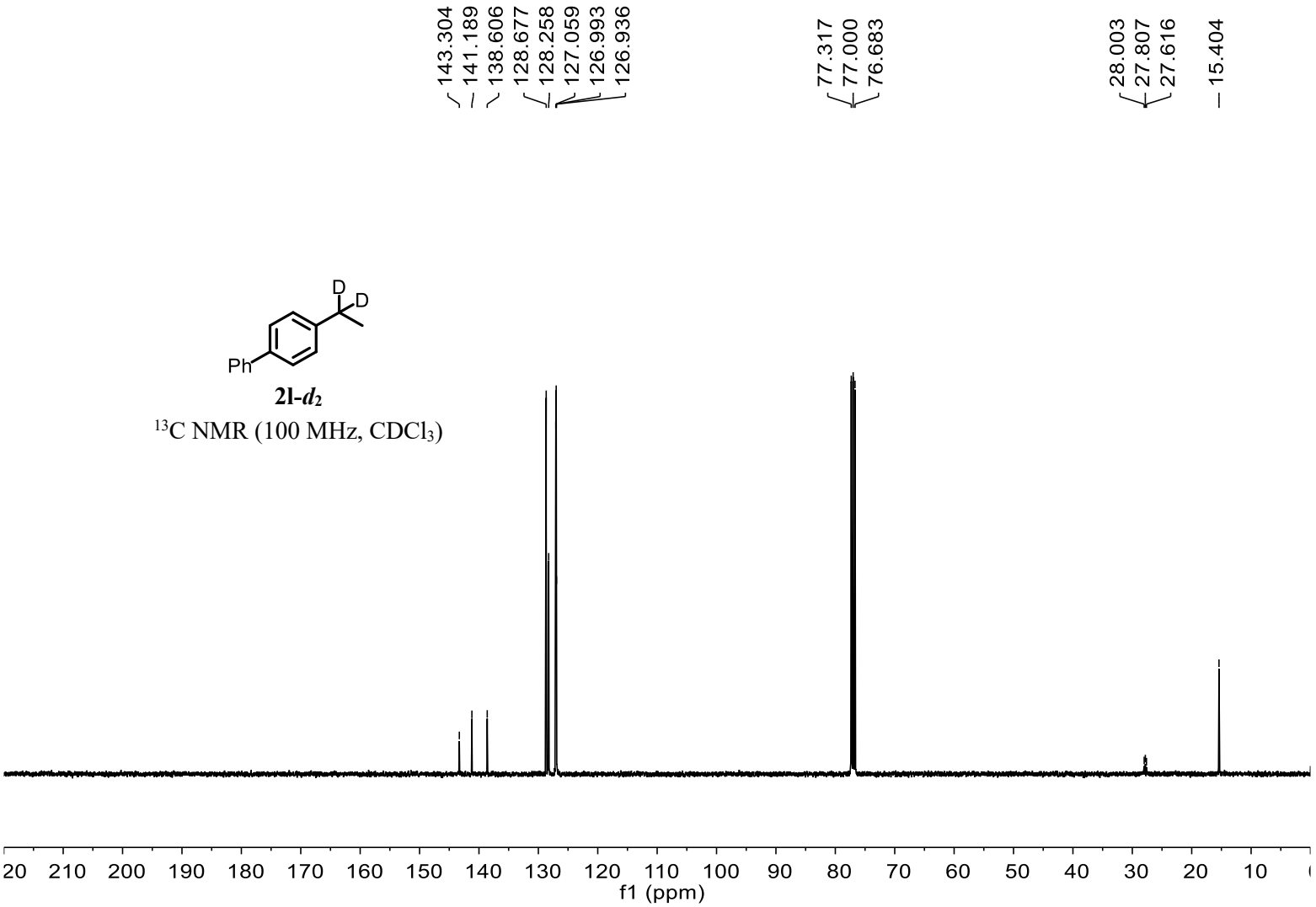

2l-d_2

^{13}C NMR (100 MHz, $CDCl_3$)

10. References

1. Xu, Y. et al., A light-driven enzymatic enantioselective radical acylation. *Nature* **625**, 74-78 (2024).
2. Tang, L. et al. Construction of "small-intelligent" focused mutagenesis libraries using well-designed combinatorial degenerate primers. *Bio Techniques.* **52**, 149-158 (2012).
3. Li, A., Acevedo-Rocha, C. G. & Reetz, M. T. Boosting the efficiency of site-saturation mutagenesis for a difficult-to-randomize gene by a two-step PCR strategy. *Appl. Microbiol. Biotechnol.* **102**, 6095-6103 (2018).
4. Liao, Y., Xing, C., Hu, Q. Rhodium(I)/diene-catalyzed addition reactions of arylborons with ketones. *Org. Lett.* **14**, 1544–1547 (2012).
5. Jin, L. et al. Unsymmetrical CNN-palladacycles with geometry-constrained iminopyridyl ligands: an efficient precatalyst in Suzuki coupling for accessing 1,1-diarylalkanes from secondary benzylic bromides. *Org. Chem. Front.* **5**, 2484-2491 (2018).
6. Chatalova-Sazepin, C., Wang, Q., Sammis, G. M. & Zhu, J. Copper-catalyzed intermolecular carboetherification of unactivated alkenes by alkyl nitriles and alcohols. *Angew. Chem. Int. Ed.* **54**, 5443-5446 (2015).
7. Tie, L., Shan, X.-H., Qu, J.-P. & Kang, Y.-B. α-Trideuteration of methylarenes. *Org. Chem. Front.* **8**, 2981-2984 (2021).
8. Finney, E. E., Ogawa, K. A. & Boydston, A. J. Organocatalyzed anodic oxidation of aldehydes. *J. Am. Chem. Soc.* **134**, 12374-12377 (2012).
9. Hari, D. P. & König, B. Synthetic applications of eosin Y in photoredox catalysis. *Chem. Commun.* **50**, 6688-6699 (2014).
10. Leibler, I. N.-M., Tekle-Smith, M. A. & Doyle, A. G. A general strategy for C(sp^3)–H functionalization with nucleophiles using methyl radical as a hydrogen atom abstractor. *Nat. Commun.* **12**, 6950 (2021).
11. Delfau, L. et al. Critical assessment of the reducing ability of Breslow-type derivatives and implications for carbene-catalyzed radical reactions. *Angew. Chem. Int. Ed.* **60**, 26783-26789 (2021).
12. Waterhouse, A. et al., SWISS-MODEL: homology modelling of protein structures and complexes. *Nucleic Acids Res.* **46**, W296-W303 (2018).
13. Trott, O. & Olson, A. J. AutoDock Vina: improving the speed and accuracy of docking with a new scoring function, efficient optimization, and multithreading. *J. Comput. Chem.* **31**, 455-461 (2010).
14. Søndergaard, C. R., Olsson, M. H. M., Rostkowski, M. & Jensen, J. H. Improved treatment of ligands and coupling effects in empirical calculation and rationalization of pKa values. *J. Chem. Theory Comput.* **7**, 2284-2295 (2011).
15. Maier, J. A. et al. ff14SB: Improving the accuracy of protein side chain and backbone parameters from ff99SB. *J. Chem. Theory Comput.* **11**, 3696-3713 (2015).
16. Wang, J., Wolf, R. M., Caldwell, J. W., Kollman, P. A. & Case, D. A. Case, Development and testing of a general amber force field. *J. Comput. Chem.* **25**, 1157-1174 (2004).
17. Bayly, C. I., Cieplak, P., Cornell, W. & Kollman, P. A. A well-behaved electrostatic

potential based method using charge restraints for deriving atomic charges: the RESP model. J. Phys. Chem. 97, 10269-10280 (1993).
18. Kräutler, V., van Gunsteren, W. F. & Hünenberger, P. H. A fast SHAKE algorithm to solve distance constraint equations for small molecules in molecular dynamics simulations. *J. Comput. Chem.* **22**, 501-508 (2001).
19. Case, A. D. et al., AMBER 2020. (2020).
20. Senn, H. M. & Thiel, W. QM/MM methods for biomolecular systems. *Angew. Chem. Int. Ed.* **48**, 1198-1229 (2009).
21. Metz, S., Kästner, J., Sokol, A. A., Keal, T. W. & Sherwood, P. ChemShell-a modular software package for QM/MM simulations. *WIRES Comput. Mol. Sci.* **4**, 101-110 (2014).
22. Ahlrichs, R., Bär, M., Häser, M., Horn, H. & Kölmel, C. Electronic structure calculations on workstation computers: The program system turbomole. *Chem. Phys. Lett.* **162**, 165-169 (1989).
23. Smith, W., Yong, C. W. & Rodger, P. M. DL_POLY: Application to molecular simulation. *Mol. Simul.* **28**, 385-471 (2002).
24. Frisch, M. J. et al., Gaussian 16 Rev. A.03. (2016).
25. Marenich, A. V., Cramer, C. J. & Truhlar, D. G. Universal solvation model based on solute electron density and on a continuum model of the solvent defined by the bulk dielectric constant and atomic surface tensions. *J. Phys. Chem. B* **113**, 6378-6396 (2009).
26. Chai, J.-D. & Head-Gordon, M. Long-range corrected hybrid density functionals with damped atom–atom dispersion corrections. *Phys. Chem. Chem. Phys.* **10**, 6615–6620 (2008).
27. Aragó, J., Sancho-García, J. C., Ortí, E. & Beljonne, D. Ab Initio Modeling of Donor–Acceptor Interactions and Charge-Transfer Excitations in Molecular Complexes: The Case of Terthiophene–Tetracyanoquinodimethane. *J. Chem. Theory. Comput.* **7**, 2068–2077 (2011).
28. Kim, J. & Yi, C.-S. Intermolecular Markovnikov-selective hydroacylation of olefins catalyzed by a cationic ruthenium–hydride complex. *ACS Catal.* **6**, 3336-3339 (2016).
29. Pichette Drapeau, M. et al. Transition-metal-free α-arylation of enolizable aryl ketones and mechanistic evidence for a radical process. *Angew. Chem. Int. Ed*. **54**, 10587-10591 (2015).
30. Liu, F., et al. N-Heterocyclic carbene-palladacyclic complexes: synthesis, characterization and their applications in the C-N coupling and α-arylation of ketones using aryl chlorides. *Tetrahedron Lett.* **74**, 5683-5690 (2018).
31. Lundin, P. M., Esquivias, J. & Fu, G. C. Catalytic asymmetric cross-couplings of racemic α-bromoketones with arylzinc reagents. *Angew. Chem. Int. Ed.* **48**, 154-156 (2009).
32. Peng, C., Zhang, W., Yan, G. & Wang, J.-B. Arylation and vinylation of α-diazocarbonyl compounds with boroxines. *Org. Lett.* **11**, 1667-1670 (2009).
33. Kim, J., Jang, J., Lee, Y. & Shin, K. Exogenous ligand-free NiH-catalyzed hydroacylation of aryl alkenes with aroyl fluorides. Org. Lett. 24, 5412-5416 (2022).
34. Scholz, M. et al. Diaryl-dithiolanes and -isothiazoles: COX-1/COX-2 and 5-LOX-inhibitory, OH scavenging and anti-adhesive activities. *Bio. Org. Med. Chem.* **17**, 558-568 (2009).
35. Schedler, M., Wang, D.-S. & Glorius, F. NHC-catalyzed hydroacylation of styrenes.

Angew. Chem. Int. Ed. **52**, 2585-2589 (2013).
36. Sim, S-B. D., Wang, M. & Zhao, Y. Phase-transfer-catalyzed enantioselective α-hydroxylation of acyclic and cyclic ketones with oxygen. *ACS Catal.* **5**, 3609-3612 (2015).
37. Zhang, Z. et al. Anodic oxidation triggered divergent 1, 2- and 1, 4-group transfer reactions of β-hydroxycarboxylic acids enabled by electrochemical regulation. *Chem. Sci.* **11**, 12021-12028 (2020).
38. Henrion, M., Chetcuti, M. J. & Ritleng, V. From acetone metalation to the catalytic α-arylation of acyclic ketones with NHC-nickel (II) complexes. *Chem. Commun.* **50**, 4624-4627 (2014).
39. Meng, Q.-Y., Lezius, L. & Studer, A. Benzylic C−H acylation by cooperative NHC and photoredox catalysis. *Nat. Commun.* **12**, 2068 (2021).
40. Wang, C. et al. Palladium-catalyzed secondary benzylic imidoylative reactions. *Org. Lett.* **22**, 6954-6959 (2020).
41. Yan, W.-J., Tu, H.-Y., Liao, Z., Shen, X.-Q. & Zhang, X.-G. Palladium-catalyzed ring-opening diarylation of cyclobutanols for the synthesis of acylindanes. *Adv. Synth. Catal.* **365**, 2147-2151 (2023).